JOURNAL OF

CHROMATOGRAPHY A

INCLUDING ELECTROPHORESIS AND OTHER SEPARATION METHODS

ELSEVIER

CONTENTS

(Abstracts / Contents Lists published in Analytical Abstracts, Biochemical Abstracts, Biological Abstracts, Chemical Abstracts, Chemical Titles, Chromatography Abstracts, Current Awareness in Biological Sciences (CABS), Current Contents/Life Sciences, Current Contents/Physical, Chemical & Earth Sciences, Deep-Sea Research/Part B: Oceanographic Literature Review, Excerpta Medica, Index Medicus, Mass Spectrometry Bulletin, PASCAL-CNRS, Referativnyi Zhurnal, Research Alert and Science Citation Index)

REGULAR PAPERS

Column Liquid Chromatography

Field-Flow Fractionation

Gas Chromatography

(Continued overleaf)

Contents (continued)

SHORT COMMUNICATIONS

JOURNAL OF CHROMATOGRAPHY A

INCLUDING ELECTROPHORESIS AND OTHER SEPARATION METHODS

Selection of stationary phases for the liquid chromatographic analysis of basic compounds using chemometric methods

R.J.M. Vervoort, M.W.J. Derksen, F.A. Maris*

AKZO Nobel, N.V. Organon, P.O. Box 20, 5340 BH Oss, Netherlands

Abstract

The analysis of basic compounds by means of reversed-phase liquid chromatography is often hampered by poor peak shapes. In this paper chemometrical methods are used to select and reduce the number of test compounds and to detect differences in applicability of stationary phases designed for the analysis of basic drugs.

In the first part principal component analysis was applied to reduce the number of test compounds necessary to characterize a stationary phase. From a data set of the asymmetry values of 32 test compounds analyzed on six different LC columns, five representative compounds were selected. Subsequently, these five compounds were used for evaluation of commercially available columns.

For the column judgement the asymmetry of the test compounds, the efficiency and the short-term reproducibility of the capacity factor and the plate number, were taken into account. Graphical presentation using bar charts, multi-criteria decision making based on the Pareto optimality and bi-plots were used to distinguish between columns. First of all eight columns were compared at individual pH values of 3.0, 7.0 and 11.0. Finally, all results were combined and revealed that for our test compounds very good results were obtained at a pH of 11 using a column containing zirconium oxide particles coated with polybutadiene (3MZ-18). At low pH values good results were obtained with a Supelcosil LC-ABZ and a Zorbax Rx-C_{18} column.

Overall it can be concluded that a chemometric approach is successfully applied for the development of a method for in-house column testing and evaluation dedicated to the Organon type of compounds. Other columns developed for the analysis of basic solutes can now be efficiently tested with the method described in this paper. Chemometric methods were useful to efficiently reduce the number of test compounds and for column evaluation. However, the final selection of a column also depends on the special requirements defined by the expert. The requirements, which are, for example, for routine quality control clearly different than for purity testing of new chemical entities in drug development, can be translated to weighing factors for the variables tested. For this the advice of the expert remains indispensable.

1. Introduction

In pharmaceutical analysis reversed-phase liquid chromatography (LC) is the most frequently used technique. It is used as a tool to quantify active ingredients in pharmaceutical formulations, to determine impurities, to investigate the stability of a product, etc. For the analysis of basic drugs, however, often asymmetric peaks are obtained due to ionic interactions of compounds with residual silanol groups of the stationary phase [1,2].

* Corresponding author.

To improve peak shape, optimization of both the mobile and stationary phase should be considered. In the literature, many suggestions have been given to optimize the mobile phase, e.g. by adding silanol blockers, using ion-pair reagents and by selecting an optimal pH [1,2]. Also the number of stationary phases specially designed for the analysis of basic compounds is exponentially increasing [1,3]. Because many possibilities are available, it is difficult to select the best system.

Recently, we reported about the analysis of 32 basic compounds using several columns with different eluents [1]. Relations between retention, asymmetry and basicity of the compounds were studied for a μBondapak C$_{18}$ column. Together with data of the peak shape of the 32 test compounds on five other columns, a data set was obtained which contains a lot of information. However, to extract useful information from such a set is often problematic and the use of chemometric methods can be helpful.

Multivariate techniques, like principal component, cluster, correspondence factor and discriminant analysis can be used to analyse and reduce the number of variables of a data set [4–8]. In the literature, Musumarra et al. [6] reported results from principal component analysis (PCA) of chromatographic retention data of drugs for identification purposes. Delaney et al. [7] used PCA to select a set of test compounds in LC. Schmitz et al. [8] compared different multivariate techniques for the characterization of stationary phases in LC and to select test compounds.

From a data set of 32 compounds and different columns, a number of test compounds was selected using PCA. The test compounds were selected on basis of the asymmetry obtained on six stationary phases which are recommended for the analysis of basic compounds. Subsequently, the test compounds were used for testing of several other stationary phases. For selecting the optimal column not only the peak shapes are important, but also the efficiency and ruggedness. In these situations methods of multi-criteria decision making (MCDM) can be applied for column judgement [9–12]. Within this approach it is not necessary to make a priori decisions and

experiments can be compared easily. Also bar charts and bi-plots can be helpful tools to characterize stationary phases [13]. For the column judgement presented in this paper the obtained asymmetry values, the plate height, and the repeatability of the capacity factor and plate height are used.

2. Experimental

2.1. Apparatus

The HPLC experiments were carried out using an HP1090M liquid chromatograph equipped with an HP1040M diode-array detector (Hewlett-Packard, Amstelveen, Netherlands). HPLC chromatograms were collected on a HP 79994A HPLC Workstation.

The software packages Unscrambler 5.03, Camo (Trondheim, Norway) and Microsoft Excel 4.0 (Redmond, WA, USA) were used to analyse the data.

2.2. Chemicals

All basic drugs were synthesized by Organon (Oss, Netherlands).

As organic modifiers methanol (MeOH) and acetonitrile (ACN) were used. Methanol was freshly distilled before use. Analytical-grade acetonitrile was obtained from J.T. Baker (Deventer, Netherlands).

For the preparation of the buffers disodium hydrogenphosphate, sodium dihydrogenphosphate and boric acid, supplied by J.T. Baker were used. To obtain 25 mM buffers, adequate amounts were dissolved in water of Milli-Q quality. Sodium hydroxide and concentrated orthophosphoric acid were obtained from Merck (Darmstadt, Germany) and were added to the buffers until the desired pH value was reached.

The amount of basic drugs injected was 2 μg and was achieved by injecting 2 μl from a 1 mg/ml solution in methanol.

The stationary phases used in this study were obtained from the suppliers as pre-packed columns (Table 1).

Table 1
Overview of the stationary phases used for selection of the test compounds (A) and for the evaluation of the column performance (B)

	Column	Abbreviation	Manufacturer	Dimensions (length × I.D., mm)	Particle size (μm)
A	μBondapak C$_{18}$	BON	Waters–Millipore	300 × 3.9	10
	NovaPak C$_{18}$	NOV	Waters–Millipore	300 × 3.9	4
	Kromasil KR100-5-C$_{18}$	KRO	Eka Nobel	250 × 4.6	5
	Exsil 100 ODS-B	EXS	Exmere	250 × 4.6	5
	Suplex pKb-100	PKB	Supelco	250 × 4.6	5
	Zorbax Rx-C$_{18}$	ZRX	Rockland Technologies	250 × 4.6	5
B	Zorbax Rx-C$_{18}$	ZRX	Rockland Technologies	250 × 4.6	5
	Hypersil BDS-C$_{18}$	BDS	Shandon Scientific	150 × 4.6	5
	Chromspher B	CHB	Chrompack	250 × 4.6	5
	Supelcosil LC-ABZ	ABZ	Supelco	150 × 4.6	5
	Polyspher RP-18	POL	Merck	150 × 4.6	10
	Asahipak ODP-50	ASA	Asahi Chemical Co.	125 × 4.0	5
	Aluspher RP-Select B	ALU	Merck	125 × 4.0	5
	3M-Z18	3MZ	Cohesive Technologies	150 × 4.6	6

2.3. Experimental set-up

The experiments carried out to characterize the columns were performed in strict order. Initially, for each column data were collected in duplicate at the highest pH to be tested. Subsequently, this was done for the lower pH. All experiments were repeated on a subsequent day.

Generally, silica-based columns are claimed to be only stable from pH values of 2 to 8. In order to avoid to operate the silica-based columns to close to the operating boundaries, they were tested at pH values of 3 and 7 using methanol as modifier. The non-silica-based columns were tested, using acetonitrile as modifier, at pH values of 7 and 11, and for the Asahipak ODP-50 and the 3MZ-18 column also at pH 3.

The modifier–buffer ratio was adjusted to ensure k' values larger than 1.

2.4. Calculations

The asymmetry factor (A_s) was calculated at 10% of the peak height and expressed as the ratio of the width of the rear and the front side of the peak. For the calculation of the plate height (HETP) the second moment of the peak was used [14].

For the stability of the column the repeatability of the plate height (RH) and the capacity factor (Rk') were determined. This was done by repeating the analyses on the next day. The difference between two days divided by the highest value (in most cases the first day) times 100% is reported.

3. Results and discussion

3.1. Selection of test compounds

Until now, the applicability of stationary phases for the analysis of basic compounds was tested using 32 compounds [1]. However, analysing 32 compounds each time is rather time consuming. The use of a representative set of test compounds, extracted from the 32 compounds, will result in a reduction of experimental work. This extraction, using the asymmetry data obtained for the test compounds on six different columns, was achieved using PCA. The information obtained with the reduced number of test compounds should be comparable with the information obtained with 32 compounds.

The data matrix used is shown in Table 2. For the missing values the particular column averages were used. The data were collected using methanol–10 mM phosphate buffer pH 7.4 as eluent [1]. The asymmetry factors for the BON column were calculated at a capacity factor 5.0. On the other columns the asymmetry values were taken at capacity factors varying from 2 to 8 with an average value of about 5.

In Fig. 1 the results of the PCA analysis of the six variables (LC columns) and the 32 objects (test compounds) are shown. Before performing PCA the data were autoscaled. With the first two principal components (PCs) 79% of the variance was described, while using the first three PCs

86% of the variance could be described. In Fig. 1A and B the score and the loading plot of the first and second PC, respectively, are given. In the loading plot can be seen that for the six different columns almost the same value is obtained for the first PC. A better distinction between the columns is obtained by plotting the second against the third PC (Fig. 1D). From this plot can be seen that the BON column and the NOV column behave very similar, which is not unexpected as they are produced by the same manufacturer. Also with the KRO column comparable results are obtained. In Fig. 1C the score plot is given for the second and the third PC.

Looking at the score plots, the compounds

Table 2
Asymmetry factors for 32 compounds (objects) and 6 LC colums (variables)

Objects	BON	NOV	ZRX	KRO	PKB	EXS
1	3.600	5.740	2.760	2.630	1.300	2.020
2	5.600	10.440	4.820	4.190	3.860	2.400
3	1.700	1.570	1.570	1.300	1.280	1.470
4	2.300	Missing	Missing	1.440	1.330	Missing
5	1.100	1.050	1.240	1.200	1.430	1.930
6	4.600	6.920	Missing	Missing	1.730	7.490
7	1.900	2.390	1.640	1.840	1.870	2.340
8	2.300	3.220	3.300	2.380	1.400	2.140
9	1.100	1.210	1.490	1.170	1.170	1.460
10	1.000	1.150	1.220	1.120	1.170	1.060
11	1.100	1.190	Missing	1.170	1.190	0.990
12	0.900	1.070	1.210	1.190	1.230	1.080
13	2.800	3.070	2.200	2.320	1.480	2.950
14	2.200	2.350	1.500	2.160	1.290	1.690
15	1.100	1.240	1.230	Missing	1.210	1.230
16	2.600	5.410	1.960	4.080	2.070	3.100
17	2.300	1.890	1.540	1.700	1.500	2.500
18	5.200	5.510	2.770	5.320	1.850	6.570
19	9.100	14.440	2.940	6.110	2.170	6.430
20	3.600	5.810	1.920	Missing	Missing	4.240
21	3.600	1.590	1.550	1.370	1.380	2.520
22	2.400	2.350	1.910	1.080	Missing	3.280
23	2.300	1.560	1.630	1.340	1.460	2.600
24	1.900	1.230	1.510	1.190	1.250	1.540
25	2.300	2.130	1.790	Missing	Missing	2.830
26	4.800	8.020	2.290	4.190	Missing	8.290
27	1.700	1.370	1.530	1.290	1.720	2.240
28	2.900	3.420	1.990	3.310	1.190	2.130
29	2.400	1.950	1.880	1.700	2.550	3.500
30	5.700	6.990	3.110	4.890	3.550	6.510
31	4.000	6.050	2.470	3.020	2.350	4.740
32	3.770	4.190	4.160	4.510	1.560	2.990
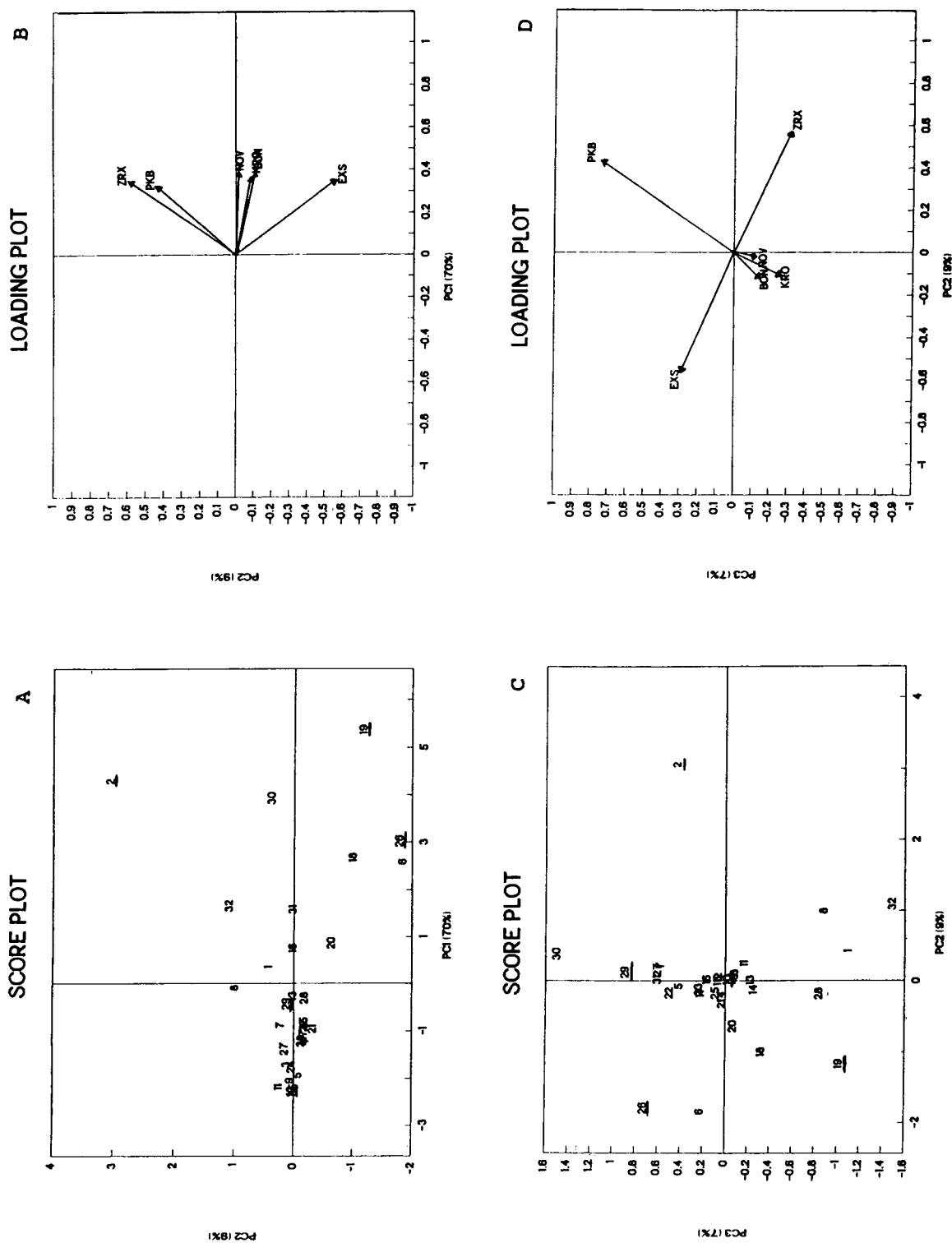
Fig. 1. Results of the p........pal components analysis. (A) Scoreplot PC1 vs. PC2; (B) loading plot PC1 vs. PC2; (C) scoreplot PC2 vs. PC3; (D) loading plot PC2 vs. PC3. Compounds selected for the test set are underlined in (A) and (C).
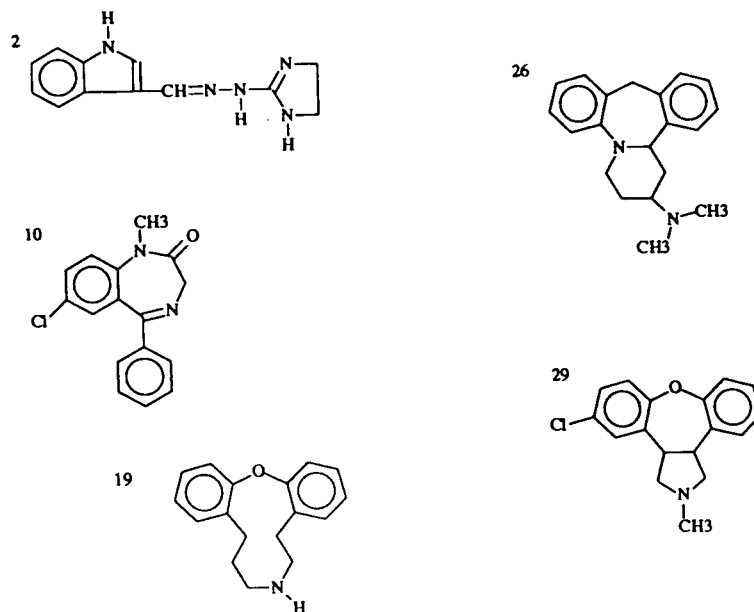
Fig. 2. Structures of the compounds selected with PCA.

positioned to the left in Fig. 1A and in the middle of Fig. 1C always gave symmetrical peaks. Compound 10 was selected as a "neutral" test compound, giving symmetrical peaks on all six columns tested. This compound is used to calculate the efficiency of the columns. The first PC seems to correspond with a general asymmetry effect; with increasing value for the PC the average asymmetry for the compounds is increasing. Other test compounds were selected from Fig. 1A and C on basis of their position somewhere on the edge of the cluster in order to obtain maximum discrimination. Compounds 2, 19, 26 and 29 were selected. Looking at Fig. 1C, compounds 30 and 32 would also have been good

choices. The selection of the test compounds on basis of PCA fitted very well with the compounds which would have been selected by the analytical expert based on the polarity, the pK_a values and the peak shapes of the compounds [1]. However, other factors involved can easily be overlooked by the expert or can be difficult to interpret. In Fig. 2 the structures of the selected compounds are shown.

The correlation matrix of the variables (columns) is given in Table 3. In this table again the high correlation between the BON and the NOV column can be noticed. For the other columns probably different mechanisms play a role which influence the (a)symmetry. These different elu-

Table 3
Correlation matrix of the variables (columns) calculated from Table 2

	BON	NOV	ZRX	KRO	PKB	EXS
BON	1.000	0.935	0.678	0.877	0.636	0.771
NOV		1.000	0.696	0.871	0.674	0.704
ZRX			1.000	0.720	0.658	0.387
KRO				1.000	0.608	0.755
PKB					1.000	0.524
EXS						1.000

tion mechanisms can be a result of the different ways residual silanols are shielded. For instance, with the ZRX stationary phase highly pure silica was used, whereas residual silanols of the PKB stationary phase are shielded electrostatically.

3.2. Testing of HPLC columns specially designed for the analysis of basic compounds

In a previous paper [1] eight HPLC columns were compared in a more qualitative way. From these results it was concluded that the PKB column was the most promising column. Later on an improved version of this column appeared on the market, viz. ABZ. Also with the ZRX column reasonable results were obtained. Therefore, these two columns and six other LC columns were further tested using the five compounds selected in the first part of this study.

The silica-based columns used in the second part of this study (Table 1B), differed in the manner the residual silanols are shielded. As mentioned before, very pure silica was used in the preparation of the ZRX column. Residual silanols in the ABZ column are shielded by electrostatic repulsion. The stationary phase used for the CHB column are polymer-coated silica particles whereas for the BDS column silica with a homogeneous surface is used which is end-capped after bonding the C_{18} phase.

For the 3MZ and the ALU stationary phase, polybutadiene was coated on particles of zirkonium oxide and aluminium oxide, respectively. The ASA column consisted of macroporous particles of polyvinylalcohol-based polymer, in which reversed-phase chains were introduced by binding stearic ester chains through an ester bond. The POL column consisted of particles of polystyrene–divinylbenzene polymer with C_{18} chains.

Besides the asymmetry factor an important parameter for the comparison of columns is the efficiency. For example for purity analysis of unknown compounds, i.e. new chemical entities in drug development, a high separation efficiency is necessary in an acceptable time. Low efficiency and high asymmetry will lead to poor purity analyses. High asymmetry will also hamper a correct integration. To make it more complicated, columns with low efficiency will mask the factors which contribute to the tailing. For mutual optimization MCDM is therefore necessary.

The primary goal of the column selection is to select the best column which can be broadly applied. Therefore the average asymmetry of the test compounds was used and not the single values. For the calculation of the efficiency of the column the results of test compound 10 were used. In order to compare the efficiency of the columns and to compensate for differences in the column length the plate height was calculated.

Table 4
Chromatographic data obtained at pH 7

Column	Asymmetry (A_s)					Capacity factor (k')					Average				
	2	10	19	26	29	2	10	19	26	29	A_s	k'	HETP (μm)	RH (%)	Rk' (%)
ZRX	3.8	1.1	6.8	5.9	3.1	3.4	4.9	7.6	5.2	4.0	4.1	5.0	17.3	1.7	10.3
BDS	7.1	0.9	8.3	7.4	2.5	3.5	6.1	2.3	2.9	2.6	5.2	3.5	19.9	2.5	3.3
CHB	4.7	1.1	7.5	6.5	3.9	5.0	2.6	24.4	16.4	8.6	4.7	11.4	31.4	1.0	1.9
ABZ	5.8	0.9	2.1	2.2	1.3	5.2	7.8	4.1	6.4	5.7	2.5	5.8	20.7	4.1	3.9
ASA	6.1	1.7	4.6	4.5	5.0	2.0	5.1	2.8	2.0	2.9	4.4	2.9	64.3	11.4	2.0
ALU	1.3	0.6	1.6	1.7	1.4	12.9	5.0	5.5	6.2	6.5	1.3	7.2	74.8	14.1	6.1
POL	3.3	1.1	1.8	1.3	1.2	0.5	5.6	1.2	3.2	8.0	1.8	3.7	298.3	69.3	9.0
BMZ	1.6	1.0	1.7	1.4	1.2.	4.5	2.6	3.2	3.1	3.1	1.4	3.3	25.2	8.9	3.9

Another factor which is important for a good column performance is the reproducibility of analyses. In this study the capacity factors and the plate heights were measured on two subsequent days. In this way the short-term reproducibility or repeatability is measured. Testing the ruggedness of a column requires more extensive testing which should be done after the initial selection described in this report. The relative difference between two days is reported for compound 10. The obtained data must be seen as qualitative data in comparison with the more precise data obtained for the asymmetry and the plate height. The repeatability of the capacity factor is an indication of the stability of the stationary phase, while the repeatability of the plate height is an indication of the stability of the packing material in combination with the stationary phase.

3.3. Testing of columns at pH 7

The results are shown in Table 4. The first question was whether k' values should be treated as a factor. In ref. [1] a correlation was found for k' and A_s. Because the k' values vary from column to column, for a honest comparison of the asymmetry factors the k' values should be included. However, in this case there was hardly any correlation between k' and A_s, as can be seen from the correlation matrix presented in Table 5. Because in the column evaluation only the asymmetry plays a role, the k' values were excluded.

In order to interpret the results, bar charts were made (see Fig. 3). For four of the columns recommended for basic solutes an average

asymmetry for the test compounds of more than 4 was observed. Lowest asymmetry factors were obtained for the 3MZ, the ALU and the POL column. From these three columns only the 3MZ column showed a reasonable low plate height. Poor efficiency was observed for the POL column. However, the repeatability of the 3MZ column is moderate in comparison with for example the CHB column. A qualitative interpretation of the bar charts is given in Table 6. In this table the repeatability of the capacity factor and of the plate height are combined. It can be concluded that the best results are obtained with the 3MZ column, although there are still doubts about the ruggedness of the column.

MCDM using the Pareto optimal (PO) points [15] is another method to interpret the results. A PO plot is the best possible combination of two criteria. Applying four factors, in principle 6 plots of 2 criteria can be made. The most important one is the asymmetry vs. plate height. As the asymmetry is the starting point for the optimization it was decided to add the PO plots for asymmetry vs. repeatability of the plate height, and asymmetry vs. the repeatability of the capacity factor. When three or more criteria are involved a stacked PO plot can be made. A stacked PO plot is a stack of scatter plots of the individual criteria. The individual plots are placed on top of each other. Points which are exactly vertical to each other (over the different plots) belong to the same stationary phase [15].

Table 5
Correlation matrix at pH 7 calculated from Table 4

	A_s	k'	Rk'	HETP	RH
A_s	1.00	0.14	−0.34	−0.40	−0.46
k'		1.00	−0.21	−0.21	−0.29
Rk'			1.00	0.46	0.48
HETP				1.00	0.99
RH					1.00

Table 6
Qualitative interpretation of the results of Fig. 3

Column	Asymmetry	Efficiency	Repeatability
ZRX	−	+	0
BDS	−	+	+
CHB	−	+	+
ABZ	0	+	+
ASA	−	0	0
ALU	+	0	0
POL	+	−	−
3MZ	+	+	0

+ = Good; 0 = moderate; − = poor.
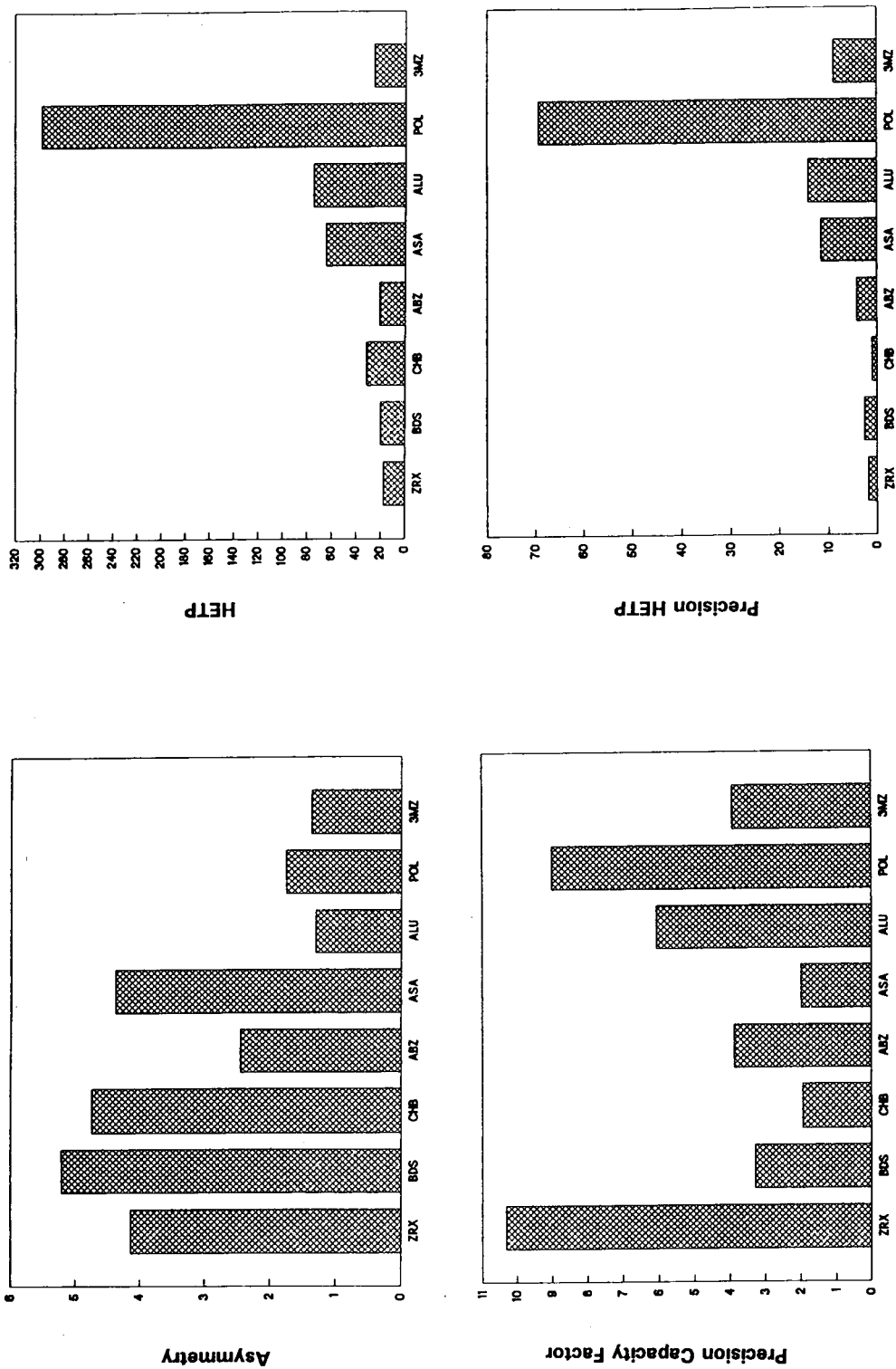
Fig. 3. Bar charts of the asymmetry, the precision of the capacity factor, height equivalent of a theoretical plate (HETP) and the precision of the HETP obtained at pH 7. The numbers are calculated as described in the Experimental section.
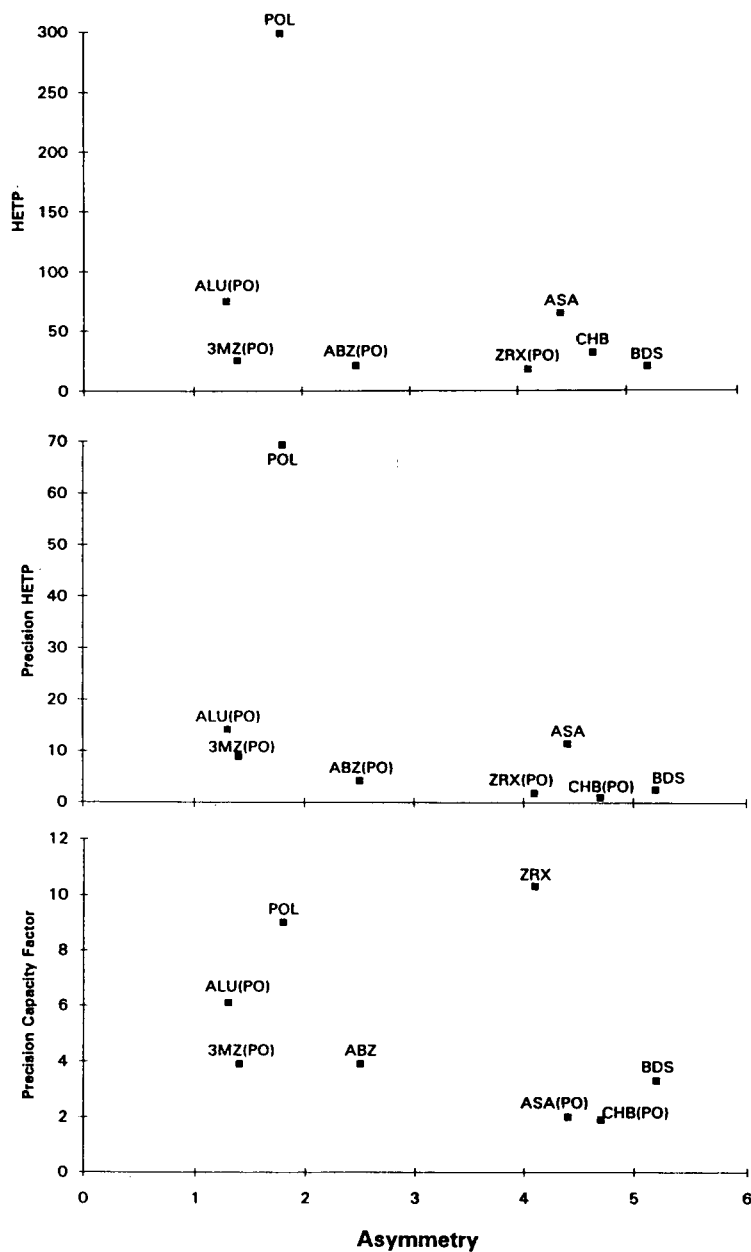
Fig. 4. Stacked PO plot of the asymmetry vs. HETP, precision of the HETP and precision of the capacity factor, obtained at pH 7. The PO points are indicated between brackets (PO) in the plot.

The stacked PO plot is shown in Fig. 4 in which the PO points are indicated. Very good asymmetry values are obtained for the ALU and the 3MZ. Comparing the efficiency, the 3MZ is clearly better. With respect to this aspect the ZRX and the ABZ are even better. However,
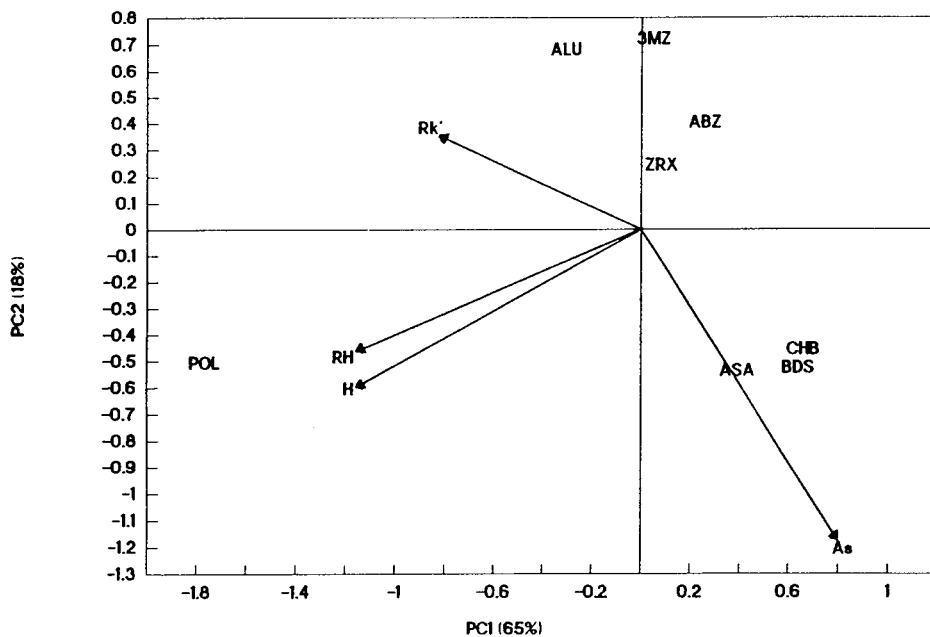
Fig. 5. Bi-plot obtained at pH 7. The data used for the bi-plot are the average values given in Table 4.

the increased asymmetry is likely to be more substantial than the gain in efficiency. Therefore, the 3MZ is to be preferred.

Still it is interesting to see whether other chemometrical methods can improve the column

evaluation. In Fig. 5 a bi-plot is given based on the information presented in Table 4. As pretreatment the data were autoscaled. The first two PCs explain 83% of the variance. As can be seen the demands on "asymmetry" and "repeatability

Table 7
Chromatographic data obtained at pH 3, 7 and 11

Column	pH 3				pH 7				pH 11			
	A_s^a	HETP (μM)	RH (%)	Rk' (%)	A_s^a	HETP (μM)	RH (%)	Rk' (%)	A_s^a	HETP (μM)	RH (%)	Rk' (%)
ZRX	3.3	17.5	5.4	4.7	4.1	17.3	1.7	10.3				
BDS	8.8	20.5	4.4	0.0	5.2	19.9	2.5	3.3				
CHB	5.1	32.6	0.5	4.1	4.7	31.4	1.0	1.9				
ABZ	1.8	21.0	5.7	4.0	2.5	20.7	4.1	3.9				
ASA	3.2	62.0	27.1	6.3	4.4	64.3	11.4	2.0	2.2	64.0	14.9	3.6
ALU					1.3	74.8	14.1	6.1	0.7	73.8	10.6	25.6
POL					1.8	298.3	69.3	9.0	1.4	323.6	89.3	6.2
3MZ	1.6	26.5	13.8	6.8	1.4	25.2	8.9	3.9	1.0	24.7	4.9	7.7

[a] Average values of compounds 2, 10, 19, 26 and 29.

Table 8
Pareto optimal (PO) points at pH 3, 7 and 11

Column	PO points at pH 3			PO points at pH 7			PO points at pH 11			PO points all pH values		
Column	A_s-HETP	A_s-RH	A_s-Rk'	A_s-HETP	A_s-RH	A_s-Rk'	A_s-HETP	A_s-RH	A_s-Rk'	A_s-HETP	A_s-RH	A_s-Rk'
ZRX	**	*		**	*		–	–	–	**	*	
BDS			*				–	–	–			*
CHB		*			*	*	–	–	–		*	
ABZ	**	*	*	**	*		–	–	–	**	*	
ASA						*			*			
ALU	–	–	–	**	*	*	**	*	*	**	*	*
POL	–	–	–						*			
3MZ	**	*	*	**	*	*	**	*	*	**	*	*

– = Not tested. **PO points are considered to be more important than *PO points.
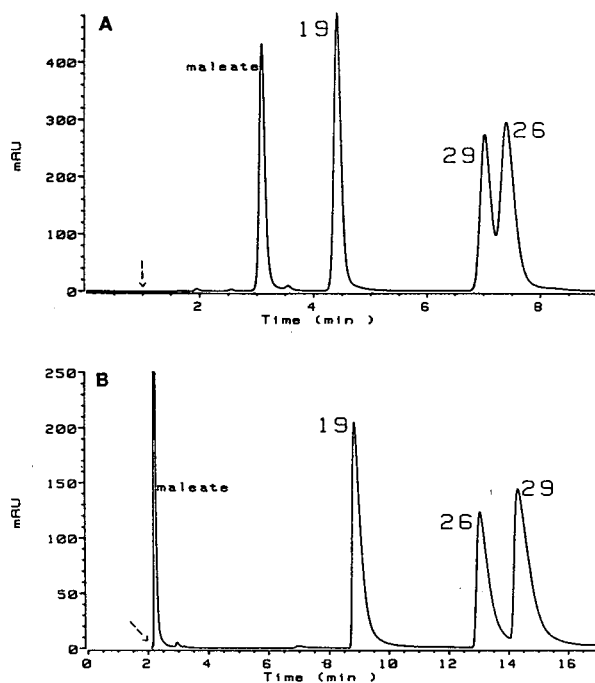
Fig. 6. LC–UV chromatograms of compounds 19, 26 and 29. Detection was done at UV 210 nm. The arrow in the chromatograms indicates the dead time. (A) A 2-μl volume from a 1 mg/ml solution was injected onto a Supelcosil LC-ABZ 150 × 4.6 mm I.D. column. The flow-rate was set to 1.0 ml/min and the eluent used was methanol–25 mM NaH$_2$PO$_4$ pH 3.0 (40:60, v/v). (B) A 2-μl volume from a 1 mg/ml solution was injected onto a Zorbax Rx-C18 250 × 4.6 mm I.D. column. The flow-rate was set to 1.0 ml/min and the eluent used was methanol–25 mM NaH$_2$PO$_4$ pH 3.0 (45:55, v/v).
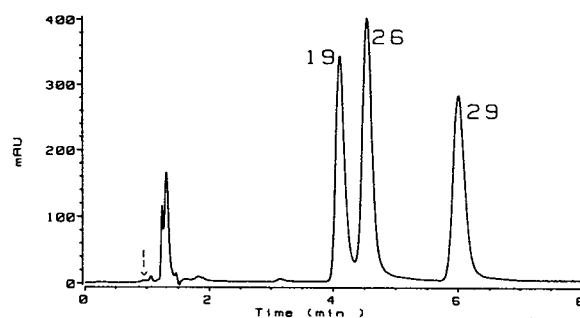
Fig. 7. LC–UV chromatogram of compounds 19, 26 and 29. A 2-μl volume from a 1 mg/ml solution was injected onto a 3MZ-18 150 × 4.6 mm I.D. column. The flow-rate was set to 1.0 ml/min and the eluent used was acetonitrile–25 mM borate pH 11.0 (45:55, v/v). Detection was done by UV at 210 nm. The arrow in the chromatogram indicates the dead time.

of the capacity factor" are contradictory to each other, while there is a high correlation between "plate height" and "repeatability of the plate height". For the optimal columns these chromatographic factors must be as low as possible, preferably in the opposite direction of the arrows in Fig. 5. The best columns are clustered together in the upper right quadrant of the figure. Also from this graph, taking the "asymmetry" and "plate height" as the most important factors, it can be concluded that the 3MZ is the most optimal column, although the differences with three other columns are small. An advantage of
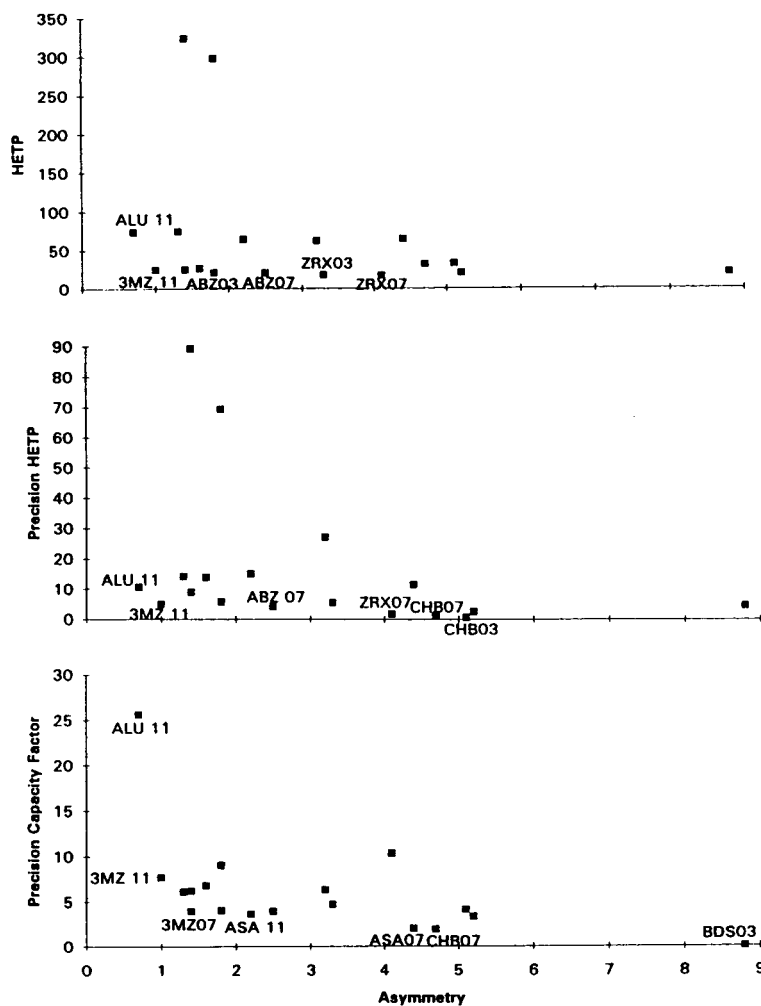
Fig. 8. Stacked PO plot of the asymmetry vs. HETP, precision of the HETP and precision of the capacity factor, obtained at pH values 3, 7 and 11. Only the PO points are indicated by giving the column abbreviation together with the pH used.

the bi-plot is that all information can be seen in one graph, while this is not the case for the bar charts and the MCDM plots. However, one has to realize that with the bi-plot information is lost, that the interpretation is sometimes difficult and that all factors are treated as being of the same importance.

3.4. Testing of columns at pH 3, 7 and 11

An overview of the results at pH values of 3, 7

and 11 is given in Table 7. Again from the original data the correlation between the capacity factors and the asymmetries was so low that the capacity factor was excluded as a factor. From the correlation matrices at pH 3 and 11 again surprisingly high correlations of 0.82 and 1.00, respectively, were found between the plate height and the repeatability of the plate height, as was also observed in the previous section at a pH of 7 (see Table 5).

Because at pH of 3 and 11 less columns were used than at the pH of 7, the interpretation is
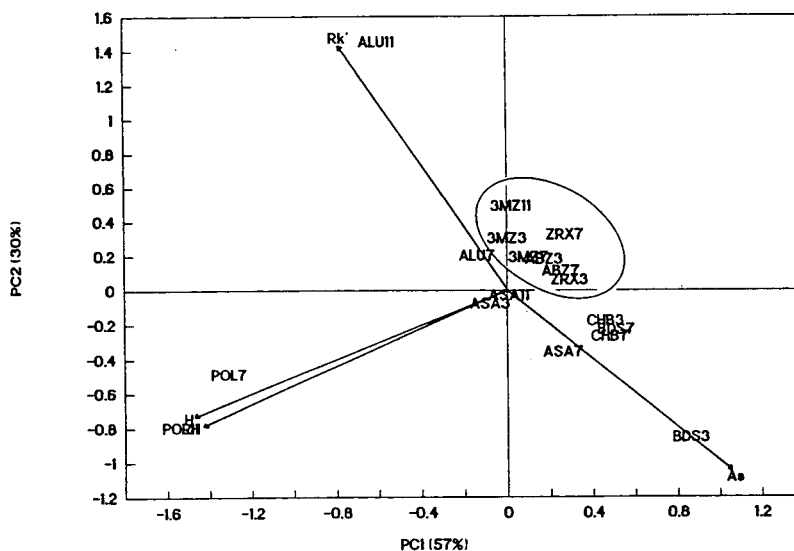
Fig. 9. Bi-plot of the data obtained at all pH values. The data used for the bi-plot are the values given in Table 7.

easier. The PO points were determined and are given in Table 8. At a pH of 3 the 3MZ column again shows the lowest tailing, although the difference with the ABZ column is very small. Even more, with the ABZ column a smaller plate height and a better repeatability is obtained. With the ZRX column a further (small) improvement in efficiency is obtained while the other factors are worse. In Fig. 6 chromatograms of compounds 19, 26 and 29 on the ABZ (Fig. 6A) and ZRX column (Fig. 6B) at pH 3 are shown. With the ABZ column the results at pH 3 are better than at pH 7.

At pH 11, both the ALU and 3MZ columns show good characteristics. However, with the ALU column fronting peaks were observed at this pH (Table 7). Also the plate height is in favour of the 3MZ column. Clearly, at pH 11 the 3MZ column is a good choice for analyzing basic solutes. This is confirmed by the repeatability data. In Fig. 7 a chromatogram of compounds 19, 26 and 29 on the 3MZ column at pH 11 is shown.

The ultimate goal of course is to select the best column operating at its optimal pH, although in practice there can be reasons to select on forehand a certain pH. In Table 8 the PO points

at all pH values are given. The results are also presented graphically in Fig. 8. On basis of this MCDM plot the user can decide which column to use by weighing the importance of the different chromatographic factors. Overall the 3MZ column seems to give the best results of the columns tested. Looking at the individual data for this column (Table 7), operating at pH 11 is preferred at which very symmetrical peaks and acceptable plate heights are obtained. A bi-plot of the overall results is given in Fig. 9. For this the results of Table 7 are used and the data are autoscaled. The first two PCs explain 88% of the variance. A cluster of optimal columns is encircled. The 3MZ column shows better asymmetry values while the ZRX and ABZ columns show a better repeatability of the capacity factor. This latter factor, however, is only a qualitative factor while the asymmetry values are quite accurately determined. With respect to the efficiency and the repeatability of the efficiency the columns are equally good. It is interesting to see that at the different pH values for some columns, e.g. the 3MZ, ZRX and ABZ column, only small differences while for other columns, e.g. the ALU and BDS column, large differences were observed.

4. Conclusions

The selection of a set of test compounds out of a larger set with PCA was carried out. Using a test set of only five compounds, information about the applicability of stationary phases developed for the analysis of basic compounds was obtained. A complete column test requires only two LC analyses using two mobile phases for the analysis of 3 and 2 test compounds. Each analysis consists of a duplicate injection and the testing is repeated on the next day.

Using bar charts and several chemometrical techniques such as bi-plots and MCDM, differences between stationary phases in their applicability for the analysis of basic solutes were successfully made. The advantage of the MCDM plots is that the factors involved can be visually weighed in order to select a column. The bi-plots are more difficult to interpret. An interesting conclusion from the results is that the columns with a high efficiency generally show a good repeatability for the plate height.

A column consisting of zirconium oxide particles coated with polybutadiene proved to be suitable at all pH values tested. The best results with this column were obtained at pH 11. However, one has to realize that at this moment too limited information is available on the ruggedness of the column. This requires specific testing on this aspect. Furthermore, the high price of this column is a limiting factor. At pH 3 a Supelcosil LC-ABZ and a Zorbax Rx-C_{18} column showed also promising results. Polymer-based columns showed inferior results because of the high plate heights obtained.

References

[1] R.J.M. Vervoort, F.A. Maris and H. Hindriks, *J. Chromatogr.*, 623 (1992) 207.
[2] M. Stadalius, J. Berus and L. Snyder, *LC·GC*, 6 (1988) 494.
[3] R. Majors, *LC·GC*, 10 (1992) 188.
[4] D.L. Massart, B.G.M. Vandeginste, S.N. Deming, Y. Michotte and L. Kaufman, *Chemometrics: a Textbook*, Elsevier, Amsterdam, 1988.
[5] G. Windhorst, J. Kelder and J.P. de Kleijn, *J. Planar Chromatogr.*, 3 (1990) 300.
[6] G. Musumarra, G. Scarlata, G. Romano, G. Cappello, S. Clementi and G. Giulietti, *J. Anal. Toxicol.*, 11 (1987) 154.
[7] M.F. Delaney, A.N. Papas and M.J. Walters, *J. Chromatogr.*, 410 (1987) 31.
[8] S.J. Schmitz, H. Zwanziger and H. Engelhardt, *J. Chromatogr.*, 544 (1991) 381.
[9] J.H. de Boer, A.K. Smilde and D.A. Doornbos, *Acta Pharm. Technol.*, 34 (1988) 140.
[10] A.K. Smilde, A. Knevelman and P.M.J. Coenegracht, *J. Chromatogr.*, 369 (1986) 1.
[11] M.M.W.B Hendriks, J.H. de Boer, A.K. Smilde and D.A. Doornbos, *Chemom. Intell. Lab. Syst.*, 16 (1992) 175.
[12] H.R. Keller and D.L. Massart, *Trends Anal. Chem.*, 9 (1990) 251.
[13] K.R. Gabriel, *Biometrika*, 58 (1971) 453.
[14] J. Foley and J. Dorsey, *Anal. Chem.*, 55 (1983) 730.
[15] J.H. de Boer, *Ph.D. Thesis*, University of Groningen, Groningen, 1992.

Chromatographic separation of 1-phenyl-3-methyl-5-pyrazolone-derivatized neutral, acidic and basic aldoses

Daniel J. Strydom

Center for Biochemical and Biophysical Sciences and Medicine and Department of Pathology, Harvard Medical School, 250 Longwood Avenue, Boston, MA 02115, USA

Abstract

Analysis, by HPLC, of reducing monosaccharides as their 1-phenyl-3-methyl-5-pyrazolone derivatives is attractive owing to its sensitivity of detection and the generation of single derivatives of each aldose molecule [Honda et al., *Anal. Biochem.* 180 (1989) 351]. The present studies establish conditions for reversed-phase chromatographic analyses of hydrolysates containing neutral, basic and acidic reducing monosaccharides. In particular, glucuronic and galacturonic acids, glucosamine and galactosamine are separated completely both from one another and from the aldoses of glycoproteins commonly found. Analyses of blank hydrolysates provide the baseline for background amounts of these carbohydrates and analyses of a variety of glycoproteins illustrate the effectiveness of these separations. Elution times were established for derivatives of all tetroses, pentoses and hexoses, as well as a variety of deoxy and phosphorylated aldoses.

1. Introduction

The state of glycosylation can have a major influence on the structure and biological activity of proteins [1,2]. The carbohydrate moieties participate in such functions as compartmentalization, transport and excretion, cell–cell communication and protein folding. The importance of proteoglycans is also increasingly apparent [3]. Analytical examination of the sugar content of peptides and proteins is therefore a fundamental requirement for research on and production of glycoproteins.

Typically, sugar compositional analyses are performed by ion-exchange chromatography of hydrolyzed sugars at high pH and with direct detection using electrochemical detectors (e.g. [4]) or through post-column reactions [5,6], or alternately by reversed-phase chromatographic analyses of variously derivatized sugars, derivatized e.g. with reagents such as dabsyl- and fluorenylmethoxycarbonyl hydrazines [7,8], phenylisothiocyanate [9] or benzoylation reagents [10]. The ion-exchange techniques require more specialized equipment than the pre-column derivatization methods, while the latter in many cases yield multiple peaks for each sugar [11,12]. Honda et al. [12] developed 1-phenyl-3-methyl-5-pyrazolone (PMP) as a pre-column derivatization reagent which yields highly absorbent single derivatives in good yield. The methodology has found use in other laboratories [13–15], but the

generation and separation of PMP derivatives of the commonly found free-amino sugars and uronic acids has not yet been described.

We describe here a chromatographic analysis of the neutral, acidic and basic reducing sugars which are found in hydrolysates of glycoproteins and proteoglycans.

2. Experimental

2.1. Materials

Ovalbumin was obtained from Pharmacia Biotech (Piscataway, NJ, USA), phósvitin and actin from Sigma (St. Louis, MO, USA) and a recombinant angiotensin-converting enzyme mutant was a gift of Dr. M.R.W. Ehlers. The various sugars were from Sigma, except for galactose (Fisher Scientific, Pittsburgh, PA, USA) and ribose (Nutritional Biochemical, Cleveland, OH, USA). PMP was from Aldrich (Milwaukee, WI, USA) and was recrystallized from methanol [13] (m.p. 127–128.5°C) before use.

2.2. Hydrolysis of glycoproteins

The samples (100–1000 pmol) were dried into 50 × 6 mm glass test tubes which had been cleaned by pyrolysis in a muffle furnace at 500°C for 18 h. Trifluoroacetic acid (200 μl, 2 M) was added into each tube and the tubes placed in a hydrolysis vial (PicoTag; Millipore, Milford, MA, USA), briefly evacuated, sealed and placed at 110°C for the required time. Hydrolysates were dried under vacuum in 2-ml conical glass tubes, ready for derivatization.

2.3. Derivatization with PMP

Dry samples were derivatized [12] with 10 μl PMP (0.5 M in methanol) and 10 μl 0.3 M sodium hydroxide at 70°C for 30 min. The derivatives were neutralized with 3.5 μl of 1 M HCl, dried, redissolved in 50 μl water and excess reagent extracted twice with 200 μl chloroform.

The aqueous layer was analyzed directly by HPLC.

2.4. Chromatography

Chromatographic conditions were generally as follows: column, NovaPak 30 × 0.39 cm (Millipore); temperature, 26°C; solvent A, 0.4% triethylamine (pH 4.86 with phosphoric acid) + 10% acetonitrile in water; solvent B, acetonitrile–water (60:40); gradient, 10–14% B in 9 min, 14–64% B in a further 21 min at 1 ml/min flow-rate. The eluate was monitored at 254 nm.

3. Results and discussion

3.1. Hydrolysis and derivatization

Hydrolysis of simple carbohydrate chains was essentially complete after 2 h of hydrolysis at 110°C, with only a slight increase in the yields of amino sugars at 4 h. The hydrolysis of ATP/ADP to ribose was slower and required a minimum of 4 h hydrolysis.

Derivatization by the procedure of Honda et al. [12] proceeded smoothly, when care was taken to ensure that the aqueous phase had been fully neutralized prior to extraction with chloroform. At high pH the extractions were inefficient and significant amounts (>50%) of the PMP-sugars were also extracted. Attempts to use ethyl acetate [16] as extractant were unsuccessful owing to excessive losses of the PMP-sugars.

The derivatization of the uronic acids and the free amino sugars also proceeded well with single peaks appearing during HPLC analyses of the reaction mixtures. The peak areas (color yields) for equal amounts of most PMP-sugars were within 10% of their average value, with glucuronate deviating the most with a color yield which was 27% low (Table 1). The derivatives are stable for a day at room temperature and in solution, which allowed convenient overnight HPLC analyses. The most labile derivatives in the group, that decrease in apparent yield over periods of days, are those of glucose, glucosamine, glucuronic acid and galactosamine.

Table 1
Relative color yields of PMP-sugars, reported as average ±
standard deviation

PMP-sugar	Relative color yield fresh standards (n = 15)	Relative color yield decayed standards (n = 5)
Mannose	1.10 ± 0.04	0.98 ± 0.17
Glucosamine	0.89 ± 0.16	0.41 ± 0.18
Lyxose	1.07 ± 0.03	1.14 ± 0.10
Ribose	0.95 ± 0.03	1.07 ± 0.11
Galactosamine	1.21 ± 0.17	0.71 ± 0.22
Glucuronate	0.73 ± 0.04	0.57 ± 0.12
Galacturonate	1.03 ± 0.06	1.12 ± 0.23
Glucose	0.86 ± 0.07	0.71 ± 0.09
Galactose	0.98 ± 0.05	0.90 ± 0.10
Xylose	1.08 ± 0.10	1.09 ± 0.10
Fucose	0.94 ± 0.08	0.99 ± 0.10

3.2. Separation of standard PMP-sugars

Initial experiments showed that a large, broad reagent peak eluted early during chromatography and could be moved relative to the PMP-sugars by changes in slope of the acetonitrile gradient or by varying the initial acetonitrile concentration. Higher acetonitrile concentrations eluted the reagent peak in very close proximity to the PMP-sugars. The chromatographic system was therefore designed to provide a large separation of reagent and the earliest eluting PMP-sugar, PMP-mannose. A very flat initial gradient proved essential to this aim. A second linear gradient provided separation of most of the other neutral compounds of interest. A separation of the common neutral, acidic and basic PMP-sugars is presented in Fig. 1. The broad reagent peak separates very well from all the PMP-sugars, and good separation was achieved for derivatives of mannose, glucosamine, lyxose, ribose, galactosamine, glucuronic acid, galacturonic acid, glucose, galactose, xylose and fucose, all of which elute as very sharp peaks.

Since good yields of PMP-glucosamine and -galactosamine were obtained using both standard compounds and glycoprotein hydrolysates, the separation was designed for hydrolysis mixtures which would obviously contain free amino sugars and not N-acetyl amino sugars, and which
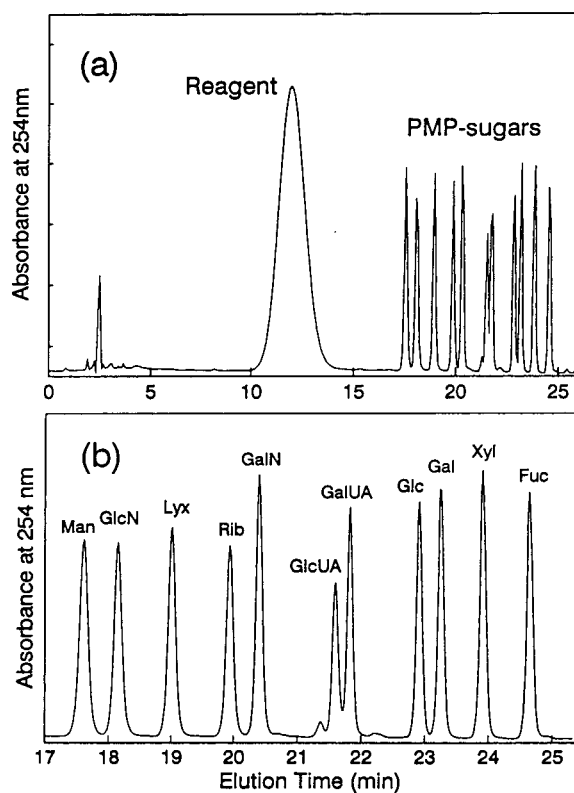
Fig. 1. Chromatography of PMP derivatives of common reducing monosaccharides. (a) Separation of the remaining reagent (broad peak) from the PMP derivatives (sharp peaks). (b) An expanded region of the chromatogram in (a): the PMP derivatives of the common neutral, basic and acidic reducing monosaccharides. Man = Mannose; GlcN = glucosamine; Lyx = lyxose; Rib = ribose; GalN = galactosamine; GlcUA = glucuronic acid; GalUA = galacturonic acid; Glc = glucose; Gal = galactose; Xyl = xylose; Fuc = fucose.

are more amenable to chromatographic manipulation. Fig. 2 shows the variation of elution times of the uronic acids and amino sugars as a function of pH. Values of pH from 4.5 to 5.3 allowed PMP-glucosamine to elute between PMP-mannose and PMP-lyxose, while PMP-galactosamine eluted between PMP-ribose and PMP-glucuronic acid. Higher pH values altered the relative elution of the charged sugars much more than that of the others. The neutral sugars show highest resolution in the tested range at pH 6.9, although the amino sugars then elute in inconvenient positions. At this pH PMP-arabin-
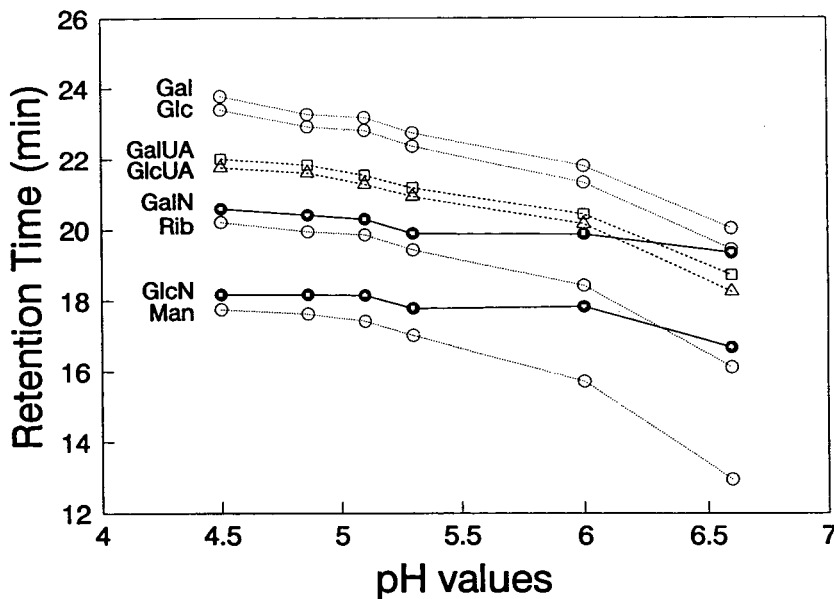
Fig. 2. Chromatographic elution times of PMP-sugars at different pH values of the eluent.

ose separates from PMP-xylose, eluting slightly later.

3.3. Separation of less common PMP-aldoses

The other hexoses, pentoses, tetroses, glyceraldehyde and some deoxy and phosphorylated sugars were derivatized and chromatographed as above. Many separated from the common sugars and their elution positions are indicated in Fig. 3. The deoxy sugars eluted later than their parent compounds, as expected for their higher hydrophobicity, while the phospho sugars eluted earlier, in accord with their higher hydrophilicity.

The elution order of the various enantiomorphic pairs of aldotetroses, -pentoses and -hexoses appears to depend on the orientation of the hydroxyl groups in positions 2 and 3. A *cis*-orientation correlates with early elution and a *trans*-orientation with late elution. This causes the slowest eluting of the 2,3-*cis* enantiomorphs of tetroses, pentoses and hexoses —PMP-erythrose— to elute before the earliest of the *trans* enantiomorphs, PMP-idose.

In addition hydrolysates of heparin and alginic

acid were analyzed to examine the potential of the method for proteoglycans. In the former case a large variety of fragments were seen, presumably sulfated products, but glucuronic acid and glucosamine were clearly identified. The expected products from hydrolysis of alginic acid are mannuronic and guluronic acids and two major peaks were found to elute between the positions of mannose and gulose. Ascorbate reacted with PMP and yielded two products which eluted very early, preceding and superimposed on the reagent peak.

3.4. Adventitious contamination by sugars

The background contribution of sugars arising during the hydrolysis process could become a problem when sensitive analytical methodologies such as the PMP method are used to estimate amounts of sugar in relatively small amounts of glycoprotein, or when a protein is examined for a potential short-chain carbohydrate modification. This contamination may be serious and is inherent in the hydrolysis acid, as well as being introduced from the environment. Table 2 records the amounts of the neutral aldoses found
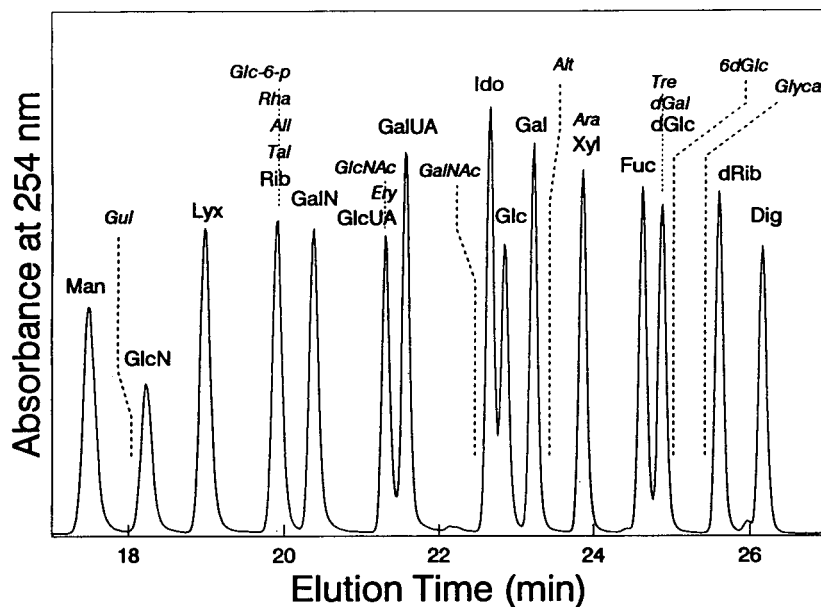
Fig. 3. Chromatography of PMP-sugars. Fifteen well resolved compounds are shown, with the elution positions of other derivatives indicated. Gul = Gulose; Glc-6-p = glucose-6-phosphate; Rha = rhamnose; All = Allose; Tal = Tallose; GlcNAc = N-acetylglucosamine; Ery = erythrose; GalNAc = N-acetylgalactosamine; Ido = idose; Alt = Altrose; Ara = arabinose; Tre = threose; d = deoxy; Glyca = glyceraldehyde; Dig = digitoxose; other abbreviations as in Fig. 1.

in hydrolysis blanks done singly over a period of time. Glucose and xylose are particularly problematic and contents of unknown samples should therefore be interpreted with caution when < 100 pmol of protein is analyzed. Reaction blanks, without hydrolysates, give very clean

Table 2
Analysis of sugars in hydrolysis blanks

Sugar	Average amount ± S.D. (pmol), n = 27	Range (pmol)
Mannose	13.6 ± 12.5	0–53.2
Glucose	74.0 ± 46.4	12.8–200.8
Galactose	9.5 ± 5.3	3.1–21.8
Xylose	43.7 ± 34.7	0–136.1
Fucose	4.0 ± 4.8	0–17.1

Blanks were made by adding 200 μl 2 M trifluoroacetic acid into clean test tubes inside hydrolysis vials and hydrolyzing together with batches of samples. Derivatization with PMP was done as described under Experimental and the derivatives were analyzed by reversed-phase HPLC

chromatograms with values of < 2 pmol on average for everything except for glucose, for which it is < 4 pmol.

The amounts of amino sugars and uronic acids in the hydrolysis blanks were as negligible as in the reaction blanks.

3.5. Applications to glycoproteins

A variety of glycoproteins were analyzed by the chromatographic methodology outlined above. The results are summarized in Table 3. Identification and quantitation correlated well with the literature values for ovalbumin and phosvitin. Actin preparations contain a mole of either ATP or ADP which yield ribose on acid hydrolysis. The analysis of a recombinant mutant of angiotensin converting enzyme demonstrates the ease with which the variety of carbohydrate residues in such a heavily glycosylated protein can be determined.

The accurate analysis of amounts of less than 100 pmol glycoprotein becomes difficult owing to

Table 3
Analysis of the sugar residues of glycoproteins by chromatography of PMP derivatives

Sugar	ACE[a] mutant	Phosvitin	Ovalbumin	Actin
Mannose	14.8	3.45 (3 [18])	5.57 (4–6 [19], 6 [20])	0.15
Glucosamine	23.3	5.23 (5 [18])	3.79 (2–5 [19], 3 [20])	0.00
Galactosamine	6.5	0.10	0.03	0.04
Glucose	1.5	0.65	0.30	0.99
Galactose	28.2	3.46 (3 [18])	0.36 (0–1 [19])	0.10
Xylose	0.5	0.36	0.16	0.16
Fucose	5.9	0.12	0.13	0.03
Glucuronic acid	0.0	0.03	0.04	0.04
Galacturonic acid	0.0	0.01	0.03	0.01
Ribose	0.4	0.17	0.07	0.44 (1)
Amount hydrolyzed (pmol)	95.2	543	1116	486

Proteins were hydrolyzed with 2 M trifluoroacetic acid for 4 h at 110°C. Values are reported as molar ratios recovered. Literature values are in parentheses.
[a] Angiotensin converting enzyme.

the prevalent background of especially glucose, seen both in blank samples and also as an additional background in protein preparations. This has also been noted in analyses done by anion-exchange chromatography with electrochemical detection [4].

4. Conclusions

The determination of the monosaccharide content of glycoproteins provides basic information, much as amino acid analyses provide a characteristic property of a protein. We have established a robust reversed-phase HPLC separation of stable derivatives of reducing sugars which allows convenient analysis of carbohydrate compositions using conventional HPLC equipment. It has already proved useful in studying the glycosylation state of angiotensin-converting enzyme [14]. Analysis of qualitatively unknown samples may occasionally provide derivatives other than the common ones. A recent example is the discovery of gulose in an algal glycoprotein [17]. The use of the high-resolution separation, which is very robust in the pH range from 4.9 to 5.3, allows such derivatives to be recognized with

ease. The use of a second eluent system, with a different pH (such as 6.9) will clearly differentiate sugars such as gulose or arabinose from the common sugars.

References

[1] A. Kobata, Eur. J. Biochem., 209 (1992) 483.
[2] H. Lis and N. Sharon, Eur. J. Biochem., 218 (1993) 1.
[3] E. Ruoslahti and Y. Yamaguchi, Cell, 64 (1991) 867.
[4] M.R. Hardy, R.R. Townsend and Y.C. Lee, Anal. Biochem., 170 (1988) 54.
[5] S. Honda, T. Konishi, S. Suzuki, M. Takahashi, K. Kakehi and S. Ganno, Anal. Biochem., 134 (1983) 483.

[6] N. Kiba, K. Shitara and M. Furusawa, *J. Chromatogr.*, 463 (1989) 183.

[7] K. Muramoto, R. Goto and H. Kamiya, *Anal. Biochem.*, 162 (1987) 435.

[8] R.-E. Zhang, Y.-L. Cao and M.W. Hearn, *Anal. Biochem.*, 195 (1991) 160.

[9] M.J. Spiro and R.G. Spiro, *Anal. Biochem.*, 204 (1992) 152.

[10] N. Jentoft, *Anal. Biochem.*, 148 (1985) 424.

[11] E.Y.J. Kang, R.D. Coleman, H.J. Pownall, A.M. Gotto, Jr. and C.-Y. Yang, *J. Protein Chem.*, 9 (1990) 31.

[12] S. Honda, E. Akao, S. Suzuki, M. Okuda, K. Kakehi and J. Nakamura, *Anal. Biochem.*, 180 (1989) 351.

[13] D.H. Hawke, K.L. Hsi, L.R. Zieske, L. Chen and P.M. Yuan, in R.H. Angeletti (Editor), *Techniques in Protein Chemistry III*, Academic Press, San Diego, CA, 1992, p. 315.

[14] M.R.W. Ehlers, Y.-N.P. Chen and J.F. Riordan, *Biochem. Biophys. Res. Commun.*, 183 (1992) 199.

[15] Y.-T. Hsu, S.Y.C. Wong, G.J. Connell and R.S. Molday, *Biochim. Biophys. Acta*, 1145 (1993) 85.

[16] S. Honda, T. Ueno and K. Kakehi, *J. Chromatogr.*, 608 (1992) 289.

[17] R. Mengele and M. Sumper, *FEBS Lett.*, 298 (1992) 14.

[18] R. Shainkin and G.E. Perlmann, *Arch. Biochem. Biophys.*, 145 (1971) 693.

[19] H. Iwase, Y. Kato and K. Hotta, *J. Biol. Chem.*, 256 (1981) 5638.

[20] Y.C. Lee and R. Montgomery, *Arch. Biochem. Biophys.*, 95 (1961) 263.

Immobilized metal-ion affinity partitioning of NAD^+-dependent dehydrogenases in poly(ethylene glycol)–dextran two-phase systems[☆]

Henrikas Pesliakas*, Vilius Žutautas, Birutė Baškevičiūtė

Department of Research, Institute of Biotechnology "Fermentas", Graičiūno 8, Vilnius 2028, Lithuania

Abstract

Affinity partitioning of yeast alcohol dehydrogenase (YADH), lactate dehydrogenase from rabbit muscle (MLDH) and lactate and malate dehydrogenases from pig heart (HLDH and HMDH, respectively) were studied in aqueous two-phase systems containing metal ions (Cu^{2+}, Ni^{2+}, Zn^{2+} and Cd^{2+}) chelated by iminodiacetate-poly(ethylene glycol) (IDA–PEG). The partitioning behaviour of the enzymes in the presence of Cu(II)–IDA–PEG was studied as a function of the concentration of NaCl, the pH of the medium and the concentration of added selected agents. It was demonstrated that the partition effect ($\Delta \log K$) of dehydrogenases in the presence of Cu(II)–IDA–PEG and the affinity of enzymes for immobilized Cu^{2+} ions increases in the order MLDH > YADH > HMDH ≥ HLDH. It was shown that the determined variations in the enzyme affinities for Cu(II)–IDA–PEG might be related to the differences in the content of histidine residues accessible to the solvent.

1. Introduction

Immobilized metal ion affinity chromatography (IMAC) of proteins was introduced by Porath et al. [1]. The basic principle of this method is the coordination between transition metal ions chelated by iminodiacetic acid (IDA) and electron-donor groups on the protein surface. Surface-exposed histidine, cysteine and tryptophan residues have attracted attention as the primary sites responsible for protein interac-

tions with immobilized metal ions [1–4]. More recent studies have demonstrated that of the amino acids, the available histidyl residues in terms of their topography on the macromolecule surface seem to be the critical factor dictating the selective retention on metal-affinity columns [4–10].

Immobilized metal ion affinity partitioning has been developed recently to enhance the selective partitioning of proteins in aqueous two-phase systems [11]. The method is based on the interactions between accessible amino acid residues on the protein surface and transition metal ions charged on IDA–poly(ethylene glycol) (PEG). The partitioning behaviour of native [12–16], genetically engineered proteins carrying high-

---

* Corresponding author.
☆ Presented at the *8th International Conference on Partitioning in Aqueous Two-Phase Systems, Leipzig, August 22–27, 1993*.

affinity His–X_3–His sites engineered into their surface [16–19], erythrocytes [20] and iso-enzymes of lactate dehydrogenase [21] has been studied in aqueous PEG–salt and PEG–dextran two-phase systems. Interactions between Cu(II)–IDA–PEG and surface-exposed histidines in aqueous two-phase systems have also been explored theoretically [13].

Recently [22,23], affinity partitioning has been used to study the interaction of many NAD(H)-dependent dehydrogenases with immobilized Cu(II) complexes of dye ligands. It was found that the Cu^{2+} ions had a discriminating ability to affect the specificity of dye–enzyme complex formation between the yeast and horse liver ADH on the one hand, and LDH from rabbit muscle on the other. In this respect, it was of interest to evaluate the binding properties of these enzymes towards Cu^{2+} and other metal ions charged on chelating ligands such as IDA, excluding the dye ligand effect.

2. Experimental

2.1. Materials

Yeast alcohol dehydrogenase (EC 1.1.1.1, specific activity ca. 400 U/mg) was obtained from Boehringer (Mannheim, Germany). Lactate dehydrogenase from rabbit muscle (EC 1.1.1.27, specific activity ca. 650 U/mg) was purchased from Serva (Heidelberg, Germany). Lactate dehydrogenase from pig heart (EC 1.1.1.27, specific activity ca. 300 U/mg) and malate dehydrogenase from pig heart (EC 1.1.1.37, specific activity ca. 1100 U/mg) were kindly provided by T. Bodneva, Institute of Biotechnology. Substrates and substances for Good's buffers —MES (morpholinoethanesulfonic acid), HEPES (N - 2 - hydroxyethylpiperazine - N' - 2 - ethanesulfonic acid) and TAPS [N- tris(hydroxymethyl)methyl - 3 - aminopropanesulfonic acid]— were obtained from Serva or Sigma (St. Louis, MO, USA). Poly(ethylene glycol) PEG 6000 was obtained from Serva or Fluka (Basle, Switzerland) and dextran 60 000

from the Factory of Clinical Preparations (Krasnojarsk, Russian Federation). Iminodiacetic acid (IDA) and epichlorohydrin were obtained from Fluka. All other chemicals were commercially available and of analytical-reagent or puriss grade.

2.2. Synthesis of IDA–PEG derivatives

IDA–PEG was synthesized in two steps by reaction of iminodiacetic acid with a monosubstituted derivative of epichlorohydrin-activated PEG. Epichlorohydrin-activated PEG was prepared according to the usual method for the synthesis of glycidyl ethers as described by Ulbrich et al. [24]. Briefly, 100 g of PEG 6000 (M_r 6000–7500) were dissolved in 500 ml of absolute benzene, then 5 ml of boron trifluoride ethyl etherate and 1.32 ml of epichlorohydrin (0.5 mol/mol PEG) were added dropwise and the reaction mixture was stored at room temperature for 48 h. Thereafter the mixture was gently stirred and 1.2 ml of a 45% solution of NaOH was slowly added dropwise and the solution was again stored at room temperature for 2 h. The reaction mixture was decanted, treated with 500 ml of diethyl ether and the precipitate was filtered off and dried. The product was dissolved in 200–300 ml of absolute benzene, precipitated repeatedly with 500 ml of diethyl ether and dried.

A 50-g amount of the product obtained was dissolved in 250 ml of 2 M Na_2CO_3 solution containing 25 g of iminodiacetic acid and the mixture was stirred at 65°C for 24 h. After the mixture had been cooled, the product was extracted with 750–1000 ml of chloroform. The chloroform phases were pooled, dried over anhydrous Na_2SO_4 and the solvent was removed by rotary evaporation. After two crystallizations in absolute ethanol, the IDA–PEG derivative was obtained (the yield was 25–30% of total PEG).

The Cu(II) complex of IDA–PEG was obtained by dissolving 25 g of IDA–PEG in 25 ml of 50 mM sodium acetate buffer (pH 4.0) containing 12.5 g of Cu_2SO_4. The solution was stirred at room temperature for 1 h and then

extracted twice with 100–150 ml of chloroform. The combined chloroform phases were dried and the solvent was evaporated. The yield of Cu(II)–IDA–PEG was 15–20 g. Other metal ion (Ni^{2+}, Zn^{2+} and Cd^{2+}) IDA–PEG complexes were obtained in a similar manner using a 10 molar excess of appropriate metal salts over IDA–PEG.

The metal ion concentration in the metal chelate–PEG derivatives was measured by atomic absorption spectrometry.

2.3. Enzyme assays

The enzyme activities were determined spectrophotometrically at 340 nm and 30°C. Alcohol dehydrogenase and both lactate dehydrogenases were determined as described previously [22,23]. The activity of malate dehydrogenase was measured as described [25].

2.4. Two-phase systems

Two-phase systems (4 g) were prepared by weighing from stock solutions of polymers in water, viz., 20–50% (w/w) PEG and 20–30% (w/w) dextran. The final concentrations of PEG and dextran in the aqueous two-phase systems were 6.5% (w/w) PEG 6000–10% (w/w) dextran 60 000. All necessary ingredients, buffer, water, enzyme samples and selected agents, were mixed with polymer solutions to give the desired final concentrations as indicated in the tables. IMA partitioning experiments were performed by replacing part of PEG with IDA–PEG or metal ion complexes with IDA–PEG. The amount of IDA–PEG derivative is given as a percentage of the total mass of PEG present in the system or expressed as metal ion concentration (mM/kg) per kg of two-phase system.

2.5. Partitioning of enzymes

After 17–24 units of YADH, 4–12 units of MLDH, 30–43 units of HLDH or 20–47 units of

HMDH has been introduced into the two-phase systems, the mixture obtained was shaken gently for about 15 s, kept for 5 min and then centrifuged for about 2 min at 2000 g to complete the phase separation. Samples of known volume were withdrawn from each phase and the enzyme activity was determined. The partition coefficient of the enzyme, K, was defined as the ratio of the enzyme concentration in the upper and lower phases. The affinities of enzymes for metal ions were expressed in terms of $\Delta \log K$, defined as the difference between the logarithmic partition coefficients of enzymes in the presence (K) and in the absence (K_0) of metal–IDA–PEG ($\Delta \log K = \log K - \log K_0$). The change in the enzyme partition coefficients when selected agents were introduced into the two-phase systems was expressed as a percentage of the initial value of $\Delta \log K$ in the presence of metal–IDA–PEG and the absence of the agent.

All partitioning experiments were carried out in duplicate at room temperature and the value of $\Delta \log K$ is given as the mean of two separate determinations.

3. Results

3.1. Synthesis of IDA–PEG derivatives

The commonly used method for coupling IDA to PEG includes a three-step synthesis starting from monomethoxy-PEG [14]. The intermediate aminomonomethoxy-PEG derivative was treated with bromoacetic acid, yielding IDA–PEG. In an attempt to obtain a water-soluble chelating polymer carrying iminodiacetate groups coupled to the polymer in a similar manner to the synthesis of the well known Porath's adsorbent on Sepharose [2], another route to IDA–PEG synthesis was chosen. PEG was activated with a stoichiometric amount of epichlorohydrin to obtain the monosubstituted derivative, which was subsequently treated with the IDA according to Porath and Olin [2].

The metal ion contents combined with IDA–PEG are given in Table 1.

Table 1
Contents of metal ions combined with IDA–PEG

Metal ion	Metal ion content (mol/mol PEG)[a]
Cu^{2+}	0.43–0.58
Ni^{2+}	0.19–0.32
Zn^{2+}	0.09–0.13
Cd^{2+}	0.20–0.30

[a] The metal ion content in IDA–PEG is expressed as moles of the respective metal ion per mole of PEG.

3.2. Partitioning of dehydrogenases as a function of salt concentration and metal ions

In the two-phase system containing 6.5% (w/w) PEG and 10% (w/w) dextran, in the absence of the IDA–PEG derivative all the dehydrogenases studied were partitioned in favour of the dextran-rich bottom phase. The partitioning behaviour of any enzyme introduced into a system containing an increasing concentration of metal ions, e.g., Cu^{2+} ions chelated by IDA–PEG, was greatly changed. This may be exemplified by the YADH partitioning data. As can be seen from Table 2 and Fig. 1, the presence of Cu^{2+} ions in two-phase system dramatically enhances the extraction of enzyme into the metal–IDA–PEG-containing upper phase. Less extraction of YADH occurs in the presence of Ni^{2+} ions and PEG–IDA with no metal ion seems to have a negligible effect on the partitioning of the enzyme even when 5% of a portion of PEG was replaced with PEG–IDA.

Table 2
Effect of liganded PEG on the partitioning of yeast ADH

Liganded PEG	$\Delta \log K$
IDA–PEG	0.41
Ni(II)–IDA–PEG	0.72
Cu(II)–IDA–PEG	2.30

Two-phase system (4 g) contained 6.5% (w/w) PEG 6000, 10% (w/w) dextran 60 000, 17–24 units of enzyme, 5% liganded PEG and 10 mM MES buffer (pH 6.5). The amount of liganded PEG is expressed as a percentage of the total mass of PEG present in the system.
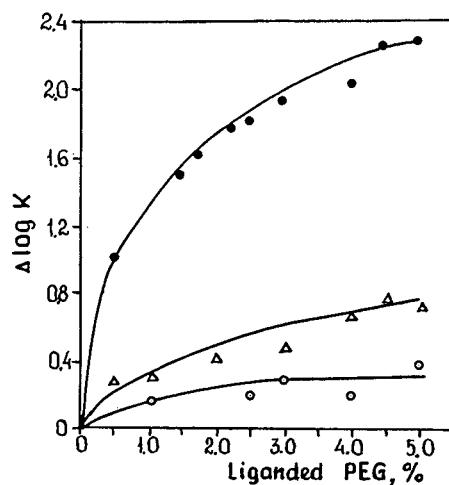
Fig. 1. Partitioning of yeast ADH in PEG–dextran systems containing increasing amounts of liganded PEG. Two-phase system (4 g) contained 6.5% (w/w) PEG 6000, 10% (w/w) dextran 60 000, 17–24 units of enzyme and 10 mM MES buffer (pH 6.5). The amount of liganded PEG is given as a percentage of the total mass of PEG in the system. ● = Cu(II)–IDA–PEG; △ = Ni(II)–IDA–PEG; ○ = IDA–PEG.

Addition of NaCl and an increase in its concentration in the two-phase systems to 0.6–1.0 M had different effects on the partitioning of the dehydrogenases studied. As can be seen from Table 3 and Fig. 2, NaCl greatly affects the partitioning of MDH and LDH from pig heart. An increase in NaCl concentration in the system to 0.6 M in the presence of Cu(II)–IDA–PEG caused an increase in the $\Delta \log K$ value of HMDH from 0.89 (in the absence of NaCl) to 1.32 (at 0.3 M NaCl). However, with HLDH an increase in NaCl concentration to 0.6 M gave a decrease in $\Delta \log K$ of the enzyme from 1.30 (in the absence of salt) to 0.41–0.56 (with 0.2–0.4 M NaCl), suppressing its binding to Cu(II)–IDA–PEG. This means that in addition to the coordination, another type of bonding, probably electrostatic, is involved in the interaction of HLDH with Cu(II)–IDA–PEG. Only the part of the $\Delta \log K$ value equal to 0.41–0.56 may be attributed to the contribution of coordination bonds. On the basis of this effect of NaCl, all further experiments on HMDH partitioning were carried out in the presence of 0.25 M NaCl, and with HLDH NaCl was omitted. Introduction of

Table 3
Effect of NaCl concentration on the partitioning of MDH and LDH from pig heart in the presence of Cu(II)–IDA–PEG

NaCl (M)	Δ log K	
	HMDH	HLDH
–	0.89	1.30
0.1	1.15	0.50
0.2	1.15	0.41
0.3	1.32	0.50
0.4	1.05	0.56
0.5	1.09	0.54
0.6	1.08	0.44

Two-phase systems (4 g) were composed of PEG and dextran as in Table 2, 10 mM HEPES buffer (pH 7.0), 22–34 units of enzyme and increasing concentration of NaCl. The Cu(II)–IDA–PEG concentration in the system is expressed as the concentration of Cu^{2+} ions per kg of two-phase system and was equal to 0.21 and 0.42 mM/kg for HMDH and HLDH, respectively.

NaCl at concentrations up to 1.0 M into the systems containing MLDH in the presence of Cu(II)–IDA–PEG had no appreciable effect on the partitioning of the enzyme, whereas with
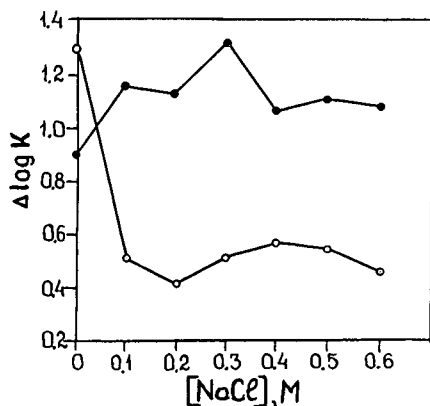
Fig. 2. Effect of NaCl concentration on the partitioning of MDH and LDH from pig heart in the presence of Cu(II)–IDA–PEG. Two-phase systems (4 g) were composed of PEG and dextran as in Fig. 1, 10 mM HEPES buffer (pH 7.0), 22–34 units of enzyme and increasing concentrations of NaCl. The Cu(II)–IDA–PEG concentration in the system is expressed as the concentration of Cu^{2+} ions in mM per kg of two-phase system and was equal to 0.21 and 0.42 mM/kg for HMDH and HLDH, respectively. ● = HMDH; ○ = HLDH.

YADH there was a slow increase in Δ log K as the NaCl concentration was increased from 0.2 to 0.6 M (see Figs. 5 and 6).

Partitioning of dehydrogenases in the presence of PEG–IDA conjugates combined with various metal ions in summarized in Table 4. According to the results in Table 4, it is evident that Cu^{2+} ions, as would be expected, exhibited the strongest effect on the partitioning of the dehydrogenases studied. Of the other metal ions, only Ni^{2+} ions had an appreciable effect on the affinity partitioning efficiency (Δ log K) of YADH and MLDH. The extraction power into the upper phase of dehydrogenases in the presence of Cu(II)–IDA–PEG differed significantly and revealed differences in the surface properties of the enzymes. For example, a high binding of YADH to Cu(II)–IDA–PEG (Δ log $K = 2.62$) might be expected, based on the predominant contribution of the Cu^{2+} ion coordination bonds previously found [22] in the interaction of this enzyme with Cu(II) complexes of many dye ligands. The possibility of coordination of the Cu^{2+} ions with the histidine residue located at the coenzyme-binding site of YADH was proposed. With LDH from rabbit muscle we observed [23] a smaller contribution of Cu^{2+} ions to the dye–enzyme complex formation. However, as can be seen from Table 4, LDH from rabbit muscle displayed a much stronger binding to Cu(II)–IDA–PEG (Δ log $K = 3.72$) than YADH. This obviously indicated that MLDH possesses surface-exposed amino acid residues available for the interaction with Cu^{2+} ions. A much weaker interaction with Cu(II)–IDA–PEG was found for HMDL (Δ log $K = 1.45$). In contrast to LDH from rabbit muscle, the enzyme from pig heart interacts with Cu^{2+} ions weakly (Δ log $K = 1.33$). The partitioning behaviour of both LDH towards Cu(II) and Ni(II)–IDA–PEG determined in this work agrees very well with the partitioning results of these enzymes obtained recently by Otto and Birkenmeier [21]. Despite the differences in the composition of the aqueous two-phase systems used, the tendency of LDH partitioning in both instances was found to be the same: LDH from rabbit muscle displayed a much stronger binding to Cu(II) and

Table 4
Effect of metal ion chelated by IDA–PEG on the partitioning of different NAD^+-dependent dehydrogenases

Metal ion– IDA–PEG	Concentration of metal ion (mM/kg)	$\Delta \log K$			
		YADH (pH 6.5)	MLDH (pH 7.0)	HLDH (pH 7.0)	HMDH (pH 7.0 with 0.25 M NaCl)
–	–	$K_0 = 0.0043$ ± 0.0011	$K_0 = 0.0089$ ± 0.0004	$K_0 = 0.0124$ ± 0.0005	$K_0 = 0.0898$ ± 0.0090
Cu^{2+}	0.42	2.62 ± 0.04	3.72 ± 0.12	1.33 ± 0.08	1.45 ± 0.028
Ni^{2+}	0.25	1.10 ± 0.10	0.70 ± 0.03	0.32 ± 0.01	0.114 ± 0.035
Zn^{2+}	0.12	n.d.[a]	n.d	0.086 ± 0.026	0.03
Cd^{2+}	0.25	n.d.	n.d.	0.22 ± 0.078	0.10

System composition as in Table 2; 10 mM buffers: HEPES (pH 7.0) and MES (pH 6.5).
[a] n.d. = Not determined.

Ni(II)–IDA–PEG than the enzyme from pig heart. The observed orders of magnitude of the $\Delta \log K$ values of the LDH obtained in this work and that reported by Otto and Birkenmeier [21] are similar: 3.72 and 0.41–0.56 (with 0.2–0.4 M NaCl) in the presence of Cu(II)–IDA–PEG for MLDH and HLDH, respectively, in this work and 4.5 and 0.4 determined by Otto and Birkenmeir [21]. In general, the partitioning behaviour of both types of LDH parallels also the chromatographic behaviour of the LDH isoenzymes from hog on an Ni(II)–nitrilotriacetic acid (NTA) column as determined by Hochuli et al. [26]. They observed the retention of the muscle-

type isoenzyme on the Ni(II)–NTA column and a lack of retention by the heart-type enzyme.

3.3. Effect of pH on affinity partitioning of dehydrogenases

The affinities of all the dehydrogenases studied, except the LDH from pig heart, for Cu(II)–IDA–PEG, and also the MLDH affinity for Ni(II)–IDA–PEG, were found to be sensitive to pH. In the presence of Cu(II)–IDA–PEG the $\Delta \log K$ values of YADH increase monotonically with increase in pH from 5.0 to 8.0, as indicated in Table 5 and Fig. 3. The alteration of

Table 5
Effect of pH on the partitioning of dehydrogenases in the presence of metal–IDA–PEG

pH	$\Delta \log K$		pH	$\Delta \log K$	
	YADH (Cu^{2+})	MLDH (Cu^{2+}; Ni^{2+})		HMDH (Cu^{2+})	HLDH (Cu^{2+})
5.0	1.68	1.60 n.d.[a]	6.0	1.04	1.37
5.5	2.04	2.00 1.24	7.0	1.45	1.33
6.5	2.20	2.79 1.86	8.0	1.74	1.46
7.0	n.d.	3.03 2.30	9.0	1.25	n.d.
7.5	2.30	n.d. n.d.			
8.0	2.38	2.99 2.09			

Two-phase systems (4 g) were composed of PEG and dextran as in Table 2. Concentrations of metal ions: Cu^{2+}, 0.2234 mM/kg for YADH and MLDH and 0.42 mM/kg for HMDH and HLDH; Ni^{2+}, 7.03 mM/kg for MLDH. Two-phase systems contained 10 mM buffers for YADH, MLDH and HLDH and 10 mM buffers with 0.25 M NaCl for HMDH: MES (pH 5.0–6.5), HEPES (pH 7.0) and TAPS (pH 8.0–9.0)
[a] n.d. = Not determined.
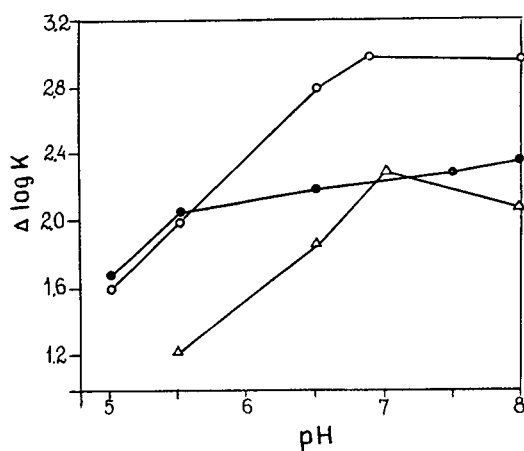
Fig. 3. Effect of pH on the partitioning of yeast ADH in the presence of Cu(II)–IDA–PEG and LDH from rabbit muscle in the presence of Cu(II) and NI(II)–IDA–PEG. Two-phase systems (4 g) were composed of PEG and dextran as in Fig. 1. Concentrations of metal ions: Cu^{2+}, 0.2234 mM/kg; Ni^{2+}, 7.03 mM/kg. 10 mM buffers: MES (pH 5.5–6.5), HEPES (pH 7.0) and TAPS (pH 8.0–9.0). $\bigcirc$ = MLDH (CU^{2+}); $\mathbf{O}$ = YADH (Cu^{2+}); $\triangle$ = MLDH (Ni^{2+}).

the partition coefficients of MLDH, Δ log K, in the presence of immobilized Cu^{2+} or Ni^{2+} ions is highly sensitive to pH, increasing in the pH range 5.0–7.0 and beginning to decrease above pH 7.0 (Table 5, Fig. 3). The dependence of the affinities of MDH and LDH from pig heart for Cu(II)–IDA–PEG on the pH of the medium differs greatly (Table 5, Fig. 4). With HMDH an
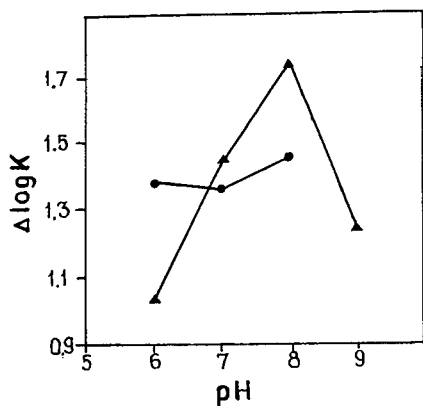
Fig. 4. Effect of pH on the partitioning of LDH and MDH from pig heart in the presence of Cu(II)–IDA–PEG. System composition as in Fig. 3. Concentration of Cu^{2+} ions, 0.42 mM/kg. $\blacktriangle$ = HMDH; $\mathbf{O}$ = HLDH.

increase in pH in the systems from 6.0 to 8.0 caused an increase in Δ log K, followed by a decrease at higher pH. In contrast, the affinity partitioning effect (Δ log K) of HLDH is virtually insensitive to pH variations in the range 6.0–8.0 (Fig. 4).

3.4. Partitioning of dehydrogenases in the presence of selected agents

The interaction of dehydrogenases with chelated Cu^{2+} ions was studied when selected agents such as nucleotide ligands, chelating agents or amino acids were present in the two-phase systems. As can be seen from Table 6 and Figs. 5 and 6, the introduction into the two-phase systems of the chelating agent EDTA at concentrations up to 1 mM was sufficient to abolish the binding of all the dehydrogenases to Cu(II)–IDA–PEG, the Δ log K values decreasing to zero. Imidazole also had a strong ability, but discriminating among the enzymes studied, to reduce their interaction with immobilized Cu^{2+} ions. Table 6 shows that the addition of 1 mM imidazole to the two-phase systems decreased Δ log K to zero with MLDH and HMDH, but was less effective with YADH and HLDH. In the latter two cases, a further increase in imidazole concentration to 5 mM caused a 92% decrease in Δ log K of HLDH, whereas the Δ log K of YADH was decreased only to 48%. Table 6 shows that among the amino acids, tryptophan was the most effective for the dissociation of the HMDH–Cu(II)–IDA complex. A 1 mM concentration of tryptophan could reduce the value of Δ log K by 88%. Low concentrations of arginine (1 mM) resulted in decreases in Δ log K by 96, 74 and 53% for HMDH, HLDH and MLDH, respectively. The observed Δ log K-decreasing capacity of ammonium ion was the same as that of arginine for LMDH and lower for HMDH.

As can be seen from Table 6, cysteine at increasing concentrations in the two-phase systems diminished the binding of HLDH and HMDH to Cu(II)–IDA–PEG but to a smaller extent than imidazole. Nucleotide ligands such as adenine and NAD were able, as was shown

Table 6
Dependence of the affinity partitioning effect ($\Delta \log K$) of dehydrogenases on the concentration of selected agents

Agent	Concentration (mM)	Residual $\Delta \log K$ (%)			
		YADH (pH 6.5)	MLDH (pH 7.0)	HLDH (pH 7.0)	HMDH (pH 8.0 with 0.25 M NaCl)
EDTA	1	0	0 (at 0.5 mM)	0	0
Imidazole	1	71	0	33	0
	5	48	0	8	0
NAD	1	49	n.d.[a]	n.d.	n.d.
	5	34	n.d.	n.d.	n.d.
NADH	1	n.d.	82	80	100[b]
	5	n.d.	71	55	100[b]
Nicotinamide	1	85	n.d.	n.d.	n.d.
	5	72	n.d.	n.d.	n.d.
Adenine	1	86	n.d.	n.d.	n.d.
	5	75	n.d.	n.d.	n.d.
Tryptophan	1	99	n.d.	61	12
	5	95	n.d.	23	0
Ammonium ion	1	n.d.	41	n.d.	59
	5	n.d.	19	n.d.	0
Arginine	1	n.d.	47	26	4
	5	n.d.	14	−12	−5
Cysteine	1	n.d.	n.d.	34	27
	5	n.d.	n.d.	21	16

System composition as in Table 2; 10 mM buffers: HEPES (pH 7.0), MES (pH 6.5) and TAPS (pH 8.0). Concentration of Cu^{2+} ions in the systems: 0.2234 mM/kg for YADH and MLDH, 0.21 mM/kg for HMDH and 0.42 mM/kg for HLDH.
[a] n.d. = Not determined.
[b] Two-phase system without NaCl.
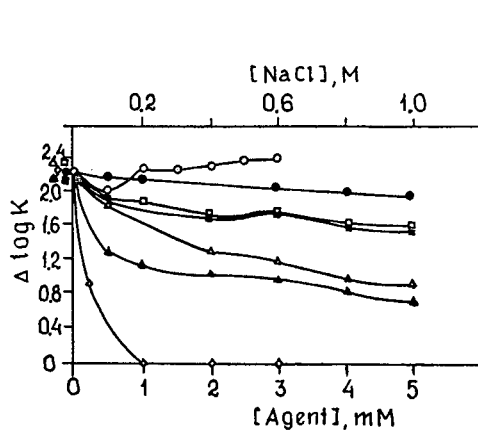
Fig. 5. Partitioning of yeast ADH in the systems containing increasing concentrations of selected agents in the presence of Cu(II)–IDA–PEG. System composition as in Fig. 1. Concentration of Cu^{2+} ions, 0.2234 mM/kg; 10 mM MES buffer (pH 6.5). ○ = NaCl; ● = tryptophan; □ = adenine; ▣ = nicotinamide; △ = imidazole; ▲ = NAD; ◇ = EDTA.
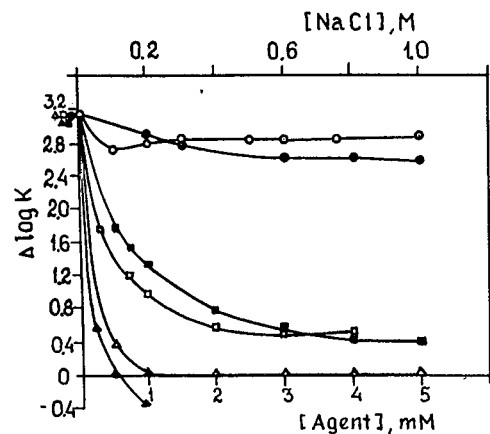
Fig. 6. Partitioning of LDH from rabbit muscle in systems containing increasing concentrations of agents in the presence of Cu(II)–IDA–PEG. System composition as in Fig. 1. Concentration of Cu^{2+} ions, 0.2234 mM/kg; 10 mM HEPES buffer (pH 7.0). ○ = NaCl; ● = NADH; □ = ammonium ions; ▣ = arginine; △ = imidazole; ▲ = EDTA.

previously [27], to elute the enzyme retained on the adsorbent with the immobilized dye–Cu(II) complex. Therefore, they might act as displacing agents causing also the dissociation of the formed Cu(II)–IDA–PEG–enzyme complexes. However, in contrast to the high eluting capacity of adenine observed earlier [27] and its relatively high Δ log K-decreasing capacity, observed previously [22,23] by studying the partitioning of dehydrogenases in the presence of dye–Cu(II) complexes, in this study we found a much smaller effect of adenine on the Δ log K values. Table 6 and Fig. 5 show that even a 5 mM concentration of adenine caused a decrease in Δ log K of YADH in the presence of Cu(II)–IDA–PEG of only 25%. However, unexpectedly, we found a relatively high capability of NAD to reduce YADH binding to Cu^{2+} ions. A 5 mM concentration of NAD decreased Δ log K of YADH by 66% and gave a larger decrease in Δ log K when the same concentration of imidazole was presence in the two-phase system. This indicates that the coenzyme-binding site of YADH might be involved in the interaction with Cu(II)–IDA–PEG. Addition of NADH and an increase in its concentration to 5 mM had an appreciable effect, decreasing Δ log K of HLDH to 55%, whereas Δ log K of MLDH was decreased to 71% and no change in Δ log K was observed with HMDH. Nicotinamide, as can be seen from Table 6, affected the YADH partitioning with respect to the Cu(II)–IDA–PEG in a similar manner to adenine.

4. Discussion

As a continuation of our attempts to explore the role of metal ions on the specific recognition of ligands, e.g., biomimetic dyes by various NAD^+-dependent dehydrogenases, in this study the binding properties of four enzymes towards metal ions chelated by IDA–PEG were evaluated in an aqueous two-phase system composed of PEG and dextran.

The determined variations in the partition coefficients (Δ log K) of dehydrogenases (YADH, MLDH, HLDH and HMDH) studied in the presence of metal ions, primarily Cu^{2+}, immobilized on IDA–PEG clearly indicated (Table 4) the presence of and differences in the accessibility of metal-binding sites on the surface of the enzymes. Further, it was found that the interactions of many dehydrogenases with Cu(II)–IDA–PEG show a pronounced dependence on the pH of the medium. The determined increase in the Δ log K values of enzymes with increase in pH (Table 5) may be related, as has been indicated previously [18], to deprotonation of the imidazole group. Therefore, the differences in the partitioning behaviour of the dehydrogenases studied in the presence of Cu(II)–IDA–PEG could be due to the possible involvement in the interaction with metal ions of histidyl residues of enzymes exposed to the solvent. The dependence of metal affinity on histidine content, with the existence of a linear proportionality between the increase in partition coefficients and the protein surface histidine content, was clearly shown recently [16,18] by studying the partitioning of native and genetically engineered histidine-containing proteins in a PEG–dextran two-phase system containing Cu(II)–IDA–PEG. Despite the lack of complete information concerning the location and number of surface-exposed histidine residues in the dehydrogenases studied, some discussion is possible.

It is well known that the dehydrogenases studied differ in the number of histidine residues available for chemical modification by diethyl pyrocarbonate. As the latter reacts with all accessible histidines in proteins, the maximum number of histidine residues modified in dehydrogenases can be regarded, to a first approximation, as a relative measure defining the partitioning efficiency (Δ log K) of an enzyme in the presence of Cu(II)–IDA–PEG. The numbers of histidine residues per subunit of enzymes studied were found to be ten for YADH [28], eleven for MLDH [21], seven for HLDH [26] and thirteen per molecule of HMDH [29]. According to the literature, the maximum numbers of histidine residues modified per enzyme subunit were three (pH 6.0) for LDH from rabbit muscle [30], 2.5 (pH 7.0) for yeast ADH [31] and one (pH 6.0) for LDH from pig heart [32]. The number of

essential histidine residues for these three enzymes was established as one per enzyme subunit [31]. For MDH from pig heart, one essential histidine residue chemically alkylated with iodo-acetamide per active site was found [29].

Taking these considerations into account, one can observe that the dehydrogenase affinity to Cu(II)–IDA–PEG (Table 4) increases according to the number of histidine residues accessible for chemical modification with diethyl pyrocarbonate in the following order: MLDH > YADH > HMDH ⩾ HLDH. Therefore, one of the possible ways to explore the location of the histidine residues that are involved at the interaction of the studied dehydrogenases with Cu^{2+} ions would be to carry out investigations with chemically modified enzymes. However, despite this, the data presented here demonstrated that immobilized metal ion affinity partitioning in aqueous two-phase systems can be used as a sensitive probe for metal-binding sites on the surface of NAD^+ dehydrogenases.

Acknowledgement

References

[1] J. Porath, J. Carlsson, I. Olsson and G. Belfrage, *Nature*, 258 (1975) 598–599.
[2] J. Porath and B. Olin, *Biochemistry*, 22 (1983) 1621–1630.
[3] J. Porath, in H. Tschesche (Editor), *Modern Methods in Protein Chemistry*, Vol. 2, Walter de Gruyter, Berlin, 1985, p. 85.
[4] J. Porath, *Trends Anal. Chem.*, 7 (1988) 254–259.
[5] E. Sulkowski, *Trends Biotechnol.*, 3 (1985) 1–7.
[6] E.S. Hemdan, Y.J. Zhao, E. Sulkowski and J. Porath, *Proc. Natl. Acad. Sci. U.S.A.*, 86 (1989) 1811–1815.
[7] T.T. Yip, Y. Nakagawa and J. Porath, *Anal. Biochem.*, 183 (1989) 159–171.

[8] M. Belew and J. Porath, *J. Chromatogr.*, 516 (1990) 333–354.
[9] Y.J. Zhao, E. Sulkowski and J. Porath, *Eur. J. Biochem.*, 202 (1991) 1115–1119.
[10] L. Andersson, E. Sulkowski and J. Porath, *Bioseparation*, 2 (1991) 15–22.
[11] G.E. Wuenschell, E. Naranjo and F.H. Arnold, *Bioprocess Eng.*, 5 (1990) 199–202.
[12] S.D. Plankett and F.H. Arnold, *Biotechnol. Tech.*, 4 (1990) 45–48.
[13] S.S. Suh and F.H. Arnold, *Biotechnol. Bioeng.*, 35 (1990) 682–690.
[14] G. Birkenmeier, M.A. Vijayalakshmi, T. Stigbrand and G. Kopperschläger, *J. Chromatogr.*, 539 (1991) 267–277.
[15] B.H. Chung and F.H. Arnold, *Biotechnol. Lett.*, 13 (1991) 615–620.
[16] F.H. Arnold, *Bio/Technology*, 9 (1991) 151–156.
[17] S.S. Suh, B.L. Haymore and F.H. Arnold, *Protein Eng.*, 4 (1991) 301–305.
[18] R.J. Todd, M.E. Van Dam, D. Casimiro, B.L. Haymore and F.H. Arnold, *Proteins Struct. Function Genet.*, 10 (1991) 156–161.
[19] F.H. Arnold and B.L. Haymore, *Science*, 252 (1991) 1796–1797.
[20] H.G. Botros, G. Birkenmeier, A. Otto, G. Kopperschläger and M.A. Vijayalakshmi, *Biochim. Biophys. Acta*, 1074 (1991) 69–73.
[21] A. Otto and G. Birkenmeier, *J. Chromatogr.*, 644 (1993) 25–33.
[22] J.-H.J. Pesliakas, V.D. Žutautas and A.A. Glemža, *Chromatographia*, 26 (1988) 85–90.
[23] V. Žutautas, B. Baškevičiūtė and H. Pesliakas, *J. Chromatogr.*, 606 (1992) 55–64.
[24] V. Ulbrich, J. Makeš and M. Mareček, *Collect. Czech. Chem. Commun.*, 29 (1964) 1466–1475.
[25] L.A. Decker (Editor). *Worthington Enzyme Manual*, Worthington Biochemical, Freehold, NJ, 1977, pp. 23–24.
[26] E. Hochuli, H. Döbeli and A. Schacher, *J. Chromatogr.*, 411 (1987) 177–184.
[27] S.S. Flaksaité, O.F. Sūdžiuviené, J.-H.J. Pesliakas and A.A. Glemža, *Biokhimiya*, 52 (1987) 73–81.
[28] H. Jörnvall, *Eur. J. Biochem.*, 72 (1977) 425–442.
[29] B.H. Anderton, *Eur. J. Biochem.*, 15 (1970) 562–567.
[30] C. Huc, A. Olomucki, Lè-Thi-Lan, D.B. Pho and N. van Thoai, *Eur. J. Biochem.*, 21 (1971) 161–169.
[31] M. Hennecke and B.V. Plapp, *Biochemistry*, 22 (1983) 3721–3728.
[32] J.J. Holbrook and V.A. Ingram, *Biochem. J.*, 131 (1973) 729–738.

ELSEVIER

Fast protein liquid chromatographic purification of poly(ADP–ribose) polymerase and separation of ADP–ribose polymers

Phyllis L. Panzeter, Barbara Zweifel, Felix R. Althaus*

Institute of Pharmacology and Toxicology, University of Zürich–Tierspital, Winterthurerstrasse 260, CH-8057 Zurich, Switzerland

(First received March 14th, 1994; revised manuscript received May 26th, 1994)

Abstract

Poly(ADP–ribose) polymerase responds to DNA strand breaks in nuclei by producing ADP–ribose polymers covalently attached to proteins. Here we report two fast protein liquid chromatographic applications to aid investigations on poly(ADP–ribosyl)ation. The first rapidly purifies poly(ADP–ribose) polymerase from crude calf thymus extract. The purification protocol, involving successive fractionations over four columns, reduces the time for polymerase purification from four days to 14 h resulting in a > 50% increase in enzyme-specific activity. The second application employs a complex salt gradient to reproducibly separate ADP–ribose polymers into individual size classes.

1. Introduction

Poly(ADP–ribosyl)ation is required for repair of DNA breaks in higher eukaryotes [1–3]. Poly(ADP–ribose) polymerase (EC 2.4.2.30) is dependent on DNA strand breaks for activation [4], and activation in turn leads to modification of polymerase molecules with long polymers of ADP–ribose (automodification). Through non-covalent interactions with histones [5–7], these polymers disrupt DNA–histone complexes making the DNA accessible to DNA processing enzymes [8,9]. Degradation of ADP–ribose polymers by poly(ADP–ribose) glycohydrolase restores the integrity of the DNA–histone complex. Polymer size and structure play an important role in this histone shuttle mechanism,

influencing both polymer affinity for chromatinic proteins [6] and polymer degradation kinetics [10,11]. We therefore found it necessary to prepare ADP–ribose polymers of distinct sizes to further elucidate the histone shuttle of chromatin.

We have established two fast protein liquid chromatographic (FPLC; Pharmacia) applications to aid our investigations. (1) Because purification of poly(ADP–ribose) polymerase requires successive fractionation of a calf thymus crude extract over four different chromatography resins [12–14], conventional chromatography techniques take at least four days before the pure enzyme is obtained. Strategic programming and continuous flow from column to column using FPLC reduced purification time to 14 h thereby yielding more active enzyme faster. (2) Separation of ADP–ribose polymers into indi-

---

* Corresponding author.

vidual size classes has recently been achieved using HPLC [15]. We have found that high-resolution separation of polymers by FPLC using a MonoQ column is highly reproducible and can process large quantities of polymers with recoveries of $98 \pm 7\%$.

2. Materials and methods

2.1. Poly(ADP–ribose) polymerase purification

Preparation of calf thymus crude extract

Frozen calf thymus (50 g) was homogenized in 250 ml of 50 mM Tris, 0.3 M NaCl, 10% glycerol, 10 mM β-mercaptoethanol (β-ME), 50 mM Na$_2$S$_2$O$_5$, pH 8.0. After centrifugation at 12 000 g for 15 min at 4°C, the supernatant was precipitated with 30% (NH$_4$)$_2$SO$_4$, centrifuged,

and reprecipitated with 70% (NH$_4$)$_2$SO$_4$. The resulting pellet was resuspended in 10 ml basis buffer (100 mM Tris–HCl, 17% glycerol, 25 mM K$_2$S$_2$O$_5$, 12 mM β-ME, 0.5 mM EDTA) and loaded into a 50-ml Superloop (Pharmacia).

Columns and FPLC configuration

DNA-cellulose (Pharmacia) was nicked [16] and packed in an HR 10/30 column (Pharmacia). 3-Aminobenzamide was cross-linked to AffiGel 10 (Bio-Rad) and packed in an HR 10/30 column. A 0.2-ml volume of hydroxyapatite (HTP Bio-Gel; Bio-Rad) was prepared fresh for each purification and packed in a 10-ml EconoColumn (Bio-Rad). FPLC (with LCC-500 Plus controller; Pharmacia) connections to columns, valves and buffers are schematically shown in Fig. 1. The system was run at 4°C; the flow-rate was maintained at 0.4 ml/min. For
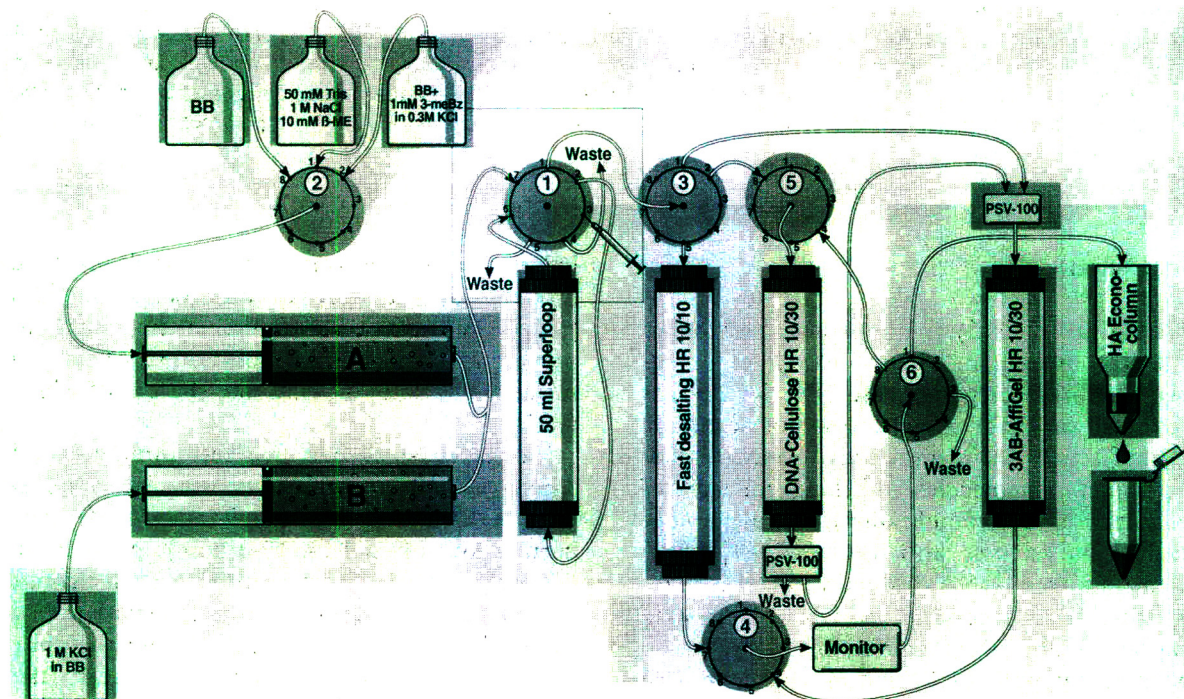
Fig. 1. Schematic diagram of FPLC system for purification of poly(ADP–ribose) polymerase. Purification of poly(ADP–ribose) polymerase from calf thymus crude extract requires successive fractionation over Sephadex G-25, DNA–cellulose, 3-aminobenzamide–AffiGel and hydroxyapatite columns. Using the basic FPLC system with strategic programming of the valves (1–6), the time needed for polymerase purification was reduced from four days to 14 h. 3-meBz = 3-Methoxybenzamide.

further details, a copy of the run program is available on request.

Enzyme activity assay

The specific activity of poly(ADP–ribose) polymerase was calculated from the amount of NAD^+-derived ADP–ribose incorporated into acid-precipitable material. A 10-μl volume of the solution to be assayed was added to 50 mM Tris (pH 8.0), 1 mM dithiothreitol, 10 mM $MgCl_2$, 2 μg nicked calf thymus DNA [16], 2 μg H1 (Boehringer Mannheim) and 10 μM [^{3}H]NAD$^+$ (45 Ci/mol; New England Nuclear) in a final volume of 100 μl. After incubation at 25°C for 10 min, samples were precipitated with 20% trichloroacetic acid, applied to glass fiber filters, washed with 5% trichloroacetic acid, and counted for radioactivity.

2.2. Separation of ADP–ribose polymers

Polymer synthesis and purification

Protein-attached polymers of [^{32}P]ADP–ribose were synthesized in a 9-ml reaction mix containing 3 mg of crude poly(ADP–ribose) polymerase (430 pmol/min mg), 50 mM Tris (pH 8.0), 1 mM dithiothreitol, 10 mM $MgCl_2$, 100 μg nicked calf thymus DNA [16], 225 μg H1, 9.6% ethanol and 1 mM [^{32}P]NAD$^+$ (10 Ci/mol; New England Nuclear). After 30 min at 25°C, protein-attached polymers were precipitated with 20% trichloroacetic acid, dissolved in 98% formic acid, and reprecipitated with trichloroacetic acid.

Each pellet was resuspended in 1 ml of 1 M KOH/50 mM EDTA and incubated at 37°C for 2 h to detach [^{32}P]poly(ADP–ribose) from protein. Conditions were adjusted to pH 8 and 50 mM $MgCl_2$ whereupon DNA was digested with 1000 U of DNase I (Sigma) for 2 h at 37°C. Proteins were subsequently digested with 200 U of proteinase K (Boehringer Mannheim) at 37°C overnight. After extraction with an equal volume of phenol–CHCl$_3$–isoamyl alcohol (49:49:2), [^{32}P]poly(ADP–ribose) was precipitated with ethanol and dried in a Speed-Vac concentrator. The polymers of [^{32}P]ADP–ribose were dissolved in water and stored at −20°C.

Columns and FPLC configuration

A 1-ml MonoQ column (Pharmacia) was used at a flow-rate of 0.4 ml/min; 0.4-ml fractions were collected. Gradient buffer A contained 20 mM Tris, pH 8.3, and buffer B consisted of 1 M KCl in buffer A. The system was run at 4°C.

High-resolution size analysis of polymers

Fractions from FPLC separation were counted for ^{32}P content. Aliquots containing 100 dpm from each peak fraction were dried, dissolved in 10 μl of loading buffer and separated on a polyacrylamide gel as previously described [17].

3. Results and discussion

Strategic design and programming of FPLC and reproducible high resolution from FPLC columns have allowed us to not only rapidly purify the nuclear enzyme poly(ADP–ribose) polymerase but also to resolve its polymeric ADP–ribose products. The significant attributes of each application are discussed below.

3.1. Poly(ADP–ribose) polymerase purification

Purification of poly(ADP–ribose) polymerase requires successive fractionation of a crude extract over four chromatography resins, three of which are affinity resins. Previous purification protocols required many technical manipulations in a cold room over a period of four days. Using FPLC, we have completely automated the column chromatography fractionations such that the technician need only perform a preparative ammonium sulfate precipitation and load the crude extract onto the FPLC. The new procedure yields pure poly(ADP–ribose) polymerase in only 14 h.

The FPLC setup is schematically shown in Fig. 1. Notable variations from usual setups include the use of a valve (valve 2) for selection of elution buffers, a valve before the UV monitor (valve 4) to select which eluent to monitor, and the use of PSV-100 valves to direct flow to/from columns. The FPLC system itself resides in a

cold room and is connected serially to the computer driver in a nearby office. Once the crude extract is loaded onto the FPLC system, all FPLC manipulations and monitoring of results are done at the computer station.

After preparation of the crude extract (see Materials and methods), the sample containing 200–300 mg of protein is loaded into the Superloop and the FPLC program initiated. Protein is desalted and automatically loaded onto nicked DNA–cellulose. Poly(ADP–ribose) polymerase binds with high affinity to DNA nicks [18] and is subsequently eluted with a 0.2–1 M KCl linear gradient in basis buffer. The polymerase elutes in a sharp peak at about 0.8 M KCl and is shunted directly to a 3-aminobenzamide AffiGel column. After four column washes, the enzyme is competitively eluted from the AffiGel resin with basis buffer containing 0.3 M KCl/1 mM 3-methoxybenzamide and is concentrated and washed on a 0.2-ml pad of hydroxyapatite. Elution of poly(ADP–ribose) polymerase from hydroxyapatite is performed manually with two 250-μl aliquots of basis buffer containing 0.5 M potassium phosphate, pH 7.2.

A comparison of purification parameters from the conventional procedure versus FPLC is given in Table 1. While the overall yields are comparable, a 53% increase in enzyme-specific activity was obtained using FPLC mainly due to the decreased processing time. Like the conventional preparation, FPLC-purified poly(ADP–ribose) polymerase contains no detectable DNA topoisomerase activity and is electrophoretically pure (Fig. 2).

Table 1
Purification of poly(ADP-ribose) polymerase from calf thymus using conventional chromatography versus FPLC

	Conventional chromatography	FPLC
Protein recovery (%)	5.2	5.8
Specific activity (nmol/min mg)	378	578
Purification (x-fold)	1026	1399
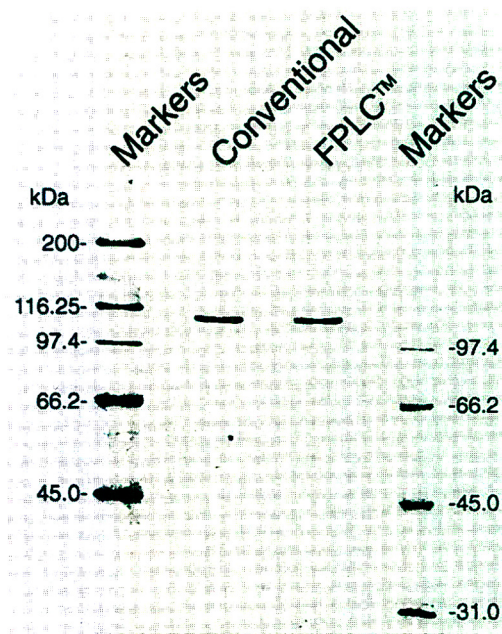
Fig. 2. Gel analysis of purified poly(ADP–ribose) polymerase. A 1-μg amount of protein prepared by conventional chromatography techniques or FPLC was separated on a 10% sodium dodecyl sulphate–polyacrylamide gel [20] and stained with Coommassie Blue. Markers with molecular masses (kDa = kilodalton) as indicated were loaded in the first and last lanes.

3.2. Separation of ADP–ribose polymers

Poly(ADP–ribose) polymerase synthesizes polymers of NAD$^+$-derived ADP–ribose, the sizes of which respond to the protein environment at the time of synthesis [19]. It has been difficult to further analyze the specific role of discrete polymer sizes since homogeneous polymer size classes could not be isolated. We have overcome this obstacle using FPLC.

After synthesis and detachment from protein (see Materials and methods), 50–100 nmol of [^{32}P]ADP–ribose in the form of polymers were injected in 0.5 ml of buffer A onto a 1-ml MonoQ column. The polymers were eluted with a KCl gradient (caption to Fig. 3) and fractions collected. A typical elution profile is shown in Fig. 3. As polymer size increases, the elution
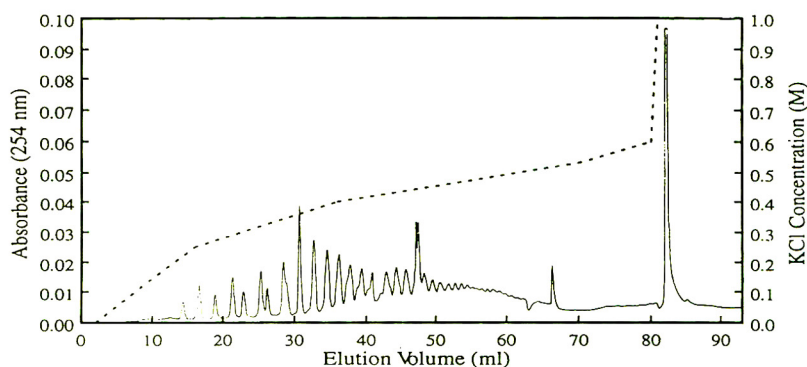
Fig. 3. Separation of ADP–ribose polymers by FPLC. Polymers of ADP–ribose in a total volume of 0.5 ml were injected onto a 1-ml MonoQ column. Absorbance (solid line) was monitored continuously during elution with a KCl gradient (broken line). The gradient program used was: 0% buffer B at 0 ml, 0% B at 2 ml, 25% B at 16 ml, 40% B at 36 ml, 53% B at 70 ml, 60% B at 80 ml, and 100% B at 81 ml (see also Materials and methods).
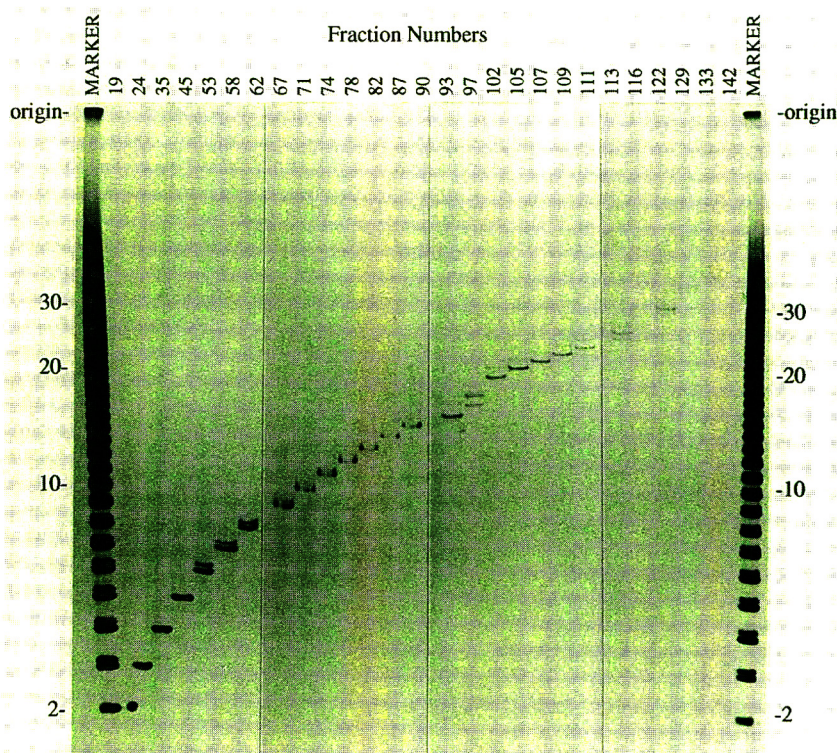
Fig. 4. Poly(ADP–ribose) size analysis following FPLC separation. A heterogeneous population of [^{32}P]ADP–ribose polymers (MARKER) was separated on a 1-ml MonoQ column and fractions collected (see Materials and methods). Aliquots containing 100 dpm of [^{32}P]poly(ADP–ribose) were analyzed on high-resolution polyacrylamide gels and subjected to autoradiography [17]. The lengths of the polymers in terms of ADP–ribose residues are indicated to the left and right of the autoradiograph.

gradient becomes more shallow to maximize resolution. Aliquots from peak fractions were analyzed by autoradiography of high-resolution polymer gels [17]. Fig. 4 shows that the MonoQ resin easily resolved polymers ranging from 2–24 ADP–ribose units and resolved polymers ranging from 26–50 ADP–ribose residues by units of 2–4. In addition, polymers eluting in 1 M KCl did not migrate upon electrophoretic analysis (not shown) and therefore may represent branched polymers [6,15]. Overall recovery of radioactivity from the MonoQ was always >90%.

Recently, Kiehlbauch et al. [15] have reported the separation of polymers on a Progel-TSK DEAE NPR HPLC column. While separation of polymers using HPLC was comparable to FPLC, they cited potential problems with reproducibility dependent on the HPLC system used. Supplied as a standard system, FPLC eliminates such variabilities. Also unlike HPLC, FPLC lends itself to the scale-up of analytical chromatography separations for preparative purposes. The MonoQ column used for this study has an ionic capacity of 0.27–0.37 mmol which is equivalent to 75–100 mg of ADP–ribose. Separation can be easily scaled up to a 20-ml column which could separate up to 2 g of ADP–ribose polymers. This becomes an important aspect for polymer preparation when one considers that, in a heterogeneous polymer population, a single size class of polymers represents only one of at least 50 size classes, and the longer the polymer, the less frequent its occurrence [17]. For these reasons, we recommend FPLC for the large-scale preparation of homogeneous ADP–ribose polymer populations as well as for poly(ADP–ribose) polymerase purification.

Acknowledgements

References

[1] F.R. Althaus and C. Richter, Mol. Biol. Biochem. Biophys., 37 (1987) 1.
[2] J.E. Cleaver and W.F. Morgan, Mutation Res., 257 (1991) 1.
[3] M.S. Satoh and T. Lindahl, Nature, 356 (1992) 356.
[4] R.C. Benjamin and D.M. Gill, J. Biol. Chem., 255 (1980) 10502.
[5] J. Wesierska-Gadek and G. Sauermann, Eur. J. Biochem., 173 (1988) 675.
[6] P.L. Panzeter, C.A. Realini and F.R. Althaus, Biochemistry, 31 (1992) 1379.
[7] P.L. Panzeter, B. Zweifel, M. Malanga, S.H. Waser, M.C. Richard and F.R. Althaus, J. Biol. Chem., 268 (1993) 17662.
[8] C.A. Realini and F.R. Althaus, J. Biol. Chem., 267 (1992) 18858.
[9] F.R. Althaus, J. Cell Sci., 102 (1992) 663.
[10] K. Hatakeyama, Y. Nemoto, K. Ueda and O. Hayaishi, J. Biol. Chem., 261 (1986) 14902.
[11] S.A. Braun, P.L. Panzeter, M.A. Collinge and F.R. Althaus, Eur. J. Biochem., 220 (1994) 369.
[12] S. Ito, Y. Shizuta and O. Hayaishi, J. Biol. Chem., 254 (1979) 3647.
[13] S.G. Carter and N.A. Berger, Biochemistry, 21 (1982) 5475.
[14] B. Kofler, E. Wallraff, H. Herzog, R. Schneider, B. Auer and M. Schweiger, Biochem. J., 293 (1993) 275.
[15] C.C. Kiehlbauch, N. Aboul-Ela, E.L. Jacobson, D.P. Ringer and M.K. Jacobson, Anal. Biochem., 208 (1993) 26.
[16] L.A. Loeb, J. Biol. Chem., 244 (1969) 1672.
[17] P.L. Panzeter and F.R. Althaus, Nucl. Acids Res., 18 (1990) 2194.
[18] J. Ménissier-de Murcia, M. Molinete, G. Gradwohl, F. Simonin and G. de Murcia, J. Mol. Biol., 210 (1989) 229.
[19] H. Naegeli and F.R. Althaus, J. Biol. Chem., 266 (1991) 10596.
[20] U.K. Laemmli, Nature, 227 (1970) 680.

Reversed-phase separation of ionic organoborate clusters by high-performance liquid chromatography

Sven Harfst, Detlef Moller, Hartmut Ketz, Jens Rösler, Detlef Gabel*

Department of Chemistry, University of Bremen, P.O. Box 330 440, D-28334 Bremen, Germany

(First received December 8th, 1993; revised manuscript received April 28th, 1994)

Abstract

Chromatographic separation on reversed-phase materials was carried out for mercaptoundecahydrododecaborate ($B_{12}H_{11}SH^{2-}$) and derivatives with organic residues attached to the sulfur. Solvent and ion-pair systems are described that allow the separation of compounds with greatly different structures. Gradient systems of ion-pair reagents with methanol could be used to separate compounds with greatly different degrees of hydrophobicity. A gradient system was developed in which $B_{12}H_{11}SH^{2-}$-substituted porphyrins and other polar and non-polar porphyrins could be separated.

1. Introduction

The preparation of boron-containing compounds for use in boron neutron capture therapy has received increased interest in recent years [1]. For compounds to be of use in BNCT, they must possess a certain degree of water solubility. This is often achieved through the introduction of solubilizing moieties [2]. Recently, the sulfhydryl-substituted derivative mercaptoundecahydrododecaborate ($B_{12}H_{11}SH^{2-}$) (BSH) of the ionic boron hydride cage $B_{12}H_{12}^{2-}$ has been found to lend itself to substitution chemistry on the sulfur [3]. Although compounds can be prepared readily, analytical separation by chromatography is not trivial, owing to the ionic nature of the boron hydride cage. One of the main problems in this connection is to achieve fast and reproducible reaction control. Simple chromatographic methods such as thin-layer chromatography suffer from bad resolution; further, BSH derivatives are difficult to detect. In contrast, high performance liquid chromatography (HPLC) with ion-pairing reagents allows analysis with good resolution and short analysis times. UV absorption monitoring allows sensitive detection for boron cage derivatives. In addition, HPLC offers easy and practicable purity assays for compounds used in clinical studies (e.g., BSH).

Heteroborane anions have been separated by reversed-phase (RP) ion-pair HPLC on C_1-bonded columns with n-alkylamines as ion-pair reagents [4]. More recently, chromatography of inorganic $B_{12}H_{12}^{2-}$ derivatives on hydroxyethylmethacrylate gels has been described [5]. For preparative chromatography of halogenated boron hydride cages, ion-exchange chromatography has been used [6]. For BSH and its oxidation products, RP-HPLC in the presence of

* Corresponding author.

tetrabutylammonium as ion-pair reagent has been used [7].

We report here that analytical separations of organic derivatives of BSH can be carried out using HPLC in the presence of ion-pair reagents. We have investigated systematically the chromatographic behaviour of many different sulfur-substituted derivatives of $B_{12}H_{11}SH^{2-}$, in order to establish the separation conditions for reaction control and purity assay with maximum resolution and minimum elution times.

2. Experimental

RP chromatography was carried out on a Merck–Hitachi system consisting of an L-6200 pump, a L-4200 UV–Vis detector and a D-2500 chromatointegrator. A Merck LiChrospher RP-18 (5 μm) column (125 × 4 mm I.D.) was used, with a precolumn containing the same material (4 × 4 mm I.D.). The injection loop held 20 μl. The flow-rate was 1 ml/min, unless indicated otherwise. Changes in the flow-rate of the gradient systems lead to shorter run times without loss of resolution. Retention times are given as

k' values. UV detection was carried out at 220 nm [BSH derivatives and BSH possess an absorption maximum at 220 nm ($\varepsilon = 2400$)] or 400 nm (porphyrin derivatives). Methanol and tetrabutylammonium hydrogensulfate (TBAS) used for the mobile phase were of analytical-reagent grade. Water was desalted and doubly distilled. Triethylammonium formate (TEAF) was prepared from triethylamine [purified with aluminium oxide (basic, super 1, ICN)] and formic acid, both of analytical-reagent grade. The solvent systems listed in Table 1 were used. The pH was adjusted to 6.5 with sodium hydroxide.

The boron compounds used are shown in Fig. 1.

BSH derivatives (Fig. 1a and b) were normally prepared by the following procedure [3]. The tetramethylammonium salt of BSH was converted into the sodium thiolate by titration with an equimolar amount of NaOH in water and recovered by lyophilization. This salt (1 g, 2.9 mmol) was suspending in 250 ml of acetonitrile. A solution of 15 mmol of alkyl bromide in 40 ml of acetonitrile was added through a dropping funnel at room temperature over 10 min. After 24 h the solvent was removed under vacuum.

Table 1
Isocratic and gradient solvent systems used
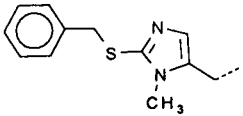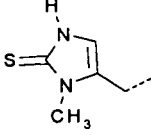
Isocratic systems
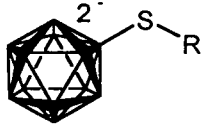
Solvent	Methanol (%)	Water (%)	TBAS (mM)	TEAF (mM)
A	57	43	20	–
B	30	70	–	30

Gradient systems

Gradient	Time interval (min)	Methanol (%)	Water (%)	TEAF (mM)	Flow-rate (ml/min)
1	0 → 1.1	20	80	30	1
	1.1 → 5.1	20 → 60	80 → 40	30 → 15	1
	5.1 → 10.1	60 → 100	40 → 0	15 → 0	2
	10.1 → 15.0	100	0	0	2
2	0 → 5.1	20 → 64	80 → 36	30 → 13.5	2
	5.1 → 30.1	64 → 100	36 → 0	13.5 → 0	1
	30.1 → 40.0	100	0	0	3

a

$B_{12}H_{11}S^{2-}$-R	
R	Designation
H	BSH
Cyanomethyl	S-1
Cyanoethyl	S-2
Allyl	S-3
Benzylmethimazole	S-4
Methimazole	S-5
Acetyl	S-6
Pentenoyl	S-7
Benzoyl	S-8

b

$B_{12}H_{11}S^-$-R_2	
R	Designation
Cyanomethyl	D-1
Cyanoethyl	D-2
Allyl	D-3
Butenyl	D-4
Pentenyl	D-5
(1,3-Dioxolanyl)-2-propyl	D-6
Cyanopropyl	D-7
3,3-Diethyloxypropyl	D-8
p-Cyanobenzyl	D-9
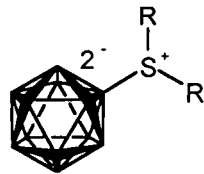
Fig. 1.

Fig. 1. *(Continued on p. 44)*

c

Porphyrins			
R^1 (propionic acid)	R^2	M	Des.
OH	H (deuteroporphyrin IX)	2H	P-1
OMe	H	2H	P-2
$B_{12}H_{11}^{2-}$-S	H	2H	P-3
OMe	t-butyl-acrylate	Zn	P-4
OMe	acrylate	2H	P-5
OMe	$B_{12}H_{11}^{2-}$-S-acrylate	2H	P-6
OMe	t-butyl-pentenoate	Zn	P-7
OMe	pentenoate	2H	P-8
OMe	$CH=CH-(CH_2)_2-SB_{12}H_{11}^{2-}$	2H	P-9
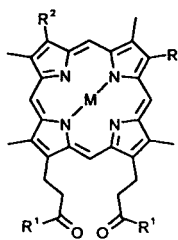
Fig. 1. Compounds studied.

The residue was suspended in acetonitrile and filtered to remove NaBr. On addition of diethyl ether, the product precipitated.

Boronated porphyrin derivatives (Fig. 1c) were normally prepared by the following procedure. The porphyrin (1 mmol) with free acid side-chains was dissolved in dichloromethane (50 ml). Oxalyl chloride (10 ml) was added and the mixture was refluxed for 45 min. The solvent was evaporated under vacuum. The residue was dissolved in acetonitrile (50 ml) and mixed with dry pyridine (1 ml) and dry tetramethylammonium BSH (1 g, 3.1 mmol, dried at 125°C for 2 h). The mixture was stirred overnight. The solvent was then removed, the residue was dissolved in acetonitrile–water and the counter ion was exchanged against sodium with an ion exchanger (Amberlite IR-120, Na$^+$ form). The solvent was evaporated, the residue was dissolved in a small amount of acetonitrile, filtered off and the solvent removed. The porphyrin was purified by two-step reversed-phase column chromatography with ion-pair reagent (methanol–water between 20:80 and 65:35, triethylammonium formate between 10 and 25 mM) in a flash column (details of preparation and purification will be reported elsewhere). The ion-pair reagent was removed by repeated lyophilization.

Subsequently, the counter ion was exchanged against sodium. The product was dissolved in acetonitrile, filtered and the solvent was evaporated. Reaction control was carried out using the HPLC gradient system 2, taking 10 μl from the reaction mixture dissolved in 100 μl of solvent. Purity assays were carried out by dissolving 1 mg of the pure compound in 250 μl of solvent. A volume of 50 μl of this solution was injected.

For the investigation in Table 2, BSH itself, a sulfonium salt with k' smaller than that of BSH (D-9) and one with k' larger than that of BSH (D-8) were chosen. The solutions of compounds used in Table 2 were prepared from the pure compounds.

Loading experiments were carried out with porphyrin P-3 with five different concentrations (55, 27.5, 14, 10.5 and 7 μg per 500 μl solvent). The retention times at all concentrations varied by only about ±5 s.

3. Results and discussion

A systematic search for optimum separation conditions was carried out. The ratio of methanol to water and the concentrations of the ion-pair reagents TBAS and TEAF were varied and

Table 2
Separation of selected compounds by buffers with various concentrations of methanol and TBAS at pH 7.0

TBAS (mM)	MeOH (%)	k' for compound			Separation of ternary mixture
		BSH	D-8	D-9	
20	60	4.03	5.88	3.37	Yes
	55	7.41	13.17	6.11	Yes
	50	15.24	32.33	12.16	Yes
10	60	2.84	4.54	2.30	Yes
	55	4.46	8.35	3.55	Yes
5	60	2.02	3.31	1.87	No
	55	2.80	5.96	2.65	No

the change in k' for a set of different compounds was recorded.

The values for k' for the three compounds BSH, D-9 and D-8 were greatly influenced by the methanol concentration. Fig. 2 shows that an increase in methanol concentration from 50% to 60% leads to a considerable decrease in the
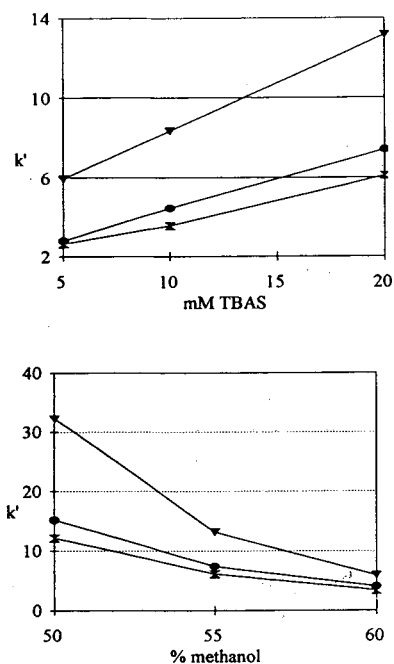
Fig. 2. Dependence of k' values on TBAS concentration (methanol-to-water ratio = 55:45) and methanol-to-water ratio (TBAS concentration = 20 mM). $\mathbf{O}$ = k'(BSH); $\mathbf{\blacktriangledown}$ = k'(D-8); $\mathbf{I}$ = k'(D-9)].

retention times of all compounds. The retention times were also influenced by the concentration of the ion-pair reagent. For TBAS, a nearly linear increase in k' was found between 5 and 20 mM concentrations (Fig. 2). Fig. 3 shows the interdependence of k' values for BSH on methanol and TBAS concentrations. The effects of methanol and TBAS concentrations appear to be additive. No reversal of elution times was found for any of the compounds investigated for any of the concentration combinations of methanol and TBAS. With low concentrations of TBAS, the difference between the k' values decreased. Table 2 summarizes these data. Fig. 4 shows a chromatogram of the reaction mixture of compound D-3.

Also for TEAF there is a strong correlation between methanol concentration and elution time. Again, an increase in methanol concentration reduced the elution times. However, there was a much weaker dependence of the
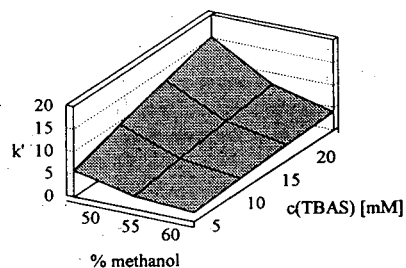
Fig. 3. Dependence of k' value of $B_{12}H_{11}SH^{2-}$ on methanol and TBAS concentrations.
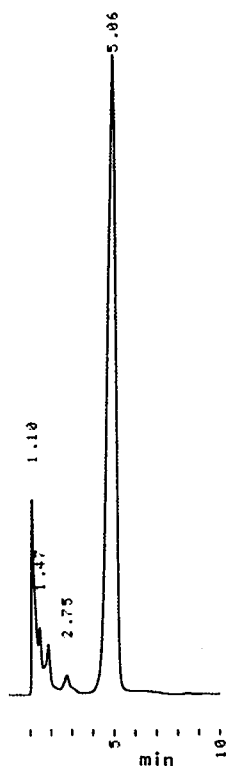
Fig. 4. Chromatogram of the reaction mixture of bisallyl-BSH (D-3). Peaks [retention times (min)]: 1.10 = acetonitrile; 1.47 and 1.86 = by-products; 2.75 = BSH; 5.06 = D-3.

Fig. 5. Dependence on k' on methanol-to-water ratio (TEAF concentration = 20 mM) and TEAF concentration (methanol-to-water ratio = 60:40). $\mathbf{O}$ = k'(BSH); $\blacktriangledown$ = k'(D-8); $\mathbf{\mathcal{I}}$ = k'(D-9).

elution time on TEAF concentration between 20 and 60 mM (Fig. 5). For TEAF, much lower k' values were found for all compounds investigated, compared with TBAS as ion-pair reagent. Exceptions are the cyanomethyl and cyanoethyl substituents, where both sulfonium salts showed longer retention times with TEAF than with TBAS.

For a greater number of compounds with similar chemical structures but different carbon side-chain lengths, increased chain length generally led to an increase in k', as shown in Table 3. Despite the fact that sulfonium salts have one more carbon chain than the corresponding thioethers, their k' values did not differ greatly from those of the thioethers (compare, e.g., D-1 with S-1, D-2 with S-2 and D-3 with S-3). This might be because sulfonium salts require only one counter ion for ion-pair formation.

Most of the BSH derivatives could be purified by recrystallization. Only some of the compounds were difficult to purify without chromatographic methods (e.g. S-4 and porphyrins). These compound mixtures contained components that varied greatly in the degree of hydrophobicity. In these cases isocratic elution led to unacceptably long elution times. Therefore, two gradient systems were developed for these separation problems. TEAF was used as ion-pair reagent because it can be removed by lyophilization. Thus, later use of this solvent in preparative chromatography is possible.

Gradient 1 is capable of resolving the highly polar S-5 ($k' = 2.56$) from the S-benzylated derivative S-4 ($k' = 11.71$) and toluene ($k' = 20.86$). In this system, BSH has a k' value of 1.03, close to the void volume. Gradient 2 allows the separation of porphyrins. With the high water concentrations necessary when using TEAF, some poorly water-soluble salts, such as the tetramethylammonoum salts of boronated porphyrins, may present problems. In such

Table 3
Retention times of different compounds in (A) MeOH–water (57:43), 10 mM in TBAS (pH 6.5) and (B) MeOH–water (30:70), 30 mM in TEAF (pH 6.5)

Substituent	Number of substituents	Designation	k'	
			Solvent A	Solvent B
H	1	BSH	2.51	0.80
Cyanomethyl	1	S-1	2.83	2.25
Cyanomethyl	2	D-1	2.05	3.20
Cyanoethyl	1	S-2	3.12	1.42
Cyanoethyl	2	D-2	2.12	3.44
Cyanopropyl	2	D-7	2.31	n.d.[a]
Allyl	1	S-3	12.44	n.d.
Allyl	2	D-3	10.80	n.d.
Pentenyl	2	D-5	34.19	n.d.
Butenyl	2	D-4	19.46	n.d.
(1,3-Dioxolanyl)-2-propyl	2	D-6	4.07	n.d.
Acetyl	1	S-6	3.12	1.24
Pentenoyl	1	S-7	7.92	n.d.
Benzoyl	1	S-8	9.92	7.34

[a] n.d. = Not determined.

cases, exchanging the counter ion to Na$^+$ and thereby enhancing the water solubility proved to be helpful. As can be seen in Table 4, porphyrins with greatly different substituents could be separated successfully. Fig. 6 shows the analytical separation of porphyrin P-6 from its monoboronated derivatives in the reaction mixture. Loading experiments for porphyrin P-3 showed no dependence of k' on sample concentration. The boronated porphyrins P-3 and P-6 must be considered very hydrophilic, based on their short retention times.

HPLC in the presence of ion-pair reagents is capable of separating ionic borates with greatly different degrees of hydrophobicity. The best separations for most of the BSH derivatives are achieved with methanol–water mixtures around 57:43 and tetrabutylammonium concentrations

Table 4
Separation of 3,8-substituted porphyrins using gradient system 2

Designation	R at 3- and 8-positions	M	R at propionic acid	k'
P-1	H	2H	OH	35.96
P-2	H	2H	OMe	57.66
P-2	H	Zn	OMe	50.37
P-3	H	2H	$SB_{12}H_{11}^{2-}$	28.84
P-4	CH = CHCOOBu^t	Zn	OMe	62.35
P-5	CH = CHCOOH	2H	OMe	32.23
P-6	CH = CHCOSB$_{12}$H$_{11}^{2-}$	2H	OMe	25.62
P-7	CH = CH(CH$_2$)$_2$COOBu^t	Zn	OMe	57.66/59.68[a]
P-8	CH = CH(CH$_2$)$_2$COOH	2H	OMe	42.40/43.76[a]
P-9	CH = CH(CH$_2$)$_2$SB$_{12}$H$_{11}^{2-}$	2H	OMe	35.96/39.01[a]

[a] *cis–trans* Isomers.
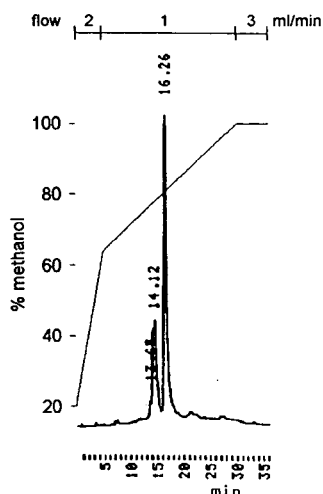
Fig. 6. Chromatogram of the reaction mixture of porphyrin P-6. Peaks [retention times (min)]: 13.65 and 14.12 = mono boronated porphyrins; 16.26 = P-6.

around 10 mM. The elution times depend very critically on the methanol-to-water ratio, as reported previously for C_1 phases and laurylamine as ion-pair reagent [4]. For the TBAS system described here, a decrease in methanol concentration of 2–3% led to a doubling of the retention time. For TEAF, an increase of the methanol concentration from 30 to 40% led to about 50% shorter retention times. Whereas laurylamine was required for the C_1 phase at concentrations around 2 mM [4], on the C_{18} phase used here higher concentrations of 10 mM TBAS were found to be necessary for adequate separation.

The separation of ionic borates has been achieved previously by ion-exchange chromatography [6]. Recovery of the compounds was achieved by eluting slices of the extruding gel. In contrast, HPLC can be carried out also under analytical conditions, and with greatly enhanced speed.

Acknowledgements

References

[1] M.F. Hawthorne, Angew. Chem., 105 (1993) 997.
[2] J. Nemeto, J.G. Wilson, H. Nakamura and Y. Yamamoto, J. Org. Chem., 57 (1992) 435.
[3] D. Gabel, D. Moller, S. Harfst, J. Rösler and H. Ketz, Inorg. Chem., 32 (1993) 2276.
[4] J. Plzák, J. Plesek and B. Stibr, J. Chromatogr., 212 (1981) 283.
[5] B. Grüner, Z. Plzák and I. Vins, J. Chromatogr., 588 (1991) 201.
[6] W. Preetz, M.G. Srebny and H.C. Marsmann, Z. Naturforsch., Teil B, 39 (1984) 189.
[7] A.K. Gianotto and W.F. Bauer, in A.H. Soloway, R.F. Barth and D.E. Carpenter (Editors), Advances in Neutron Capture Therapy, Plenum Press, New York, 1993, p. 459.

Isolation of four tocopherols and four tocotrienols from a variety of natural sources by semi-preparative high-performance liquid chromatography ☆

Tai-Sun Shin, J. Samuel Godber*

Department of Food Science, Louisiana Agricultural Experimental Station, Louisiana State University Agricultural Center, Baton Rouge, LA 70803, USA

Abstract

Quantitative measurements of tocopherols and tocotrienols required isolation of four tocopherols from a mixture of soybean oil and wheat germ and four tocotrienols from a mixture of wheat bran and rubber latex. Semi-preparative HPLC was accomplished using a 250 mm × 10 mm I.D. column packed with 10-μm silica gel in hexane containing 2–15% tetrahydrofuran. Identification of isolated and purified tocopherols and tocotrienols was confirmed from mass spectra, and concentrations of identified vitamers were determined by absorption coefficients. Recovery of tocopherols and tocotrienols ranged from 54 to 83%. Isomer purities were found to be above 99% by capillary GC and HPLC.

1. Introduction

There are four known naturally occurring tocopherols termed α-, β-, γ- and δ-tocopherol, as well as four closely related compounds termed tocotrienols, which have three double bonds in the isoprenoid side chain (Fig. 1). Tocopherols are widely distributed in animals, cereals, fruits, vegetable oil, nuts and vegetables. Tocotrienols are mostly absent in nuts, fruits and vegetables. Small amounts of tocotrienols are found in carrots, sweetcorn and cereal bran and germ oils. These endogenous antioxidants each have a

* Corresponding author.
☆ Approved for publication by the direction of the Louisiana Agricultural Experiment Station as manuscript number 93-21-7182.

different specific activity, necessitating a separate determination.

Thin-layer chromatography (TLC) has been used widely to prepare tocopherol and tocotrienol standards, which were not available commercially. Natural sources were soybean oil for α-, γ- and δ-tocopherol, whole ground barley for α- and β-tocotrienol, corn for α-tocotrienol, and barley germ oil for γ-tocotrienol [1–5]. The primary disadvantage of the TLC procedure is its inability to distinguish between γ-tocopherol and β-tocotrienol in a one-dimensional system. Also, since tocopherols are antioxidants and are known to be light-sensitive, the TLC system has the disadvantage of leaving them vulnerable to oxidation during the time they are on the plate [1]. In 1979, Thompson and Hatina [6] used a preparative column to isolate α- and γ-toco-

Position of methyl group	Tocopherols	Tocotrienols
5,7,8-Trimethyl	α-T	α-T3
5,8-Dimethyl	ß-T	ß-T3
7,8-Dimethyl	γ-T	γ-T3
8-Monomethyl	δ-T	δ-T3

Fig. 1. Structures of tocopherols and tocotrienols.

trienol as standards from wheat flour and rubber latex. More recently, Bruns et al. [7,8] applied technical-scale preparative liquid chromatography using a silica column to isolate tocopherols from vegetable oil. Saito and Yamauchi [15] isolated α-and β-tocopherol from wheat germ oil by recycle, semi-preparative supercritical fluid chromatography. For this isolation, special equipment is needed, such as a CO_2 pump, pre-heating coil and air-circulating oven, normally unavailable in typical laboratories.

Pure standard grade tocopherols (α, γ, δ) are available commercially, but tocotrienol standards are not. Recently released standards for γ- and δ-tocopherol (ICN Biochemicals, Division, CA, USA) are expensive and/or of lower purity. Research in our laboratory on rice bran composition and oxidative stability required analysis of endogenous tocopherols and tocotrienols. The purpose of the present study was to develop a procedure for isolation of highly purified tocopherols and tocotrienols as analytical standards from natural sources using semi-preparative liquid chromatography.

2. Experimental

2.1. Chemicals and materials

All solvents were HPLC grade from Mallinckrodt (Paris, KY, U.S.A). L-Ascorbic acid was from Sigma (St. Louis, MO, USA). Rubber latex was obtained from Malaysia, and soybean oil, wheat bran and wheat germ were purchased from a local grocery.

2.2. Extraction of crude oil

Rubber latex was used as a source for α-, γ- and δ-tocotrienols, soybean oil for α-, γ- and δ-tocopherol, wheat bran for β-tocotrienol, and wheat germ for β-tocopherol. To facilitate isolation, a mixture of soybean oil and wheat germ oil was used for tocopherols, as was a mixture of rubber latex lipid and wheat bran oil for tocotrienols.

For extraction of crude wheat germ and bran oil, 20 g of wheat germ or 40 g of wheat bran were placed in a 500-ml Erlenmeyer flask with 200 ml ethanol and 5 g ascorbic acid. The mouth of the flask was covered with a beaker and placed in a 60°C water bath for 10 min. Then 1.2 ml of 80% KOH were quickly added and mixed by vortexing. The sample was saponified for 10 min at 80°C. During saponification, the sample was agitated using a wrist-type shaker. After saponification, the flask was placed in an ice bath, and 30 ml water and 50 ml hexane were added. The mixture was vortexed, transferred to centrifuge bottles, and centrifuged at 120 g for 1 min. The upper layer was transferred to a 500-ml separatory funnel. Extraction of the sample with 50 ml hexane was repeated twice. The pooled hexane layer was washed three times with 30 ml water to remove residual KOH, filtered through Na_2SO_4, and then evaporated to dryness on a rotary evaporator. The crude oil sample was diluted with 10 ml methanol and the mixture was allowed to stand overnight at − 20°C. The mixture was centrifuged, 12 000 g at − 20°C for 30 min, and the supernatant filtered through a 0.45-μm filter. The filtrate was diluted with 20 ml water and extracted with 20 ml hexane twice.

Solvent was evaporated to dryness under a stream of nitrogen and sample diluted with a known amount of hexane and placed under nitrogen at $-20°C$.

For extraction of latex oil, the method of Whittle et al. [9] was employed with modification. Samples of latex (50 ml) were added to 500 ml chloroform with stirring and then homogenized in a Tissumizer (Tekmar, Cincinnati, OH, USA) for 5 min. To this mixture 250 ml methanol were added and stirred until the rubber coagulated. The coagulated rubber was filtered, then dried on a rotary evaporator under reduced pressure.

Saponification and crystallization [9] of latex oil (4 g) and commercial soybean oil (4 g) were as described previously.

2.3. Apparatus

Semi-preparative HPLC

The semi-preparative HPLC system that was used consisted of Waters (Milford, MA, USA) M-45 and 510 pumps, a Waters 680 automated gradient controller, a Waters 470 scanning fluorescence detector with 18 nm spectral bandwidth for excitation and emission, a Hewlett-Packard (San Fernando, CA, USA) UV–Vis diode-array detector (series 1050) and a Waters 715 Ultra WISP injector equipped with a 2000-μl loop and 200-μl syringe. Chromatograms were recorded and peaks determined using a Baseline 810 Chromatography workstation (Waters). Concentrated extracts were injected into a 25 cm × 10 mm diameter column of 10-μm Alltech Econosil silica (Deerfield, IL, USA). The column was used with 5 cm × 4.6 mm I.D. guard column packed with 40-μm Supelco pellicular silica (Bellefonte, PA, USA). The mobile phase consisted of a gradient of 0–15% tetrahydrofuran (THF) in hexane at a flow-rate of 8–9 ml/min, and the eluate was monitored from the fluorescence detector at 290 nm excitation and 330 nm emission. Eluates considered as α-, β-, γ- and δ-tocopherols and tocotrienols in each experiment were collected into 250-ml amber bottles with PTFE cap using a Gilson Model 202 fraction collector (Beltline-Middleton, WI, USA).

Collection bottles were placed in a 50°C water bath and solvent evaporated in the dark using ultra-high-purity nitrogen. The pooled specimens of α-, β-, γ- and δ-tocopherols and tocotrienols were rechromatographed until the specimens were pure chromatographically and spectrophotometrically. The pooled specimens were also concentrated. To check purity of each isomer, the absorption ratio of 295 nm to 245 nm wavelength with 4 nm bandwidth and 390 nm reference wavelength were compared using a diode array detector. The concentrations of fractionated vitamin E vitamers were determined using a Gilford UV–Vis spectrophotometer (Oberlin, OH, USA).

For semi-preparative HPLC, solvent A was 40% (v/v) THF in hexane, and solvent B was 100% hexane. The solvents were filtered through Millipore 0.45-μm membranes prior to use. THF was distilled [10] to remove peroxides that might form during storage prior to mobile phase incorporation.

Analytical HPLC

The analytical HPLC system was similar to the semi-preparative system with modifications as follow. Samples (0.5–5 μl) were injected using a 200-μl loop and 25-μl syringes into a 25 cm × 4.6 mm diameter column of 5-μm Sulpelcosil LC-Si (Supelco). The column was preceded by a 5 cm × 4.6 mm I.D. guard column packed with 40-μm pellicular silica. The mobile phase consisted of 2.4% ethyl acetate in isooctane at a flow-rate of 2.0 ml/min, and the eluate was monitored from the fluorescence detector. Isolated and purified tocopherols and tocotrienols were used as standards.

Gas chromatography (GC) and mass spectrometry (MS)

Purities of isomers were determined using a J & W Scientific (Folsom, CA, USA) 95% dimethyl-/5% diphenylpolysiloxane capillary column (0.25-μm stationary phase thickness, 30 m × 0.25 mm I.D.) on a Hewlett-Packard 5890 gas chromatograph equipped with a split/splitless capillary inlet system and a flame ionization detector. Column oven temperature was pro-

grammed to increase from an initial temperature of 40°C to a final temperature of 280°C. Oven temperature was maintained at the initial temperature for 3 min after injection and then increased at 20°C/min to a temperature of 280°C for 40 min. Other operation parameters were as follows: injector temperature, 300°C; detector temperature, 350°C; helium carrier gas flow, 30 cm/s; split ratio, 1/50. A Maxima 820 Chromatography workstation was used to determine peak areas (Waters).

Mass spectra of tocopherols and tocotrienols were obtained by a Hewlett-Packard 5890 series II gas chromatograph/5971A mass spectrometer with splitless (holding time, 0.75 min) injection. GC column and temperature program were as described previously. Additional conditions were as follows: ionization voltage, 70 eV; electron multiplier voltage, 1800; scan range, 40–450 u; interface temperature, 280°C; injector temperature, 250°C.

3. Results and discussion

3.1. Sample preparation

Saponification of oils concentrated vitamin E vitamers and removed interfering glycerides and other hydrolyzable materials. At the same time, saponification liberated tocopherols and tocotrienols from esters that may have been present. Chow et al. [11] reported that rubber latex lipid contains about 68% esterified tocotrienol. The unsaponifiable matter contains higher aliphatic alcohols (waxes), sterols, pigments, and hydrocarbons. In wheat germ and soybean oil, the major components of the unsaponifiable matter are sterols [12]. Some sterols may be removed by precipitation at low temperature and filtration [6,11,13,14]. During sample preparation it is important to reduce mass of sample as much as possible to increase sample loading, reduce analysis time, and improve column stability. Table 1 shows changes in mass balance of sample during separation steps. With saponification and crystallization, over 95% of sample mass could be reduced from commercial soybean oil and extracted oils.

3.2. Isolation of tocopherols and tocotrienols

Fig. 2 shows a chromatogram of vitamin E vitamers from soybean and wheat germ oil. Before sample injection, the column was flushed with a gradient system (Table 2) for 25 min. The mixture had a concentration of 479 mg/ml in 2.5% THF in hexane, and 60 μl (about 28.8 mg)

Table 1
Mass balance of sample preparation

Sample	Mass (g)			
	Soybean oil	Wheat germ	Wheat bran	Latex
Sample before extraction	2	20	40	20
Sample after extraction	–	0.0471[a]	0.0395[a]	0.2194[b]
Sample after saponification	0.0165	–	–	0.07635
Sample after crystallization[c]	0.00907	0.0164	0.0146	0.05008

[a] Extracted with saponification.
[b] Extracted without saponification.
[c] Crystallized at −20°C for 12 h and centrifuged at −20°C.
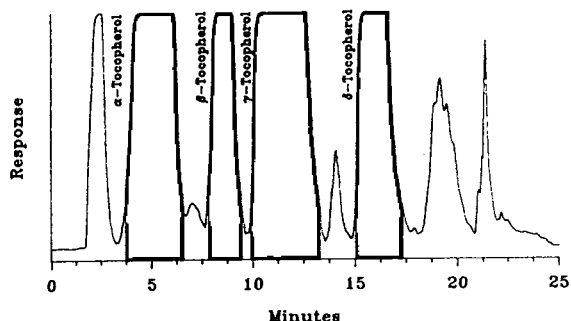
Fig. 2. Chromatogram of a mixture of a soybean oil and wheat germ oil; solid peaks represent fraction cuts. Chromatographic conditions are described in text and in Table 2.

were injected. Injection of over 35 mg of the mixture decreased vitamers' resolution. A flow-rate between 8 and 9.99 ml/min, which was the maximum flow-rate of our controller, had no influence on resolution. Peaks of α-, β-, γ- and δ-tocopherol in Fig. 2 represent amounts of 0.68, 0.29, 2.02 and 0.84 mg per injection, respectively. α-Tocotrienol eluted between α-tocopherol and β-tocopherol, and β-tocotrienol eluted between γ-tocopherol and δ-tocopherol. After 17 min, more polar compounds such as sterols eluted. Tocotrienols and most late eluates came from wheat germ oil. An injection of soybean oil alone produced level base line after δ-tocopherol

Table 2
Mobile phase gradient program for mixture of soybean oil and wheat germ oil

Time (min)	Solvent A (%)[a]	Solvent B (%)[b]	Curve[c]
Initial	30	70	*
0.5	6	94	5
2.0	10	90	5
9	10	90	6
13.7	35	65	6
14.5	35	65	6
20	30	70	6

Flow-rate 8 ml/min.
[a] Hexane–THF (60:40).
[b] Hexane (100%).
[c] Pre-programmed gradient curve in Waters 680 automated gradient controller. * = No curve.

eluted. Sterols could not be removed completely with precipitation at low temperature. To remove sterols completely, crystallization and digitonin precipitation were used [9].

The column required cleaning between injections to obtain constant retention time and pure fractions. Hexane with 14% THF (Table 2, from 13.7 to 14.5 min) was used to remove late-eluting compounds and stabilize retention time. A higher concentration of THF could be applied to accelerate elution of late compounds, but analysis time would be similar because the column would require reequilibration to the 12% THF mobile phase. Solvent A was prepared with 40% THF in hexane rather than pure 100% THF to improve control of the gradient system.

Fig. 3 shows the chromatogram of a mixture of a latex oil and wheat bran oil (gradient in Table 3). The mixture of latex oil and wheat bran oil with concentration of 485 mg/ml in hexane containing 2.5% THF was prepared, and 180 μl (about 87.3 mg) were injected. Injection of over 95 mg decreased resolution of tocopherols and tocotrienols. The eluate between α-tocotrienol and β-tocotrienol was β-tocopherol. The peak between γ-tocotrienol and δ-tocotrienol was presumably δ-tocopherol. But δ-tocopherol was not detected in wheat bran oil and latex lipid using an analytical column. Peaks of α-, β-, γ- and δ-tocotrienol in Fig. 3 represent amounts of 0.78, 0.55, 3.37 and 0.77 mg per injection, respectively. The sample matrix of wheat germ oil and wheat bran oil was complex, so isolation of β-
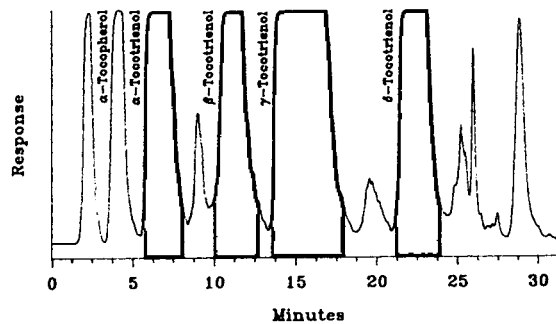
Fig. 3. Chromatogram of a mixture of a wheat bran oil and latex lipid; solid peaks represent fraction cuts. Chromatographic conditions are described in text and in Table 3.

Table 3
Mobile phase gradient program for latex lipid and wheat bran oil

Time (min)	Flow (ml/min)	Solvent A (%)[a]	Solvent B (%)[b]	Curve[c]
Initial	8	30	70	*
0.7	8	8	92	6
1.1	8	5	95	5
5	8	5	95	6
13	8	7	93	5
14.5	8	8	92	4
16.5	8	10	90	9
20	8	15	85	8
22	9	35	65	10
25	9	35	65	6
27	8	30	70	8

[a] Hexane–THF (60:40).
[b] Hexane (100%).
[c] Pre-programmed gradient curve in Waters 680 automated gradient controller. * = No curve.

tocopherol or β-tocotrienol from wheat germ oil took over 20 min.

3.3. Fraction purification

Purities of first fraction were over 88% and those of second fraction over 97% by analytical HPLC. Isocratic mobile phase systems were used during purification steps. The concentrations of THF in hexane as a modifier solvent ranged from 7% for α-tocopherol to 18% for δ-tocotrienol. To reduce the purification time in the last steps, the amounts of THF in hexane were increased.

3.4. Purity checks and concentration determination

To characterize fraction purity to a greater extent, the ratio of UV absorptions (295/245 nm) was determined using a UV diode array detector (Fig. 4). Saito and Yamauchi [15] used the ratio of 230 to 295 nm to check purities of α- and β-tocopherol fraction. Absorption at 230 nm represents tocopherols, fatty acids, and their esters, and the absorption at 295 represents only tocopherols. Presumably, our samples were free from fatty acids and triglycerides, so we used 245 nm to check for sterols in isomer fractions. Eluates from the fluorescence detector were
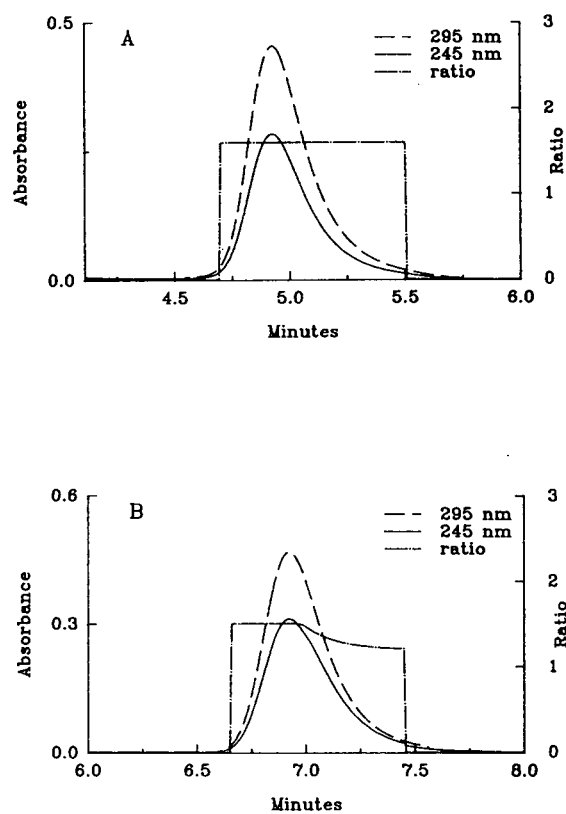
Fig. 4. Chromatograms at wavelengths 295 nm, 245 nm and the ratio of the two for (A) δ-tocopherol and (B) δ-tocotrienol.

Table 4
Analytical data for isolated and purified tocopherols and tocotrienols fractions from 6 g of a mixture of soybean oil and wheat germ oil and 8 g of a mixture of wheat bran oil and latex lipid

Sample	α-T	β-T	γ-T	δ-T	α-T3	β-T3	γ-T3	δ-T3
Purity (%)[a]	99	99	99	99	99	99	99	99
Recovery (%)	79	75	83	78	76	72	81	54
Yield (mg)	112.2	45.22	350.4	136.5	54.16	33.96	250.5	38.2

[a] By gas chromatography.

passed through the UV detector with HPLC conditions similar to the purification procedure, except injection quantity was reduced to 5–20 μl. As shown in Fig. 4A, the δ-tocopherol peak produced a constant signal ratio (295 nm/245 nm) throughout the peak's elution. However, the δ-tocotrienol peak evidenced a change in the signal ratio (295 nm/245 nm). Impurities in the δ-tocotrienol fraction eluted at a similar time, so purification with the column could not be obtained. The impurities were not identified.

Fractionated δ-tocotrienol were scanned at UV–Vis wavelengths from 200 to 350 nm. The chromatogram had high absorption values in the wavelength range around 260 nm (minimum wavelengths of δ-tocotrienol). The fraction of δ-tocotrienol after three HPLC passes still contained impurities, which were then chromatographed two additional times using TLC with

silica gel G (250 μm) and 20% diisopropyl ether in light petroleum (b.p. 35–60°C) [9]. After TLC fractionation the purity was satisfactory as is shown in Table 4.

Each fractionated solution in the last purification steps was evaporated to dryness, weighed, and diluted with known amount of hexane. A known amount of each tocopherol and tocotrienol solution was evaporated to dryness and diluted with ethanol to determine the concentration of vitamin E vitamers in hexane solution by published molar absorbance values $E_{1\ cm}^{1\ \%}$ in Table 5. However, absorption maxima and molar absorbance values found in the literature differ. Absorption maxima that matched published $E_{1\ cm}^{1\ \%}$ were chosen in accordance with UV–Vis spectrum maxima of purified vitamers in Fig. 5. For β-tocotrienol, two $E_{1\ cm}^{1\ \%}$ values at 294 nm have been published, so the average value of

Table 5
UV absorption maxima and molar absorbance of tocopherols and tocotrienols in ethanol solution taken from the literature

Compound	λ_{max} (nm)[a]	λ_{max} (nm)	$E_{1\ cm}^{1\ \%}$
Tocopherol			
α-	292	292 [16,20]	75.8 [16,19]
β-	296	296 [16]	89.4 [16]
γ-	298	298 [16]	91.4 [16]
δ-	298	298 [16]	87.3 [16]
Tocotrienol			
α-	292	292.5 [17], 290 [18]	91 [17], 77.2 [18]
β-	294	294 [16,18], 295.5 [20]	87.3 [16], 85.5 [18], 87.5 [20]
γ-	296	296 [19], 298 [20]	90.5 [17], 103 [20]
δ-	297	297 [9], 292 [20]	88.1 [9], 83.0 [20]

Italicized values used to determine the concentration of vitamers.
[a] Isolated and purified vitamers in Fig. 5.
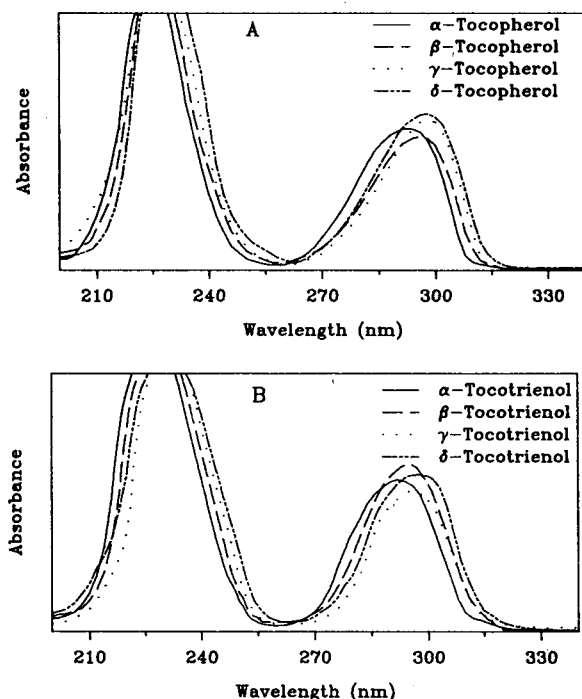
Fig. 5. UV–visible spectra of isolated and purified tocopherols and tocotrienols.

86.4 was used for calculation of β-tocotrienol concentration. The concentrations of purified vitamin E vitamers as determined were used as standards for HPLC assays.

3.5. GC–MS

Table 6 shows molecular masses and major peaks (m/z) of purified vitamin E vitamers in mass spectra. The major mass fragmentations of β- and γ-tocopherol and β- and γ-tocotrienol were the same, since these are positional vitamers having the same molecular masses. Also, they had a similar retention time on GC. However, using HPLC, differences in absorption maximum and retention time were noted (Table 5). The peaks of m/z 205, 191 or 177 ($M_r - 255$ or 219) indicates the loss of a side chain ($C_{16}H_{33}$ for tocopherols or $C_{16}H_{27}$ for tocotrienol), and peaks of m/z 165, 151 or 137 (205, 191 or $177 - 40$) originated from the cleavage of the side chain accomplished by the breakdown of

Table 6
Molecular masses and major m/z ratios of vitamin E vitamers in mass spectrum

Compound	M_r	m/z
Tocopherol		
α-	430	43, 55, 57, 165, 205, 430
β-	416	43, 55, 57, 107, 151, 191, 416
γ-	416	43, 55, 57, 107, 151, 191, 416
δ-	402	43, 55, 69, 137, 163, 177, 402
Tocotrienol		
α-	424	41, 55, 69, 81, 165, 203, 205, 424
β-	410	41, 55, 69, 81, 151, 189, 191, 410
γ-	410	41, 55, 69, 81, 151, 189, 191, 410
δ-	396	41, 55, 69, 81, 137, 177, 189, 396

chroman structure with hydrogen rearrangement and loss of a methyl acetylene $CH_3 = C \equiv CH$ fragment [21].

Fig. 6 shows chromatograms of purified α-tocopherol and α-tocotrienol. As can be seen,
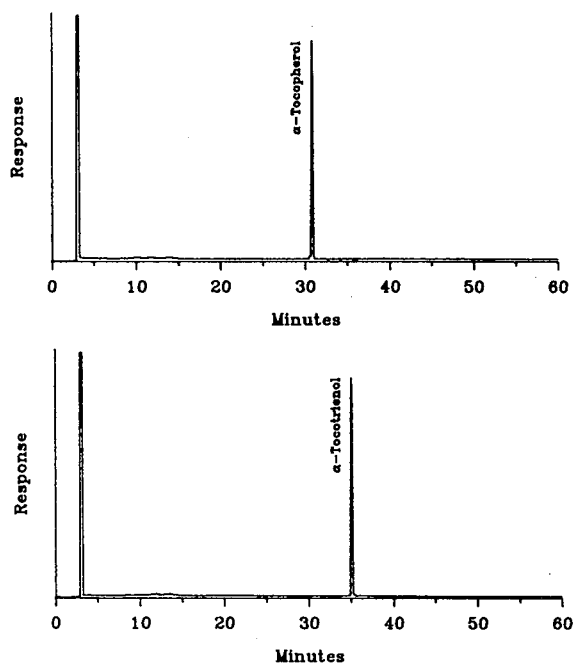
Fig. 6. Gas chromatograms of isolated and purified α-tocopherol and α-tocotrienol. Chromatographic conditions are given in the text.

the chromatograms have a single peak and clear baseline. Other chromatograms for β- + γ- and δ-tocopherols and tocotrienols had similar characteristics. Purities of vitamers were over 99% based on the peak area percentage.

3.6. Analytical HPLC analysis of isolated and purified vitamers

Baseline resolution was obtained for all vitamers in the mixtures of soybean oil and wheat germ oil, and wheat bran oil and latex. Table 7 shows the concentrations using analytical HPLC. Concentrations of tocopherols and tocotrienols were calculated from peak areas and corresponding standard curves ranging from 0.1 to 1.5 μg/ml. Table 4 shows recoveries, purities and yields of isolated and purified vitamers. Purities of all vitamers were over 99% by GC and HPLC. Analytical HPLC chromatograms were clearer than GC ones due to the high selectivity of fluorescence detection for vitamin E vitamers. γ-Tocopherol and tocotrienol had higher recovery than other vitamers because concentrations of these vitamers in source oils were higher than those of other vitamers. Recovery of δ-tocotrienol was lower than the other vitamers because it required additional TLC procedures to attain purification.

4. Conclusions

Four vitamers of tocopherol and tocotrienol were isolated from a mixture of natural sources by semi-preparative HPLC for use in analytical HPLC. Recovery was higher than by conventional TLC. The semi-preparative HPLC column is useful to obtain small amounts of pure tocopherols and tocotrienols as an alternative to conventional methods that tend to be tedious and time consuming, such as distillation, extraction, crystallization and TLC. Isolation also was more efficient because all tocopherols and tocotrienols can be obtained from a mixture of several natural sources simultaneously and each fraction collected and rechromatographed to obtain pure standards.

References

[1] J.F. Cavins and G.E. Inglett, Cereal Chem., 51 (1974) 605.
[2] E.J. Wever, J. Am. Oil Chem. Soc., 61 (1984) 1231.
[3] E.J. Wever, J. Am. Oil Chem. Soc., 64 (1987) 1129.
[4] W.M. Cort, T.S. Vicente, E.H. Waysek and B.D. Williams, J. Agric. Food Chem., 31 (1983) 1330.
[5] P.J. Van Niekerk, Anal. Biochem., 52 (1973) 533.
[6] J.H. Thompson and G. Hatina, J. Liq. Chromatogr., 2 (1979) 327.
[7] A. Bruns, D. Berg and A. Werner-Busse, J. Chromatogr., 450 (1988) 111.

Table 7
Contents of tocopherols and tocotrienols in a mixture of soybean and wheat germ oil and a mixture of wheat bran oil and latex lipid

Sample	Contents (mg/g)							
	α-T	β-T	γ-T	δ-T	α-T3	β-T3	γ-T3	δ-T3
Mixture of soybean oil and wheat germ oil[a]	23.66	10.05	70.29	29.171	0.114	0.491	–	–
Mixture of wheat bran oil and latex lipid[b]	4.164	0.612	–	–	8.914	5.901	38.66	8.846

[a] Soybean oil (1 g)–wheat germ oil (1 g) in 2.5% THF in hexane.
[b] Wheat bran oil (1 g)–latex lipid (2 g) in 2.5% THF in hexane.

[8] A. Bruns, J. Chromatogr., 536 (1991) 75.
[9] K.J. Whittle, P.J. Dunphy and J.F. Pennock, Biochem. J., 100 (1966) 138.
[10] J.A. Riddick and W.B. Bunger, Organic Solvents, Wiley-Interscience, New York, 3rd ed., 1973.
[11] C.K. Chow, H.H. Draper and A.S. Csallany, Anal. Biochem., 32 (1969) 81.
[12] T. Itoh, T. Tamura and T. Matsumoto, J. Am. Oil Chem. Soc., 50 (1973) 122.
[13] R.H. Bunnell, Lipids, 6 (1971) 245.
[14] J.F. Pennock, G. Neiss and H.R. Mahler, Biochem. J., 85 (1962) 530.
[15] M. Saito and Y. Yamauchi, J. Chromatogr., 505 (1990) 257.

[16] P.W.R. Eggit and F.W. Norris, J. Sci. Food Agr., 6 (1955) 689.
[17] J. Green, S. Marchnkiewicz and P.R. Watt, J. Sci. Food Agr., 6 (1955) 274.
[18] P. Schudel, H. Mayer, J. Metzger, R. Rüegg and O. Isler, Helv. Chim. Acta, 46 (1963) 2517.
[19] H. Mayer, J. Metzger and O. Isler, Helv. Chim. Acta, 50 (1967) 1376.
[20] R.A. Morton, Biochemical Spectroscopy, Wiley, New York, 1975, p. 410.
[21] M.K. Govind Ras and E.G. Perknis, J. Agr. Food Chem., 20 (1972) 241.

ELSEVIER

Rapid determination of glufosinate in environmental water samples using 9-fluorenylmethoxycarbonyl precolumn derivatization, large-volume injection and coupled-column liquid chromatography

J.V. Sancho[a], F.J. López[a], F. Hernández[a], E.A. Hogendoorn[b], P. van Zoonen[b,*]

[a]Environmental and Natural Resources, Experimental Sciencies Department, Universitat Jaume I, P.O. Box 224, 12080 Castellón, Spain

[b]Laboratory of Organic–Analytical Chemistry, National Institute of Public Health and Environmental Protection (RIVM), P.O. Box 1, 3720 BA Bilthoven, Netherlands

Abstract

The application of 9-fluorenylmethoxycarbonyl (FMOC) derivatization prior to coupled-column LC with fluorescence detection using a reversed-phase C_{18} column (C-1) coupled to an ion-exchange column (C-2) proved to be useful for the rapid determination of the very polar pesticide glufosinate in a variety of environmental water samples at the sub-ppb level. The separation power of the first column is used to provide (i) sensitivity by means of large-volume injection and (ii) selectivity by an efficient preseparation of the very polar analyte from the less polar interferences including the excess of unreacted FMOC reagent. Conditions for the important parameters with respect to separation and sensitivity, viz., sample injection volume, separation power of the columns and composition of the buffer and modifier in the mobile phases, were established, resulting in a method with which glufosinate in water samples, after FMOC derivatization, can be assayed at a level of 0.25 μg/l (signal-to-noise ratio = 3) in less than 15 min. The overall procedure has a sample throughput of more than 50 per day. Drinking, ground and surface water samples spiked at levels between 0.5 and 5.0 μg/l yielded average recoveries between 90 and 105% ($n = 5$ for each sample type and spiked level) with relative standard deviations between 1 and 5%. The method is linear over at least three orders of magnitude ($r > 0.999$). The limit of detection can be lowered to 0.1 μg/l by means of a simple preconcentration step with a Rotavapor.

1. Introduction

A recent report on Water Pollution published by the Commission of the European Communities [1] clearly emphasizes that information on the occurrence of a number of very polar pesticides is not yet available. The major reason for this is the lack of adequate analytical methodology to determine efficiently such very polar compounds at the sub-μg/l level in aqueous samples.

One of these "problem" analytes is glufosinate, which is used as a non-selective contact

---

* Corresponding author.

SSDI 0021-9673(94)00447-H

Table 1
Structural formulae and water solubilities of glufosinate and glyphosate

Pesticide	Formula	Solubility in water (mg/l at 20°C)
Glufosinate	CH_3—P(=O)(OH)—CH_2CH_2—C(H)(NH_2)—C(=O)—OH	$2 \cdot 10^5$
Glyphosate	OH—P(=O)(OH)—CH_2—N(H)—CH_2—C(=O)—OH	$0.1 \cdot 10^5$

herbicide with increasing popularity in both Netherlands and Spain. As indicated in Table 1, glufosinate is a very polar compound and its structural formula is similar to that of the older and widely used herbicide glyphosate (first marketed in 1974), for which a variety of analytical residue methods are available [2–18]. Probably for reasons of later marketing (since the early 1980s) and its (so far) less widespread application, information on analytical methodology for glufosinate is poor in comparison with glyphosate. For example, official handbooks on pesticide residue analysis in foodstuffs [19,20] refer only to the analytical method supplied by the manufacturer [21]. A modification of this method [22] has been included in German official handbooks [23,24] to determine glufosinate in drinking water. However, this method is very laborious, involving enrichment on an anion-exchange column, a derivatization step and clean-up on silica gel prior to analysis by GC with nitrogen–phosphorus detection.

The aim of this study was to develop a method for the determination of glufosinate in water samples which is faster and, hence, more suitable for monitoring purposes. Regarding their chemical similarity, the published method for glyphosate was used as the starting point in method development. Glyphosate and its major metabolite aminomethylphosphonic acid (AMPA) can be determined by both GC [3–7] and LC [8–17].

Both techniques require derivatization of the analytes, necessary for the chromatographic separation in GC and improve detectability in LC with fluorescence detection. The possibility of performing derivatisation in aqueous solutions, which are compatible with both water samples and reversed-phase chromatographic separation, usually makes LC the preferred technique.

Recent work [25–27] has demonstrated that the combination of direct large-volume injection and coupled-column RPLC is a suitable technique for the rapid, sensitive and selective determination of polar pesticides in environmental water samples. As has been experimentally determined [25–27] and explained rationally [26], the applied separation power and dimensions of the first C_{18} column made it possible to inject large sample volumes (sensitivity) and perform an efficient clean-up (selectivity) between the polar analyte and the large excess of UV-absorbing early interferences.

This paper reports the development of a coupled-column method for the rapid determination of glufosinate, after 9-fluorenylmethoxycarbonyl (FMOC) derivatisation, in environmental water samples using a C_{18} column for efficient separation between the analyte and FMOC (and interferences) coupled to an amino column for the anion-exchange separation of the fluorescent glufosinate derivative.

2. Experimental

2.1. Chemicals

Glufosinate (content >99%) was obtained from Riedel-de Haën (Seelze, Germany). Acetonitrile and ethyl acetate, both of HPLC-grade, were purchased from Scharlau Science (Barcelona, Spain). Analytical-reagent grade potassium dihydrogenphosphate, disodium tetraborate decahydrate, orthophosphoric acid (50% pure), hydrochloric acid (37%), potassium hydroxide and 9-fluorenylmethyl chloroformate (FMOC-Cl) were bought from Merck. HPLC-grade water was obtained by purifying demineralized water in a Nanopure II system (Barnstead, Newton, MA, USA).

A stock standard solution (ca. 500 μg/ml) of glufosinate and dilutions were prepared with HPLC-grade water. A 0.025 M borate buffer solution (pH 9) and a 100 μg/ml FMOC-Cl solution were prepared in HPLC-grade water and acetonitrile, respectively.

Acetonitrile–0.05 M phosphate (pH 5.5) in water (35:65, v/v) and acetonitrile–0.1 M phosphate (pH 5.5) in water (35:65, v/v) were used as the first (M-1) and second (M-2) mobile phases, respectively. The pH of the aqueous buffer solutions was adjusted with 2 M KOH and 1 M HCl.

2.2. Equipment

The HPLC set-up is illustrated schematically in Fig. 1. The modular system consisted of a Model 1050 sampler (Hewlett-Packard, Waldbronn, Germany), the manual injector of which, equipped with a 2.0-ml loop, was used to perform large-volume injections (LVI), a Model 1050 gradient pump (P-1, Hewlett-Packard), a Model C6W six-port switching valve (HV) driven by a WE-II actuator from Valco (VIGI, Schenkon, Switzerland) and time controlled by the sampler, a Model 2150 pump (P-2) from LKB (Bromma, Sweden), a Model 1046A fluorescence detector (Hewlett-Packard) set at 263 nm (excitation) and 317 nm (emission), a 30 × 4.6
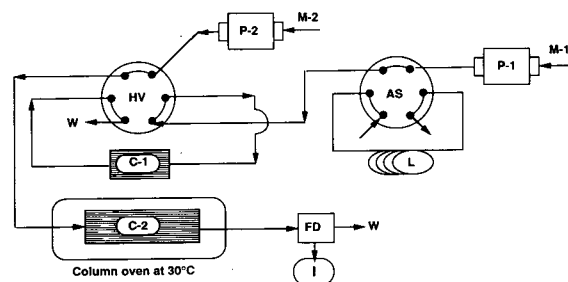
Fig. 1. HPLC set-up for column-switching. AS = sample injector with a 2-ml loop (L); HV = six-port high-pressure value; P-1 = gradient LC pump; P-2 = isocratic LC pump; C-1 = first separation column; C-2 = second separation column; M-1 and M-2 = mobile phases on C-1 and C-2, respectively; FD = fluorescence detector; I = integrator system; W = waste.

mm I.D. separation column (C-1) packed with 5-μm Nucleosil C_{18} from Scharlau Science and a 250 × 4.6 mm I.D. separation column (C-2) packed with 5-μm Adsorbosphere NH_2 from Alltech (Carnforth, UK). C-2 was kept at 30°C in the column heater of the Model 1050 pump (P-1).

Recording of chromatograms and quantitative measurements of peak heights were performed with a Hewlett Packard HPLC Chem Station (software version G1034A). A Digilab 517 pH meter and Pipetmans (200 and 1000 μl) were obtained from Crison Instruments (Barcelona, Spain) and Gilson, respectively.

2.3. Sample preconcentration

To lower the limit of detection for glufosinate from 0.25 to 0.1 μg/l, 25 ml of water sample were transferred into a 250-ml round-bottomed flask and evaporated to dryness with a Rotavapor using a water-bath temperature of 40°C. The residue was dissolved in 5 ml of HPLC-grade water.

2.4. Precolumn derivatisation

A 0.5-ml volume of water sample or a water sample concentrated fivefold by means of

Rotavapor evaporation was pipetted into a 9-ml glass tube together with 1.0 ml of borate buffer and 1.0 ml of FMOC reagent. The tube was swirled and left at room temperature for 30 min. After reaction, 5 ml of borate buffer were added and the tube was swirled again for thorough mixing.

2.5. LC analysis

The mobile phases (see Fig. 1) were set at a flow-rate of 1 ml/min. A volume of 2.00 ml of the solution obtained after derivatization was injected on to C-1. After clean-up with 2.25 ml of M-1 (injection volume included), C-1 was switched on-line with C-2 for 18 s to transfer the fraction (300 μl) containing the glufosinate derivative to C-2. Two minutes after injection, C-1 was rinsed and conditioned by applying gradient elution from 35 to 65% acetonitrile in 2 min, holding at 65% acetonitrile for 2 min, then to 35% acetonitrile in 2 min. Quantification of glufosinate was done by external calibration with standard solutions of glufosinate in water which were processed with the precolumn derivatization procedure.

3. Results and discussion

This study was focused on the development of an efficient method for the determination of glufosinate in water samples using published information on the LC determination of glyphosate. Two different derivatization procedures for glyphosate are commonly used: (i) precolumn derivatization using FMOC reagent [8–12] and (ii) postcolumn derivatization using o-phthaldehyde (OPA) reagent [8,13–18]. FMOC forms easily and quantitatively derivatives with both primary and secondary amines in aqueous solutions. However, the excess of the less polar highly fluorescent reagent must be removed with an additional liquid–liquid extraction step [9–12] or with gradient elution after the RPLC separation of the analytes [8]. The recommended method for the determination of glyphosate in foodstuffs [2,15] and used in the USA as an

Environmental Protection Agency method for the determination of glyphosate in drinking water [18] is based on the use of postcolumn derivatization with OPA. The non-fluorescence of unreacted OPA allows on-line derivatization of primary amines with the chromatographic separation without removing the excess of reagent. Therefore, glyphosate (secondary amine) requires postcolumn hydrolysis prior to the OPA reaction, which involves more instrumentation and careful maintenance. Moreover, the underivatized analytes are separated on an anion-exchange column, usually with a low separation power.

In contrast to OPA, FMOC reacts with both primary and secondary amines and it use does not require a previous hydrolysis step. Hence FMOC seems to be attractive for improving both the simplicity of the chromatographic set-up and the detectability. As has been shown for FMOC-glyphosate [8], the approach of precolumn derivatization with FMOC offers the possibility of separating the analyte and FMOC on a C_{18} column. The applicability of column switching using a first C_{18} column to perform an automated and effective clean-up prior to a selected off-line standard FMOC derivatization procedure for glyphosate [11] was investigated. The several steps in the method development are discussed below.

3.1. Sample pretreatment

The selected procedure [11] uses, for the complete precolumn derivatization of glyphosate and AMPA, 1 ml of aqueous sample, 1 ml of FMOC solution (1000 μg/ml in acetonitrile) and 1 ml of borate buffer and a reaction time of 20 min at room temperature. Because glufosinate is a primary amine, it can be expected that in comparison with glyphosate (secondary amine) lower FMOC concentrations can be used. Employing the same procedure, experiments showed that with a tenfold decrease in the FMOC concentration the signal of FMOC-glufosinate remained constant. Expecting some increase in selectivity towards secondary amines present in water samples and less interference of

the unreacted excess of reagent, the lower FMOC concentration was selected for further work (for the final procedure, see Experimental).

3.2. Separation on second column

Glufosinate forms with FMOC a derivative by reaction of the amine (analyte) and the acid chloride (FMOC-Cl), yielding an anionic compound. According to the literature [9–12], the separation of FMOC-glyphosate is preferably performed on an amino-bonded silica column in combination with aqueous phosphate solution. The important factors for the separation, viz., percentage of modifier and the ionic strength and pH of the buffer, have been discussed in detail [11]. Using this information, a 250×4.6 mm I.D. amino column with a mobile phase of acetonitrile–0.05 M phosphate in water (35:65, v/v) were selected as the initial LC conditions. Investigating the influence of the pH (tested pH range = 3–7), it appeared that the retention was maximum at pH 4 ($k' = 12$) and decreased at lower pH ($k' = 4$ at pH 3) or higher pH ($k' = 2$ at pH 7). Further, a decrease in the ionic strength (tested phosphate concentration = 0.05–0.005 M, pH = 5.5) increased the retention considerably ($k' = 3.3$ and 20 at 0.05 and 0.005 M phosphate, respectively). In this case, however, the high retention leads to excessive band broadening. Hence a decrease in ionic strength is not advantageous for improving retention. Acetonitrile–0.05 M phosphate (pH 5.5) in water (35:65, v/v) was therefore selected as a good compromise between separation ($k' = 4$) and the peak shape of FMOC-glufosinate. It is well known that a phosphate solution at the selected pH of 5.5 will not have any buffer capacity and therefore fluctuations in retention can be expected. At such a pH, a citrate buffer is more suitable. In comparison with phosphate, the application of a 0.05 M citrate (pH 5.5) solution resulted in considerable band broadening of the analyte at a similar retention. A mixture of phosphate–citrate buffer did not improve this situation. Apparently, only the presence of phosphate ions favourably influences the elution profile of

FMOC-glufosinate on the amino-bonded column. Therefore, a new experiment was performed, increasing the ionic concentration to 0.1 M phosphate, which reduced the peak volume of FMOC-glufosinate (the retention was not affected) and provided a 25% increase in peak height. Owing to possible damage of the pistons and seals, higher salt concentrations were not investigated and 0.1 M phosphate was finally selected for mobile phase M-2. Increasing the column temperature (range 30–50°C) did not improve the elution profile of the analyte.

3.3. Clean-up procedure on first column

The first step in obtaining an efficient preseparation between FMOC and FMOC-glufosinate was to employ a small column (4×4 mm I.D.) packed with 5-μm C_{18} (Waters–Millipore). In order to minimize disturbances of the ion-exchange separation on the second column (C-2), a mobile phase of acetonitrile–0.05 M phosphate (pH 5.5) in water (35:65, v/v) was selected on C-1. As discussed in earlier work [24–26], the attainable sensitivity and selectivity and selectivity of a column-switching procedure will depend on how much sample can be injected on to the first column and transferred to the second column without excessive band broadening of the analyte. Actually, two processes are crucial: (i) elution of the analyte during injection, which in this instance will be determined by the degree of retention of the analyte on C_{18}, and (ii) peak compression prior to transfer, which will depend on the eluotropic strength of the mobile phase(s). Applying large-volume injections, elution on C-1 must be considered as a step gradient in which the same volume acts as the first mobile phase. Consequently, the eluotropic strength (percentage of acetonitrile) of the sample solution will be a determining parameter and it should be kept as low as possible to minimize band broadening of the analyte during injection. Experiments clearly indicated that a quantitative FMOC reaction of glufosinate requires the presence of at least 40% (v/v) of acetonitrile, which is in agreement with the selected procedure [11]. Under the selected LC conditions, the maximum

sample injection volume avoiding excessive band broadening of the analyte (sensitivity) and also providing the minimum required separation between the compound and unreacted FMOC (selectivity) was about 20 μl. The sample loadability could be significantly increased by an aqueous dilution the sample prior to injection. For example, a tenfold diluted solution (with borate buffer) containing 4% of acetonitrile allowed an injection volume of 500 μl. Establishing the obtainable sensitivity and selectivity with respect to sample dilution and injection volume, a threefold dilution with borate buffer appeared to optimum (15% of acetonitrile). From this solution about 200 μl could be injected on to the C_{18} precolumn, giving a marginal separation between the analyte and FMOC. Dilution with pure water or aqueous 0.05 M phosphate solutions (pH range 1–5) resulted in an insufficient separation between FMOC and the analyte.

In order to increase the sample loadability (sensitivity), a 5-μm C_{18} column (30 × 4.6 mm I.D.) with a greater separation power than the 5-μm C_{18} column (4 × 4 mm I.D.) was selected as C-1. Maintaining the same mobile phase, it appeared that large-volume injections (up to at least 1.0 ml) on this column resulted in a very favourable elution of the FMOC-glufosinate peak. It appeared that the sample mobile phase (15% of acetonitrile) results in a sufficient retention and acceptable peak volume of the analyte, whereas with the mobile phase of the column (35% of acetonitrile) the analyte elutes as an unretained compound well separated from the later eluting FMOC. This favourable elution behaviour is illustrated in Fig. 2A, showing the chromatogram obtained on C-1 of a 1-ml injection of spiked glufosinate solution (100 μg/l) diluted threefold with borate buffer after derivatization (for procedure, see Experimental).

Fig. 2B shows the chromatogram obtained for a 330-μl injection of an undiluted solution (40% of acetonitrile) containing the same amount of sample as the diluted solution (15% of acetonitrile) in Fig. 2A. The chromatograms clearly demonstrate the usefulness of the dilution step to prevent excessive peak tailing and, consequently, to improve sensitivity. Moreover, the dilution
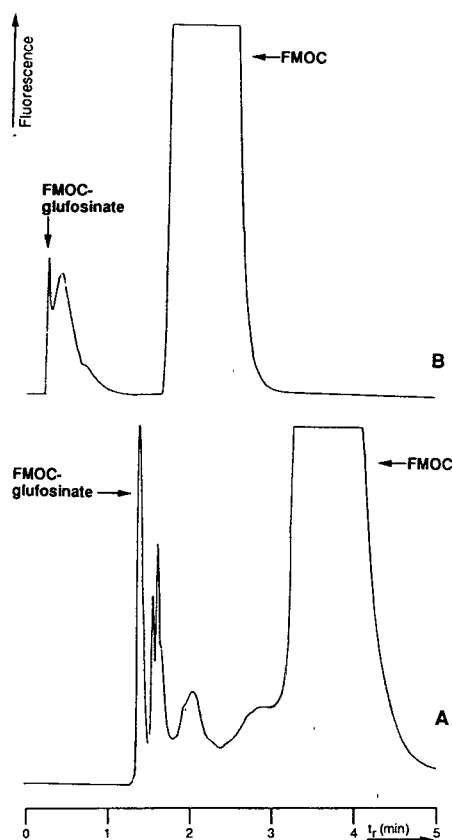
Fig. 2. Chromatograms recorded on C-1 connected to the fluorescence detector of a glufosinate standard solution (100 μg/l) obtained after FMOC derivatization. (A) 1000 μl of the solution after a threefold dilution with borate buffer; (B) 330 μl of the undiluted solution. See text for further explanation.

step allows the application of a small transfer volume (300 μl), which is favourable for the selectivity.

In order to enhance the sensitivity further, the injection of larger sample volumes (up to 4 ml) was investigated. It appeared that volumes larger than 2 ml did not substantially increase the signal of the analyte.

Fig. 3 shows the chromatogram of a 10 ppb glufosinate standard solution obtained with the proposed procedure, which employs a "clean-up" volume of 2.3 ml after injection (injection volume included) and a transfer volume of 300 μl.
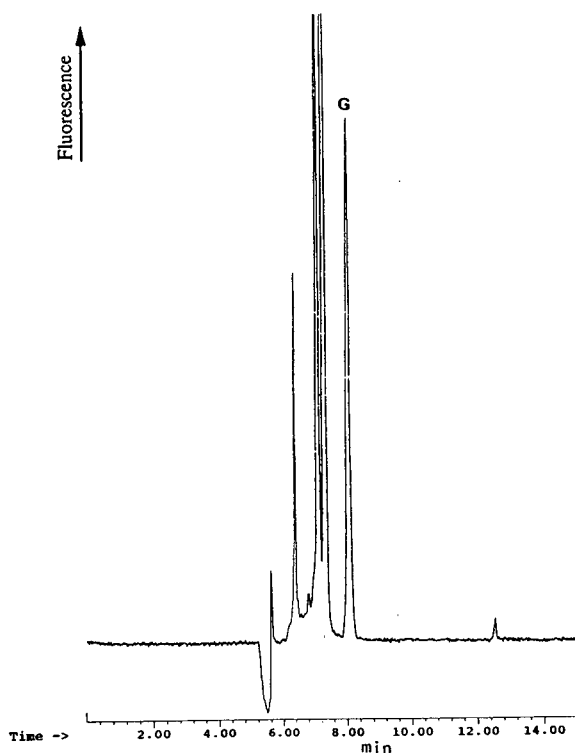
Fig. 3. Column-switching LC with fluorescence detection (FD) with large-volume (2.0 ml) sample injection of a surface water sample spiked with glufosinate at a level of 10 μg/l. For LC conditions, see Experimental.

Complete automation of the whole procedure including precolumn derivatization by means of the autosampler used seems an interesting feature. However, the maximum available volume of the autosampler vials (<1.8 ml) limited the possibility of making proper dilutions after reaction and to perform large-volume injections (2 ml). Making no concession to sensitivity, the simple off-line precolumn derivatization procedure was preferred to a completely automated procedure.

4. Results

The response of FMOC-glufosinate was linear for standard solutions of glufosinate in water with concentrations between 0.25 and 100 μg/l ($r = 0.9996$, $n = 5$). The described procedure (see

Experimental) was validated by analysing various types of water samples spiked with glufosinate. The recoveries at several levels are given in Table 2. The performance of the procedure is illustrated in Fig. 4, which shows the LC analysis of surface water spiked with glufosinate at 1 μg/l. It appeared that for all types of water samples the resulting chromatograms were very similar, rendering a sensitive and selective procedure. Partly owing to good reproducibility of the chromatographic patterns, the limit of detection was found to be 0.25 μg/l (signal-to-noise ratio = 3). The LC analysis of a surface water sample spiked at this low level is shown in Fig. 5, in which the chromatogram was obtained by means of blank subtraction. Three different water matrices (ground, surface and drinking water, $n = 2$ for each sample type) spiked at 1 μg/l were analysed on different days. As indicated in Table 2, the corresponding recovery and reproducibility ($n = 6$) of these experiments was 97% and 10%, respectively.

The rapid precolumn derivatization procedure (see Experimental) and the short time of the subsequent LC analysis result in a sample throughput of at least 50 per day. The method appears to be very robust. During the time of experiments (3 months of daily use), the C_{18} column (C-1) maintained its performance and readjustment of column-switching conditions was

Table 2
Recoveries and relative standard deviations (R.S.D.) for environmental water samples spiked at different levels with glufosinate

Spiked level (μg/l)	Recovery (%)	R.S.D. (%)
5[a]	100	2.1
0.5[a]	95	2.0
0.25[a]	118	11
1[b]	97	10
0.1[c]	78	12

[a] Surface water ($n = 5$).
[b] Surface water ($n = 2$), ground water ($n = 2$) and drinking water ($n = 2$), analysed on different days.
[c] Ground water ($n = 5$); values obtained after fivefold preconcentration of water sample.
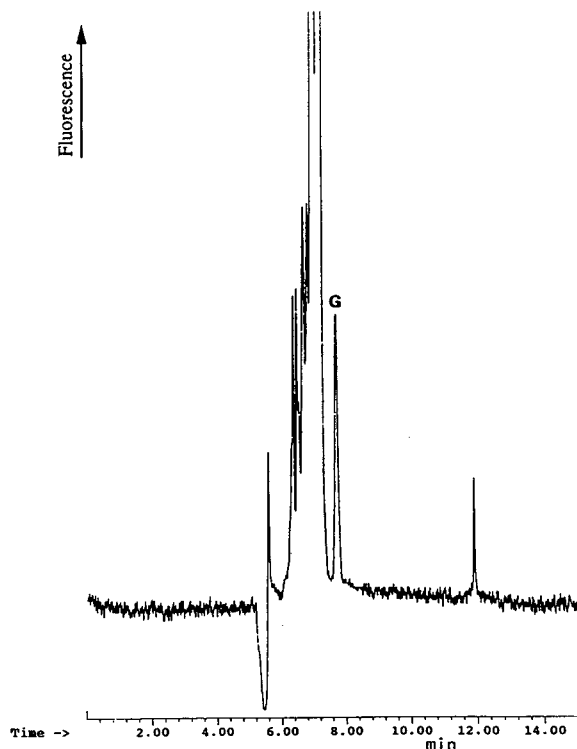
Fig. 4. Column-switching LC–FD with large-volume (2.0 ml) injection of a surface water sample containing 1.0 μg/l of glufosinate. (For LC conditions, see Experimental).

Fig. 5. Column-switching LC–FD of a surface water sample spiked with glufosinate at the 0.25 μg/l level. Chromatogram obtained after blank subtraction. LC conditions as in Fig. 4.

not necessary. The amino column (C-2) suffered a gradual decrease in efficiency only noticeable after 2 months of use.

The possibility of lowering the limit of detection to 0.1 μg/l by simply concentrating a certain volume of water sample prior to derivatization was investigated. A fivefold decrease in sample volume by means of a Rotovapor (see Experimental) was sufficient to determine glufosinate in groundwater down to a level of 0.1 μg/l. Fig. 6 shows a chromatogram for a surface sample spiked at 0.1 μg/l and concentrated fivefold. The recovery and repeatability ($n = 5$) at this level were 78% and 12% (relative standard deviation), respectively.

5. Conclusions

The combination of precolumn FMOC derivatization and coupled-column LC with fluores-cence detection appears to be a viable approach for the rapid determination of glufosinate in environmental water samples down to a level of 0.25 μg/l. The sample throughput of about 50 per day makes the procedure highly suitable for screening purposes. If necessary, the limit of detection can be lowered to 0.1 μg/l by means of a simple preconcentration step.

Acknowledgements
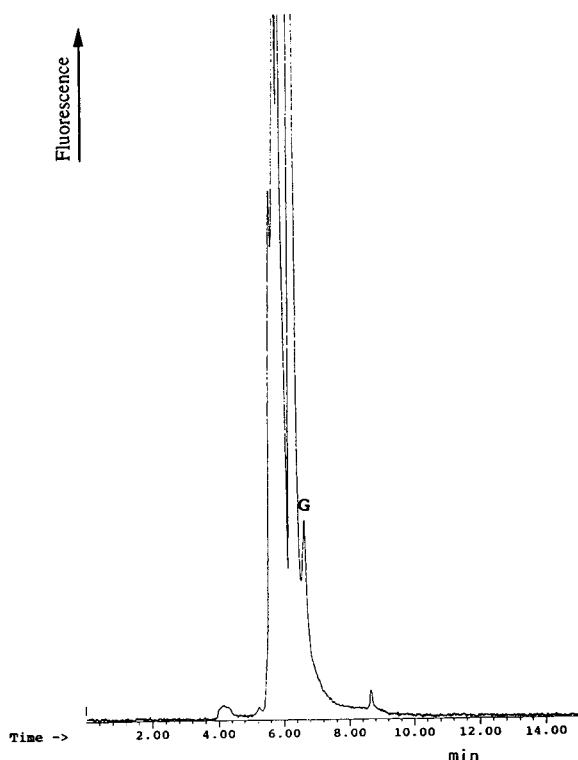
Fig. 6. Column-switching LC–FD of a fivefold concentrated surface water sample spiked with glufosinate at the 0.1 μg/l level. LC conditions as in Fig. 4.

References

[1] M. Fielding, D. Barceló, A. Helweg, S. Galassi, L. Torstensson, P. van Zoonen, R. Wolter and G. Angeletti, in M. Fielding (Editor), *Pesticides in Ground and Drinking Water* (*Water Pollution Research Report*, 27), Commission of the European Community, Brussels, 1992, pp. 1–67.

[2] S. Dubbelman, in J. Sherma (Editor), *Analytical Methods for Pesticides and Plant Growth Regulations, Specific Applications*, Vol. XVI, Academic Press, New York, 1988, Ch. 6, p. 69.

[3] N.J. Seiber, M.M. McChesney, R. Kon and R.A. Leavitt, *J. Agric. Food Chem.*, 32 (1984) 681.

[4] H.A. Moye and C.L. Deyrup, *J. Agric. Food Chem.*, 32 (1984) 193.

[5] D.N. Roy and S.K. Konar, *J. Agric. Food Chem.*, 37 (1989) 441.

[6] S.K. Konar and D.R. Roy, *Anal. Chim. Acta*, 229 (1990) 227.

[7] N. Tsunoda, *J. Chromatogr.*, 637 (1993) 167.

[8] R. Schuster and A. Gratzfeld-Hüsgen, *A Comparison of Pre- and Post-Column Sample Treatment for the Analysis of Glyphosate* (*Hewlett-Packard Application Note*, Publication No. 12-5091-3621 E) Hewlett-Packard, Avondale, PA, 1992.

[9] R.L. Glass, *J. Agric. Food Chem.*, 31 (1983) 280.

[10] H. Rosenboom and C.J. Berkhoff, *Anal. Chim. Acta*, 135 (1982) 373.

[11] C.J. Miles, L.R. Wallace and H.A. Moye, *J. Assoc. Off. Anal. Chem.*, 69 (1986) 458.

[12] R. Gauch, U. Leuenberger and U. Müller, *Z. Lebensm.-Unters.-Forsch.*, 188 (1989) 458.

[13] H.A. Moye, C.J. Miles and S.J. Scherer, *J. Agric. Food Chem.*, 31 (1983) 69.

[14] L.G.M.Th. Tuinstra and P.G.M. Kienhuis, *Chromatographia*, 24 (1987) 696.

[15] J.E. Cowell, J.L. Kunstman, P.J. Nord, J.R. Steinmetz and G.R. Wilson, *J. Agric. Food Chem.*, 34 (1986) 955.

[16] Y.Y. Wigfield and M. Lanouette, *Anal. Chim. Acta*, 233 (1990) 311.

[17] M.E. Oppenhuizen and J.E. Cowell, *J. Assoc. Off. Anal. Chem.*, 74 (1991) 317.

[18] *EPA Method 547, Analysis of Glyphosate in Drinking Water by Direct Aqueous Injection HPLC with Post-Column Derivatisation*, Office of Research and Development, United States Environmental Protection Agency, Cincinatti, OH, 1990.

[19] C.R. Worthing and R.J. Hance (Editors), *The Pesticide Manual, a World Compendium*, British Crop Protection Council, Old Woking, 1991, 9th ed., p. 458.

[20] P.A. Greve (Editor), *Analytical Methods for Residues of Pesticides in Foodstuffs, Part III*, SDU, The Hague, 5th ed., 1988, p. 75.

[21] *Report Hoe 039866*, Hoechst, Frankfurt, 1983.

[22] H. Sochor, Ch. Eichelmann and G. Schuld, *Gaschromatographische Bestimmung von Hoe 039866 (Glufosinateammonium) sowie dessen Metaboliten Hoe 061517 in Trinkwasser*, Report No. AL 66/88-0, Hoechst, Frankfurt, 1988.

[23] M. Blacha-Puller and J. Siebers (Editors), *Rückstandsanalysenmethoden, Teil I*, Biologische Bundesanstalt für Land- und Forstwirtschaft, Braunschweig, 1989, p. 185.

[24] H.P. Thier and I. Kirchhoff (Editors), *Manual of Pesticide Residue Analysis*, Vol. II, DFG, Pesticides Commission, VCH, Weinheim, 1992, p. 477.

[25] E.A. Hogendoorn, P. van Zoonen and U.A.Th. Brinkman, *Chromatographia*, 31 (1991) 285.

[26] E.A. Hogendoorn, C. Verschraagen, U.A.Th. Brinkman and P. van Zoonen, *Anal. Chim. Acta*, 268 (1992) 205.

[27] E.A. Hogendoorn, U.A.Th. Brinkman and P. van Zoonen, *J. Chromatogr.*, 644 (1993) 307.

Determination of (2S, 3S, 5R)-3-methyl-7-oxo-3-(1H-1,2,3-triazol-1-ylmethyl)-4-thia-1-azabicyclo[3.2.0]heptane-2-carboxylic acid 4,4-dioxide (YTR-830H) and piperacillin in pharmaceutical preparations by high-performance liquid chromatography

Tsuyoshi Tsukamoto*, Takanori Ushio

Department of Analytical Research, Pharmaceutical Research Laboratory, Taiho Pharmaceutical Co., Ltd., 224-2, Ebisuno, Hiraishi, Kawauchi-cho, Tokushima 771-01, Japan

Abstract

A high-performance liquid chromatographic method using a wavelength-scanning system was developed for the determination of (2S, 3S, 5R)-3-methyl-7-oxo-3-(1H-1, 2, 3-triazol-1-ylmethyl)-4-thia-1-azabicyclo[3.2.0]heptane-2-carboxylic acid 4,4-dioxide (I) and piperacillin (PIPC) in pharmaceutical preparations. I and PIPC were determined using a reversed-phase column with a mixture of 10 mM tetra-n-butylammonium hydroxide and 5 mM K_2SO_4 (pH 4.1), acetonitrile and methanol (1000:300:25) as the mobile phase. Addition of SO_4^{2-} to the mobile phase was useful for the separation of related substances and improving the peak tailing of I and PIPC. This mobile phase was also suitable for the determination of PIPC, I and their degradation products in pharmaceutical preparations. Detection was based on the ultraviolet absorption of I at 220 nm and of PIPC at 270 nm using a wavelength-scanning system. The calibration graphs were linear over the ranges 0–7.5 μg for I and 0–30 μg for PIPC. The precisions (relative standard deviations of six analyses) of I and PIPC were 0.45% and 0.33%, respectively.

1. Introduction

The combined use of β-lactam antibiotics with β-lactamase inhibitor was effective against β-lactamase-producing antibiotic-resistant strains. Clavulanic acid and sulbactam have been developed as potent β-lactamase inhibitors [1,2] and have been commercialized world-wide. A novel β-lactamase inhibitor, YTR-830H, (2S, 3S,

5R)-3-methyl-7-oxo-3-(1H-1,2,3-triazol-1-ylmethyl)-4-thia-1-azabicyclo[3.2.0]heptane-2-carboxylic acid 4,4-dioxide (I) (Fig. 1), was introduced by Micetich et al. [3]. Various investigations of I with β-lactam antibiotics [4–12] showed that the combined use of I with piperacillin (PIPC) was most effective against various β-lactamase-producing bacteria [13].

An analytical method was required for the combined formulation of I and PIPC. At first I and PIPC in pharmaceutical preparations were

* Corresponding author.
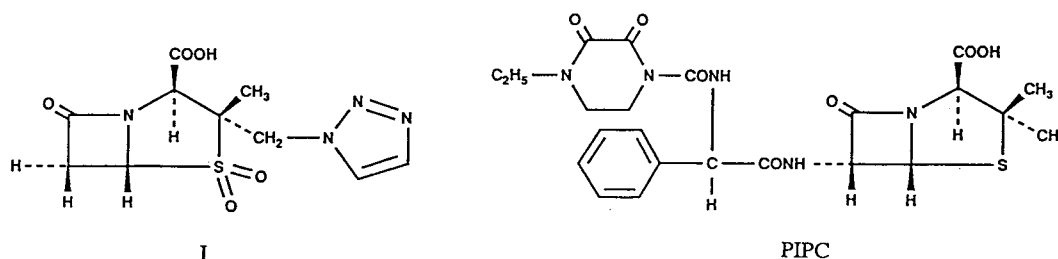
Fig. 1. Structures of I and piperacilln (PIPC).

separately determined by using individual HPLC methods. However, a simple and reliable HPLC method was required for pharmaceutical preparations, involving routine quality control and stability assays. I and PIPC have no UV absorption maxima above 210 nm. Degradation of I [14,15] and PIPC [16] yielded many structurally related compounds. This paper describes an HPLC method for the simultaneous determination of I and PIPC using ion-pairing and wavelength-scanning techniques. The method was successfully applied to the separation of degradation products of I and PIPC in a stability study of pharmaceutical preparations.

2. Experimental

2.1. Chemicals and reagents

Methanol, acetonitrile and tetra-n-butylammonium hydroxide (TBAH) solution (0.5 M) of HPLC-grade were obtained from Wako (Osaka, Japan). Tetra-n-butylammonium hydrogensulphate (TBAHS) of analytical-reagent grade was purchased from Aldrich (Steinheim, Germany). Diammonium hydrogenphosphate, potassium sulphate and phosphoric acid of analytical-reagent grade were purchased from Wako. Water purified with a Milli-Q water-purification system (Millipore, Bedford MA, USA) was used in all procedures. Combined formulations of I and PIPC, with a mass ratio of 1:4, were prepared by Taiho Pharmaceutical (Tokyo, Japan).

2.2. Instrumentation

The HPLC system consisted of a Model 600E multi-solvent delivery system, a Model 468 pro-

grammable multi-wavelength detector and a WISP Model 712 autosampler (Waters Chromatography Division, Millipore, Milford, MA, USA) or a Model LC-7A multi-solvent delivery system, a Model SPD-6AV programmable multi-wavelength detector (Shimadzu, Kyoto, Japan) and a WISP model 712 autosampler (Waters Chromatography Division). A Model C-R4A integrator (Shimadzu) was used to record chromatograms and calculate peak areas. A Waters Model 990J photodiode-array detector was used when assessing the homogeneity of the YTR-830H and PIPC peaks.

2.3. Columns

The analytical columns used were as follows: column A, Ultron phenyl; column B, Ultron N-C_{18}; column H, Ultron ODS-X; and column I, Ultron N-C_8 (all from Shinwa Chemical Industries, Kyoto, Japan); column C, TSK-Gel ODS 80TM (Tosoh, Tokyo, Japan); column D, Wakopak 5C_{18} (Wako); column E, Unisil Q C_{18} (GL Science, Tokyo, Japan); column F, Capcellpak C_{18} (Shiseido, Tokyo, Japan); and column G, Cosmosil 5C_{18} (Nacalai Tesque, Osaka, Japan). All packing materials were made from silica gels except for the Capcellpak C_{18}, which is made from a polymer-coated silica gel. All materials were packed into a 150 mm × 4.6 mm I.D. stainless-steel column.

2.4. Sample preparation

Known amounts of I and PIPC were dissolved in mobile phases or a mixture of acetonitrile and mobile phase. The concentrations of I and PIPC were adjusted to about 0.5 and 2.0 mg/ml, respectively.

2.5. HPLC analysis

A 10-μl aliquot of the sample solution was injected on to a column. Other chromatographic conditions are given in the figures and tables. The influence of the mobile phase pH and concentrations of ion-pairing reagent, SO_4^{2-} and methanol on capacity factors, peak tailing, separation factor and the resolution of I and PIPC were examined as described under Results and Discussion. Chromatographic parameters such as tailing and resolution were calculated according to the Pharmacopoeia of Japan [17]. The concentrations of I and PIPC in the sample were calculated from a calibration graph of concentration *vs.* peak area.

3. Results and discussion

3.1. Influence of mobile phase pH

The retention of I and PIPC was investigated with and without addition of TBAHS as an ion-pairing reagent. The ion-pairing reagent was useful for the simultaneous determination of I and PIPC under isocratic conditions. When the pharmaceutical preparation was stored in heated conditions, degradation of I and PIPC yielded many structurally related compounds. Therefore, we focused just on a main unknown degradation product. First, 5 mM TBAHS was used as an ion-pairing reagent. The pH of the mobile phase was adjusted with phosphoric acid. The relationships between the capacity factors (k') of I, PIPC and the main unknown degradation product and the pH of the mobile phase were investigated at pH 3.8, 5.3 and 7.0. When the pH of the mobile phase was increased to 7.0, the k' values of I and PIPC decreased. The separation of degradation products from I and PIPC was then investigated under acidic conditions. The chromatograms obtained with the use of TBAH and TBAHS were almost identical. However, for the separation of degradation products from PIPC, TBAH was better than TBAHS. In subsequent investigations 6.5 mM TBAH was used as the ion-pairing reagent.

The relationships between the capacity factors

Table 1
Influence of the mobile phase pH on the capacity factors of I, PIPC and the main degradation product

Compound	Capacity factor (k')		
	pH 5.0	pH 4.0	pH 3.1
I	1.36	1.53	1.55
PIPC	4.50	4.89	4.18
Main degradation product	3.33	2.84	2.53
α[a]	1.35	1.72	1.65

I and PIPC was stored at room temperature for 8 days. Chromatographic conditions: column, Ultron N-C_8; mobile phase, mixture of water containing 6.5 mM TABH (pH is adjusted with phosphoric acid) and acetonitrile (100:45); column temperature, room temperature; flow-rate, 0.7 ml/min; detection wavelength, 220 nm. Mean results ($n = 3$).
[a] Separation factor of PIPC and main degradation product.

and the pH of the mobile phase at pH 3.1, 4.0 and 5.0 are shown in Table 1. As the pH of the mobile phase was increased to 5.0, the k' value of the unknown degradation product increased. The capacity factor of I remained unchanged, and that of PIPC was maximum at pH 4.0. Taking into account the separation of I and PIPC and the separation of degradation products from I and PIPC, the optimum pH of mobile phase was about 4 for the simultaneous determination of I and PIPC.

3.2. Column selection

Various commercially available reversed-phase columns were examined for the separation of I and PIPC by using a mobile phase (pH 4.1, adjusted with phosphoric acid) containing 6.5 mM TBAH as an ion-pairing reagent. Degradation of pharmaceutical preparations yielded many structurally related compounds. The separation of degradation products from I and PIPC was investigated using the degraded sample. The capacity factors and tailing factors of I and PIPC and the resolution between I and PIPC are shown in Table 2. All the reversed-phase columns were efficient for the separation of I and PIPC. However, the peaks were broad with the use of phenyl and polymer-coated ODS columns. Columns G and H were better for the separation

Table 2
Capacity factors (k'), tailing factors (T) and resolution (R_s) of I and PIPC on various columns

Column	I		PIPC		R_s
	k'	T	k'	T	
A	1.40	1.21	5.63	1.62	14.9
B	1.25	1.58	4.12	2.60	15.1
C	2.35	1.72	8.26	2.94	18.1
D	1.63	—	5.29	—	—
E	1.75	1.22	5.83	2.04	13.1
F	1.12	1.67	3.28	2.79	9.1
G	1.43	1.88	4.51	3.12	10.6
H	1.19	1.70	3.52	2.73	11.0
I	1.24	1.62	3.79	2.36	12.0

Chromatographic conditions: mobile phase, mixture of 6.5 mM TBAH (pH 4.1, adjusted with phosphoric acid) and acetonitrile (1000:450 or 1000:400); column temperature, room temperature; flow-rate, 0.7 ml/min. Column H = Ultron ODS-X. Mean results ($n = 3$).

of degradation products from I and PIPC. Taking into account the analytical time and tailing factor, column H (Ultron ODS-X, 5 μm particle size, 16% carbon content) was selected for the simultaneous determination of I and PIPC.

3.3. Influence of concentration of ion-pairing reagent

Table 3 shows the influence on the capacity factors and tailing factors of I and PIPC and the resolution between I and PIPC of the concen-

Table 3
Influence of concentration of TBAH on the capacity factors (k'), tailing factors (T) and resolution (R_s)

Concentration of TABH (mM)	I		PIPC		R_s
	k'	T	k'	T	
3	1.94	1.79	6.35	3.95	13.2
10	1.76	1.60	6.14	3.25	16.3
15	1.72	1.55	6.22	2.95	17.6

Chromatographic conditions: column, Ultron ODS-X; mobile phase, mixture of each concentration of TBAH (pH 4.1, adjusted with phosphoric acid) and acetonitrile (10:4); column temperature, room temperature; flow-rate, 0.7 ml/min; detection wavelength, 220 nm. Mean results ($n = 3$).

tration of an ion-pairing reagent with a mobile phase of pH 4.1. At pH 4.1, changes in the TBAH concentration in the mobile phase had almost no effect on the retentions of I and PIPC. However, an increase in the concentration of the ion-pairing reagent gave an increase in resolution between I and PIPC and a decrease in the peak tailing of I and PIPC. In the degraded sample, the degradation products were not separated from I at a concentration of 3 mM TBAH and PIPC at a concentration of 15 mM TBAH. Therefore 10 mM TBAH was selected.

3.4. Influence of SO_4^{2-} ion and methanol

The influence of the SO_4^{2-} ion on the tailing of I and PIPC at concentrations of 2, 5 and 10 mM K_2SO_4 in the mobile phase was investigated. Addition of 2–10 mM SO_4^{2-} ion to the mobile phase gave significant improvements to the PIPC peak tailing and the resolution between I and PIPC. The tailing factor of PIPC was dependent on the concentration of SO_4^{2-}. When the concentration of SO_4^{2-} in the mobile phase was increased from 2 to 10 mM, the tailing of PIPC decreased from 2.88 to 2.23 and the retention of PIPC decreased. This gave a change in resolution between I and PIPC. In the degraded sample, the degradation products were not separated from I at a concentration of 10 mM SO_4^{2-} and from PIPC at a concentration of 2mM SO_4^{2-}. Therefore, 5 mM SO_4^{2-} was selected. Addition of methanol to the mobile phase was also effective for the separation of degradation products from PIPC.

Based on the above findings, a mixture of 10 mM TBAH and 5 mM K_2SO_4 (pH 4.1), acetonitrile and methanol (1000:300:25) was selected for routine assays of I and PIPC.

3.5. Determinations of I and PIPC in pharmaceutical preparations

The mass ratio of I and PIPC in pharmaceutical preparations was 1:4, whereas their peak-area ratio was 1:8 at 220 nm under the HPLC conditions described above. Detection of

I and PIPC was investigated using the wave-length-scanning technique for the assay of low concentrations of **I**. The repeatabilities of the assays of **I** and PIPC detection at 220 nm and with wavelength-scanning detection (**I** at 220 nm and PIPC at 270 nm) are shown in Table 4, where the wavelength was scanned from 220 to 270 nm 8 min after injection. This result revealed that the repeatabilities based on wavelength-scanning detection are better than those based on detection at 220 nm. Hence wavelength-scanning detection was obviously useful for assays of **I** and PIPC in pharmaceutical preparations and was selected in order to obtain higher repeatabilities. A typical chromatogram of standard **I** and PIPC is shown in Fig. 2, where methyl benzoate was used as an internal standard.

3.6. Linearity and precision

The linearity of the response was good for both **I** and PIPC throughout the range of concentrations studied (**I**, 0–7.5 μg per 10 μl; PIPC, 0–30 μg per 10 μl). Regression analysis of mass (x) *versus* peak-area ratio of **I** and PIPC to the internal standard (y) gave straight lines with correlation coefficients of 1.000 and 0.9998 ($y = -0.003 + 0.1153x$, $y = -0.019 + 0.0585x$), respectively. The relative standard deviations (R.S.D.) for **I** and PIPC for six or seven replicates assays were 0.45% and 0.33% respectively, for within-day assay, and 0.78% and 0.52%, respectively for day-to-day assay.
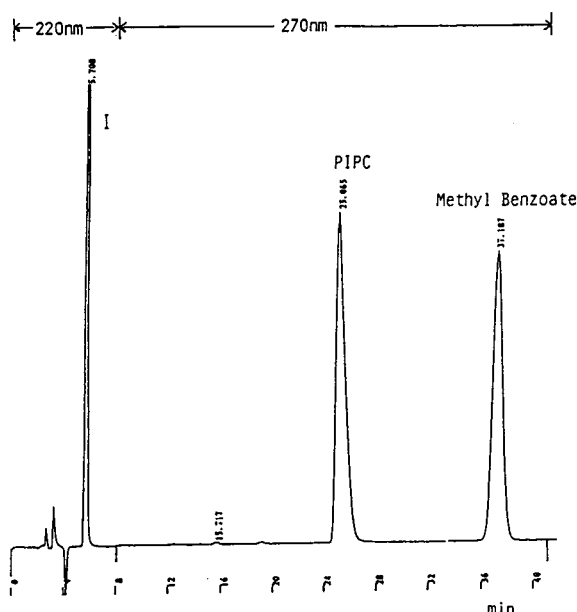
Fig. 2. Chromatogram of standard in the determination of pharmaceutical preparations. Chromatographic conditions: column, Ultron ODS-X; mobile phase, mixture of 10 m*M* tetrabutylammonium hydroxide (TBAH) and 5 m*M* K$_2$SO$_4$ (pH 4.1, adjusted with phosphoric acid), acetonitrile and methanol (1000:300:25); column temperature, room temperature; flow-rate, 0.7 ml/min; detection, **I** at 220 nm, PIPC at 270 nm; sample size, 25 μg.

3.7. Application of the proposed method

The stability of the solution of a sample of the combined formulation of **I** and PIPC at 5°C was investigated by the proposed method. After

Table 4
Repeatabilities of assays of **I** and PIPC with detection at 220 nm or with wavelength scanning from 220 to 270 nm

Parameter	I		PIPC	
	220 nm	220–270 nm[a]	220 nm	220–270 nm[a]
Mean (%)[b,c]	100.4	99.9	100.0	99.8
R.S.D. (%)[c]	0.50	0.27	0.54	0.15

Chromatographic conditions as in Fig. 2.
[a] The wavelength was scanned 8 min after injection.
[b] Percentage to the labelled amounts of **I** and PIPC in pharmaceutical preparations.
[c] $n = 6$.
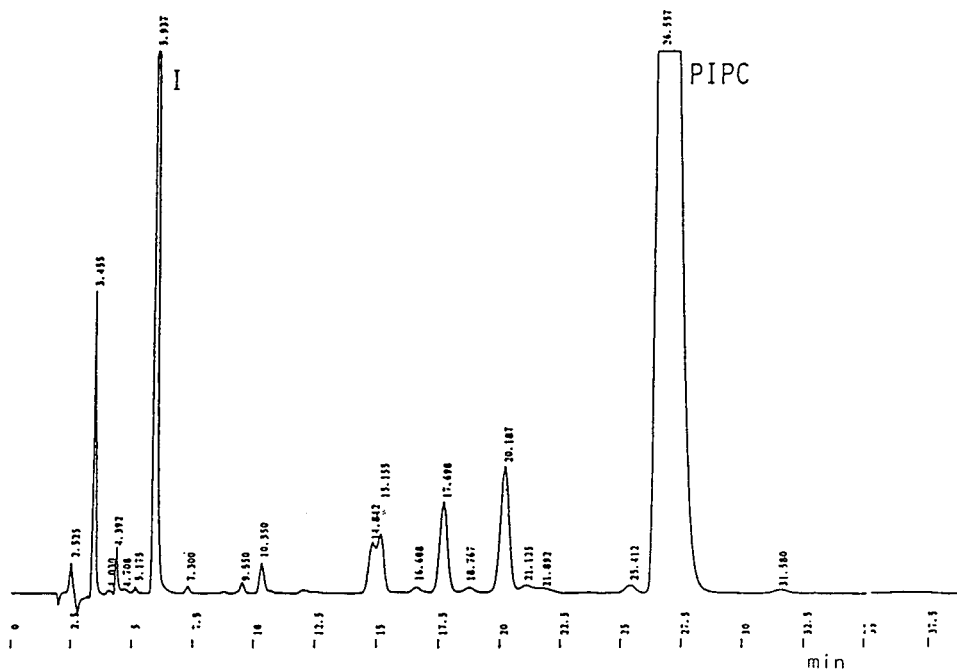
Fig. 3. Chromatogram of skin test ampoule. An ampoule was stored at 40°C for 3 months was used. The sample was treated as described under Experimental. Chromatographic conditions as in Fig. 2, except for detection wavelength, 220 nm.

storage for 36 h at 5°C, the residual contents of I and PIPC were 99.5% and 101.1%, respectively.

Fig. 3 shows the chromatogram of I and PIPC in a skin test ampoule (40°C, 3 months), in the form of a pharmaceutical preparation for al-

lergenic testing. The homogeneities of the I and PIPC peaks were verified by using photodiode-array detection. The specific chromatogram of the degraded sample at 220 and 230 nm is shown in Fig. 4. The ratios of the absorbances at 220
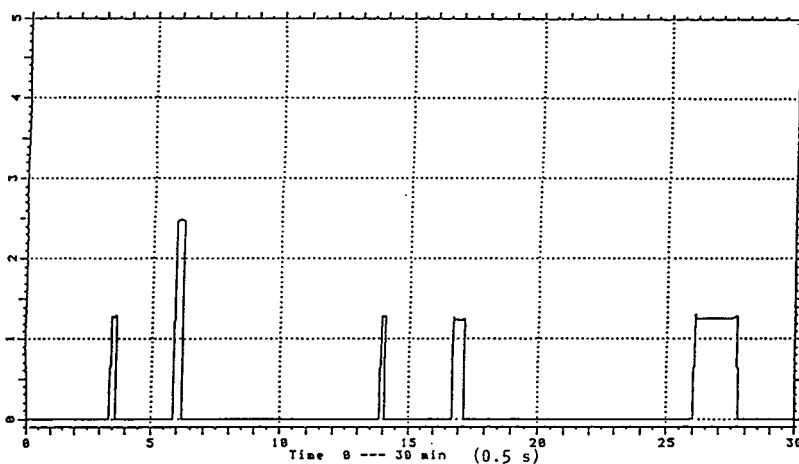
Fig. 4. Specific chromatogram of heat-degraded sample. Sample and chromatographic conditions as in Fig. 3, except for detection wavelength.

and at 230 nm for **I** and PIPC were constant, and a rectangular chromatogram was obtained. These results reveal that **I** and PIPC are well separated from their degradation products, and that none of the degradation products interfere with the assays of **I** and PIPC.

When a sample of the combined formulation of **I** and PIPC was degraded for 3 months at 40°C, the resulting mixtures contained many degradation products. The chromatogram of the degraded sample at 220 nm is shown in Fig. 5. Double the volumes used to obtain the chromatogram in Fig. 3 were injected, but **I** and PIPC were still well separated from their degradation products. Six replicate analyses of the sample showed that the content of degradation products was $16.27 \pm 0.20\%$ (mean $\pm$ S.D.), based on the UV absorbance at 220 nm.

In conclusion, the proposed method using wavelength scanning was successfully applied to routine quality control and stability assays of **I** and PIPC. Also, with the slight modification the method will be applicable to the determination of degradation products and the determination of **I** and PIPC in biological fluids.

Acknowledgement

References

[1] P.A. Hunter, K. Coleman, J. Fisher and D. Talor, *J. Antimicrob. Chemother.*, 6 (1980) 455; and references cited therein.
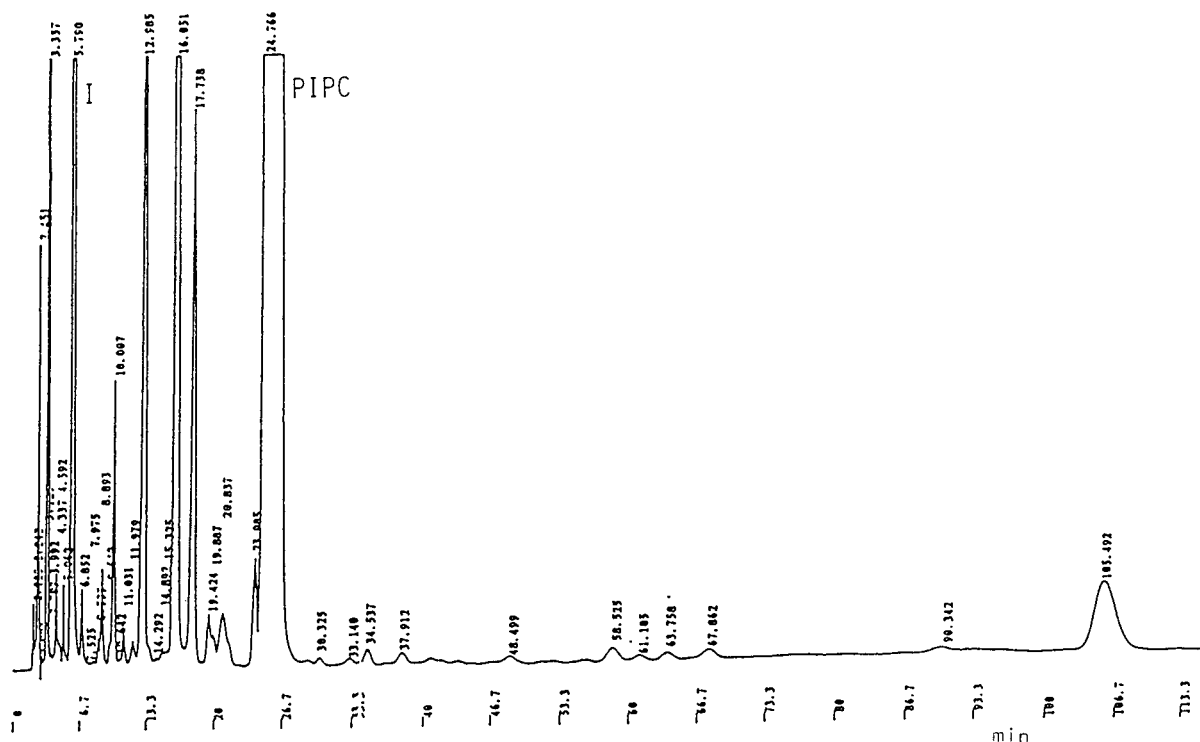
Fig. 5. Chromatogram of heat-degraded sample. Sample and chromatographic conditions as in Fig. 3, except for sample size, 50 μg.

[2] A.R. English, J.A. Retsema and A.E. Girand, J.E. Lynch and W.E. Barth, *Antimicrob. Agents Chemother.*, 14 (1978) 414.

[3] R.G. Micetich, T.W. Hall, S.N. Maiti, P. Sevak, S. Yamabe, N. Ishida, K. Ogawa, M. Tanaka, T. Yamasaki and A. Nakai, in J. Ishigami (Editor), *Proceedings of the 14th International Congress of Chemotherapy, Kyoto, 1985*, University of Tokyo Press, Tokyo, 1985, pp. 249–250.

[4] S. Aronoff, P. Labrozzi and S. Yamabe, in J. Ishigami (Editor), *Proceedings of the 14th International Congress of Chemotherapy, Kyoto, 1985*, University of Tokyo Press, Tokyo, 1985, pp. 1268–1269.

[5] S. Aronoff, P. Labrozzi, M. Jacobs and S. Yamabe, in J. Ishigami (Editor), *Proceedings of the 14th International Congress of Chemotherapy, Kyoto, 1985*, University of Tokyo Press, Tokyo, 1985, pp. 1270–1271.

[6] F. Moosdeen, J.D. Williams and S. Yamabe, in J. Ishigami (Editor), *Proceedings of the 14th International Congress of Chemotherapy, Kyoto, 1985*, University of Tokyo Press, Tokyo, 1985, pp. 1272–1273.

[7] N. Ishida, A. Hyodo, C. Hanehara, M. Miyake, Y. Kawaguchi and S. Yamabe, in J. Ishigami (Editor), *Proceedings of the 14th International Congress of Chemotherapy, Kyoto, 1985*, University of Tokyo Press, Tokyo, 1985, pp. 1274–1275.

[8] M.D. Kitzis, L. Gutmann, S. Yamabe and J.F. Acar, in J. Ishigami (Editor), *Proceedings of the 14th International Congress of Chemotherapy, Kyoto, 1985*, University of Tokyo Press, Tokyo, 1985, pp. 1276–1277.

[9] M.R. Jacobs, S.C. Aronoff, S. Johenning and S. Yamabe, in J. Ishigami (Editor), *Proceedings of the 14th International Congress of Chemotherapy, Kyoto, 1985*, University of Tokyo Press, Tokyo, 1985, pp. 1278–1279.

[10] S.C. Aronoff, M.R. Jacobs, S. Johenning and S. Yamabe, *Antimicrob. Agents Chemother.*, 26 (1984) 580.

[11] P.C. Appelbaum, M.R. Jacobs, S.K. Spangler and S. Yamabe, *Antimicrob. Agents Chemother.*, 30 (1986) 789.

[12] L. Gutmann, M.D. Kitzis, S. Yamabe and J.F. Acar, *Antimicrob. Agents Chemother.*, 29 (1986) 955.

[13] F. Higashitani, A. Hyodo, N. Ishida, M. Inoue and S. Mitsuhashi, *J. Antimicrob. Chemother.*, 25 (1990) 567.

[14] T. Marunaka, E. Matsushima, Y. Minami, K. Yoshida and R. Azuma, *Chem. Pharm. Bull.*, 36 (1988) 4478.

[15] E. Matsushima, K. Yoshida, R. Azuma, Y. Minami and T. Marunaka, *Chem. Pharm. Bull.*, 36 (1988) 4593.

[16] I. Saikawa, S. Takano, C. Yoshida, E. Saitoh, T. Mochida, H. Sakai, H. Takashita, F. Yamamoto and Y. Sugimoto, *Yakugaku Zasshi*, 97 (1977) 995.

[17] *The Parmacopoeia of Japan*, The Society of the Japanese Pharmacopoeia, Tokyo, 12th ed., 1991, p. 36.

Preparative separation of components of the color additive D&C Red No. 28 (phloxine B) by pH-zone-refining counter-current chromatography☆

Adrian Weisz[a,*], Denis Andrzejewski[b], Yoichiro Ito[c]

[a]Office of Cosmetics and Colors, US Food and Drug Administration, Washington, DC 20204, USA
[b]Office of Scientific Analysis and Support, US Food and Drug Administration, Washington, DC 20204, USA
[c]Laboratory of Biophysical Chemistry, National Heart, Lung, and Blood Institute, National Institutes of Health,
Bethesda, MD 20892, USA

Abstract

A pH-zone-refining counter-current chromatographic method was developed for the preparative (multigram) separation and purification of components of the commercial color additive D&C Red No. 28 (phloxine B). The chromatography of 3 and 6 g of color additive yielded 1.07 and 4.06 g, respectively, of pure 2',4',5',7'-tetrabromo-4,5,6,7-tetrachlorofluorescein, the principal component of D&C Red No. 28. The importance of the quantity of retainer acid (trifluoroacetic acid) relative to the amount of salt in the color additive is discussed.

1. Introduction

D&C Red No. 28 (Colour Index No. 45410) is a xanthene color additive used in drugs and cosmetics in the USA. It is identified as principally 1 (the disodium salt of 2',4',5',7'-tetrabromo-4,5,6,7-tetrachlorofluorescein), and may contain ≤4% of lower-halogenated subsidiary colors (including 2) and ≤2% of the ethyl ester 3 [1]. Under the name phloxine B, this dye is used as a biological stain [2,3]. D&C Red No. 28 is manufactured by bromination of 4,5,6,7-tetra-

chlorofluorescein (TCF), followed by alkaline hydrolysis of the reaction product (Fig. 1).

D&C Red No. 28 is subject to batch certification by the US Food and Drug Administration (FDA) [1] before it may be used for coloring drugs or cosmetics. For FDA's color additive certification program, pure 1 and pure lower-brominated subsidiary colors are needed for use as reference materials. Pure xanthene dyes are also desirable for use as biological stains. Their use would allow comparison of specimens stained in different laboratories [4–6] and promote standardization of biological stains [4,7].

Several methods for preparative-scale separation and purification of phloxine B were reported [8–10]. One of these uses acid precipitation [8] and does not separate the lower-halogenated isomers from 1. The other methods use

* Corresponding author.
☆ Presented at the *10th International Symposium on Preparative Chromatography, Arlington, VA, June 14–16, 1993.*
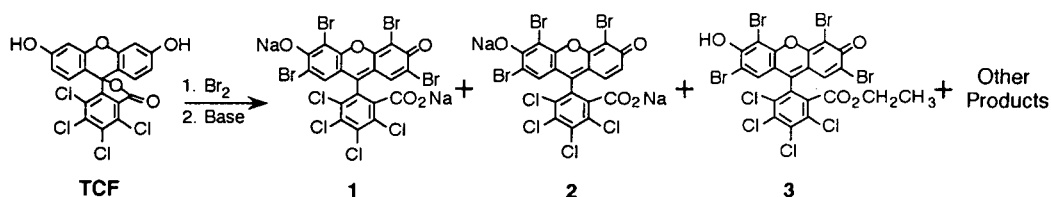
Fig. 1. Bromination of 4,5,6,7-tetrachlorofluorescein, followed by alkaline hydrolysis of the reaction product.

gel chromatography [9] and conventional high-speed counter-current chromatography (HSCCC) [10], and separate relatively small quantities (10–30 and 50 mg, respectively) of dye in each trial.

In the present study, a modified HSCCC technique, pH-zone-refining CCC [11–15], was used for the separation of multigram quantities of 1 from D&C Red No. 28. pH-Zone-refining CCC allows the separation, with high resolution, of the components of multigram mixtures of organic acids. The method requires the addition of an acid, such as trifluoroacetic acid (TFA), to the sample solution or stationary phase, followed by isocratic elution with a basic mobile phase. The acids elute as well-resolved rectangular peaks, in the order of their pK_a values and hydrophobicities [11–14]. Although UV detection may not indicate that separations have occurred, giving one broad rectangular peak, monitoring of the eluted fractions with a pH meter results in a series of plateaus that correspond to the separated components. An increase in sample size results in lengthening each plateau without changing the overall elution profile [11–14]. In this work, pH-zone-refining CCC was used to separate components from 3- and 6-g portions of commercial D&C Red No. 28.

2. Experimental

2.1. Materials

Two lots of D&C Red No. 28 were selected from samples of commercial lots submitted to FDA for batch certification. Ammonium acetate (NH$_4$OAc), methanol, water and acetonitrile were chromatography grade. Diethyl ether (anhydrous), hydrochloric acid (36.5–38.0% HCl)

and ammonium hydroxide (28–30% NH$_3$) were ACS-reagent grade. Anhydrous sodium sulfate (granular) was analytical-reagent grade. TFA (Sigma, St. Louis, MO, USA), deuterium oxide (99.9% ^{2}H, MSD Isotopes, Montreal, Canada) and sodium deuteroxide (99.9% ^{2}H, ca. 40% NaO^{2}H in ^{2}H$_2$O; Fluka, Buchs, Switzerland) were used as received.

2.2. pH-Zone-refining CCC

The separations were performed using a commercial high-speed CCC centrifuge (P.C. Inc., Potomac, MD, USA) that holds an Ito multilayer-coil separation column and a counterweight whose centers revolve 10 cm around the centrifugal axis. The multilayer column was constructed by one of us (Y.I.) from polytetrafluoroethylene tubing (ca. 165 m × 1.6 mm I.D., with a total capacity of approximately 325 ml). The β value (a centrifugal parameter) [16] ranged from 0.5 at the internal terminal to 0.85 at the external terminal. The column consisted of 16 coiled layers. (Similar columns are commercially available from P.C. Inc.; Pharma-Tech Research Corp., Baltimore, MD, USA, and Shimadzu, Kyoto, Japan.)

The two-phase solvent system, used for both separations (experiments I and II) described below, consisted of diethyl ether–acetonitrile–0.01 M aqueous NH$_4$OAc (4:1:5). The solvent system was thoroughly equilibrated in a separatory funnel and the two phases were separated shortly before use. The basic aqueous eluent was prepared by addition of concentrated NH$_4$OH to the lower (mobile) phase. TFA was added either to the upper organic (stationary) phase (experiment I) or to the sample solution (experiment II). The sample preparation is described under Results and discussion.

The separation was initiated by using a metering pump (Beckman Accu-Flo pump; Beckman, Palo Alto, CA, USA) to fill the entire column with the stationary (upper) phase, and then the suspension of the color additive was loaded into the column by syringe. The mobile (lower) phase was pumped into the column at 3 ml/min while the column was rotated at 800 rpm in the forward mode. The column effluent was monitored with a UV detector (Uvicord S; LKB, Stockholm, Sweden) at 206 nm, to which was attached an LKB 6-channel strip-chart recorder set at a chart speed of 1 cm/20 min and a full-scale response of 2 absorbance units. Fractions (6 ml) were collected using a fraction collector (Ultrorac, LKB). The pH of each eluted fraction was measured with a pH meter (Accumet 1001; Fisher Scientific, Pittsburgh, PA, USA). The separated fractions were analyzed by analytical reversed-phase high-performance liquid chromatography (RP-HPLC).

2.3. Analytical RP-HPLC

The system used was previously described [10,17]. It consisted of a Model 8800 ternary pump, Model 8500 dynamic mixer, Model 8780 autosampler, Model 4270 integrator (all Spectra-Physics, San Jose, CA, USA) and a Model 490 multiwavelength UV–Vis detector set at 254 and 520 nm (Waters Assoc., Milford, MA, USA). The autosampler was equipped with a Model 7010 injector (Rheodyne, Cotati, CA, USA) with a 20-μl sample loop. A Hypersil MOS-1 RPC-8 column (5-μm particle size, 250 × 4.6 mm I.D., Keystone Scientific, Bellefonte, PA, USA) was used throughout.

The eluents were 0.1 M aqueous NH_4OAc and methanol. The column was eluted by using consecutive linear gradients of 25 to 90% methanol in 25 min, 90 to 100% methanol in 5 min, and 100% methanol for 5 min. The column was re-equilibrated with 25% methanol for 15 min. Other conditions were injection volume, 20 μl; full scale response, 0.128 absorbance units; and flow-rate, 1 ml/min.

An aliquot of each selected fraction from the pH-zone-refining CCC separation was diluted with approximately 2 ml of methanol–water (50:50, v/v). The solution was filtered through a UniPrep 0.45-μm glass microfiber syringeless filter unit (Whatman, Clifton, NJ, USA) prior to chromatography.

2.4. Isolation of the halogenated fluoresceins from pH-zone-refining CCC fractions

The halogenated fluoresceins were isolated in the lactone form, as previously described [17]. Fractions with the same pH values and RP-HPLC retention times were combined and concentrated to ca. 5 ml on a rotary evaporator at ca. 30 Torr (1 Torr = 133.322 Pa) and 50°C. The residue was acidified with 20–40 ml of 10% HCl, and the precipitated lactones were extracted into ethyl acetate. The organic layer was washed twice (10 or 20 ml water), dried (anhydrous Na_2SO_4), and the solvent was evaporated.

Recoveries of the main component **1** were calculated from the amounts of **1** in the dyes as determined during certification analyses by the FDA (94.5% in the lot used for experiment I and 89.5% in the lot used for experiment II).

2.5. Mass spectrometry

Positive ion chemical ionization (PICI) mass spectra were obtained on a Finnigan Mat TSQ-46 quadrupole mass spectrometer interfaced to an INCOS 2300 data system. The instrument was operated at a source temperature of 100°C, ionization energy of 70 eV, emission current of 0.35 mA, 0.25 Torr methane and preamplifier setting of 10^{-8} A/V, and was scanned from m/z 100 to 900 in 1.0 s. The fluoresceins (lactone form) were dissolved in methanol and were introduced into the mass spectrometer via the direct chemical ionization probe at a probe heating rate of 20 mA/s. The protonated molecular ions [m/z (relative intensity)] for 2′,4′,5′,7′-tetrabromo-4,5,6,7-tetrachlorofluorescein and 2′,4′,5′ - tribromo - 4,5,6,7 - tetrachlorofluorescein (corresponding to A and B, respectively, in Figs. 2 and 3) were 783/785/787/789/791 (40.65:82.49:100.0:87.99:47.38, MH$^+$) (Fig. 4b) and 703/705/707/709/711 (15.78:63.43:
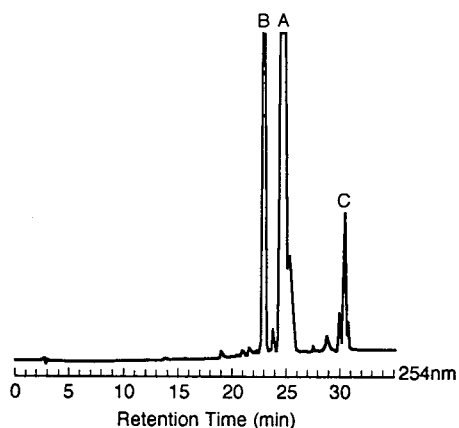
Fig. 2. Analytical RP-HPLC of the commercial lot of color additive D&C Red No. 28 used in experiment I.

100.0:91.05:47.49, MH^+) (Fig. 5b), which are similar to values previously reported for this compound [17].

2.6. ^1H Nuclear magnetic resonance

^1H NMR spectra were obtained on a Varian XL 300 Fourier transform NMR spectrometer at 300 MHz. Typical concentrations consisted of 4 mg of separated component, in the lactone form, dissolved in 0.5 ml of 0.5% NaO^2H in ^2H_2O. 2',4',5',7'-Tetrabromo-4,5,6,7-tetrachlorofluorescein (Fig. 4c): 7.38 ppm (s, 2H-a). 2',4',5'-Tribromo-4,5,6,7-tetrachlorofluorescein (Fig. 5c): 7.40 ppm (s, H-a), 7.00 ppm (d, H-b), 6.70 ppm (d, H-c). The NMR spectrum of 2',4',5'-tribromo-4,5,6,7-tetrachlorofluorescein is similar to that previously reported for this compound [17].

3. Results and discussion

3.1. Experiment I: Separation of components in 3 g of commercial D&C Red No. 28

Analytical RP-HPLC of D&C Red No. 28 gave three main peaks (Fig. 2); 3 g of this mixture were used for the preparative separation by pH-zone-refining CCC. The counter-current chromatogram of the separation is shown in Fig. 3. The two-phase solvent system used consisted
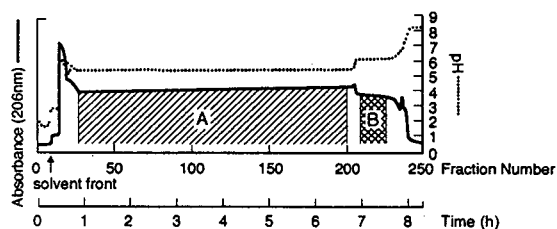
Fig. 3. pH-Zone-refining counter-current chromatogram of the separation of components in 3 g of the D&C Red No. 28 used to obtain Fig. 2. Hatched areas A and B represent fractions containing single components corresponding to peaks A and B, respectively, in Fig. 2.

of diethyl ether–acetonitrile–0.01 M NH_4OAc (4:1:5, v/v/v). The pH of the lower (mobile) phase was adjusted to 8.1 by addition of ammonium hydroxide. TFA (600 μl) was added to the upper, stationary phase (500 ml). The sample mixture was prepared by mixing 3 g of dye in a solvent consisting of 20 ml of the lower phase and 10 ml of the upper phase. The solvent front (first fraction containing mobile phase) emerged at fraction 8. The resulting chromatogram has a broad rectangular shape (Fig. 3) characteristic of pH-zone-refining CCC [11–15]. The two absorbance plateaus (solid line) correspond to the two pH plateaus (dotted line). Each pH plateau represents elution of a pure compound. A decrease in absorbance occurs before the first plateau (fractions 18–25). These fractions contained the main component, 1, as a suspension, slightly contaminated with other impurities. The fractions corresponding to the pH plateaus (fractions 27–200 and 209–225) contained single components whose RP-HPLC peaks (Figs. 4a and 5a) corresponded to peaks A and B, respectively, in Fig. 2. The compounds were isolated in the lactone form (1.07 g and 61 mg, respectively) and identified by CI-MS (Figs. 4b and 5b) and ^1H NMR (Figs. 4c and 5c) as 2',4',5',7'-tetrabromo-4,5,6,7-tetrachlorofluorescein and 2',4',5'-tribromo-4,5,6,7-tetrachlorofluorescein, respectively. The least polar component of the mixture, which corresponds to peak C in Fig. 2, remained in the stationary phase in the column in a relatively purified form, as shown by RP-HPLC in Fig. 6. It was tentatively identified as the ethyl ester, 3, on the basis of an analytical RP-HPLC
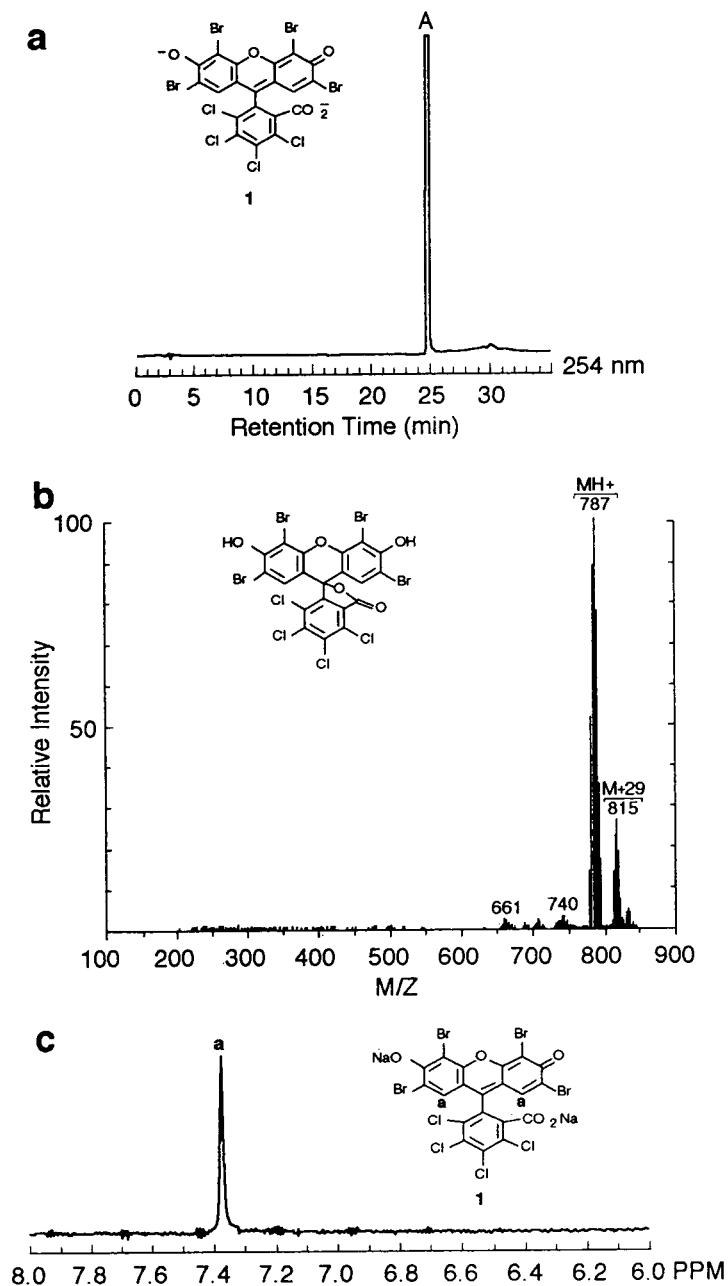
Fig. 4. Characterization of the compound contained in fractions 27–200 of the pH-zone-refining CCC separation in Fig. 3. (a) Analytical RP-HPLC of the combined fractions 27–200, (b) PICI (methane) mass spectrum and (c) ^{1}H NMR spectrum (in NaO^{2}H–^{2}H$_2$O, 300 MHz).

retention time similar to that of the compound which was synthesized according to a procedure for preparing the ethyl ester of Rose Bengal [18].

The ca. 39% recovery of the pure main component, **1**, in this experiment is considerably less than would be expected on the basis of previous
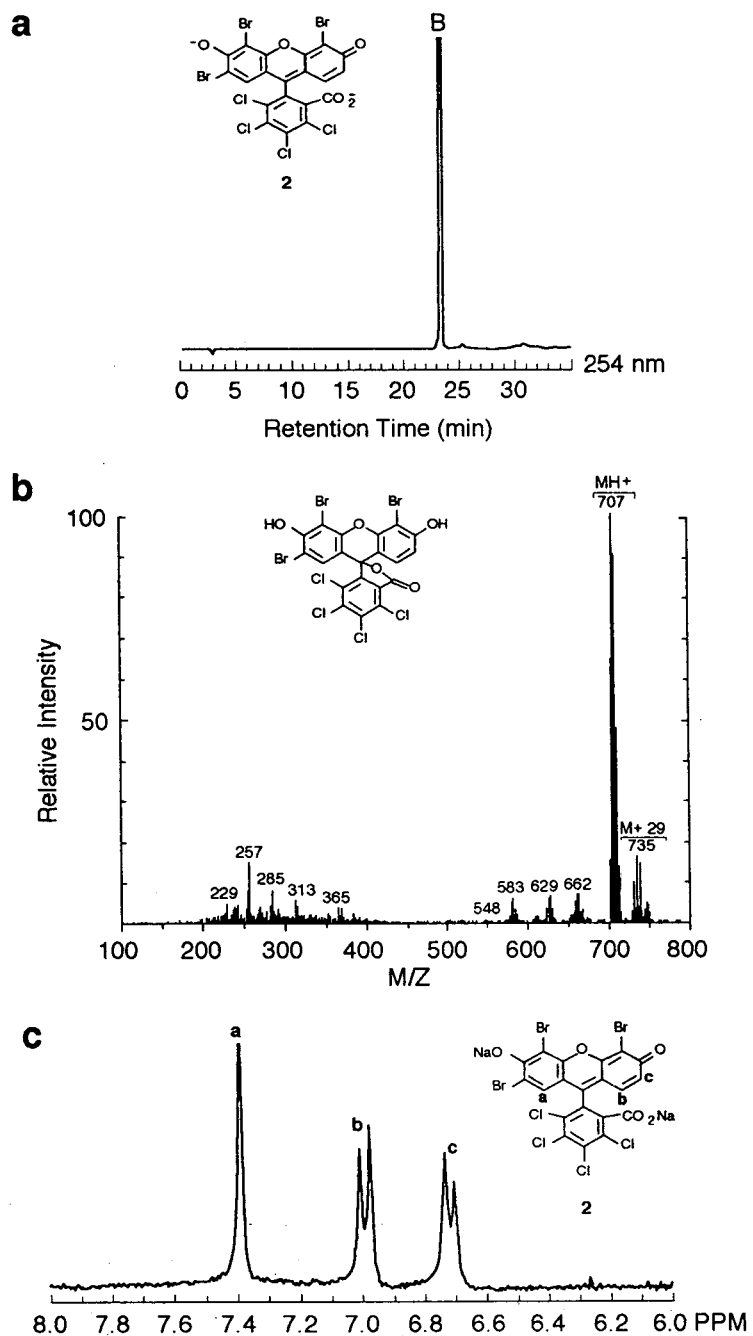
Fig. 5. Characterization of the compound contained in fractions 209–225 of the pH-zone-refining CCC separation in Fig. 3. (a) Analytical RP-HPLC of the combined fractions 209–225, (b) PICI (methane) mass spectrum and (c) ^{1}H NMR spectrum (in NaO^{2}H–^{2}H$_2$O, 300 MHz).
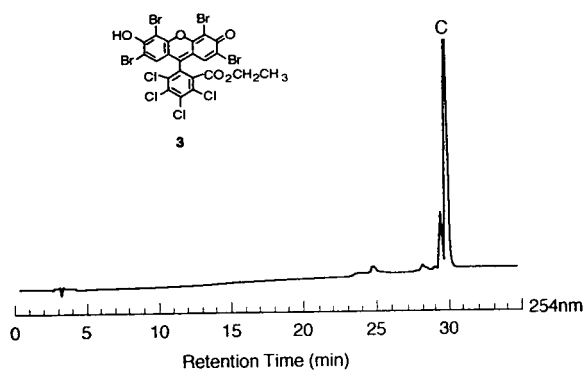
Fig. 6. Analytical RP-HPLC of the column content after the pH-zone-refining CCC separation of D&C Red No. 28 shown in Fig. 2.

experience with pH-zone-refining CCC [11–15]. This lower yield is apparently due to the elution of the suspension in fractions 18–25. It is thought that the elution of the suspension was caused by an insufficient amount of retainer acid (TFA) in the column. The retention of the stationary phase, calculated after the separation, was 61.3% of the total column capacity. This implies that 38.7% of the stationary phase and the corresponding amount of TFA (230 μl) were lost from the column before the separation. The remaining quantity of TFA in the column (0.0050 mol) was not enough to acidify the sodium salt of the dye present in the color additive (0.0072 equivalents). The part of the color additive that remained in the sodium salt form was not retained in the stationary phase and consequently was eluted as a suspension with the mobile phase. It appears that the recovery of pure 1 would have been higher if enough TFA had been added to ensure that the retained stationary phase would acidify all the dye in the sample solution. In the following experiment the loss of retainer acid from the column was circumvented by the addition of the retainer acid to the sample solution. Thus, the components in 6 g of D&C Red No. 28 were separated by the addition of TFA to the sample solution in sufficient quantity to convert all the dye to the acid form.

3.2. Experiment II: Separation of components in 6 g of commercial D&C Red No. 28

Analytical RP-HPLC of the D&C Red No. 28 used in this separation gave four peaks (Fig. 7); 6 g of this mixture were used for the preparative separation by pH-zone-refining CCC. The counter-current chromatogram of the separation is shown in Fig. 8. The two-phase solvent system used consisted of diethyl ether–acetonitrile–0.01 M NH$_4$OAc (4:1:5, v/v/v). The pH of the lower (mobile) phase was adjusted to 9.2 by addition of ammonium hydroxide. The sample mixture was prepared by mixing 6 g of dye in a solvent consisting of 20 ml of the lower phase and 30 ml of the upper phase. TFA (1.2 ml) was added to the sample solution. The solvent front (first fraction containing mobile phase) emerged at fraction 7. The retention of the stationary phase, calculated after the separation, was 54.7% of the total column capacity. The resulting chromatogram has a broad rectangular shape (Fig. 8a) that includes two pH plateaus (dotted line): a short and a long one (fractions 45–47 and 55–215, respectively). In this case, no suspension was eluted and no decrease occurred in the absorbance intensity before the elution of the main component. Fractions 55–215 contained a
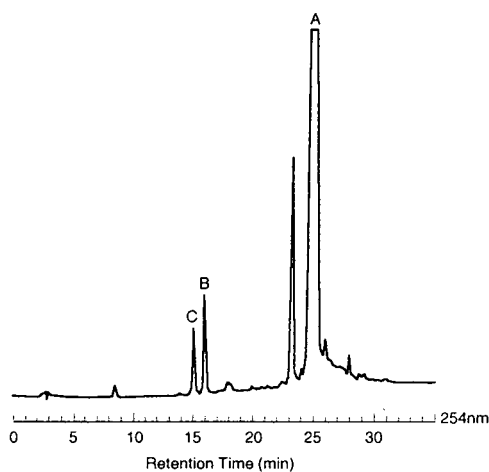
Fig. 7. Analytical RP-HPLC of the commercial lot of color additive D&C Red No. 28 used in experiment II.
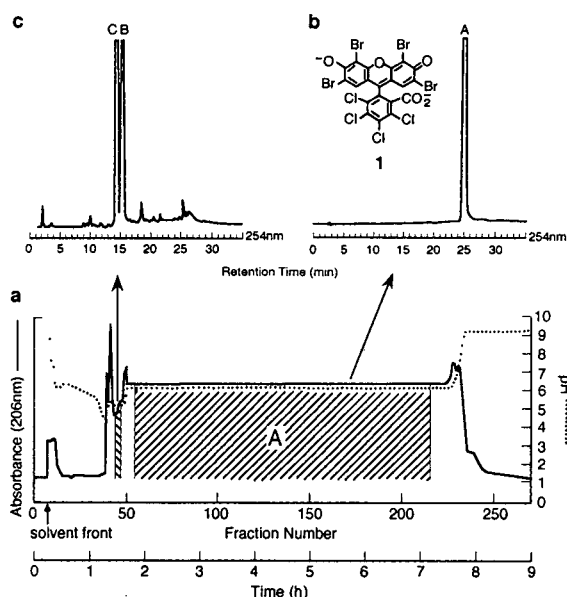
Fig. 8. (a) pH-Zone-refining counter-current chromatogram of the separation of components in 6 g of the D&C Red No. 28 used to obtain Fig. 7, (b) analytical RP-HPLC of the combined fractions 55–215 and (c) analytical RP-HPLC of the combined fractions 45–47.

single component whose RP-HPLC peak (Fig. 8b) corresponded to peak A in Fig. 7. The compound was isolated as the lactone (4.06 g) and identified by CI-MS and ^{1}H NMR as 2′,4′,5′,7′-tetrabromo-4,5,6,7-tetrachlorofluorescein. The ca. 80% recovery of pure **1** was improved in this separation by avoiding elution of the contaminated suspension through the presence of sufficient retainer acid (0.016 mol TFA) to acidify the sodium salt of the dye (0.014 equivalents). The two components corresponding to peaks B and C in Fig. 7 eluted in a very concentrated form in fractions 45–47 (Fig. 8c). On the basis of preliminary studies, it appears that these two acidic components have very closely related structures [19].

4. Conclusions

This study and previous work [11,15,20–22] demonstrate that pH-zone-refining CCC is an effective method for the separation and purification of multigram quantities of acidic components of hydroxyxanthene dye mixtures.

References

[1] *Code of Federal Regulations*, Title 21, Part 74.1328, US Government Printing Office, Washington, DC, 1993.
[2] G. Clark, *Staining Procedures*, Williams & Wilkins, Baltimore, MD, 4th ed., 1981.
[3] F.J. Green, *The Sigma–Aldrich Handbook of Stains, Dyes, and Indicators*, Aldrich, Milwaukee, WI, 1990, p. 577.
[4] E.K.W. Schulte, *Histochemistry*, 95 (1991) 319–328.
[5] P.N. Marshall and S.M. Lewis, *Stain Technol.*, 49 (1974) 235–240.
[6] P.N. Marshall, S.A. Bentley and S.M. Lewis, *J. Clin. Pathol.*, 28 (1975) 920–923.
[7] P.N. Marshall, S.A. Bentley and S.M. Lewis, *Scand. J. Haematol.*, 20 (1978) 206–212.
[8] A.J. Emery, Jr., F. Knapp Hazen and E. Stotz, *Stain Technol.*, 25 (1950) 201–208.
[9] E. Gandin, J. Piette and Y. Lion, *J. Chromatogr.*, 249 (1982) 393–398.
[10] A. Weisz, A.J. Langowski, M.B. Meyers, M.A. Thieken and Y. Ito, *J. Chromatogr.*, 538 (1991) 157–164.
[11] A. Weisz, A.L. Scher, K. Shinomiya, H.M. Fales and Y. Ito, *J. Am. Chem. Soc.*, 116 (1994) 704–708.
[12] Y. Ito, K. Shinomiya, H.M. Fales, A. Weisz and A.L. Scher, presented at the *44th Pittsburgh Conference and Exposition on Analytical Chemistry and Applied Spectroscopy, Atlanta, GA, March 8–12, 1993*, abstract 54P.
[13] Y. Ito, K. Shinomiya, H.M. Fales, A. Weisz and A.L. Scher, presented at the *ACS National Meeting, Chicago, IL, Aug. 22–27, 1993*.
[14] Y. Ito, in Y. Ito and W.D. Conway (Editors), *High-Speed Countercurrent Chromatography (Chemical Analysis Series)*, Wiley, New York, submitted for publication.
[15] Y. Ito and A. Weisz, *pH-Zone-Refining Countercurrent Chromatography*, US Pat., pending.
[16] Y. Ito, *J. Chromatogr.*, 301 (1984) 387–403.
[17] A. Weisz, A.L. Scher, D. Andrzejewski, Y. Shibusawa and Y. Ito, *J. Chromatogr.*, 607 (1992) 47–53.
[18] J.J.M. Lamberts and D.C. Neckers, *Z. Naturforsch. B*, 39 (1984) 474–484.
[19] A. Weisz, unpublished results.
[20] A. Weisz, K. Shinomiya and Y. Ito, presented at the *44th Pittsburgh Conference and Expositon on Analytical Chemistry and Applied Spectroscopy, Atlanta, GA, March 8–12, 1993*, abstract 865.
[21] A. Weisz, D. Andrzejewski, R.J. Highet and Y. Ito, *J. Chromatogr. A*, 658 (1994) 505–510.
[22] A. Weisz, A.L. Scher, D. Andrzejewski and Y. Ito, presented at the *10th International Symposium on Preparative Chromatography, Arlington, VA, June 14–16, 1993*, abstract 320.

Velocity profiles in thermal field-flow fractionation

Jamel Eddine Belgaied, Mauricio Hoyos, Michel Martin*

École Supérieure de Physique et Chimie Industrielles, Laboratoire de Physique et Mécanique des Milieux Hétérogènes (URA CNRS 857), 10 Rue Vauquelin, 75231 Paris Cedex 05, France

Abstract

Exact velocity profiles in thermal field-flow fractionation (FFF) were numerically computed for twelve solvents and forty different combinations of the temperature drop ΔT across the channel and of the cold wall temperature, T_c. An expression with six coefficients relating the ν parameter of a third-degree polynomial velocity profile which approximates the exact profile with ΔT and T_c was derived for each solvent. Under typical experimental conditions, it provides a nearly two orders of magnitude improvement in the accuracy of the prediction of the retention over the equation based on the classical parabolic profile. A procedure is suggested for using this ν vs. ΔT and T_c expression for extracting the basic FFF parameter λ from retention data.

1. Introduction

Field-flow fractionation (FFF) is a method of separation of macromolecular or particulate materials which is performed in a thin, ribbon-like channel. A flow of carrier liquid transports the sample components along the channel at various rates depending on their degree of interaction with an external field applied perpendicular to the main axis of the channel [1]. The retention time of a sample component (which, in the following, will be called an analyte) depends on both its concentration distribution and the axial velocity distribution in the field direction. Therefore, in order to predict the retention of an analyte or to characterize an analyte from its FFF retention data, one needs to know these two distributions precisely. The concentration distri-

bution depends on the forces acting on the analyte and on its diffusivity. In fact, the shape of this distribution determines the operating retention mode [2].

Because the analytes generally have a small size, it can be correctly assumed in most cases, that they are transported along the channel by the flow with the axial flow velocity at the position of their centre of gravity. Knowing the axial velocity distribution of the analytes in the field direction then amounts to knowing the axial flow profile. Because the channel is essentially made of two long and wide parallel walls, the flow profile is frequently assumed to be parabolic, except for a small perturbation near the channel edges [3,4]. Such a velocity profile is obtained for the flow of an isothermal fluid between two infinite parallel plates. Indeed, if z is the direction of the flow, x the distance from one of the plates, w the distance between the

---

* Corresponding author.

two plates, dP/dz the pressure gradient driving the flow and η the fluid viscosity, the velocity profile, $v(x)$, is then obtained from the simple form of the differential Navier–Stokes equation:

$$\eta \cdot \frac{d^2 v}{dx^2} = \frac{dP}{dz} \tag{1}$$

which gives, after integration:

$$\frac{v(x)}{\langle v \rangle} = 6\left[\left(\frac{x}{w}\right) - \left(\frac{x}{w}\right)^2 \right] \tag{2}$$

where $\langle v \rangle$ is the mean flow velocity. There are, however, situations encountered in FFF where these two underlying assumptions (infinite parallel plates geometry and constant viscosity) are not fulfilled. Such is the case, for instance, in sedimentation FFF because of the curved geometry of the channel, or in flow FFF because of a transverse flow component through at least one of the channel walls. Nevertheless, under typical operating conditions, the correction to be brought to the flow profile is then negligibly small [2].

The situation is clearly different in thermal FFF in which the variations of the fluid viscosity resulting from the temperature gradient applied across the channel thickness are sufficiently large to induce significant distortion of the flow profile from the parabolic limit. This was recognized in earlier papers on thermal FFF. Myers et al. [5] solved Eq. 1 in which η is no longer a constant but is given as a function of x as

$$\eta = \eta_c \exp(-\beta x / w) \tag{3}$$

where $\beta = B \, \Delta T / T_c^2$, η_c is the viscosity at temperature T_c of the cold wall, ΔT is the temperature difference between the two plates and B a solvent constant in the Andrade equation relating the viscosity and the absolute temperature T:

$$\eta = \eta_c \exp\left[B\left(\frac{1}{T} - \frac{1}{T_c}\right) \right] \tag{4}$$

Comparison of Eqs. 3 and 4 shows that the following relationship was implicitly assumed for the temperature profile across the channel thickness:

$$T = \frac{T_c}{1 - \dfrac{\Delta T}{T_c} \cdot \dfrac{x}{w}} \tag{5}$$

this equation may provide a satisfactory approximation of the temperature profile near the cold wall but is not consistent with the fact that ΔT represents the temperature drop between the two plates.

It was later pointed out that, when the viscosity is not constant, the left-hand term of Eq. 1 is not correct, even when taking η as a function of x, but must also include a $d\eta/dx$ term [6]. The flow profile was accordingly calculated using Eq. (4) and a linear relationship between T and x [7]. However, the calculation is complex and has to be made numerically for specific values of B, T_c and ΔT, as some of the integrals involved have no analytical solution.

Further, the temperature profile across the channel thickness is actually not linear because of the temperature dependence of the thermal conductivity of the liquid. Knowing this dependence, one can calculate the resulting temperature profile [8]. This further complicates the calculation of the velocity profile. A treatment was performed by Gunderson et al. [9] using the complete Navier–Stokes equation, a third-degree polynomial expression of the fluidity, which is the reciprocal of the viscosity, as a function of the temperature and a third-degree polynomial dependence of the temperature vs. x/w, obtained as a Taylor series about the cold wall in terms of $d\kappa/dT$, the coefficient of variation of the thermal conductivity κ with temperature. By this means, they were able to obtain an analytical solution of the velocity profile given as a fifth-degree polynomial expression in terms of the reduced coordinate x/w. Then the retention equation, for an exponential concentration profile, was obtained as a particular case of the general expression for a n-degree polynomial velocity profile given previously [10].

In spite of the fact that analytical expressions of the velocity profile and of the retention factor are obtained, this procedure is sometimes considered complicated because various successive calculations must be performed to obtain the coefficients of the velocity profile expression

[11]. In addition, the Taylor expansion of the temperature profile about the cold wall cannot rigorously provide the correct value of the temperature at the hot wall and is therefore not, in principle, rigorously consistent with the fact that the temperature drop between the two plates is equal to ΔT. Further, the computation of the dispersion coefficients for a fifth-degree polynomial velocity profile becomes very complex and has not yet been attempted, although general expressions for an n-degree polynomial velocity profile exist [10].

For this reason, it has been suggested that one can approximate the true velocity profile by a third-degree polynomial profile in such a way that the slope of the relative velocity profile becomes equal to that of the true profile as one approaches the cold wall [10,12,13]. This method is justified by the fact that it has been observed that all investigated polymeric samples analysed so far using thermal FFF move in the vicinity of the cold wall where they form a thin cloud. This method has been applied in some instances for predicting or interpreting retention data [12–16]. A third-degree polynomial velocity profile contains a single adjustable coefficient as the three other possible coefficients of a third-degree polynomial are fixed by the no-slip condition (which implies a zero velocity at each of the two walls) and the normalization condition (the mean value of the relative profile $v/\langle v \rangle$ across the thickness must be equal to 1). The main problem is selecting the appropriate third-degree coefficient for specific solvent and temperature conditions. This has mainly been done by graphical interpolation of calculations at various B/T_c and $\Delta T/T_c$ values [17]. The purpose of this work was to provide a method for calculating the third-degree coefficient for various solvents and temperature conditions, which can be easily used for practical application in both predicting and interpreting thermal FFF retention data.

2. Theory

The basic Navier–Stokes equation describing the flow velocity in the case of a non-constant viscosity is written as [6,18,19]

$$\frac{d}{dx}\left(\eta \frac{dv}{dx}\right) = \eta \frac{d^2v}{dx^2} + \frac{d\eta}{dx} \cdot \frac{dv}{dx} = \frac{dP}{dz} \qquad (6)$$

By double integration of this equation, the relative velocity profile, $v/\langle v \rangle$, is obtained as a function of the reduced transverse coordinate, x/w:

$$\frac{v}{\langle v \rangle} = \frac{\displaystyle\int_0^{x/w} \frac{x/w}{\eta}\,d(x/w) - C\int_0^{x/w}\frac{d(x/w)}{\eta}}{\displaystyle\int_0^1\left(\int_0^{x/w}\frac{x/w}{\eta}\,d(x/w) - C\int_0^{x/w}\frac{d(x/w)}{\eta}\right)d(x/w)} \qquad (7)$$

where η depends on x/w through the temperature T. The constant C in Eq. 7 is equal to

$$C = \frac{\displaystyle\int_0^1 \frac{x/w}{\eta}\,d(x/w)}{\displaystyle\int_0^1 \frac{d(x/w)}{\eta}} \qquad (8)$$

The relationship between the viscosity and the temperature used in this work is given by Eq. (4). This form of the Andrade equation is consistent with experimental data [20] and with approximate theories of the liquid state [21]. Considering Eq. 4 as an Arrhenius-type law, kB, where k is the Boltzmann constant, can be considered as an activation energy for viscous flow.

The thermal FFF system is generally operated in such a way that a constant energy flux, q, is input to the channel by means of electrical resistances in the vicinity of the hot wall, while a flow of water evacuates the heat at the cold wall. The temperature profile across the channel thickness is then given by the Fourier law of heat conduction [22]:

$$q = -\kappa \cdot \frac{dT}{dx} \qquad (9)$$

where κ is the thermal conductivity. Over the typical temperature ranges encountered in ther-

mal FFF experiments, the thermal conductivity changes slightly and linearly with temperature [23] so that one can write

$$\kappa = \kappa_c + \frac{d\kappa}{dT}(T - T_c) \qquad (10)$$

where κ_c is the thermal conductivity at the cold wall temperature and $d\kappa/dT$ is a constant specific for the carrier liquid. Integration of Eq. 9 in combination with Eq. 10 and elimination of q by replacement in terms of ΔT, the temperature drop between the two plates, gives the temperature profile across the channel thickness [9]:

$$T = T_c + \frac{1}{\dfrac{1}{\kappa_c} \cdot \dfrac{d\kappa}{dT}}$$
$$\times \left(\sqrt{1 + \frac{2}{\kappa_c} \cdot \frac{d\kappa}{dT} \cdot \Delta T \left(1 + \frac{1}{\kappa_c} \cdot \frac{d\kappa}{dT} \cdot \frac{\Delta T}{2}\right) \frac{x}{w}} - 1 \right) \qquad (11)$$

Replacement of T in Eq. 4 by its expression in Eq. 11 provides the dependence of η as a function of x/w which is needed for evaluating the integrals which gives the velocity profile in Eq. 7 for given B, T_c, η_c, ΔT, κ_c and $d\kappa/dT$ values. As B, η_c, κ_c and $d\kappa/dT$ depend on the nature of the carrier liquid and on T_c, the three independent parameters which determine the velocity profile are ΔT, T_c and the nature of the carrier liquid. The relative velocity profiles were numerically calculated according to Eqs. 7, 4 and 11 for various liquids, ΔT and T_c values. They are referred to as "exact" velocity profiles, $(v/\langle v \rangle)_{ex}$.

As discussed above, it is interesting, from a practical point of view, to approximate the exact relative velocity profile by a third-degree polynomial profile, $(v/\langle v \rangle)_3$, in terms of x/w. It has been found convenient to write this profile, which depends on the single adjustable coefficient v, in such a way that one retrieves the parabolic profile when $v = 0$ [10,13]. This gives

$$\left(\frac{v}{\langle v \rangle}\right)_3 =$$
$$6\left[(1 + v)\left(\frac{x}{w}\right) - (1 + 3v)\left(\frac{x}{w}\right)^2 + 2v\left(\frac{x}{w}\right)^3\right] \qquad (12)$$

In order to select v so that the slope of the exact relative velocity profile equals that of the third-degree profile near the cold wall, the procedure developed by Brimhall et al. [7] cannot be employed as it is specific for a linear temperature profile. We therefore use the following general approach.

One can compare a given relative velocity profile with the ideal parabolic shape, $(v/\langle v \rangle)_2$, given by Eq. 2 and obtained for $\Delta T = 0$ or for a hypothetical liquid with $B = 0$, by means of the relative deviation, ε, defined as

$$\varepsilon = \frac{(v/\langle v \rangle) - (v/\langle v \rangle)_2}{(v/\langle v \rangle)_2} \qquad (13)$$

This relative deviation depends, of course, on x/w. In fact, a plot of ε vs. x/w can be considered as a modified representation of a velocity profile. Let ε_{ex} and ε_3 be the ε functions for the exact and third-degree polynomial velocity profiles, respectively. The slope of the exact relative velocity profile is, according to Eq. 13, equal to

$$\frac{d(v/\langle v \rangle)_{ex}}{d(x/w)} = (1 + \varepsilon_{ex})\frac{d(v/\langle v \rangle)_2}{d(x/w)}$$
$$+ (v/\langle v \rangle)_2 \frac{d\varepsilon_{ex}}{d(x/w)} \qquad (14)$$

It is easily seen from Eq. 12 that the slope of the third-degree relative velocity profile at cold wall is equal to $6(1 + v)$. In order to approximate the exact velocity profile by a third-degree polynomial velocity profile in such a way that the two profiles have the same slope at the cold wall, one therefore must have

$$\frac{d(v/\langle v \rangle)_{ex}}{d(x/w)}\bigg|_{x/w=0} = 6(1 + v) \qquad (15)$$

Noting that, at the cold wall ($x/w = 0$), $(v/\langle v \rangle)_2 = 0$ and $d(v/\langle v \rangle)_2/d(x/w) = 6$ according to Eq. 2, the combination of Eqs. 14 and 15 gives

$$\lim_{x/w \to 0} \varepsilon_{ex} = v \qquad (16)$$

One notes that, according to Eq. 12, ε becomes undefined for vanishing x/w, so one has then to write ε_{ex} as a limit. The physical property of the

parameter ν expressed by eqn. 16 provides an easy graphical representation of the ν parameter: this is the limiting value of ε_{ex} for $x/w = 0$. This property is used in the following for the determination of ν.

Assuming that the concentration profile of a given solute is exponential and characterized by the basic FFF parameter, λ, of that solute, its retention factor, R, is then obtained, when the velocity profile is represented by Eq. 12, in terms of λ and ν as [10,13]

$$R = 6\lambda\left\{\nu + (1 - 6\lambda\nu)\left[\coth\left(\frac{1}{2\lambda}\right) - 2\lambda\right]\right\} \qquad (17)$$

3. Basic solvent data and computational procedure

The computation of the relative velocity profile for a given solvent at various T_c and ΔT values requires that the values of the constants B and $d\kappa/dT$ of that solvent and the value of κ at some reference temperature are known. The values of B for the various organic solvents were calculated as the slopes of the linear regressions of $\ln \eta$ vs. $1/T$ from experimental viscosity data at various temperatures [20,24]. The resulting B values for the various solvents investigated are reported in Table 1.

When experimental thermal conductivity data for a given solvent were reported at different temperatures [23], $d\kappa/dT$ was calculated as the slope of a linear regression of κ vs. T. In other cases, values of κ were estimated at various temperatures using the Latini et al. method recommended for organic solvents by Reid et al. [23], which gives

$$\kappa = \frac{A^* T_b^\alpha}{M^\beta T_{crit}^\gamma} \cdot \frac{(1 - T_r)^{0.38}}{T_r^{1/6}} \qquad (18)$$

where T_r is the reduced temperature T/T_{crit}, T_{crit} the critical temperature, T_b the normal boiling temperature, M the solvent molecular mass and A^*, α, β, γ parameters which are tabulated for various classes of organic compounds [23]. Although this expression is not rigorously consistent with the hypothesis of the constancy of $d\kappa/dT$, it is found that the variation of κ with T in the typical temperature range used in FFF is nearly linear, which justifies the approximation expressed by Eq. 10. The values of κ at 20°C and of $d\kappa/dT$ are reported in Table 1.

Once the viscosity profile, $\eta(x/w)$, across the channel thickness is known from the combination of Eqs. 4 and 11 for a given solvent and fixed values of T_c and ΔT, the integrals entering Eqs. 7 and 8 are numerically computed by means

Table 1
Solvent properties used in the calculations

Solvent	B (K)	κ at 293 K ($Wm^{-1}K^{-1}$)	$d\kappa/dT$ ($Wm^{-1}K^{-2}$)
Benzene	1315.79	0.148	$-3.53 \cdot 10^{-4}$
2-Butanone	975.90	0.160[a]	$-2.80 \cdot 10^{-4}$[a]
Carbon tetrachloride	1242.32	0.103	$-1.87 \cdot 10^{-4}$[a]
Cyclohexane	1516.57	0.124	$-2.48 \cdot 10^{-4}$[a]
Cyclohexanone	1791.00	0.170[a]	$-2.86 \cdot 10^{-4}$[a]
p-Dioxane	1311.17	0.159[a]	$-2.95 \cdot 10^{-4}$[a]
Ethyl acetate	1042.33	0.147	$-1.50 \cdot 10^{-4}$
Ethylbenzene	1095.78	0.132	$-2.33 \cdot 10^{-4}$
Tetrahydrofuran	923.21	0.166[a]	$-3.51 \cdot 10^{-4}$[a]
Toluene	1085.00	0.141[a]	$-2.59 \cdot 10^{-4}$[a]
o-Xylene	1183.00	0.139[a]	$-2.11 \cdot 10^{-4}$[a]
p-Xylene	1052.24	0.136[a]	$-2.35 \cdot 10^{-4}$[a]

[a] Values estimates by the Latini et al. method [23].

of the Simpson integration procedure. The relative velocity profile is determined for successive x/w values differing by 0.01 unit. Between two consecutive x/w values, the integrals are computed by dividing the 0.01 interval for x/w in as many sub-intervals as necessary to ensure that the results of the integration of two consecutive two fold division steps differ in relative value by less than 10^{-5}. This integration procedure was tested with some usual functions for which the analytical solution of the finite integral is known. In all cases, the relative difference between the numerical and analytical integration results was less than $5 \cdot 10^{-7}$.

Then, knowing the exact relative velocity profile, the relative deviation, ε_{ex}, from the parabolic profile is calculated and the ν parameter is estimated according to the property expressed by Eq. 16, by extrapolation to $x/w = 0$ of the ε_{ex} vs. x/w curve for small x/w values. In practice, ν is obtained as the intercept of the linear regression of ε_{ex} vs. x/w in the x/w range from 0.01 to 0.1.

4. Results and discussion

The temperature profile given by Eq. 11 is represented in Fig. 1 together with two approximate profiles previously used, the linear profile [7] and the profile given by Eq. 5 [5]. Clearly, this latter profile does not describe the true profile satisfactorily. The deviation of this true profile from linearity depends on ΔT, on the solvent used and, to a lesser extent, on T_c. Since for all organic solvents investigated the thermal conductivity decreases with increasing temperature, the shape of the temperature profile is similar to that shown in Fig. 1 and at any position across the channel the actual temperature is lower than it would be if the profile was linear.

The relative velocity profiles and the associated ν parameters were determined for the twelve organic solvents listed in Table 1, which have been or may be used in thermal FFF. For each solvent, 40 sets of calculations were performed for four T_c values ($T_c = 10$, 20, 30 and
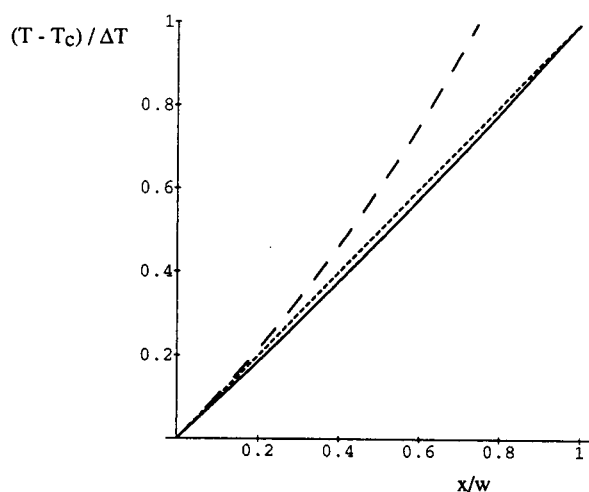
Fig. 1. Temperature profiles in thermal FFF plotted as $(T - T_c)/\Delta T$ vs. x/w. From bottom to top curves: exact profile with temperature-dependent thermal conductivity; linear profile (temperature-independent thermal conductivity); profile given by Eq. 5. Solvent, ethylbenzene; $\Delta T = 100°C; T_c = 20°C$.

40°C) and ten ΔT values ($\Delta T = 10$, 20, 30, 40, 50, 60, 70, 80, 90 and 100°C).

For all solvents except two (cyclohexanone and o-xylene), the overall temperature range covered from the lowest cold wall temperature (10°C) to the highest hot wall temperature (140°C) exceeds the liquid temperature range at atmospheric pressure. When performing the calculations it was implicitly assumed that the values of the solvent parameters B, κ_c and $d\kappa/dT$ obtained or estimated at atmospheric pressure were also correct at the pressure necessary to maintain the carrier fluid in the liquid state at the hot wall temperature selected. In fact, it is relatively rare that thermal FFF experiments are performed in a pressurized channel. Exceptions concern the analysis of relatively low-molecular mass species for which a large ΔT is necessary to obtain the required selectivity [25], the analysis of polymers, such as polyethylenes, for which a high T_c is needed to satisfy the solubility requirement [26] or, still, the case of solvents with low boiling points. Therefore, even if pressure effects on viscosity and thermal conductivity are significant, the above assumption remains applicable to

derive trends in the variations of ν when changing ΔT and/or T_c at atmospheric pressure, which is done below.

A typical velocity profile is shown in Fig. 2 together with the corresponding third-degree polynomial profile and the ideal parabolic profile. Obviously, as follows from the definition of ν, the exact and third-degree profiles become identical as one approaches the cold wall ($x/w = 0$). They are close to each other but differ significantly from the parabolic profile. The position of the maximum velocity appears to be shifted from the channel centre ($x/w = 0.5$) towards the hot wall. It can be shown that, for the third-degree polynomial velocity profile, this position is given by

$$(x/w)_{\max} = \frac{1 + 3\nu - \sqrt{1 + 3\nu^2}}{6\nu} \qquad (19)$$

The maximum relative velocity, which is equal to

$$\frac{v_{\max}}{\langle v \rangle} = -\frac{1}{9\nu^2}[1 - 9\nu^2 - (1 + 3\nu^2)\sqrt{1 + 3\nu^2}] \qquad (20)$$

is slightly larger than for the parabolic profile. For instance, for $\nu = -0.2$, one obtains $(x/w)_{\max} = 0.549$ and $v_{\max}/\langle v \rangle = 1.515$.

The relative deviations of the exact and corresponding third-degree polynomial velocity profiles from the parabolic profile are more easily observed in the plots of ε_{ex} and ε_3, respectively, vs. x/w as seen in Fig. 3. In this kind of ε vs. x/w plot, the parabolic profile is simply represented as the straight horizontal line $\varepsilon = 0$ for all x/w. It is easily seen from Eq. 12 that the relative deviation, ε_3, for a third-degree velocity profile is a straight line with a slope equal to -2ν and passing through the point [$\varepsilon_3 = 0$, $x/w = 1/2$]:

$$\varepsilon_3 = \nu\left(1 - 2 \cdot \frac{x}{w}\right) \qquad (21)$$

The exact relative velocity profile has, in the ε vs. x/w representation, a more complex shape as seen in Fig. 3. As mentioned in the theoretical section, the ν parameter is given as the value of the limiting value of ε_{ex} when one approaches $x/w = 0$. As the viscosity decreases with increasing temperature, the velocity in the vicinity of the cold wall is lower than it would be if the profile was parabolic. Therefore, the ν parameters in thermal FFF are negative as long as the cold wall is the accumulation wall. In the case of ethylbenzene with $\Delta T = 100°C$ and $T_c = 20°C$ corresponding to the curves in Fig. 3, one has $\nu = -0.2922$. This value is large and shows that the temperature effect on the velocity profile must be taken into account when interpreting retention data in thermal FFF. Indeed, neglecting this effect by using the classical retention
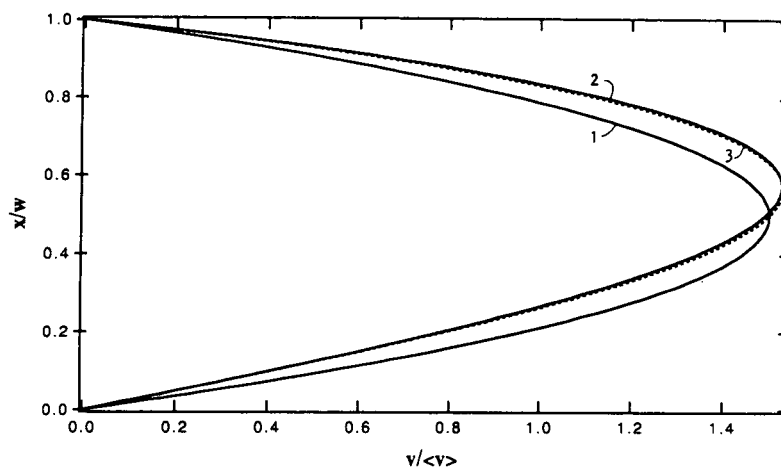
Fig. 2. Relative velocity profiles plotted as x/w vs. $v/\langle v \rangle$. 1 = parabolic profile; 2 = exact profile; 3 = third-degree polynomial profile. Solvent, ethylbenzene; $\Delta T = 100°C$; $T_c = 20°C$.
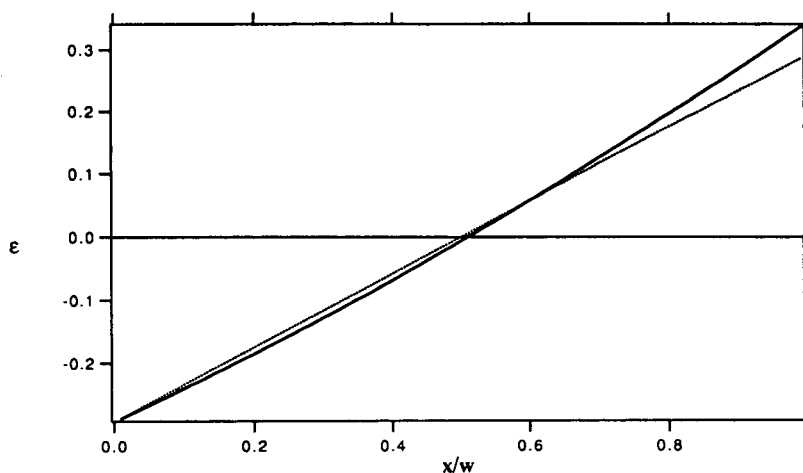
Fig. 3. Relative deviation, ε, of the exact relative velocity profile from the parabolic profile vs. x/w (solid curve). The straight line (dotted line) represents the relative deviation of the corresponding third-degree polynomial velocity profile from the parabolic profile. The ν parameter is given as the intercept of this straight line (in this case $\nu = -0.29218$). Solvent, ethylbenzene; $\Delta T = 100°C$; $T_c = 20°C$.

equation for a parabolic profile will, in the high retention domain, result in a nearly 29% error in the basic FFF parameter λ, which, in turn, will correspond to a 87% error in the determination of the molecular mass of a polystyrene sample from a known relationship between λ and molecular mass.

The deviation of the velocity profile from the parabolic shape arises from the temperature dependence of the carrier liquid viscosity. However, the influence of this effect depends on the temperature profile. The influence of the variation of the thermal conductivity with temperature has only a minor effect on the resulting velocity profile. Indeed, it can be shown that, for ethylbenzene with $T_c = 20°C$, in the relatively extreme case where $\Delta T = 100°C$, the exact relative velocity profile and the relative velocity profile that would be obtained if the thermal conductivity was independent of the temperature are very close to each other. Their maximum values differ by less than 0.2%. The corresponding ν parameters are equal to -0.2922 and -0.2999, respectively.

The dependence of ν with ΔT is plotted for ethylbenzene in Fig. 4a at various T_c values; ν, which reflects the distortion of the flow profile

from the parabolic shape, is seen to increase in absolute value with increasing ΔT. For a given ΔT, $|\nu|$ increases with decreasing T_c. A three-dimensional representation of ν vs. ΔT and T_c is shown for ethylbenzene in Fig. 4b. Similar curves are obtained for other organic solvents listed in Table 1.

In order to allow an easy determination the ν parameter corresponding to the solvent and temperature conditions of a given thermal FFF experiment without performing the lengthy calculations involved in the procedure described above, the set of 40 ν values obtained for a given solvent served as a database for finding a correlation for ν as a function of ΔT and T_c. Because the variation of ν with T_c at a given ΔT is nearly linear and that with ΔT at a given T_c is nearly quadratic, the following regression was tested by means of the least-mean square method:

$$\nu = (a_1 T_c + a_2)\,\Delta T + (a_3 T_c + a_4)\,\Delta T^2$$
$$+ (a_5 T_c + a_6)\,\Delta T^3 \qquad (22)$$

The fit is satisfactory for the twelve solvents. The relative error in ν arising from the regression was determined by comparing values given by Eq. 22 with the original ν values. It is found to be lower

Fig. 4. Variations of the ν parameter with ΔT and T_c. (a) ν vs. ΔT at $T_c = 10, 20, 30$ and $40°C$ from bottom to top curve; (b) three-dimensional representation of ν vs. ΔT and T_c. Solvent, ethylbenzene.

expressed in K instead of °C, the numerical values of a_2, a_4 and a_6 would be changed, but the value of ν would be unaffected).

It is instructive to evaluate the susceptibility of ν to small variations in the experimental conditions. In the case of ethylbenzene with $\Delta T = 60°C$ and $T_c = 20°C$, one finds $d \ln |\nu| / d \ln \Delta T = 0.79$ and $d \ln |\nu| / d \ln T_c = -1.72$ (with T_c expressed in K). Accordingly, 1°C variations in ΔT and T_c induce 1.3% and 0.6% variations in ν, respectively. These variations, which are larger than typical temperature fluctuations observed experimentally, will therefore have a negligible influence on the determination of λ in thermal FFF, as far as the velocity profile is concerned (of course, these variations, especially the variation of ΔT, will directly influence the concentration profile and, hence, the retention factor, but this effect is not considered in the present study).

The correctness of the a_i coefficients reported in Table 2 lies on the accuracy of the experimental physico-chemical parameters of the solvent which influence the velocity profile. The most important one is the parameter B entering the viscosity Eq. 4. In the case of ethylbenzene with $\Delta T = 60°C$ and $T_c = 20°C$, one finds $d \ln |\nu| / d \ln B = 0.91$. Therefore, a 1% variation of B (i.e. $\delta B = 11$ K for ethylbenzene) leads to a 0.9% variation in ν. In practice, the B parameter obtained by fitting experimental viscosity data according to Eq. 4 may not be rigorously equal to the true B parameter of the solvent investigated owing to the experimental uncertainty in the basic viscosity data, or Eq. 4 may not fit correctly the viscosity data in the whole temperature domain, in spite of its theoretical foundation. This source of error is probably the most important although its significance cannot easily be estimated. Nevertheless, the relatively high value of the correlation coefficient (generally larger than 0.999) obtained when fitting experimental data according to Eq. 4 gives confidence in the accuracy of the B parameter and of the resulting a_i coefficients in Eq. 22.

The influence of B on ν is shown in Fig. 5 for $T_c = 20°C$ and two ΔT values (50 and 100°C). In the B range spanned by the twelve investigated

than 0.4% in all instances and, on average, is about 0.2%, which is satisfactory. Indeed, in the high-retention domain, a 1% error in the determination of ν with $\nu \approx -0.2$ results in only a 0.25% error in the FFF parameter λ determined from retention data. Accordingly, the error in λ resulting from the use of Eq. 22 instead of the exact ν value will be at most about 0.1%, which is negligible in comparison with the experimental uncertainty in the measurement of the retention factor R. This error in λ will be smaller for smaller $|\nu|$ values. The numerical values of the a_i coefficients determined for the twelve solvents investigated are reported in Table 2 with ΔT and T_c expressed in °C (note that if T_c and ΔT were

Table 2

Values of the a_i parameters entering the ν vs. ΔT and T_c relationship, $\nu = (a_1 T_c + a_2)\,\Delta T + (a_3 T_c + a_4)\,\Delta T^2 + (a_5 T_c + a_6)\,\Delta T^3$, with ΔT and T_c in °C

Solvent	a_1	a_2	a_3	a_4	a_5	a_6
Benzene	$3.2890 \cdot 10^{-5}$	$-5.7476 \cdot 10^{-3}$	$-2.3355 \cdot 10^{-7}$	$2.7828 \cdot 10^{-5}$	$7.9610 \cdot 10^{-10}$	$-7.7659 \cdot 10^{-8}$
2-Butanone	$2.4391 \cdot 10^{-5}$	$-4.2698 \cdot 10^{-3}$	$-1.4870 \cdot 10^{-7}$	$1.8096 \cdot 10^{-5}$	$4.5769 \cdot 10^{-10}$	$-4.6985 \cdot 10^{-8}$
Carbon tetrachloride	$3.1100 \cdot 10^{-5}$	$-5.4295 \cdot 10^{-3}$	$-2.1386 \cdot 10^{-7}$	$2.5182 \cdot 10^{-5}$	$7.0947 \cdot 10^{-10}$	$-6.9182 \cdot 10^{-8}$
Cyclohexane	$3.7850 \cdot 10^{-5}$	$-6.6216 \cdot 10^{-3}$	$-2.8678 \cdot 10^{-7}$	$3.3675 \cdot 10^{-5}$	$9.9830 \cdot 10^{-10}$	$-9.7197 \cdot 10^{-8}$
Cyclohexanone	$4.4449 \cdot 10^{-5}$	$-7.8087 \cdot 10^{-3}$	$-3.6313 \cdot 10^{-7}$	$4.3010 \cdot 10^{-5}$	$1.2979 \cdot 10^{-9}$	$-1.2948 \cdot 10^{-7}$
p-Dioxane	$3.2829 \cdot 10^{-5}$	$-5.7365 \cdot 10^{-3}$	$-2.3105 \cdot 10^{-7}$	$2.7502 \cdot 10^{-5}$	$7.6947 \cdot 10^{-10}$	$-7.7352 \cdot 10^{-8}$
Ethyl acetate	$2.6196 \cdot 10^{-5}$	$-4.5583 \cdot 10^{-3}$	$-1.6611 \cdot 10^{-7}$	$1.9285 \cdot 10^{-5}$	$5.2939 \cdot 10^{-10}$	$-5.0727 \cdot 10^{-8}$
Ethylbenzene	$2.7579 \cdot 10^{-5}$	$-4.7923 \cdot 10^{-3}$	$-1.8286 \cdot 10^{-7}$	$2.1212 \cdot 10^{-5}$	$6.1322 \cdot 10^{-10}$	$-5.6833 \cdot 10^{-8}$
Tetrahydrofuran	$2.3140 \cdot 10^{-5}$	$-4.0363 \cdot 10^{-3}$	$-1.3965 \cdot 10^{-7}$	$1.6848 \cdot 10^{-5}$	$4.3405 \cdot 10^{-10}$	$-4.2795 \cdot 10^{-8}$
Toluene	$2.7169 \cdot 10^{-5}$	$-4.7429 \cdot 10^{-3}$	$-1.7549 \cdot 10^{-7}$	$2.0883 \cdot 10^{-5}$	$5.6398 \cdot 10^{-10}$	$-5.5386 \cdot 10^{-8}$
o-xylene	$3.1016 \cdot 10^{-5}$	$-5.2335 \cdot 10^{-3}$	$-2.0980 \cdot 10^{-7}$	$2.3803 \cdot 10^{-5}$	$6.9511 \cdot 10^{-10}$	$-6.4920 \cdot 10^{-8}$
p-xylene	$2.6337 \cdot 10^{-5}$	$-4.5996 \cdot 10^{-3}$	$-1.6614 \cdot 10^{-7}$	$1.9918 \cdot 10^{-5}$	$5.1909 \cdot 10^{-10}$	$-5.2239 \cdot 10^{-8}$

solvents (from about 900 to 1800 K), ν is seen to vary approximately linearly, although their intercepts are not equal to 0 as they should be since a hypothetical $B = 0$ solvent would have a constant viscosity at all temperatures. Nevertheless, as
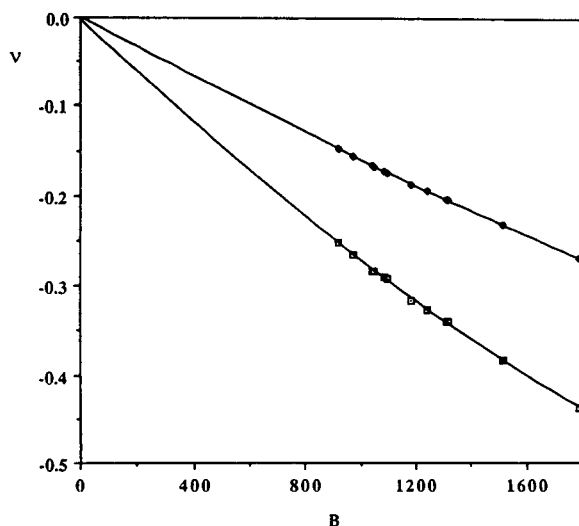
Fig. 5. Variations of the ν parameter with the solvent B constant. Upper curve, $\Delta T = 50$°C; lower curve, $\Delta T = 100$°C. $T_c = 20$°C.

organic solvents have B values lying within the range covered in Fig. 5, this near-linearity property can be used to obtain a rough estimate of the ν value for a solvent not listed in Table 1 but for which B is known. However, one cannot expect to obtain precise estimates as the temperature dependence of the thermal conductivity differs from one solvent to another, as reflected by the slight fluctuations of the data points in Fig. 5 around the regression line.

The major interest in the calculation of ν according to Eq. 22 in connection with the data in Table 2 is that it allows one to take into account, with fair accuracy, the effect that deviations in the velocity profile have on calculations of the retention factor. Indeed, the calculation of the retention factor, R, of a polystyrene sample with molecular mass 300 000 using the exact velocity profile of the ethylbenzene carrier with $\Delta T = 60$°C and $T_c = 20$°C gives a value of 0.195. If the velocity profile was assumed to be parabolic, the error in R would be 19.5%, whereas using the third-degree polynomial velocity profile with the ν value estimated as indicated above as -0.200, the error in R is only 0.25%. The error in R appears in this instance to be reduced nearly by two orders of magnitude when taking into account the deviation of the

velocity profile from the parabolic shape by means of the third-degree profile.

5. Conclusions

Thermal FFF is mainly used to obtain information on the thermal diffusion properties and the molecular mass or size of a sample. The first step in this direction is to determine the basic FFF parameter λ from retention data. In order to take into account the deviation of the velocity profile from the ideal parabolic shape due to the temperature dependence of the viscosity, one suggests first calculating the ν parameter of the third-degree polynomial velocity profile to approximate the exact velocity profile by means of Eq. 22 and Table 2, for the actual operating conditions (solvent, ΔT, T_c). Then the basic FFF parameter λ can be obtained from the retention factor R using Eq. 17 for that calculated value of ν. Solving Eq. 17 for λ when R and ν are known can be done numerically using a classical iterative methods such as Newton's method or, most conveniently, by listing R values for as close as desired λ values with various spreadsheet applications, such as Excel, on microcomputers.

This study was motivated by the need for a practical method to take into account retention perturbations in thermal FFF arising from deviations of the velocity profile from the ideal parabolic shape due to the temperature dependence of the relevant parameters. It has been pointed out that, similarly, retention perturbations may also arise from deviations of the concentration profile from the ideal exponential shape [8]. Although the latter perturbations might be of the same order as the former and that the assumption of an exponential concentration profile made for obtaining Eq. 17 is not rigorously correct, Eq. 17 still serves as a very useful basis for taking into account the effect of the concentration profile distortion on retention. Work is in progress in this direction and will be presented in a forthcoming publication [16].

Acknowledgement

References

[1] J.C. Giddings, *Science*, 260 (1993) 1456–1465.
[2] M. Martin and P.S. Williams, in F. Dondi and G. Guiochon (Editors), *Theoretical Advancement in Chromatography and Related Separation Techniques (NATO ASI Series: Mathematical and Physical Sciences*, Vol. 383), Kluwer, Dordrecht, 1992, pp. 513–580.
[3] T. Takahashi and W.N. Gill, *Chem. Eng. Commun.*, 5 (1980) 367–385.
[4] J. Janča, M. Hoyos and M. Martin, *Chromatographia*, 33 (1992) 284–286.
[5] M.N. Myers, K.D. Caldwell and J.C. Giddings, *Sep. Sci.*, 9 (1974) 47–70.
[6] G. Westermann-Clark, *Sep. Sci. Technol.*, 13 (1978) 819–822.
[7] S.L. Brimhall, M.N. Myers, K.D. Caldwell and J.C. Giddings, *J. Polym. Sci., Polym. Phys. Ed.*, 23 (1985) 2443–2456.
[8] J.C. Giddings, K.D. Caldwell and M.N. Myers, *Macromolecules*, 9 (1976) 106–112.
[9] J.J. Gunderson, K.D. Caldwell and J.C. Giddings, *Sep. Sci. Technol.*, 19 (1984) 667–683.
[10] M. Martin and J.C. Giddings, *J. Phys. Chem.*, 85 (1981) 727–733.
[11] G. Liu and J.C. Giddings, *Chromatographia*, 34 (1992) 483–492.
[12] M. Martin, M.N. Myers and J.C. Giddings, *J. Liq. Chromatogr.*, 2 (1979) 147–164.
[13] J.C. Giddings, M. Martin and M.N. Myers, *Sep. Sci. Technol.*, 14 (1979) 611–643.
[14] M. Martin and R. Reynaud, *Anal. Chem.*, 52 (1980) 2293–2298.
[15] M.E. Schimpf, P.S. Williams and J.C. Giddings, *J. Appl. Polym. Sci.*, 37 (1989) 2059–2076.
[16] M. Martin, J. Belgaied, C. Van Batten and M. Hoyos, in preparation.
[17] K.D. Caldwell, M. Martin and J.C. Giddings, unpublished results.
[18] R.B. Bird, W.E. Stewart and E.N. Lightfoot, *Transport Phenomena*, Wiley, New York, 1960, Ch. 3.
[19] A.B. Shah, J.F.G. Reis, E.N. Lightfoot and R.E. Moore, *Sep. Sci. Technol.*, 14 (1979) 475–497.
[20] R.C. Reid, J.M. Prausnitz and B.E. Poling, *The Properties of Gases and Liquids*, McGraw-Hill, New York, 4th ed., 1987, Ch. 9.

[21] E. Guyon, J.-P. Hulin and L. Petit, *Hydrodynamique Physique*, InterEditions et Editions du CNRS, Paris and Meudon, 1991, Ch. 2.

[22] R.B. Bird, W.E. Stewart and E.N. Lightfoot, *Transport Phenomena*, Wiley, New York, 1960, Ch. 8.

[23] R.C. Reid, J.M. Prausnitz and B.E. Poling, *The Properties of Gases and Liquids*, McGraw-Hill, New York, 4th ed., 1987, Ch. 10.

[24] H.-G. Elias, in J. Brandrup and E.H. Immergut (Editors), *Polymer Handbook*, Wiley, New York, 2nd ed., 1975, Ch. 7.

[25] J.C. Giddings, L.K. Smith and M.N. Myers, *Anal. Chem.*, 47 (1975) 2389–2394.

[26] S.L. Brimhall, M.N. Myers, K.D. Caldwell and J.C. Giddings, *Sep. Sci. Technol.*, 16 (1981) 671–689.

Gas chromatographic separation of deuterated and optical isomers of di-2-butyl ethers

Buchang Shi, Robert A. Keogh, Burtron H. Davis*

Center for Applied Energy Research, 3572 Iron Works Pike, Lexington, KY 40511, USA

Abstract

By connecting a DB-5 column in series with a Cyclodex-B column, nine of ten isomers of a mixture of di-2-butyl ether-d_0, di-2-butyl ether-d_5 and di-2-butyl ether-d_{10} produced during the dehydration of a 1:1 mixture of 2-butanol-d_0 and 2-butanol-d_5 using an Al_2O_3 catalyst, were separated and identified. The (R,S) and (S,R) isomers of di-2-butyl ether-d_5 could not be separated due to the similarity of their interactions toward the DB-5 and Cyclodex-B columns.

1. Introduction

Gas chromatographic methods permit pairs of isotopic molecules to be separated completely and determined quantitatively [1–5]. The introduction of highly efficient capillary GC columns in recent years permits this analysis to be accomplished in just a few minutes [6,7]. The heavier species (deuterated) always elutes first. This phenomenon is an inverse isotope effect to which intermolecular Van der Waals forces make the major contribution [1–8].

The separation of the components of an enantiomeric pair has also been accomplished by chromatographic methods [9–14]. The separation of chiral compounds by GC is an important and growing application area and has the potential to replace most classical methods of optical purity determination, such as optical

rotation measurements and diastereomeric separations [14].

The separation of a pair of isotopic molecules or the separation of a pair of enantiomeric molecules is usually difficult, but either can be accomplished by the proper selection of the column and the GC separation conditions. However, when the separation of pairs of isotopic *and* enantiomeric molecules is desired, especially when the enantiomeric molecules are deuterated to different degrees, the separation of the mixture becomes more difficult and more challenging. This problem may be rare today, but it does occur in mechanistic studies, and interest in this will increase in the future.

We report here the results where nine of the ten isomers of a mixture of di-2-butyl ether-d_0, di-2-butyl ether-d_5 and di-2-butyl ether-d_{10} were separated, identified and quantitatively determined by connecting a DB-5 column in series with an optically active Cyclodex-B column.

* Corresponding author.

2. Experimental

The DB-5 column, purchased from J & W Scientific, was a 60 m × 0.32 mm fused-silica column (0.25 μm film thickness). The liquid phase was 5% phenyl- and 95% dimethylsilicone. The Cyclodex-B column, also purchased from J & W Scientific, is a 30 m × 0.32 mm column (0.25 μm). The liquid phase was β-cyclodextrin. The columns were connected in series using a capillary connector (Supelco), in such a way that the compounds were separated first on the DB-5 column and then on the Cyclodex-B column. A Hewlett-Packard 5890 Series II gas chromatograph, interfaced with an HP5971A mass-selective detector, and operated under the control of a Vectra 05/165 computer using HPG1034B software, was used for identification. A Hewlett-Packard 5880 gas chromatograph equipped with a flame ionization detector was used for quantitative analysis. Helium was used as the carrier gas.

Retention volumes have been corrected using the retention time of methane to determine the dead volume. The mixture of di-2-butyl ethers was obtained from a reaction of a 1:1 mixture of (±)-butanol-d_5 and (±)-2-butanol-d_0 with Al_2O_3 at 230°C.

3. Results and discussion

In a study of the mechanism of dehydration of 2-butanol on Al_2O_3, an intermolecular competition technique has been utilized to determine the deuterium isotope effect for the rate of conversion of the alcohol and for the formation of butenes. For this purpose, a 1:1 mixture of 2-butanol-d_0 and 2-butanol-d_5 (C^2H_3–CHOH–C^2H_2–CH_3) was used as the feed. The liquid products were collected at timed intervals and were analyzed. Six peaks were always observed in the gas chromatogram when using only the DB-5 column (Fig. 1a). To determine the identity of the compounds responsible for these peaks, an experiment using only 2-butanol-d_0 as the reactant was conducted. In this case, only two peaks with about equal areas were observed

(Fig. 1b). The compounds responsible for these peaks were separated and collected using liquid chromatographic techniques. These two compounds were identified from ^1H NMR, ^{13}C NMR, two-dimensional NMR and GC–MS data to be di-2-butyl ethers.

An optically active GC column (Cyclodex-B) was used to identify the two isomers of the ether formed from 2-butanol-d_0. The earlier eluting peak in Fig. 1b using the DB-5 column was split into two peaks (Fig. 2) by the optically active column Cyclodex-B. This result indicates that the first peak eluting from the DB-5 column corresponds to the (R,R) and (S,S) isomers. A known mixture of di-2-butyl ether was used to identify the peaks from the Cyclodex-B experiment. The results indicate that the first peak eluting from Cyclodex-B column corresponds to the (R,R) isomer, the second to the (S,S) isomer and the third to the (R,S) isomer.

When a reaction involves the conversion of a 1:1 mixture of (±)-2-butanol-d_0 and (±)-2-butanol-d_5, ten isomers of di-2-butyl ether are expected, and they are (D = deuterium):

CD_3-CH-CD_2-CH_3
|
O
|
CD_3-CH-CD_2-CH_3

1. (R,R)-d_{10}
2. (S,S)-d_{10}
3. (R,S)-d_{10}

CD_3-CH-CD_2-CH_3
|
O
|
CH_3-CH-CH_2-CH_3

4. (R,R)-d_5
5. (S,S)-d_5

CD_3-CH-CD_2-CH_3
|
O
|
CH_3-CH-CH_2-CH_3

6. (R,S)-d_5

CD_3-CH-CD_2-CH_3
|
O
|
CH_3-CH-CH_2-CH_3

7. (S,R)-d_5

CH_3-CH-CH_2-CH_3
|
O
|
CH_3-CH-CD_2-CH_3
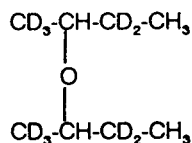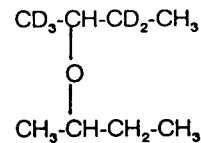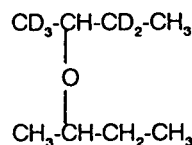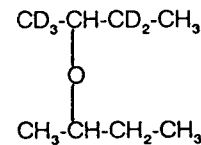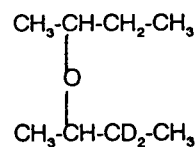
8. (R,R)-d_0
9. (S,S)-d_0
10. (R,S)-d_0
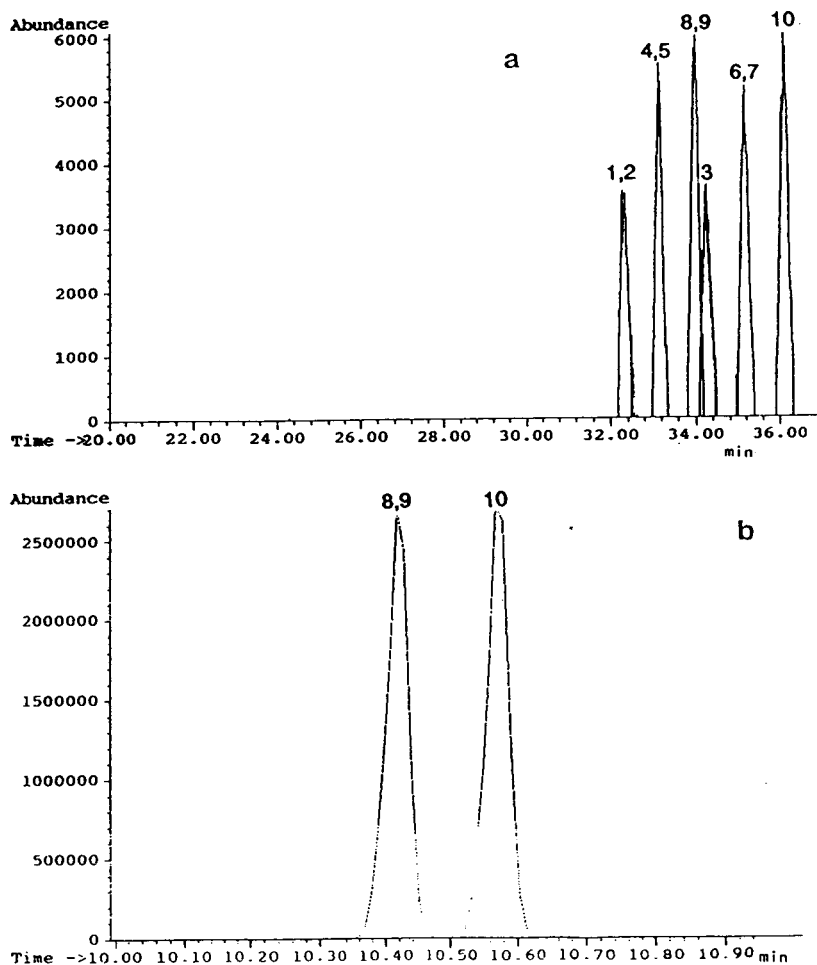
Fig. 1. Gas chromatograms using a DB-5 column to separate the ethers formed during the dehydration of 2-butanol: (a) 1:1 mixture of 2-butanol-d_0 and 2-butanol-d_5 as the feed, column temperature 15°C; (b) 2-butanol-d_0 as the feed, column temperature 45°C. See text for compound identities.

Complete separation of these ten isomers is not possible using the DB-5 column or the Cyclodex-B column alone. Using the DB-5 column, only six peaks were obtained as shown in Fig. 1a. The first peak on this chromatogram was identified as a mixture of 1 and 2; the second peak corresponds to a mixture of 4 and 5; the third peak corresponds to a mixture of 8 and 9; the fourth corresponds to isomer 3; the fifth corresponds to a mixture of 6 and 7 and the last one is due to compound 10. Using only the Cyclodex-B column, the deuterium-containing compounds cannot be separated from the undeuterated compounds.

In order to separate these ten isomers completely, a DB-5 column has been connected in series to a Cyclodex-B column. It was anticipated that the deuterated compounds would be separated from the undeuterated ones, and that the optically active isomers would be separated from the meso isomers by the DB-5 column, and then the optical active isomers would be separated into the (S,S) and (R,R) isomers on the Cyclodex-B columns. The early experiments showed that the situation was not so simple. In isothermal runs, whether at a low temperature (12°C) or at a high temperature (45°C), poor separations were obtained. The results from
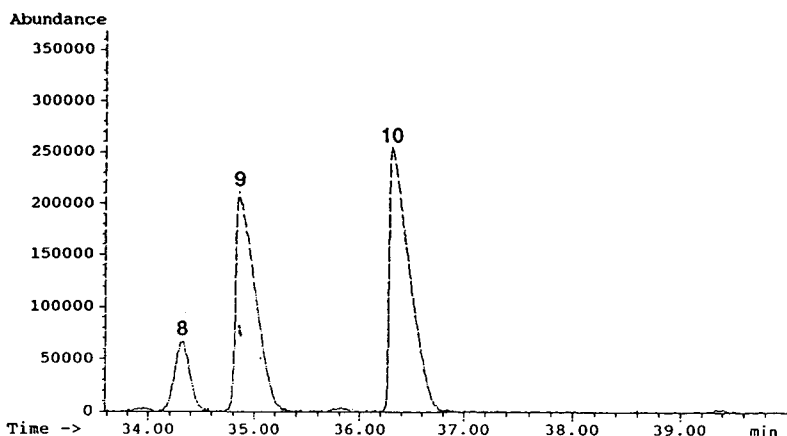
Fig. 2. GC separation of di-2-butyl ether on Cyclodex-B column. Column temperature: 25°C. See text for compound identities.

these experiments indicated that just simply connecting the two columns did not result in a chromatogram (or total ion chromatogram) that initially had the six compounds separated by the DB-5 column, which in turn were separated into the optical isomers on the Cyclodex-B column, to produce the expected ten peaks.

The obvious overlap was due to the good enantiomeric separation on the Cyclodex-B column. It is well known [3–7] that the isotopic separation is temperature dependent, and the lower the column temperature, the better the separation. To obtain the most favorable operating temperature, the separation factor has been measured from 15 to 55°C on the DB-5 column. As indicated in Fig. 3, the best separation factors are observed around 15°C and the inverse isotope effect of di-2-butyl ether-d_{10} is larger than that of di-2-butyl ether-d_5. The difference in enthalpy of the pairs of isotopic molecules related to the chromatographic process on DB-5 column are calculated according to Eq. 1 (Table 1)

Table 1
Difference in enthalpy for the pairs of isotopic molecules related to the chromatographic process on the DB-5 column

Pairs of isotopic molecules	$\Delta H_H - \Delta H_D$ (J)
Di-2-butyl ether-d_0/-d_{10} (R,R; S,S)	−247.7
Di-2-butyl ether-d_0/-d_5 (R,R; S,S)	−118.8
Di-2-butyl ether-d_0/-d_{10} (R,S)	−386.3
Di-2-butyl ether-d_0/-d_5 (R,S)	−116.7

$$\log (V_R)_H/(V_R)_D = -(\Delta H_H - \Delta H_D)/2.3RT + c$$

$$(1)$$

where $(V_R)_H$ and $(V_R)_D$ are the retention volumes of hydrogen-containing compound and deuterated compound, respectively, and c is a constant. The optical active and meso isomers of di-2-butyl ether-d_5 have the same response toward the temperature (Table 1); however, the meso isomer of di-2-butyl ether-d_{10} is more sensitive to temperature than the optically active isomer of di-2-butyl ether-d_{10}. It is also known [14] that the enantioselectivity of a chiral pair,
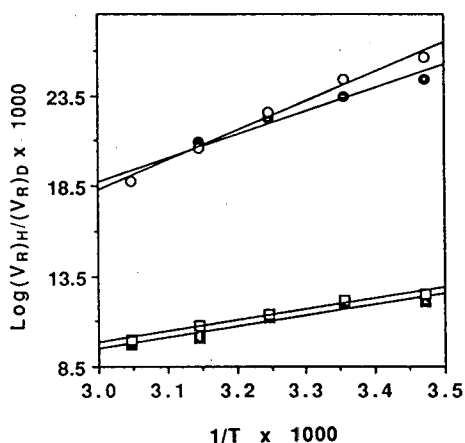
Fig. 3. Plot of the logarithms of the retention volumes versus $1/T$. ○ = Di-2-butyl ether-d_0/-d_{10} (R,S); ● = Di-2-butyl ether-d_0/-d_{10} (R,R; S,S); □ = Di-2-butyl ether-d_0/-d_5 (R, S); ■ = Di-2-butyl ether-d_0/-d_5 (R,R; S,S).

Table 2
GC data on the separation of di-2-butyl ether-d_0 on Cyclodex-B column

Temperature (°C)	$r_{S,S/R,R}$	$k_{S,S} - k_{R,R}$ (min)
15	1.02	1.23
25	1.03	0.93
35	1.02	0.46
45	1.02	0.24
55	1.02	0.13

Inlet pressure, 0.6 bar.

Table 3
Relative amounts of each isomer of di-2-butyl ether-d_0, -d_5 and -d_{10}

Compound	Determined by GC (%)	Expected[a]
1	5.0	6.3
2	4.7	6.3
3	10.3	12.5
4	11.5	12.5
5	13.2	12.5
6, 7	25.1	25.0
8	8.3	6.3
9	8.3	6.3
10	13.7	12.5

[a] Assuming an SN_2 type mechanism for the formation of the ethers.

$r_{R/S}$, can be expressed in terms of the retention factors as shown in Eq. 2:

$$r_{R/S} = \frac{k_R}{k_S} \qquad (2)$$

The value of $r_{R/S}$ is independent on the temperature; however, the value of $(k_R - k_S)$ is temperature dependent according to Eq. 3:

$$k = A \cdot \frac{RT_c}{P^0 r^0} \qquad (3)$$

where A is the stationary phase contribution, T_c is the column temperature, R is the gas constant, P^0 is the vapor pressure of the compound and r^0 is the activity of the compound. The value of $(k_R - k_S)$ determines how good the separations are. As can be seen from Table 2, the (R,R) isomer of di-2-butyl ether eluted first from the Cyclodex-B column and the value of $r_{S,S/R,R}$ is around 1.02 over the temperature range of 15 to 55°C. However, the value of $(k_{S,S} - k_{R,R})$

changes from 0.13 min at 55°C to 1.23 min at 15°C.

The above experiments suggest that if the temperature is adjusted so that the isotopic separation is at its maximum and the enantiomeric separation is kept to a minimum, a satisfactory separation may be possible. As expected, when the GC temperature program included holding the temperature at 12°C for 20 min, then increasing the temperature at a rate of 4°C/min to 45°C, a very good separation was obtained (Fig. 4). The identities of each component, verified by GC–MS, are also shown in Fig. 4.

Compounds 6 and 7 could not be separated. They are different compounds, but they have the same behavior on the DB-5 and Cyclodex-B columns.

The relative amounts of each isomer are given in Table 3. The data determined by GC using a
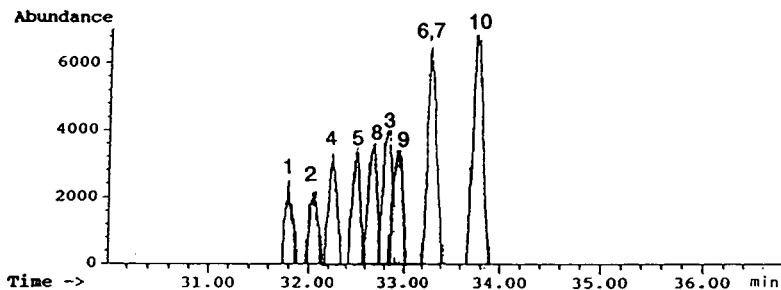
Fig. 4. GC separation of a mixture of di-2-butyl ether-d_0, -d_5 and -d_{10} on a DB-5 and Cyclodex-B column in series (12°C, hold 20 min, then 4°C/min to 45°C). See text for compound identities.

flame ionization detector are close to those expected if the ether formation follows a SN_2 type mechanism.

4. Conclusions

Deuterated enantiomeric isomers can be separated by a GC method that combines two columns, one of which is responsible for the separation of isotopic pairs and the other for the separation of the enantiomeric pairs. The separation of nine of the ten isomers of di-2-butyl ether-d_{10}, di-2-butyl ether-d_5 and di-2-butyl ether-d_0 provides an excellent example for the utility of this technique.

References

[1] W.A. van Hook, *Adv. Chem.*, 89 (1969) 99.
[2] F. Bruner, G.P. Carboni and A. Liberti, *Anal. Chem.*, 38 (1966) 298.
[3] F. Bruner and G.P. Cartoni, *J. Chromatogr.*, 18 (1965) 390.
[4] A. Liberti and G.P. Cartoni, *J. Chromatogr.*, 12 (1963) 8.
[5] W.A. van Hook and J.T. Phillips, *J. Chromatogr.*, 30 (1967) 211.
[6] M. Mohnke and J. Heybey, *J. Chromatogr.*, 417 (1989) 27.
[7] B. Shi and B.H. Davis, *J. Chromatogr. A*, 654 (1993) 319.
[8] W.A. van Hook and J.T. Phillips, *J. Phys. Chem.*, 70 (1966) 1515.
[9] C.E. Dalgliesh, *J. Chem. Soc.*, (1952) 3940.
[10] D.M. Sand and H. Schleak, *Anal. Chem.*, 33 (1961) 1624.
[11] T. Koscielski, D. Sybilska and J. Jarezak, *J. Chromatogr.*, 364 (1986) 299.
[12] W.A. König, S. Lutz, P. Mischnick-Lübecke, B. Brassat and G. Wenz, *J. Chromatogr.*, 447 (1988) 193.
[13] D.W. Armstrong and W.Y. Li, *Anal. Chem.*, 62 (1990) 217.
[14] J.V. Hinshaw, *LC · GC*, 11 (1993) 644.

Degradation of furosine during heptafluorobutyric anhydride-derivatization for gas chromatographic determination

A. Ruttkat, H.F. Erbersdobler*

Institut für Humanernährung und Lebensmittelkunde der Christian-Albrechts-Universität zu Kiel, Düsternbrooker Weg 17, 24105 Kiel, Germany

Abstract

To evaluate further the reported degradation of furosine during gas chromatographic (GC) determination, a set of experiments with different derivatization conditions were carried out, utilizing a pure furosine standard. The results showed that the decomposition of furosine is not a consequence of the GC separation process, but a result of the derivatization procedure applied. Depending on the derivatization conditions, distinct differences in the percentage degradation were observed. Particularly, an incorrect strong drying during the second and third evaporation steps resulted in substantial degradation (up to ca. 21%), suggesting that the isobutyl ester and the heptafluorobutyryl isobutyl ester of furosine are sensitive to dryness. This demonstrates that the GC determination of furosine as a heptafluorobutyryl isobutyl ester derivative cannot be recommended for routine analytical application. Even under optimum derivatization conditions, degradation in the range 3–5% cannot be completely avoided.

1. Introduction

In the early stages of the Maillard reaction, lysine and sugar compounds react to form derivatives such as fructoselysine, lactuloselysine or maltuloselysine. During hydrolysis with 7.8 M HCl these Amadori compounds form furosine [ϵ-N-(2-furoylmethyl)-L-lysine], an indicator of Maillard-type heat damage [1,2]. Furosine determinations are often applied in food science and nutrition, clinical research and medical biochemistry.

For furosine determination, chromatographic techniques including ion-exchange chromatog-

raphy (IEC) with commonly used amino acid analysers [3,4], reversed-phase high-performance liquid chromatography (HPLC) [5–7], gas chromatography (GC) [8], respectively gas chromatography–mass spectroscopy [9] have been applied. The GC determination of furosine as the heptafluorobutyryl isobutyl ester, using nitrogen–phosphorus-selective detection (NPD), was first established by Büser and Erbersdobler [8]. The simultaneous determination of amino acids and furosine by GC, using a capillary column and NPD, allows the successful resolution of these compounds with high selectivity, linearity and sensitivity [10–12]. Resmini et al. [6] proposed that during GC analysis according to the above method [8], considerable decomposition

_____
* Corresponding author.

of furosine may take place. They determined furosine in heat-treated milk samples after acid hydrolysis, first using an HPLC method and subsequently examined the collected furosine peak by GC. In addition to the furosine peak an unexpected lysine peak was detected.

To examine further the probability that furosine can be destroyed during GC determination, in this work the degradation of furosine under different derivatization conditions was measured, using pure furosine standard.

2. Experimental

2.1. Reagents

Furosine standard with a purity of >99% was obtained from Neosystem (Strasbourg, France). Norleucine hydrochloride, used as an internal standard, was purchased from Serva (Heidelberg, Germany) and heptafluorobutyric anhydride (HFBA), isobutanol and ethyl acetate, all of analytical-reagent grade, from Merck (Darmstadt, Germany). Isobutanol–3 M HCl was prepared by bubbling anhydrous HCl through two successive traps containing concentrated sulfuric acid and then into isobutanol at 0°C.

In all experiments the furosine standard was used at a concentration of 0.2 μmol/ml and the norleucine standard at a concentration of 0.25 μmol/ml.

The percentage degradation of furosine was calculated from the recovery of lysine compared with the initial lysine content in furosine.

2.2. Instrumentation

Chromatography was performed using a DANI Model 65.00 gas chromatograph equipped with a nitrogen–phosphorus detector, a programable temperature vaporizer (PTV)–injection system and a OV-1–CB fused-silica capillary column (25 m × 0.32 mm O.D. × 0.25 mm I.D.) from CS (Langerwehe, Germany). The injector was operated in the split mode with a splitting

ratio of 1:20 and the injection temperature was varied form 54 to 260°C. The detector temperature was set at 280°C. The detector was provided with air (140 ml/min) and hydrogen (3 ml/min).

Nitrogen was used as the make-up gas at a flow-rate of 25 ml/min. The carrier gas (helium) flow-rate was typically 2.6 ml/min. After 2 min at 54°C, the oven temperature was programmed to 260°C at 6°C/min, the final temperature being held for about 12 min. The chromatograph was linked to a C-R5A Chromatopac integrator from Shimadzu (Duisburg, Germany), which performed data acquisition.

2.3. Derivatization

The heptafluorobutyryl isobutyl ester was prepared according to the reaction scheme summarized in Fig. 1. Additionally a possible degradation route of the furosine derivatives is shown. Compared with the method described by Büser and Erbersdobler [8], two slight modifications were introduced. First, the heating times in the oven were both increased by about 5 min, and second, no co-injection with acetic anhydride was carried out. In a set of experiments, the impact of each individual evaporation step on the percentage degradation was studied. The experiments are summarized in Table 1.

3. Results and discussion

Typical chromatograms, one for a sample with a high percentage degradation of furosine and one for a sample with a low percentage degradation are shown in Fig. 2. Between the norleucine peak (retention time 18 min), used as an internal standard, and the furosine peak (retention time 36 min), a lysine peak (retention time 26 min) is recognizable in both instances.

As a pure furosine standard (purity >99%) was used and confirmed by other chromatographic techniques [7], lysine can only be a decomposition product of furosine. Repeated injections of the same volumes from the same sample solution revealed that the percentage degradation did not differ. Hence, the main

Dispensation of the furosine and norleucine standard
solutions into a 1 ml screw-capped glass tube

| Evaporation step 1 | Evaporation at 40 °C, using a stream of dry nitrogen |

furosine

Esterification
Addition of 100 µl isobutanol-
3M HCl, heating for 35 min at
120 °C, cooling in an ice-bath
bath

furosine isobutyl ester

| Evaporation step 2 | As step 1 |

Acylation
Addition of 100 µl HFBA,
heating for 15 min at 150 °C,
cooling in an ice-bath

furosine HFB isobutyl
ester

| Evaporation step 3 | As step 2 |

Dissolution in 100 µl ethyl acetate

* possible degradation site, leading to the corresponding lysine
   derivatives

Fig. 1. Derivatization procedure.

Table 1
Experimental conditions

Experiment	Extent of dryness in different evaporation steps		
	Step 1	Step 2	Step 3
A	Dry	Dry	Close to dryness
B	Dry	Close to dryness	Dry
C	Dry	Close to dryness	Close to dryness
D	Dry	Moist	Close to dryness

Close to dryness means that after the evaporation step concerned, a very slight residual moisture remained behind in the
screw-capped glass tube.
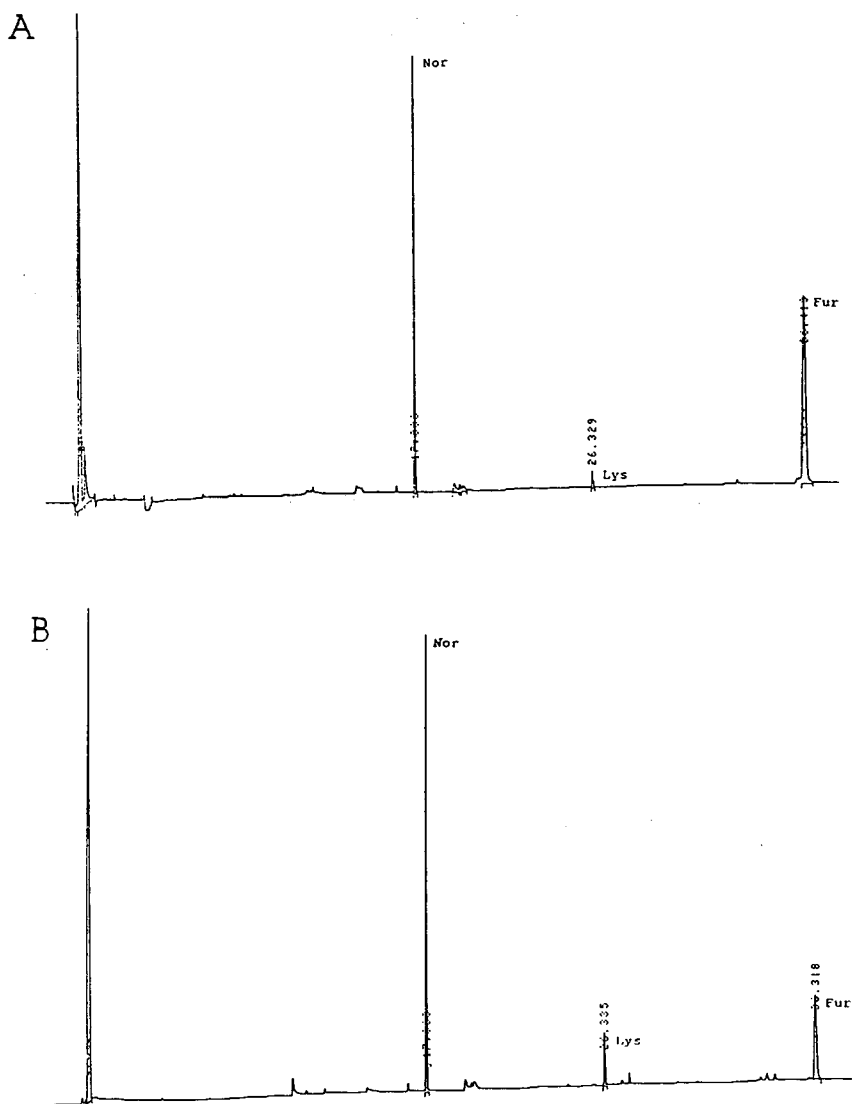
Fig. 2. Typical chromatograms for (A) a low and (B) a high percentage degradation of furosine. The HFB derivatives were prepared according to Fig. 1. Peaks: Nor = norleucine; Lys = lysine; Fur = furosine. Numbers at peaks are retention times in min.

cause of the different degradation rates lies in the derivatization procedure.

In Fig. 3, the percentage degradation under different derivatization conditions (see Table 1) is compared. Each column represents the mean + standard deviation of six to ten determinations.

Evaporation of the underivatized furosine (step 1, Fig. 1) to dryness did not lead to an increased degradation as compared with an evaporation performed close to dryness, suggesting that furosine itself is stable against dryness. Therefore, in subsequent experiments, evaporation in step one was always carried out to dryness.

Different results were obtained when in step 2 (experiment A) or in step 3 (experiment B) excess solvent was evaporated to complete dry-
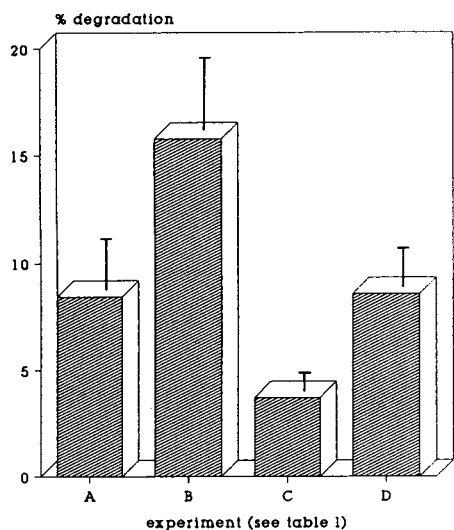
Fig. 3. Percentage degradation of furosine under different derivatization conditions.

ness. Then the percentage degradation was high, ranging from 5.3 to 11.3% for step 2 and from 11.9 to 20.3% for step 3. These results suggest that the HFB isobutyl ester of furosine is very sensitive to dryness. Experiments A and B show that a low percentage degradation of furosine is obtainable only when in evaporation steps 2 and 3 evaporation is carried out not too far, i.e., close but not completely to dryness.

The third evaporation step is especially critical, because the excess HFBA and also the HFB isobutyl ester are relatively volatile and hence the optimum extent of drying can easily be missed. Moreover, when a large batch of samples are derivatized simultaneously, the correct degree of dryness seems difficult to achieve for all samples.

In experiment D, the effect of an insufficient evaporation in step 2 was tested. In this instance, unremoved water, which is formed during esterification, can react with HFBA to form HFBA acid. Possibly this contamination leads to the poor furosine response, with a simultaneous increase in the variability. Unexpectedly, the percentage degradation also increased. Similar observations were made by Moodie et al. [13] and described for arginine.

Careful evaporation in steps 2 and 3 close to dryness (experiment C) yielded the best results, but a percentage degradation ranging from 3.2 to 4.6% has to be accepted.

In conclusions, these experiments have demonstrated that the GC determination of furosine as the HFB isobutyl ester derivative is affected by technical difficulties. For this reason, this method may be useful for comparative and confirmative assays, but is unsuitable for routine analytical applications.

Acknowledgements

References

[1] H. Erbersdobler and H. Zucker, Milchwissenschaft, 21 (1966) 564–568.
[2] H.F. Erbersdobler and A. Hupe, Z. Ernährungswiss., 30 (1991) 46–49.
[3] A. Brandt and H. Erbersdobler, Landwirtsch. Forsch., Sonderh., 28/II (1972) 115–119.
[4] H.F. Erbersdobler, B. Dehn, A. Nangpal and H. Reuter, J. Dairy Res., 54 (1987) 147–151.
[5] F. Schleicher and O.H. Wieland, J. Clin. Chem. Clin. Biochem., 19 (1981) 81–87.
[6] P. Resmini, L. Pellegrino and G. Batelli, Ital. J. Food Sci., 3 (1990) 173–183.
[7] J. Hartkopf and H.F. Erbersdobler, J. Chromatogr., 635 (1993) 151–154.
[8] W. Büser and H.F. Erbersdobler, J. Chromatogr., 346 (1985) 363–368.
[9] K.J. Knecht, J.A. Dunn, K.F. McFarland, D.R. McCarce, T.J. Lyons, S.R. Thorpe and J.W. Baynes, Diabetes, 40 (1991) 190–196.
[10] U. Bending, H. Stenner, A. Kettrup, Fresenius' Z. Anal. Chem., 309 (1981) 370–372.
[11] B. Kolb, M. Lindner and B. Kemphen, in Schriftenreihe: "Angewandte Gaschromatographie", Heft 21, Bodenseewerk Perkin-Elmer, Überlingen, 1974.
[12] W. Büser and H.F. Erbersdobler, Z. Lebensm.-Unters.-Forsch., 186 (1988) 509–513.
[13] M. Moodie, J.A. Burger, B.J. Hough, G.S. Shephard and D. Labadarios, J. Chromatogr., 347 (1985) 179–182.

Clean-up and confirmatory procedures for gas chromatographic analysis of pesticide residues. Part II

E. Viana, J.C. Moltó*, J. Mañes, G. Font

*Laboratory of Toxicology, Faculty of Pharmacy, University of Valencia, C/Vicent Andrés Estellés s/n,
46100 Burjassot Valencia, Spain*

(First received February 7th, 1994; revised manuscript received May 2nd, 1994)

Abstract

The behaviour of standard solutions of fourteen simple organohalogenated pesticides, nine individual polychlorinated biphenyls (PCBs) and Aroclor 1242, 1248, 1254 and 1260 on treatment with sulphuric acid, potassium hydroxide and chromium(IV) oxide was studied by capillary gas–liquid chromatography (cGC) using electron-capture detection. These methods were applied to confirm the presence of organochlorine residues in river water and human milk. Positive confirmation with the three treatments were in agreement with capillary GC(cGC)–MS determinations carried out in the electron impact and selected-ion monitoring mode. After cGC analyses, the extracts containing possible pesticides or Aroclors were treated with the three chemicals and re-analysed under the same cGC conditions. The new chromatographic profiles showed many missing artifact peaks, and some pesticides or PCBs were also destroyed. The presence or disappearance of the peaks after chemical attack makes it possible to identify the specific pesticides and PCBs analysed. PCBs resist both acid and alkali attacks, but some low-chloride PCBs are totally or partially destroyed by oxidative treatment. The methods studied are useful for intralaboratory purification and confirmation of residues of pesticides and PCBs, although they can be insufficient for identifying organochlorine pesticide residues from some very polluted samples.

1. Introduction

Capillary gas chromatography (cGC) with electron-capture detection (ECD) for the determination of organochlorine compound residues is a sensitive and selective method that is used in most research laboratories. However, extracts of plant, animal or environmental origin can contain electron-capturing materials other than pesticides or polychlorinated biphenyls (PCBs), and this can lead to incorrect identifica-

tions even if two different polarity capillary columns are employed.

To eliminate interferences normally occurring in halogenated residue analyses, several methods have been proposed. Most of them include adsorption column chromatography to clean up the extracts before cGC determination. This additional step is a major factor affecting the reproducibility of the overall analytical procedure and it is time, solvent and adsorbent consuming.

Adsorbents for column chromatography have also been mixed or impregnated with other compounds, such as acids, alkalis or oxidizing

---

* Corresponding author.

reagents, to help in the clean-up process. For example, Extrelut-1 was impregnated with sulphuric acid [1], Celite with sulphuric acid or magnesium oxide [2], alumina with potassium hydroxide or *tert.*-butoxide [3] and Florisil with silver nitrate [4].

Alternative methods for purifying extracts containing organochlorine residues or confirming some of the possible identified residues include chemical treatments. These treatments can be carried out on-line in a gas chromatographic system, with a liner filled with the chemical reagent, generally sodium or potassium hydroxide [5–7], magnesium oxide [8] or reducing, oxidizing, Lewis acid or weak alkali agents [9]. Most chemical treatments, however, are carried out off-line by mixing the extracts with acid, alkali, oxidizing or reducing reagents. These procedures do not require any modification of the chromatographic system, are inexpensive and are applicable in most research laboratories. However, they are not fully utilized by residue laboratories in routine confirmatory analyses, and no studies on the behaviour toward potassium hydroxide, sulphuric acid and chromium(VI) oxide treatments of some interesting pesticide metabolites such as endrin aldehyde and endrin ketone and individual PCBs were found in the literature.

Chemical treatments were originally applied to confirm organochlorine pesticide peaks in residue analyses when they were determined on packed columns [10–13]. Sulphuric acid dissolves many organic compounds other than saturated or chlorinated hydrocarbons. For this reason, it is used to purify food extracts in organochlorine pesticide and PCB analyses [14–20]. Alkali metal hydroxides in ethanolic solution dehydrochlorinate pesticides from the bis (phenyl) chloroethane group [21,22]. This effect has been employed to distinguish DDT and its metabolites from PCB residues [1,23,24]. Chromium(VI) oxide in acetic acid solution makes it possible to determine Aroclors in the presence of DDT and its analogues [25,26], and to determine total DDT metabolites as dichlorobenzophenones present in the interfering Aroclors [27]. The reactions between cyclodiene pesticides and dif-

ferent acidic, basic and derivatization agents have investigated to identify the mechanisms of the reactions [28–30].

Our interest centres on the ability of the most widely accepted chemical treatments, such as with concentrated sulphuric acid, ethanolic potassium hydroxide and chromium(VI) oxide in acetic acid solution, to purify environmental extracts and identify pesticide residues. A preliminary report gave the results for the three cited treatments when they were applied to eleven organochlorine and ten organophosphorus pesticides [31].

2. Experimental

2.1. Reference materials

Aldrin (purity 98%), endrin (95%), endrin ketone (98%), heptachlor (99%), heptachlor epoxide (99%), hexachlorobenzene (HCB) (99%), lindane (99%) and methoxychlor (99%) were purchased from Promochem (Wesel, Germany), *o,p'*-DDD (99%), *p,p'*-DDD (99%) from Aldrich, (Alcobendas, Spain) and *P,p'*-DDE (99%), *p,p'*-DDT (99%), dicofol (99%), endrin aldehyde (98%) and individual PCBs from Riedel-de Haën (Seelze, Germany). Commercially available PCB mixtures, Aroclor 1242, 1248, 1254 and 1260, were purchased from Supelco (Bellefonte, PA, USA).

2.2. Solvents

Ethyl acetate, *n*-hexane, ethanol and methanol (Nanograde quality) were purchased from Promochem.

2.3. Reagents

Sulphuric acid (sp. gr. 1.84), glacial acetic acid, potassium hydroxide and chromium(VI) oxide were of analytical-reagent grade from Merck (Darmstadt, Germany). Reagent solutions were as follows: acidic solution, 90% sulphuric acid; alkaline solution, 2 M potassium hydroxide in ethanol; and oxidative solution, 5 g

of chromium(VI) oxide dissolved in 3 ml of distilled water with addition of 60 ml of glacial acetic acid.

2.4. Apparatus

A Konik KNK 2000C gas chromatograph (Sant Cugat del Vallés, Barcelona, Spain) equipped with a Ni[63] electron-capture detector and a Spectra-Physics SP 4290 integrator were used. A Hewlett-Packard HP 5890 gas chromatograph equipped with an HP 5970 mass-selective ion detector (quadrupole), HP 59970 MS-CHEM station and HP 59973 NBS mass spectral library was also used.

The working fused-silica capillary column for both gas chromatographs was 0.25 μm bonded-phase BP-5 (5% phenyl–methylsiloxane) (25 m × 0.22 mm I.D.) provided by Scientific Glass Engineering (Ringwood, Victoria, Australia). For confirmatory purposes a 0.25-μm bonded-phase DB-17, (50% phenyl–methylsiloxane) column (30 m × 0.24 mm I.D.) provided by J & W Scientific (Folsom, CA, USA) was employed.

2.5. Gas chromatographic conditions

With the KNK 2000C system, the injector temperature, operating in splitless mode (0.7 min), was set at 285°C, the detector temperature was set at 300°C and the oven temperature was programmed as follows: initial temperature 50°C (0.8 min), increased at 30°C min^{-1} to 140°C, held for 2 min, then increased at 5°C min^{-1} to 280°C, the final temperature being held for 12 min.

With the HP 5890 system, the injector and oven temperatures were the same as for the KNK 2000C system, the transfer line was set at 300°C, the mass spectrometric source was set at 200°C, the electron impact (EI) energy was set at 70 eV and selected-ion monitoring (SIM) was performed according to characteristic ions of the pesticides and PCBs to be analysed.

2.6. Extraction procedures

Water analysis was based on solid-phase ex-

traction (SPE) with preparative octadecylsilica placed in a glass minicolumn, as in previous work [32–34].

Human milk was analysed as described by Mañes and co-workers [35,36]. The samples were treated with methanol and distilled water to destroy the fat globules and then extracted with a glass minicolumn of octadecylsilica.

2.7. Acid, alkali and oxidative treatment procedures

These procedures were fully described in a previous paper [31], and can be summarized as follows: extract-containing pesticides or PCBs were mixed with 90% sulphuric acid, chromic (VI) oxide in glacial acetic acid at 75–80°C or 2 *M* ethanolic potassium hydroxide, shaken for a few minutes, washed to eliminate the excess of the reagents and then the organic layers were recovered and re-analysed by cGC.

3. Results and discussion

Tables 1 and 2 give the recoveries of the studied organochlorine pesticides and PCBs, respectively, after the chemical treatments at two concentration levels. The results show the applicability of the three chemical treatments at trace levels of the studied compounds.

Of the three treatments, the sulphuric acid treatment gives the least degradation. It is usually applied to purify extracts containing lipids in organochlorine pesticide analyses [4] and in PCB analyses [19].

Our results agree with other reports of the use of sulphuric acid in all instances except for heptachlor epoxide, which some workers [12,17,37] state is not degraded by sulphuric acid attack. Another report [18] describes a lower recovery for heptachlor epoxide than for other pesticides that do not contain oxygen. In some studies heptachlor epoxide was destroyed by a mixture of acetic anhydride in hydrobromic acid [10], hydrochloric acid [29] and trifluoroacetic acid [38]. Under our experimental conditions the degradation occurs at both levels of concentra-

Table 1
Recoveries (% not destroyed by acid, alkali and oxidant treatments) of standard organochlorine pesticide solutions at two concentration levels

Pesticide	Working solution (μg/ml)		Recovery after treatment (%)					
			Acid		Alkali		Oxidant	
	Level 1	Level 2	Level 1	Level 2	Level 1	Level 2	Level 1	Level 2
Aldrin	0.10	1.00	57 ± 12	60 ± 5	84 ± 15	87 ± 3	0	0
o,p'-DDD	0.35	2.55	92 ± 10	95 ± 2	75 ± 13	79 ± 6	78 ± 11	81 ± 4
p,p'-DDD	0.60	5.50	92 ± 10	94 ± 4	0	0	0	0
p,p'-DDE	0.15	1.50	85 ± 14	88 ± 2	85 ± 12	90 ± 5	0	0
p,p'-DDT	0.25	2.00	80 ± 14	88 ± 5	0	0	49 ± 17	50 ± 9
Dicofol	0.75	6.00	65 ± 15	79 ± 8	0	0	0	0
Endrin	0.25	2.00	0	0	85 ± 12	89 ± 6	0	0
Endrin aldehyde	0.30	2.50	87 ± 10	94 ± 3	69 ± 15	72 ± 5	0	0
Endrin ketone	0.30	2.50	94 ± 11	96 ± 6	0	0	94 ± 10	98 ± 6
HCB	0.10	0.50	72 ± 12	75 ± 5	70 ± 14	78 ± 4	73 ± 14	77 ± 4
Heptachlor	0.10	1.00	79 ± 12	89 ± 8	85 ± 16	94 ± 7	0	0
Heptachlor epoxide	0.10	1.00	0	0	71 ± 13	76 ± 8	85 ± 12	91 ± 8
Lindane	0.10	1.00	90 ± 13	92 ± 8	0	0	50 ± 14	50 ± 7
Methoxychlor	0.35	2.95	50 ± 15	53 ± 9	80 ± 11	83 ± 7	0	0

See Experimental for details of the treatments. Results are means ± relative standard deviations for quintuplicate analyses.

Table 2
Recoveries (% not destroyed by acid, alkali and oxidant treatments) of standard PCBs and Aroclors at two concentration levels

Pesticide	Working solution (μg/ml)		Recovery after treatment (%)					
			Acid		Alkali		Oxidant	
	Level 1	Level 2	Level 1	Level 2	Level 1	Level 2	Level 1	Level 2
2'-PCB	5.00	35.00	97 ± 11	97 ± 4	96 ± 13	97 ± 4	64 ± 17	66 ± 6
2'2'-PCB	4.00	28.00	92 ± 10	95 ± 3	95 ± 14	97 ± 3	68 ± 15	68 ± 5
2,4'-PCB	0.60	3.60	97 ± 13	97 ± 4	98 ± 10	98 ± 3	0	0
4,4'-PCB	4.00	24.50	97 ± 12	98 ± 4	99 ± 14	99 ± 3	0	0
2,4,5'-PCB	0.40	2.40	98 ± 14	98 ± 6	97 ± 10	98 ± 5	60 ± 14	62 ± 7
3,3',4,4'-PCB	0.35	1.80	96 ± 10	97 ± 3	96 ± 12	97 ± 4	0	0
2,2',4,5,5'-PCB	0.25	1.25	94 ± 14	97 ± 5	96 ± 15	97 ± 6	95 ± 13	96 ± 5
2,2',4,4',5,5'-PCB	0.15	0.60	96 ± 12	98 ± 7	95 ± 11	97 ± 8	97 ± 10	98 ± 6
Decachlorobiphenyl	0.10	0.50	95 ± 10	99 ± 7	98 ± 14	99 ± 5	98 ± 11	99 ± 4
Aroclor 1242	0.35	2.55	97 ± 10	98 ± 5	96 ± 12	96 ± 10	87 ± 14	88 ± 8
Aroclor 1248	0.20	2.00	97 ± 12	99 ± 5	97 ± 14	96 ± 9	91 ± 14	95 ± 5
Aroclor 1254	0.20	2.00	96 ± 11	97 ± 7	95 ± 14	96 ± 6	95 ± 10	95 ± 6
Aroclor 1260	0.10	1.50	97 ± 11	97 ± 8	96 ± 12	97 ± 8	98 ± 11	97 ± 8
Aroclor 1262	0.10	1.60	97 ± 10	98 ± 7	97 ± 13	95 ± 4	97 ± 12	97 ± 4

See Experimental for details of the treatments. Results are means ± relative standard deviations for quintuplicate analyses.

tion studied. The 20-μg concentration level was also studied by cGC–MS in the scanning mode, and the profile clearly showed the disappearance of the heptachlor epoxide peak. The discrepancy can be attributed to the presence of an artifact peak when packed columns are used with ECD detection in place of capillary columns with a highly stable bonded phase in an MS detector, or more probably to a longer reaction time with sulphuric acid under our analytical conditions. The behaviour of endrin aldehyde and endrin ketone towards sulphuric acid treatment has not been reported in the literature so no comparison can be made.

The results of potassium hydroxide treatment are substantially different from those reported in the literature because all the reference studies were carried out at 100°C whereas our treatment was done at room temperature; at 100°C o,p'-DDD [12,21–22], heptachlor [29], dicofol [11] and methoxychlor [11,21,23] were destroyed. This destruction does not occur at room temperature (see Table 1) even if 5 *M* KOH is employed instead of 2 *M* KOH. These results suggest that KOH treatment is highly temperature dependent and this parameter must be controlled carefully. For example, carrying out the reaction in steam of water destroys only 30% of the heptachlor [21].

When the alkaline reaction is carried out at 100°C, it is more destructive than the same reaction at room temperature. At room temperature o,p'-DDD, o,p'-DDT [31], β-HCH [31], heptachlor, dicofol and methoxychlor were not destroyed and could be determined, but the purification power was also diminished. No references to reaction products of alkaline attack on endrin aldehyde and endrin ketone were found. The stability of the cyclodienes aldrin, endrin, dieldrin [31] and isodrin [31] when subjected to alkaline attack at room temperature is remarkable (Table 1). Aldrin [3,21], dieldrin [3], endrin [3] and isodrin [3,21] remain unaltered under alkaline attack at 70–100°C. Endrin aldehyde is slightly affected at room temperature and endrin ketone is virtually destroyed (Table 1).

Fig. 1a shows the chromatographic profiles of a standard mixture of organochlorine pesticides.

Peaks remaining after the acidic, alkaline and oxidative treatments are shown in Fig. 1b, c and d, respectively. Chromium(VI) oxide is the most destructive of the three treatments.

Chromium(VI) oxide treatment yields the cleanest chromatographic profiles (see Fig. 2), although a large part of the pesticides studied were partially or totally destroyed. For this reason chromium(VI) oxide is frequently applied to determine residues of PCBs from Aroclors in environmental samples [24–27], but it degrades some PCBs that have low or medium chlorine contents (see Table 2). This means that the determination of Aroclors is carried out with losses, which are higher for low chlorine-content Aroclors. This effect has been reported by most researchers [24,26,27] but not reproduced by some [25]. It can be seen from Table 2 that Aroclors with a low chlorine content are degraded more than those with a high chlorine content. In addition, individual PCBs were studied, but the effects of the position of chlorine and the number of chlorine atoms on the rings and the degradation relationship were not evident. Of the individual PCBs studied, only those containing less than five chlorine atoms were destroyed. A lower chlorine presence and degradation were not directly correlated. For example, 2-PCB containing only one chlorine was not destroyed. More chlorine substitution on the same ring does not always protect against degradation (e.g., 2,4,5-PCB was not degraded whereas 2,4-PCB was virtually destroyed).

Some compounds from the degradation of the studied compounds after such treatments are well known. Sulphuric acid degrades endrin to its metabolites endrin aldehyde and endrin ketone [1,18,30]. This conversion was not quantitative, and the metabolites only appeared on the chromatogram if a sufficient amount of endrin was present in the extract. The ability of strong acids to destroy endrin has been well established [30,37]. Trifluoroacetic acid also destroys endrin and partially destroys endrin aldehyde [38].

Alkaline treatment degrades p,p'-DDD to p,p'-DDMU, dicofol to dichlorobenzophenone, p,p'-DDT to p,p'-DDE at room temperature and o,p'-DDD to o,p'-DDMU [12,21], o,p'-
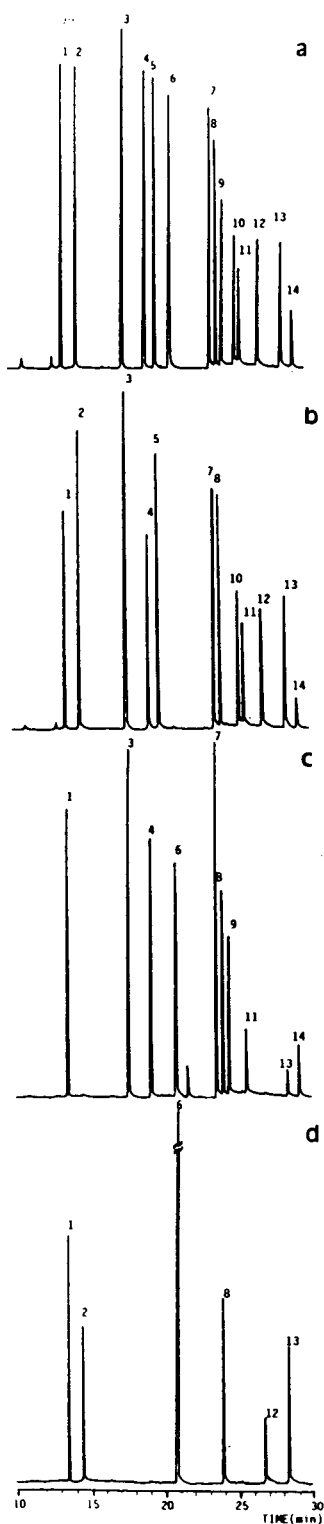
DDT to o,p'-DDE [12] and methoxychlor to its corresponding olefin [11,23] at 100°C.

Chromium(VI) oxide reacts with p,p'-DDE and dicofol to form dichlorobenzophenones [25] and with heptachlor to from heptachlor epoxide [11]. Trichlorobenzoic acids were found via NBS mass spectral standards to be possible degradation products of some individual PCBs, and endrin ketone was partially formed from endrin on chromium(VI) oxide attack.

Some degradation products must be mentioned because they are interesting organochlorine residues and present retention times similar to those of the other compounds studied. Other degradation products such as benzophenones or trichlorobenzoic acids show retention times shorter than that of lindane under our cGC conditions and they are poor indicators of the presence of their precursors because elution occurs in a peak-rich zone of the chromatogram when real samples are processed. The presence of benzophenones is therefore poorly selective because they are known degradation compounds of many diphenyl-substituted compounds such as drugs [39,40].

In Table 1 it can be observed that the behaviour of pesticides (cyclodienes, diphenylethane derivatives, HCH isomers) on chemical treatments of the same chemical kind are dissimilar. With the same chemical treatment, some of the pesticides in a family are degraded whereas others persist. It should be pointed out that all of the diphenylethane derivatives are acid resistant and only o,p'-substituted diphenylethane derivatives are more chemically resistant than their p,p'-analogues (Table 1) [31].

This chemical resistance could be a partial reason for the remaining of o,p'-DDT metabolites in environmental samples even when gener-

Fig. 1. Chromatogram of working organochlorine pesticide solution obtained (a) without any treatment, (b) after acid treatment, (c) after alkali treatment and (d) after oxidant treatment. Peaks: 1 = HCB; 2 = lindane; 3 = heptachlor; 4 = aldrin; 5 = dicofol; 6 = heptachlor epoxide; 7 = p,p'-DDE; 8 = o,p'-DDE; 9 = o,p'-DDD; 10 = endrin; 11 = p,p'-DDD; 12 = endrin aldehyde; 13 = endrin ketone; 14 = methoxychlor.

ally high-purity p,p'-DDT was utilized as pesticide.

Minor changes in the methods can change the results. In the sulphuric acid treatment, a small variation in the acid concentration strongly affects the recovery of methoxychlor [1]. This explains the irregular recoveries and poor R.S.D.s with the sulphuric acid treatment (see Table 1).

Fig. 2. (a) Chromatograms for a human milk sample, obtained by GC–ECD, (a) without any chemical treatment and after (b) acid, (c) alkali and (d) oxidant treatment. ★ = Peak at the same retention time as HCB; □ = peak at the same retention time as p,p'-DDE; ● = peak at the same retention time as methoxychlor. See text for operating conditions.
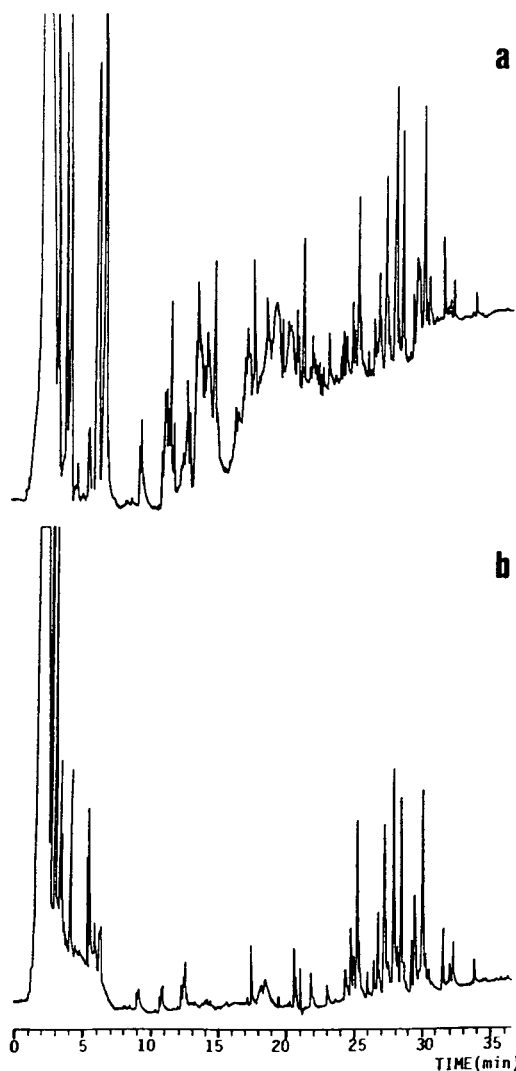
Fig. 3. Chromatograms obtained from a water sample containing Aroclor 1254, (a) before treatment and (b) after treatment with chromium(VI) acid.

When the alkaline treatment was carried out in the presence of water, DDT was not degraded to DDE [10]. On the other hand, important differences were found when the reactions were carried out at 100°C (results in the literature) instead of room temperature (this work). The reaction of p,p'-DDD with chromium(VI) oxide is reported to be temperature dependent and moisture sensitive [13]. To minimize these differences, treatments can be carried out in parallel with standards containing a pesticide or Aroclor at the suspected concentrations.

The purification power of the treatments studied may be insufficient for samples very highly contaminated with compounds other than pesticides or Aroclors. In such cases, chromium(VI) oxide is the best of the three treatments for Aroclor analyses and for the few organochlorine pesticides that resist oxidation, such as o,p'-DDD, p,p'-DDT, HCB, heptachlor epoxide, lindane and endrin ketone. o,p'-DDT, endosulfan sulphate, mirex and, to a certain extent, α-HCH, β-HCH and δ-HCH [31], can be also included in this group.

Another drawback with the proposed method is a poor limit of detection because three aliquots of sufficient concentration are required. This drawback can be minimized by working without fractionation of the extract and starting with the least destructive method, i.e., acid treatment, followed by alkali treatment and finally by the most destructive oxidative treatment.

To confirm the applicability of the treatments to real samples, the proposed method was used to confirm the presence of organochlorine compound residues in surface water and human milk extracts.

The water samples were extracted and analysed by cGC with ECD and the working BP-5 column. If peaks of possible pesticides or PCBs appear in the first chromatogram, a second analysis is carried out on the DB-17 column. If the retention times do not confirm the presence of the possible pesticides or PCBs, the result is negative. If the retention times coincide with those of possible identified compounds, aliquots of organic extracts are treated using chemical procedures. Only if the three results of the chemical treatments agree with the results in Table 1 are the analyses positive. Fig. 3 shows the chromatograms obtained from a water sample containing ·Aroclor 1254, (a) prior to any treatment and (b) after treatment with chromium(VI) oxide.

As can be in Table 3, the organochlorine pesticides aldrin and o,p'-DDD were confirmed after treatment in some water sample, whereas in two other samples, aldrin and heptachlor epoxide gave false-positive results.

The human milk analyses were performed in the same way as for water samples but samples containing possible residues were also analysed by EI-MS-SIM. In all instances, chemically positive identifications agreed with the EI-MS-SIM analyses.

In conclusion, chemical treatment offers a means of achieving residue analyses with significant savings of reagents, glassware and equip-

Table 3
Pesticides present in surface water samples from the Valencia area

Sample No.	Pesticide possible	Chemical treatment			Confirmation
		Acid	Alkali	oxidant	
1	Aldrin	+	−	−	Negative
2	Aldrin	+	+	+	Positive
	o,p'-DDD	+	+	+	Positive
3	Heptachlor epoxide	−	−	−	Negative
4	o,p'-DDD	+	+	+	Positive

+ = Unaltered; − = destroyed.

ment. If the analyses do not include chemical confirmation, it must be assumed that some of the positive analyses are false.

However, sulphuric acid treatment, only allows the determination of acid-stable compounds and column chromatographic clean-up has to be used if the determination of acid-labile compounds is required. For example, dieldrin, α-endosulfan, β-endosulfan, isodrin [31], endrin and heptachlor epoxide are degraded by sulphuric acid and cannot be determined by this technique.

Chromium(VI) oxide provides clean chromatographic profiles, but this technique is not recommended for the determination of low chlorine-containing Aroclors in environmental samples. Quantification errors can be diminished by carrying out parallel runs with similar concentrations of suspected Aroclors or choosing individual PCBs that are not degraded by this method.

Acknowledgements

References

[1] A. Di Muccio, A. Santilio, R. Dommarco and A. Ausili, J. Chromatogr., 553 (1990) 333.
[2] P.A. Mills, J. Assoc. Off. Anal. Chem., 42 (1959) 734.
[3] A.S.Y. Chau and M. Lanouette, J. Assoc. Off. Anal. Chem., 55 (1972) 1058.
[4] T. Suzuki, K. Ishikawa, N. Sato and K. Sakai, J. Assoc. Off. Anal. Chem., 62 (1979) 689.
[5] F. Broto, M. Zapata, L. Comellas and M. Gassiot, Afinidad, 45 (1988) 9.
[6] G.A. Miller and C.E. Wells, J. Assoc. Off. Anal. Chem., 52 (1969) 548.
[7] A. Pastor, J. Medina, R. Melero and F. Hernández, Int. J. Environ. Anal. Chem., 30 (1987) 265.
[8] B. Luckas, H. Pscheidl and D. Haberland, J. Chromatogr., 147 (1978) 41.
[9] J.P. Minyard and E.R. Jackson, J. Agric. Food Chem., 13 (1965) 50.
[10] J.H. Hamence, P.S. Hall and D.J. Caverly, Analyst, 90 (1965) 649.
[11] W.W. Sans, J. Agric. Food Chem., 15 (1967) 192.
[12] J.L. Sericano and A.E. Pucci, Bull. Environ. Contam. Toxicol., 33 (1984) 138.
[13] A.J. Trim, P.M. Brown, E.M. Odam and P.I. Stanley, Analyst, 108 (1983) 33.
[14] P.P. Singh, R.M. Battu and R.L. Kalra, J. Chromatogr., 457 (1988) 387.
[15] V. Contardi, B. Cosma, G. Zanicchi and V. Minganti, Talanta, 7 (1985) 479.
[16] D. Veierov and N. Aharonson, J. Assoc. Off. Anal. Chem., 63 (1980) 202.
[17] D. Veierov and N. Aharonson, J. Assoc. Off. Anal. Chem., 63 (1980) 532.
[18] D. Veierov and N. Aharonson, J. Assoc. Off. Anal. Chem., 61 (1978) 253.
[19] A. Canals, R. Forteza and V. Cerdá, Chromatographia, 34 (1992) 35.
[20] M. Ahnoff and B. Josefsson, Bull. Environ. Contam. Toxicol., 13, (1975) 159.
[21] R.T. Krause, J. Assoc. Off. Anal. Chem., 55 (1972) 1042.
[22] A.K. Klein and J.O. Watts, J. Assoc. Off. Anal. Chem., 47 (1964) 312.
[23] S.J.V. Young and J.A. Burke, Bull. Environ. Contam. Toxicol., 7 (1972) 160.
[24] W.J. Trotter, J. Assoc. Off. Anal. Chem., 58 (1975) 461.
[25] J.C. Underwood, Bull. Environ. Contam. Toxicol., 21 (1979) 787.
[26] B. Cavic and G. Boncic-Caricic, J. Serb. Chem. Soc., 53 (1988) 485.
[27] J.R.W. Miles, J. Assoc. Off. Anal. Chem., 55 (1972) 1039.
[28] W.P. Cochrane, J. Assoc. Off. Anal. Chem. 52 (1969) 1100.
[29] A.S.Y. Chau and M. Lanouette, J. Assoc. Off. Anal. Chem. 52 (1969) 1092.
[30] A.S.Y. Chau and M. Lanouette, J. Assoc. Off. Anal. Chem. 52 (1969) 1220.
[31] E. Viana, J.C. Moltó, J. Mañes and G. Font, J. Chromatogr. A, 655 (1993) 285.
[32] J.C. Moltó, C. Albelda, G. Font and J. Mañes, Int. J. Environ. Anal. Chem., 41 (1990) 21.
[33] J. Mañes, Y. Picó, J.C. Moltó and G. Font, J. High Resolut. Chromatogr., 13 (1990) 843.
[34] J.C. Moltó, Y. Picó, J. Mañes and G. Font, J. Assoc. Off. Anal. Chem., 75 (1992) 714.
[35] J. Mañes, G. Font and Y. Picó, J. Chromatogr., 642 (1993) 195.
[36] M.J. Redondo, Y. Picó, J. Server, J. Mañes and G. Font, J. High Resolut. Chromatogr., 14 (1991) 597.
[37] F. Hernández, F.J. López and J. Medina, J. Assoc. Off. Anal. Chem., 70 (1987) 727.
[38] J.C. Moltó, B. Lejeune, P. Prognon and D. Pradeau, Int. J. Environ. Anal. Chem., 54 (1994) 81.
[39] P. Hartvig, Acta Pharm. Suec., 11 (1974) 109.
[40] J. Vessman and P. Hartvig, Acta Pharm. Suec., 7 (1970) 373.

Determination of the age of ballpoint pen ink by gas and densitometric thin-layer chromatography[☆]

Valery N. Aginsky

Forensic Science Centre, Ministry of the Interior, 22 Raspletina Street, Moscow 123060, Russian Federation

(First received October 8th, 1993; revised manuscript received March 31st, 1994)

Abstract

Two procedures for dating ballpoint inks are considered that use gas chromatography (a combination of the technique for determining the extent of extraction of ink volatile components and of the accelerated ageing technique) and densitometric thin-layer chromatography (separation of ink components and evaluation of the resulting chromatograms using a specially developed mass-independent technique that is also a very effective tool for the comparative TLC examination of similarly coloured inks, paints, fibres and other materials of forensic interest). The procedures have been used in many real case situations and the results of the examinations were accepted as conclusive evidence by courts of law.

1. Introduction

Gas chromatography (GC) and densitometric thin-layer chromatography (TLC) have been demonstrated to be useful tools for the solution of many problems frequently encountered in ink analysis, including ink dating problems [1–4]. Recently, five new procedures for dating ballpoint inks have been described [5,6]. Two of them, based on using chromatographic methods, are as follows.

(1) A GC method is used to determine the extent of extraction of ink volatile components, which decreases as ink ages on paper. The procedure considered in this paper combines the capabilities of this method and of the accelerated ageing technique. The procedure allows discrimi-

nation between "fresh" (age less than several months) and "old" ballpoint ink entries and it does not need dated reference entries written with ink having the same formula as that of the questioned ink.

(2) A TLC method is used for determining age changes in resins and other colourless non-volatile ballpoint ink components; these changes are detected by observing the resulting thin-layer chromatograms under UV illumination and evaluated by using scanning densitometry. The modified TLC procedure described in this paper includes a new, mass-independent approach to evaluating thin-layer chromatograms that allows one to obtain the values of an "ink ageing parameter" [7] directly proportional to the ratios of the masses of the separated ink components (dyes, resins, etc.). For this reason, the proposed procedure gives more reliable results for ink age determination than those obtainable with the

widely used peak signal-to-peak signal ratio technique. The described approach is also a powerful tool for the comparative examination of similarly coloured inks, paints, fibres and other materials of forensic interest as its discriminating power is much greater than that usually produced by the peak ratioing technique [8–10].

2. Experimental

2.1. Materials

Up to 15-year-old entries written with Soyuz ballpoint inks of different colours having similar compositions of colourless components were analysed by GC. Entries of known ages (1 day, 1 month, 1, 2, 3 and 6 years old) written with a Parker blue ballpoint ink were analysed by TLC.

Camag N-11 polypropylene micro vials with cone-shaped interiors and a 10-μl Hamilton syringe were used.

2.2. Gas chromatography

A Hewlett-Packard Model 5890 gas chromatograph equipped with a flame ionization detector and an HP split–splitless injection system was used. A SCOT column containing SP-1000 (polyethylene glycol 20M terminated with nitroterephthalic acid) (Supelco) (25 m × 0.5 mm I.D.) was used with nitrogen (4 p.s.i.) as the carrier gas at a flow-rate of 40 ml/min. The column oven temperature was programmed from 50°C (held for 0.5 min) at 10°C/min to 220°C (held for 6 min). The injection volume was 2 μl (splitless) at 250°C. A flame ionization detector was used at 250°C.

Each sample was obtained by cutting out a ca. 1-cm sliver of ink of approximately equal thickness from the paper using a safety razor and placed in a micro vial. A 10-μl volume of carbon tetrachloride as a "slowly extracting weak solvent", containing 10 μg/ml of benzyl alcohol as an internal stranded (if benzyl alcohol is detected in ink samples in significant amounts, another appropriate substance can be used as an internal

standard) was added and the vial was capped. After 30 min a ca. 2-μl aliquot of each sample was removed and analysed by GC.

The samples were removed from the extraction solutions, dried and placed into other micro vials. A second extraction was carried out for 1 min, stirring with a needle, with 10 μl of chloroform ("fast-extracting strong solvent") also containing benzyl alcohol in the same concentration. About 2 μl of each extract were removed and analysed by GC.

The masses of a vehicle component determined in each of the two extracts analysed (M_1 and M_2 for the first and second extractions, respectively) were calculated by means of the internal standard method. The percentage extraction [1,5], that is, the percentage of the mass of the ink vehicle component, %M, extracted in the "weak" solvent (relative to its total amount contained in the sample analysed), was calculated as follows:

$$\%M = [M_1/(M_1 + M_2)] \cdot 100$$

The values of %M obtained for all samples analysed were plotted against the age of the known ink entries (see Fig. 1).

2.3. Thin-layer chromatography

To obtain an "ageing curve", samples as two 1-cm slivers of ink of approximately equal thickness were taken from five entries of known ages (X_1–X_5). Three more samples were taken from a 2-year-old entry that was analysed as a questioned (Q) entry. Each sample was placed in a micro vial and extracted for 2 min with 15 μl of chloroform, stirring with a needle. A calibration standard solution was prepared by the treatment of eight 1-cm slivers taken from a 1-month-old entry with 60 μl of chloroform. Volumes of 10 μl of the obtained extracts and 5,8,11 and 15 μl of the calibration standard solution (calibration standards, S_1–S_4) were applied to a 20 × 10 cm precoated Merck HPTLC silica gel 60 F_{254} plate as 8-mm bands by means of a Camag Linomat-3 applicator. One-dimensional ascending development was performed with ethanol–acetone–hex-

ane (1:5:20, v/v/v). The development distance was 50 mm.

The resulting chromatograms contained zones of two ink components, A and B. For five samples, X_1–X_5, the relative proportion of these components was obviously linked with the age of the ink (see Fig. 2). The chromatograms were scanned densitometrically by reflectance in the absorbance mode for fluorescence quenching at 254 nm using a Camag TLC/HPTLC scanner (with a mercury lamp, monochromator bandwidth 30 nm, slit dimensions 0.3 × 5 mm and scanning speed 1 mm/s) connected to an SP4100 integrator (Spectra-Physics). The densitometric data obtained were evaluated with external standards in the following way.

For the calibration standards S_1–S_4, it was assumed that the contents of components A and B per zone (their real values are unknown, as follows from the procedure used for preparing the calibration standard solution) were equal to the corresponding values of the volumes of the calibration standard solution applied to the plate (see Table 1).

For each calibration standard component, A and B, a logarithmic (this function gave the best correlation coefficient in all non-linear calibrations that were tested in the given case) approximated calibration graph was constructed and then the contents C_A and C_B of components A and B per zone were determined for the chromatograms of the samples taken from the known and Q aged entries.

The ratio C_A/C_B was calculated for each

Table 1
Contents of components A and B in the chromatographic zones of the calibration standards

Standard[a]	Volume applied (μl)	Component content (mg per spot)	
		A	B
S_1	5	5	5
S_2	8	8	8
S_3	11	11	11
S_4	15	15	15

[a] Extract from the 1-month ink entry.

sample. The values obtained were plotted against the actual age of the known ink entries and the age of the Q ink entry was determined (see Table 3 and Fig. 3).

3. Results and discussion

3.1. Gas chromatography

Figure 1 shows ageing curves obtained for Soyuz ballpoint inks of different colours having similar compositions of colourless components. The curves show that significant ageing taking place over a period from about 6 months to more than 2 years for different inks. After this period until the age of 15 years the extent of the extraction of the volatile component, phenoxyethanol, from the ink entries remained at about $20 \pm 10\%$.

An explanation of this result characterizing the mechanism of evaporation of volatile components (such as phenoxyethanol, phenoxyethoxyethanol and other high-boiling vehicles frequently used as the ingredients of ballpoint inks) from ageing inks has been given previously [5]. It was considered that the evaporation process includes a limiting stage of diffusion of a vehicle from the interior layers of the ink body
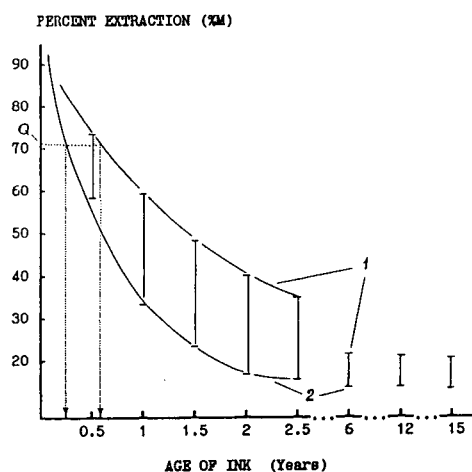

Fig. 1. Ageing curves obtained for violet, blue, green and black Soyuz ballpoint inks: 1 and 2 relate to the maximum and minimum values of %M obtained for the inks analysed.

to the surface of the film. For the same vehicle and thickness (depth) of the ink film, the efficiency of the diffusion process is mainly a function of the nature of ingredients of inks such as resins and polymers. Moreover, if the resin is capable of polymerizing, i.e., of cross-linking, the diffusion process slows as an ink ages on paper, and at a certain stage of ageing it can virtually stop. For this reason the remaining ink volatile components can be detected in the ink line even after a long period of time; this is shown in Fig. 1 for up to 15-year-old entries written with Soyuz ballpoint inks.

In such situations, a "weak" solvent (with regard to hardened ink resins), being unable to penetrate inside an old ink line, extracts the ink volatile components only from its exterior layers. However, the newer the ink, the more exterior layers of the ink become available to the weak solvent, and hence a greater amount of the volatile components is extracted.

Fig. 1 is a good illustration of the above observation that the extraction efficiency of a "weak" solvent decreased from about 90% for fresh writings to about 20% for old writings.

It should be noted that the proposed method includes also an important stage that is carried out if the values of $\%M$ determined for the Q ink entry are larger than ca. 60%. In this event, another sample (1-cm sliver) is taken from the ink entry, heated moderately, e.g., at 80°C for 5 min, and analysed as described under Experimental. The percentage extraction value, $\%M_t$, is calculated for the heated sample and compared with the value of $\%M$ that was determined for the unheated sample. If the difference between $\%M$ and $\%M_t$ is ca. 10% or larger, it can be concluded that the ink entry analysed is a fresh one. If the difference is less than 10%, it means that a more suitable "weak solvent" should be chosen for a given ink.

For example, as a result of studying the ageing process of many ballpoint inks of different formulae by using the proposed method, it has been established that if, for a given ink, the analytical results are $\%M > 70\%$ and $\%M - \%M_{t=80°C, 5\ min} > 10\%$, then the age of the ink analysed is less than ca. 6 months (depending on

the ink formula, this value may decrease to ca. 2 months).

As an example, Fig. 1 shows the results of the age determination obtained for the Q entry (in fact, it was a 3-month old entry written with a Soyuz blue ballpoint ink) using the proposed method.

The method demonstrated high efficiency in many actual case situations when it was necessary to determine whether the age of the Q entry was less than several months or not less than 1 year. Such cases are fairly typical when the investigator suspects that the given entry or signature was made after the time the investigation began. Some similar examples have been presented by Cantu [11].

3.2. Thin-layer chromatography

Fig. 2 demonstrates the view under UV illumination of the fragment of the thin-layer chromatogram (without the chromatographic zones of the paper's ingredients) and corresponding densitograms obtained for samples taken from entries written with Parker blue ballpoint ink. A and B represent separated colourless components of interest in the ink analysed.

It is clearly seen in Fig. 2 that there is an
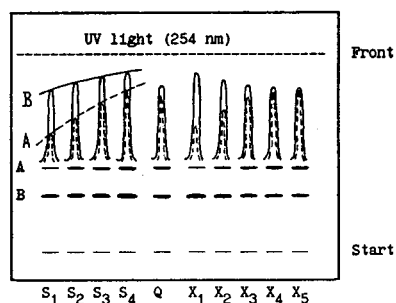

Fig. 2. Fragment of the thin-layer chromatogram (UV detection at 254 nm) and corresponding densitograms obtained for Parker blue ballpoint ink entries of different ages. S_1–S_4 are calibration standards; Q relates to an entry of questionable age; X_1–X_5 relate to known ink entries: $X_1 = 1$ day, $X_2 = 1$ month, $X_3 = 1$ year, $X_4 = 3$ years, $X_5 = 6$ years old.

obvious link between the relative proportion of substances A and B and the age of the ink writings examined: the substance A/substance B ratio gradually increases as the ink ages (it is a minimum for a fresh, 1-day-old entry, the X_1 track, and maximum for a 6-year-old entry, the X_5 track).

As a rule, the relative proportions of the components separated by TLC are evaluated by obtaining related densitometric data and further by calculating the ratios of the components' peak signals [1-3,8,9]. However, this approach has been shown to produce erroneous results because, in densitometric TLC, when chromatograms are scanned by reflectance in the absorbance mode, the relationship between signal output (peak height or peak area) and the content of a separated zone is hardly ever a directly proportionality [10,12,13].

In this connection, a more reliable approach is offered here. It can be considered as a version of the external standard method for evaluating thin-layer chromatograms for cases typical in forensic analysis when information on the quantitative and even qualitative composition of samples to be analysed is not available and, therefore, calibration graphs cannot be obtained for the analytes. (Another way to avoid erroneous results produced by the signal-to-signal ratio technique includes the application of the approach based on the mass-independent version of the peak ratioing technique [10,13].)

The proposed method allows one to obtain the actual mathematical functions of signal *versus* content for any two components, A and B, of the materials analysed within a certain calibration range of the contents of these components, $C_{min}-C_{max}$. This calibration range is formed by applying at least four or five calibration standards on a TLC plate as follows.

If samples are sprayed on as narrow bands, different volumes of only one standard solution can be applied to form a calibration range, $C_{min} - C_{max}$. An important characteristic of the method is that the real values of C_{min} and C_{max} can be unknown to the examiner: only the values of C_{max}/C_{min} and C_i/C_{min} (where i relates to a calibration standard characterized by the content

of a component per zone that is less than C_{max} and larger than C_{min}) must be known, as was described under Experimental.

If samples are applied as spots, calibration standards should be prepared in different concentrations and spotted as a fixed constant volume: multiple spotting of a single standard solution to generate a calibration graph is not acceptable for accurate quantification as there is no simple correlation between signal response for a constant amount of substance and spot size in scanning densitometry [12]. In this case, the contents of components A and B per zone are assumed to be equal (or directly proportional, if only dilution factors, not real concentrations, are known for the calibration standard solutions) to the corresponding concentrations of the calibration standard solutions. Hence the value of the ratio of the contents of any component in the chromatographic zones corresponding to any two prepared calibration solutions will be equal to the value showing how many times one of these solutions is more (or less) concentrated than the other.

Further, for each component A and B, an appropriate approximation function is found and used as a calibration function for calculating the contents, C_A and C_B, of components A and B per spot of the samples taken from the entries of the known and questionable ages. Although these content values are not real, this is not sufficient for the considered method: the main point is that the ratios of these values, C_A/C_B, are independent of mass, in contrast to the peak ratioing technique that is based on using the mass-dependent values of $signal_A/signal_B$ (see Table 2).

Tables 2 and 3 show peak-height values calculated by an integrator for the separated components of the Parker ink analysed, PH_A (for component A) and PH_B (for component B), and the values characterizing the relative proportions of the components A and B calculated by using the peak rationing technique (fourth column) and the proposed "content" ratioing method (last column).

Fig. 3 shows ageing curves obtained for the Parker ink by plotting the values of the ratios

Table 2
Data obtained for calibration standards

Standard	Integrator reading[a]		Ratio of peaks, PH_A/PH_B	Ratio of contents[a], C_A/C_B
	PH_A	PH_b		
S_1	31 032	90 506	0.34	1.02
S_2	51 716	99 126	0.52	0.98
S_3	73 261	107 745	0.68	0.96
S_4	88 782	112 056	0.79	1.04
Mean			0.58	1.00
R.S.D.			0.34	0.04

[a] Peak heights, PH_A and PH_B, were plotted against the contents C_A and C_B (see Table 1). As a result, the following regression equations and correlation coefficients (r^2) of the logarithmic calibration graphs were obtained: $PH_A = -56\,496 + 53\,529 \log C_A$ ($r^2 = 0.9929$) and $PH_B = 57\,816 + 20\,258 \log C_B$ ($r^2 = 0.9894$). Using these equations, the values of C_A and C_B were recalculated for each standard, $S_1–S_4$, and used for calculating the content ratio values listed in the last column.

listed in the last two columns of Table 3 against the actual age of the known ink entries.

The results of determining the age of the Q entry (in fact, the age of this entry was 2 years) are also shown in Fig. 3 and presented in Table 3.

It is clearly follows from Fig. 3 and the data in Tables 2 and 3 that, in comparison with the peak ratioing technique, the proposed mass-independent content ratioing method gives a significant increase in the accuracy and precision of ink age determination.

It should also be noted that this method can be successfully applied to a comparative TLC examination of similarly coloured inks, paints, fibres and other materials of forensic interest, as

Table 3
Data obtained for ink entries

Ink entry	Integrator reading		Ratio of peaks, PH_A/PH_B	Ratio of contents, C_A/C_B
	PH_A	PH_B		
X_1	39 659	110 334	0.36	0.45
X_2	64 644	103 435	0.63	1.01
X_3	79 735	94 817	0.84	2.04
X_4	84 472	94 388	0.89	2.27
X_5	88 351	93 093	0.95	2.60
Q	81 887	93 529	0.88	2.26
	87 963	96 975	0.91	2.14
	80 168	93 394	0.85	2.20
Age determined for the Q entry (years)			1.3	1.4
			2.6	2.4
			4.1	3.0
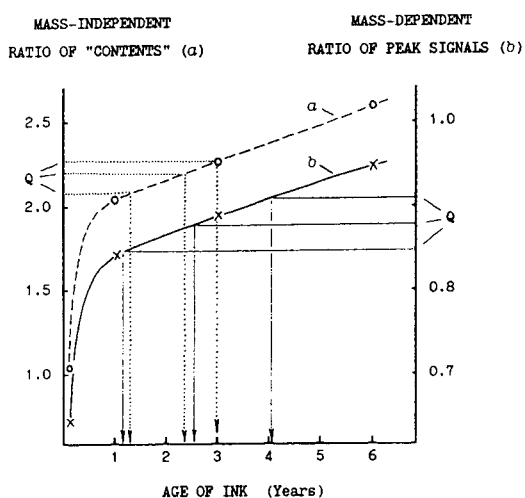
Fig. 3. Ageing curves obtained for the Parker ink using (a) the content ratioing method and (b) the peak ratioing technique.

its discriminating power is much greater than that usually produced by the widely used mass-dependent signal-to-signal ratio technique.

4. Conclusions

Two complementary methods for dating ballpoint inks have been considered. The method using GC allows discrimination between fresh (age not greater than a few months) and old ballpoint inks, including inks with formulae unknown to the examiner. It is effective for analysing ballpoint inks that contain phenoxyethanol, phenoxyethoxyethanol or similar high-boiling vehicles.

The method using TLC allows the detection of age changes in resins and other non-volatile ink components. It includes a new procedure for evaluating thin-layer chromatograms of separated ink components. Being mass-independent, this procedure gives much more correct results for dating inks than those obtained with the aid of the widely used signal-to-signal ratio technique.

Both methods, together and separately, have been used in many actual case situations and the results of the examinations have been accepted as conclusive evidence by courts.

Further work is necessary to evaluate the limits of the applicability of the methods to numerous inks that are on the market.

References

[1] A.A. Cantu and R.S. Prough, J. Forensic Sci., 32 (1987) 1151.
[2] R.L. Brunelle and A.A. Cantu, J. Forensic Sci., 32 (1987) 1522.
[3] R.L. Brunelle, J. Forensic Sci., 37 (1992) 113.
[4] L.F. Stewart, J. Forensic Sci., 30 (1985) 405.
[5] V.N. Aginsky, J. Forensic Sci., 38 (1993) 1134.
[6] V.N. Aginsky, in Proceedings of the 13th IAFS Meeting, Düsseldorf, Germany, August 1993, in press.
[7] A.A. Cantu, J. Forensic Sci., 33 (1988) 744.
[8] R.L. Brunelle and H. Lee, J. Forensic Sci., 34 (1989) 1166.
[9] G.M. Golding and S. Kokot, J. Forensic Sci., 35 (1990) 1310.
[10] V.N. Aginsky, J. Forensic Sci., 38 (1993) 1111.
[11] A.A. Cantu, Anal. Chem., 63 (1991) 847A.
[12] C.F. Poole and S.K. Poole, J. Chromatogr., 492 (1989) 539.
[13] V.N. Aginsky, J. Planar Chromatogr., 4 (1991) 167.

Determination of lipophilicity by means of reversed-phase thin-layer chromatography
III. Study of the TLC equations for a series of ionizable quinolone derivatives

Gian Luigi Biagi[a,*], Anna Maria Barbaro[a], Maurizio Recanatini[b]

[a]*Dipartimento di Farmacologia, Università di Bologna, Via Irnerio 48, 40126 Bologna, Italy*
[b]*Dipartimento di Scienze Farmaceutiche, Università di Bologna, Via Belmeloro 6, 40126 Bologna, Italy*

Abstract

The R_M values of a series of antibacterial quinolones were measured at pH 9.0 and 1.2 using a reversed-phase TLC system with acetone, methanol or acetonitrile as the organic modifier of the mobile phase and silicone DC 200 as the impregnating agent of the silica gel layer. The data obtained provide a further contribution to the assessment of the basic aspects of the chromatographic determination of lipophilicity for ionizable compounds. The very good correlations between experimental and extrapolated R_M values support the validity of the extrapolation technique. The overlapping of the extrapolated R_M values from three different systems shows that they are not dependent on the nature of the organic solvent. In a series of congeneric compounds there is a relationship between intercepts (a) and slopes (b) of the TLC equations. Factors affecting chromatographic congenerity are discussed. The slopes of the TLC equations and those of the equations correlating the parameters a and b are related to the solvent strength of the organic modifiers.

1. Introduction

During the last 25 years, we have been measuring the R_M values, as an expression of the lipophilic character of drugs and chemicals, by means of a reversed-phase TLC system with the silica gel layer impregnated with silicone DC 200. The chromatographic determination of lipophilicity is mainly based on the linear relationship between the R_M values and the organic solvent concentration in the mobile phase. In

fact, the TLC equations describing this relationship allow the calculation of a theoretical R_M value at 0% organic solvent in the mobile phase, even for those compounds which do not migrate with an aqueous buffer alone. The chromatographic work carried out in our laboratory provided the TLC equations for about 750 drugs and chemicals. In two recent papers, the main features of the TLC equations were reviewed [1,2]. In particular, the very good correlations between experimental and extrapolated R_M values support the validity of the extrapolation technique. The overlapping of the extrapolated R_M values

* Corresponding author.

from different chromatographic systems shows that they are not dependent on the nature of the organic solvent in the mobile phase when the solvent is acetone, methanol or acetonitrile. However, as already pointed out [1], it might be questionable whether this aspect has general relevance for any chromatographic system. Grünbauer et al. [3] reached our conclusion when using acetone or methanol. On the other hand, with N,N-dimethylformamide (DMF) the extrapolated R_M values were significantly lower. They suggested that this behaviour could be due to the fact that DMF deviates the most from water as far as its liquid structure is concerned. Moreover, Smith and Burr [4] found different chromatographic parameters when analysing a series of monosubstituted aromatic compounds with an HPLC system using methanol or acetonitrile in the mobile phase. Finally, our attention was drawn to two other aspects: (a) the relationship between intercepts and slopes of the TLC equations [1] and (b) the influence of different organic modifiers on the slope of the TLC equations [2].

The aim of our previous chromatographic work was the determination of the lipophilic character of non-ionized molecules, so that the R_M values could be compared with the classical octanol–water log P values. As a consequence, the pH in reversed-phase TLC was chosen in such a way that most of the compounds were non-ionized. While the aforementioned features of the TLC equations were mostly referred to non-ionized molecules, it would be interesting to assess if the presence of ionized substituent groups is consistent with the above aspects of the TLC equations. In an attempt to investigate this point, we took advantage of some preliminary results obtained with a series of quinolones. In fact, for some time in our laboratory a research project on quinolones has been in progress. The aim is to study the lipophilic character of this important class of synthetic antibacterial drugs. The amphoteric nature of some of the investigated quinolones allowed us to study the chromatographic behaviour of compounds bearing both an acidic and a basic group. As either of these groups may be ionized depending on the pH of the chromatographic system, the reversed-

phase TLC of quinolones was carried out at pH 9.0 and 1.2. At pH 9.0, the carboxyl group was ionized whereas the basic piperazine group was mostly non-ionized. In contrast, at pH 1.2 the basic moiety was fully protonated and the carboxyl group was non-ionized. In this way, by just changing the pH of the TLC system, it was possible to study the influence of both a cationic and an anionic group on the chromatographic behaviour of a single series of compounds.

2. Experimental

2.1. Chemicals

Quinolone derivatives were a generous gift from drug companies (Fig. 1). All drugs were used as received. All solvents were of analytical-reagent or HPLC grade.

2.2. Determination of R_M values by means of RP-TLC

The details of the reversed-phase (RP) TLC were described previously [5]. Glass plates (20 × 20 cm) were coated with silica gel GF_{254} (Merck, Darmstadt, Germany). In order to control the pH of the stationary phase, a slurry of silica gel GF_{254} was obtained with 0.09 M hydrochloric acid or 0.36 M sodium hydroxide when the pH of the mobile phase was to be 1.2 or 9.0 respectively. A non-polar stationary phase was obtained by impregnating the silica gel layer with silicone DC 200 (350 cSt) from Applied Science Labs. (State College, PA, USA). The mobile phases, saturated with silicone, were aqueous buffers alone or mixed with various amounts of acetone, methanol or acetonitrile. Glycine buffers of pH 1.2 and 9.0 were used. The test compounds were dissolved in water or acetone (1–2 mg/ml) and 1 μl of solution was spotted randomly on the plates. The developed plates were dried and sprayed with an alkaline solution of potassium permanganate. After a few minutes at 120°C, yellow spots appeared on an intense pink background. The R_M values were calculated by means of the equation $R_M = \log[(1/R_F) - 1]$.

3. Results

The RP-TLC of the quinolone derivatives showed that at pH 9.0 most of them did not move from the starting line when the mobile phase was aqueous buffer alone. Only with the four most hydrophilic compounds, i.e., **4**, **7**, **10** and **12**, could reliable R_M values be obtained, even with no organic modifier in the mobile phase. On the other hand, at pH 1.2 all the
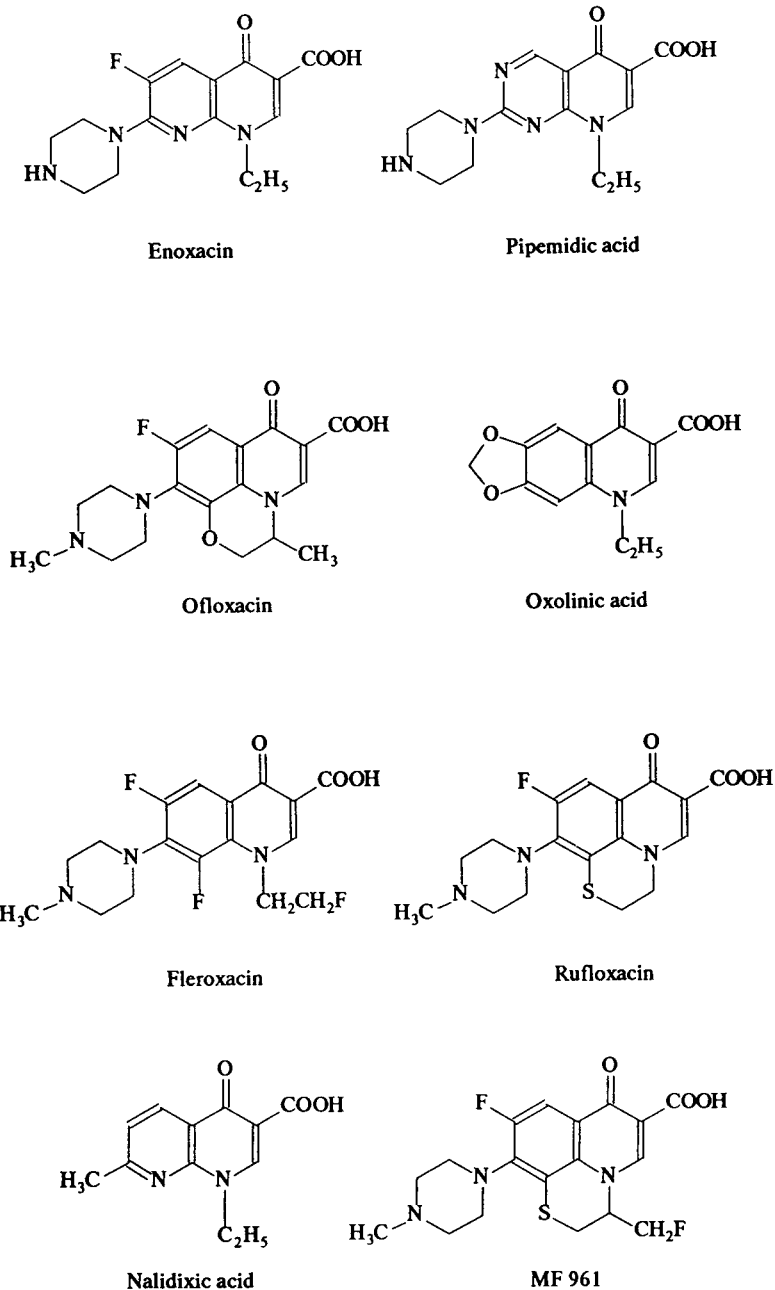
Fig. 1. *(Continued on p. 130)*
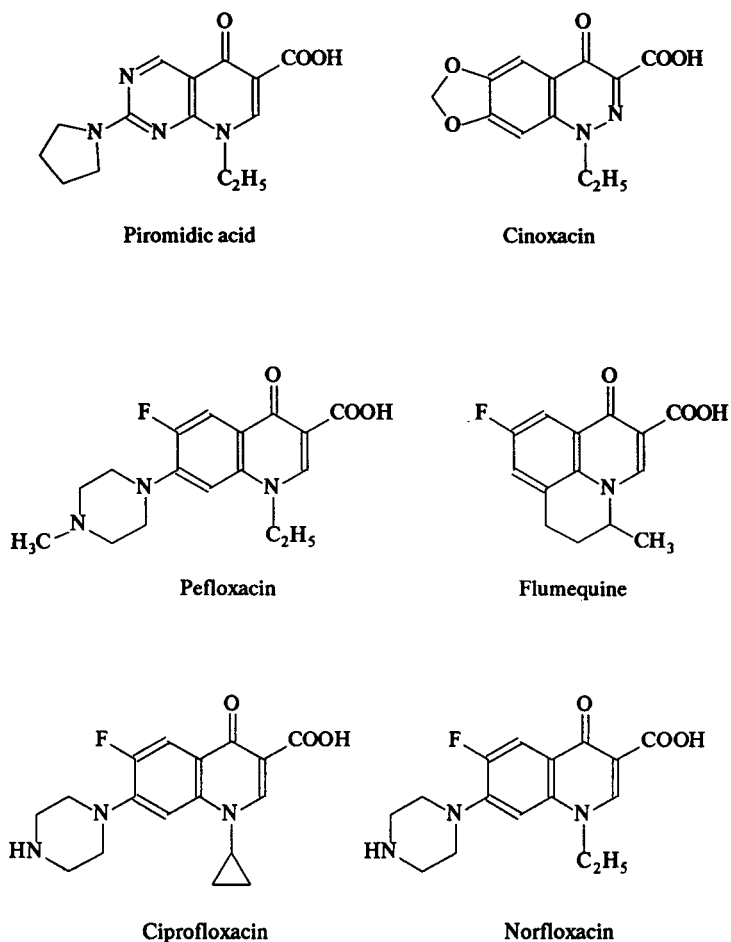
Fig. 1. Structural formulae of the compounds investigated.

derivatives except piromidic acid (9) moved with aqueous buffer alone. In order to obtain suitable R_M values for all the compounds at both pH values, an organic solvent was added to the mobile phase. The equations describing the linear relationship between R_M values and organic modifier concentration allowed the calculation of extrapolated R_M values also for the compounds that did not move with aqueous buffer alone. Experimental R_M values, TLC equations and ranges of organic solvent concentrations used for their calculation are reported in Tables 1 and 2.

As a first step in the analysis of the data in Tables 1 and 2, the relationship between ex-

perimental and extrapolated R_M values in each RP-TLC system was examined. In Table 3, Eqs. 1–4, with intercepts and slopes close to 0 and 1, respectively, show the overlapping of the experimental and extrapolated R_M values. As at pH 9.0 only four compounds yielded experimental R_M values with no organic solvent in the mobile phase, Eqs. 1–3 were calculated with only four data points. Nevertheless, the present results are in agreement with our recent equation correlating experimental and extrapolated R_M values for 240 compounds [1].

A second basic aspect of the TLC equations at pH 9.0 is illustrated by the intercepts and slopes of Eqs. 5–7 in Table 4. Very close extrapolated

Table 1
TLC equations of quinolones at pH 9.0 in acetone, methanol and acetonitrile systems

$R_M = a + b$(% organic modifier)

No.	Compound	$R_{M\ expt}$	Acetone				Methanol				Acetonitrile			
			a	b	r	Range	a	b	r	Range	a	b	r	Range
1	Enoxacin		1.80	-0.035	0.983	16–50	1.79	-0.023	0.997	24–60	1.80	-0.030	0.990	12–55
2	Pipemidic acid		1.64	-0.031	0.975	12–45	1.68	-0.022	0.987	16–60	1.56	-0.027	0.994	20–40
3	Ofloxacin		1.92	-0.039	0.981	20–45	1.90	-0.025	0.998	24–50	1.80	-0.032	0.979	16–45
4	Oxolinic acid	1.04	1.03	-0.040	0.963	0–12	0.98	-0.027	0.992	0–40	0.95	-0.036	0.978	0–28
5	Fleroxacin		1.97	-0.041	0.941	16–50	1.93	-0.028	0.999	24–55	2.02	-0.035	0.988	16–36
6	Rufloxacin		1.98	-0.042	0.994	20–50	1.93	-0.029	0.993	20–50	1.92	-0.036	0.972	20–36
7	Nalidixic acid	1.05	1.08	-0.050	0.985	0–24	1.06	-0.029	0.992	0–40	1.01	-0.045	0.987	0–20
8	MF961		1.95	-0.045	0.985	12–50	1.97	-0.032	0.993	20–50	1.81	-0.037	0.946	20–45
9	Piromidic acid		1.21	-0.050	0.980	4–36	1.22	-0.032	0.997	4–50	1.24	-0.043	0.960	0–40
10	Cinoxacin	0.50	0.49	-0.094	0.992	0–12	0.48	-0.090	0.933	0–8	0.42	-0.077	0.998	0–16
11	Pefloxacin		1.61	-0.031	0.989	16–45	1.67	-0.020	0.992	16–50	1.63	-0.027	0.993	20–55
12	Flumequine	1.16	1.17	-0.060	0.995	0–24	1.19	-0.045	0.992	0–40	1.20	-0.057	0.986	0–20
13	Ciprofloxacin		1.49	-0.025	0.993	4–45	1.41	-0.017	0.984	12–60	1.50	-0.024	0.983	12–36
14	Norfloxacin		1.58	-0.027	0.961	16–40	1.53	-0.018	0.992	20–60	1.69	-0.026	0.991	20–45

Table 2
TLC equations of quinolones at pH 1.2 in acetone system and ΔR_M values

No.	Compound	$R_{M \text{ exptl}}$	$R_M = a + b(\%$ organic modifier$)$					
			a	b	r	Range	ΔR_M [a]
1	Enoxacin	0.70	0.68	−0.063	0.999	0–12	1.12
2	Pipemidic acid	0.46	0.47	−0.053	0.999	0–12	1.17
3	Ofloxacin	1.02	0.99	−0.081	0.997	0–12	0.93
4	Oxolinic acid	1.25	1.18	−0.056	0.991	0–28	−0.15
5	Fleroxacin	0.88	0.88	−0.082	0.999	0–12	1.09
6	Rufloxacin	0.99	0.87	−0.075	0.944	0–12	1.11
7	Nalidixic acid	1.30	1.31	−0.059	0.998	0–28	−0.23
8	MF961	1.08	1.07	−0.084	0.999	0–12	0.88
9	Piromidic acid		1.84	−0.061	0.970	20–40	−0.63
10	Cinoxacin	1.17	1.20	−0.093	0.998	0–12	−0.71
11	Pefloxacin	1.00	0.95	−0.076	0.991	0–12	0.66
12	Flumequine	1.30	1.22	−0.047	0.992	0–40	−0.05
13	Ciprofloxacin	0.83	0.81	−0.076	0.999	0–12	0.68
14	Norfloxacin	0.83	0.81	−0.068	0.998	0–12	0.77

[a] Difference between the extrapolated R_M values at pH 9.0 and 1.2 in acetone system.

Table 3
Correlations between experimental and extrapolated R_M values at pH 9.0 and 1.2

Mobile phase		$R_{M \text{ exptl}} = a + bR_{M \text{ extrap}}$					
pH	Solvent	a	b	n	r	s	Eq.
9.0	Acetone	0.028	0.964	4	0.998	0.019	1
9.0	Methanol	0.058	0.948	4	0.993	0.044	2
9.0	Acetonitrile	0.151	0.979	4	0.989	0.053	3
1.2	Acetone	0.014	1.015	13	0.986	0.043	4

R_M values were obtained whether the organic modifier in the mobile phase was acetone, methanol or acetonitrile. In other words, the nature of the organic modifier does not affect the extrapolated R_M values.

Another interesting point arises from the anal-

ysis of the correlation between the intercepts ($a = R_{M \text{ extrap}}$) and slopes (b) of the TLC equations in Tables 1 and 2. As already discussed in a previous paper [1], for series of congeneric compounds the relationship between the two parameters can be described by a straight line. In

Table 4
Correlations between extrapolated R_M values obtained with different organic modifiers at pH 9.0

Organic modifier		$R_{M \text{ I}} = a + bR_{M \text{ II}}$					
I	II	a	b	n	r	s	Eq.
Methanol	Acetone	−0.007	0.996	14	0.996	0.040	5
Acetonitrile	Acetone	−0.022	0.997	14	0.987	0.074	6
Acetonitrile	Methanol	0.000	0.991	14	0.981	0.090	7

Fig. 2 the intercepts of the TLC equations for the present series of quinolones are plotted against the corresponding slopes. At pH 9.0 (plots a, b and c) in all three chromatographic systems, the intercepts and slopes of nine compounds are linearly related. These derivatives are characterized by the presence of the piperazine ring. On the other hand, four derivatives, **4**, **7**, **9** and **12**, lacking the piperazine ring, are grouped below that line. Compound **10**, lacking the piperazine ring and bearing a cinnoline ring, lies even further away. At pH 1.2 (plot d, Fig. 2), the compounds are apparently divided into two groups. In fact, only compounds **4**, **7**, **9** and **12** deviate from the linear relationship, and **10** seems to be grouped with the other nine compounds. In Table 5 the equations describing these linear relationships between intercepts and slopes are reported. Compound **10** was included in the calculation of Eq. 11.

In previous reports it was shown that the slopes of the TLC equations in a given solvent system are related to the eluting power of the organic modifier, as expressed by its solvent strength parameter E_0 [2,6]. In particular, the ratios between the mean slopes in two different solvent systems are close to the ratios between the $1/E_0$ values for the corresponding solvents. The solvent strength parameter of an organic solvent in a reversed-phase chromatographic system is expressed by $1/E_0$ [7,8]. The slopes of the TLC equations of quinolones at pH 9.0 in acetone, methanol and acetonitrile systems (Table 1) were averaged and are reported in Table 6, where they can be compared with the mean slopes calculated for other series of chemical agents [2]. It can be pointed out that for all the listed chemical series the ratios between the mean slopes in different solvent systems are not far from the ratios between the corresponding $1/E_0$ values. When considering the mean ratios (x in Table 6), those referred to acetone–acetonitrile and acetonitrile–methanol, i.e., 1.09 and 1.41, are close to the ratios between the corresponding $1/E_0$ values, i.e., 1.15 and 1.47, respectively.

More recently it was shown that the same aspect could be illustrated by the b values of the equations correlating intercepts and slopes of the TLC equations [2]. For the present series of quinolones the b values of the equations in Table 5 are reported in Table 7, and their ratios are compared with those of the E_0 values for the corresponding solvents. Again, the present findings are similar to those obtained with other series of compounds [2] and reported in Table 7. The mean acetone-to-acetonitrile ratio (x in Table 7), i.e., 0.89, is particularly close to the corresponding ratio between the E_0 values, 0.86. In a previous paper [2] it was shown why in this case the E_0 values were used instead of their reciprocals ($1/E_0$ values) as in Table 6.

4. Discussion and conclusions

The present data show that the basic factors determining the chromatographic behaviour described by the TLC equations are the same when dealing with either non-ionized or ionized molecules. In fact, the four main points characterizing the TLC equations and outlined in the Introduction seem to be confirmed also for the ionized compounds. In particular, the results in Table 4 further support the finding that at least in our chromatographic system the presence of acetone, methanol or acetonitrile in the mobile phase does not change the extrapolated R_M values.

Notwithstanding, the linear relationship between slopes and intercepts of the TLC equations deserves more detailed comment. In our previous study [1], it was observed that in several instances not all the members of a chemical series fit the same straight line. Moreover, with cephalosporins, xanthines and adenosines the chromatographic data did not reveal any relationship between intercepts and slopes. Therefore, it was assumed that the linear relationship must be based on some kind of congenerity among the members of the chemical series under investigation [1]. We proposed that congenerity might be related to the shape of the hydrophobic surface area, which is available for the interaction with the non-polar stationary phase. The deviations from linearity were attributed to sev-
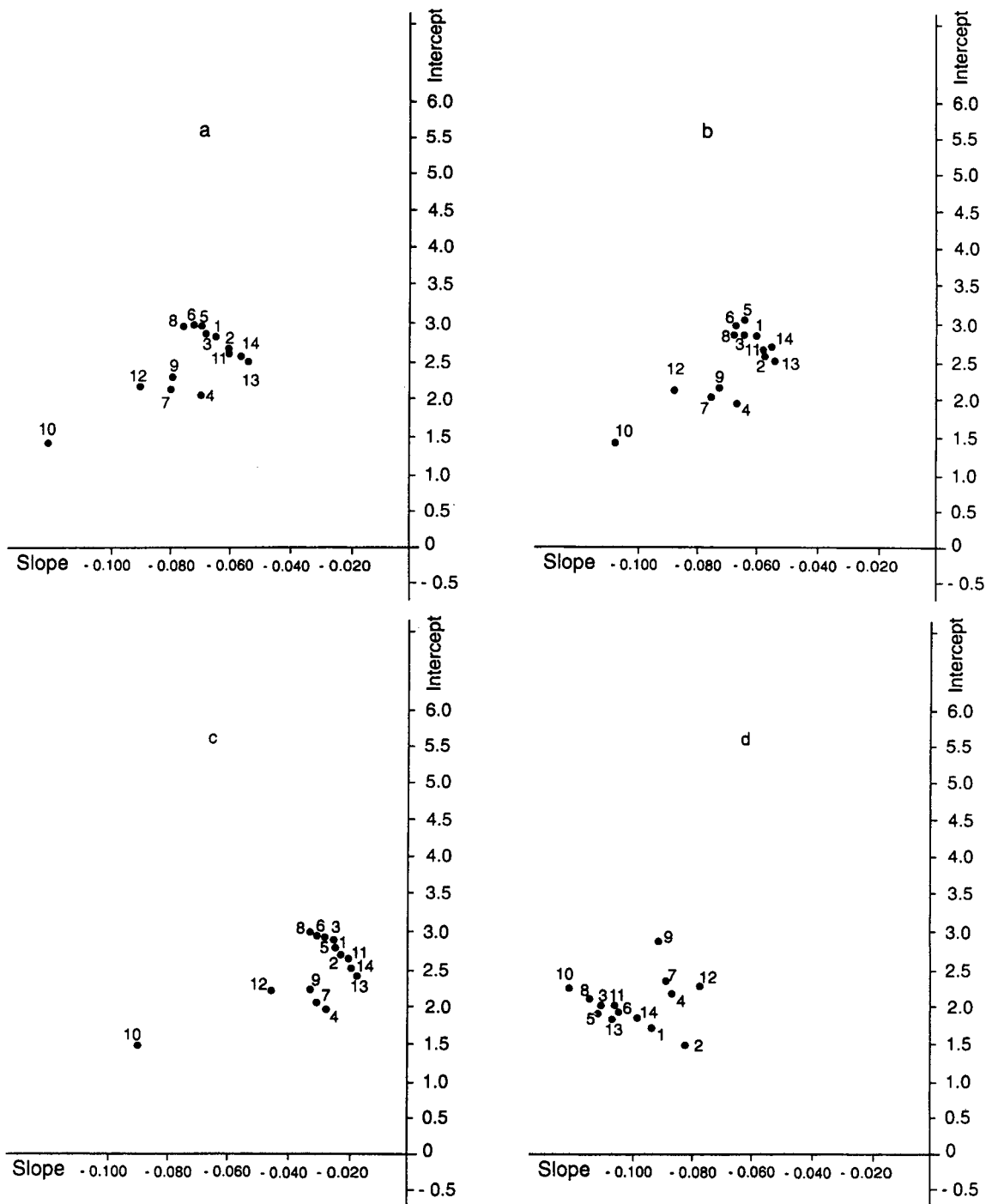
Fig. 2. Relationships between intercepts and slopes of the TLC equations at pH 9.0 (a, b and c) and 1.2 (d) in different solvent systems: (a, d) acetone, (b) acetonitrile and (c) methanol.

Table 5
Correlations between intercepts and slopes of the TLC equations at pH 9.0 and 1.2

Mobile phase		Intercept = $a + b$ (slope)					
pH	Solvent	a	b	n	r	s	Eq.
9.0	Acetone	0.838	−26.579	9	0.972	0.048	8
9.0	Methanol	0.895	−36.224	9	0.943	0.070	9
9.0	Acetonitrile	0.817	−30.561	9	0.866	0.090	10
1.2	Acetone	−0.415	−17.150	10	0.960	0.060	11

Table 6
Ratios between slopes in different TLC systems

Compound	Mean slope in solvent system			Ratio		
	Acetone	Acetonitrile	Methanol	Acetone/ acetonitrile	Acetone/ methanol	Acetonitrile/ methanol
Quinolones	−0.043(±0.005)	−0.038(±0.005)	−0.031(±0.004)	1.13	1.39	1.22
Steroids	−0.046(±0.002)	−0.041(±0.001)	−0.027(±0.001)	1.12	1.70	1.52
Triazines	−0.037(±0.001)	−0.036(±0.001)	−0.027(±0.001)	1.03	1.37	1.33
Prostaglandins	−0.072(±0.002)	−0.067(±0.001)	−0.043(±0.002)	1.07	1.67	1.56
Dermorphins	−0.064(±0.003)		−0.047(±0.003)		1.36	
Naphthalenes and quinolines	−0.046(±0.001)		−0.030(±0.001)		1.53	
$\bar{x} \pm$ S.E.[a]				1.09 ± 0.02	1.50 ± 0.06	1.41 ± 0.08
Solvent strength ($1/E_0$)	1.78	1.54	1.05	1.15	1.70	1.47

[a] Standard error of the mean.

Table 7
Ratios between the b values of the equations correlating intercepts and slopes of the TLC equations

| Compound	Slope in solvent system			Ratio		
	Acetone	Acetonitrile	Methanol	Acetone/ acetonitrile	Acetone/ methanol	Acetonitrile/ methanol
Quinolones	−26.579	−30.561	−36.224	0.87	0.73	0.84
Steroids	−72.872	−80.365	−122.802	0.91	0.59	0.65
Triazines	−69.484	−74.194	−109.730	0.94	0.63	0.68
Prostaglandins	−61.014	−73.829	−86.005	0.83	0.71	0.86
Dermorphins	−56.775		−69.317		0.82	
Naphthalenes and quinolines	−62.704		−87.810		0.71	
$\bar{x} \pm$ S.E.[a]				0.89 ± 0.02	0.70 ± 0.03	0.76 ± 0.05
Solvent strength (E_0)	0.56	0.65	0.95	0.86	0.59	0.68

[a] Standard error of the mean.

eral structural features of the chemical agents. With benzodiazepines, penicillins and β-carbolines, the compounds deviating from the linear relationship were the only ionized members of their series, the other compounds being non-ionized at the pH of the chromatographic system. Therefore, it was suggested that at least in these series, congenerity could be broken down by the presence of ionized groups [1].

As regards the present series of quinolone drugs, Eqs. 8–11 in Table 5 show that ionized compounds can be members of a congeneric series. In this case deviations from linearity seem rather to be due to different patterns of ionization. In fact, at pH 9.0 the compounds fitting Eqs. 8–10 are characterized by the fact that their carboxyl group is fully ionized and their basic group is also at least partly ionized. On the other hand, the compounds deviating from Eqs. 8–10, i.e., **4**, **7**, **9**, **10** and **12** (plots a, b and c, Fig. 2) are lacking the partially ionized basic group. The larger deviation for **10** might be related to the presence of the N atom in position 2 of the cinnoline ring.

The ionization patterns of the quinolone drugs could also help in explaining the ranking of the R_M values at pH 9.0 in Table 1 and Fig. 2 (plots a, b and c). The higher R_M values of the compounds fitting Eqs. 8–10 compared with those of the anionic compounds **4**, **7**, **9** and **12** might result from the association of molecules in their zwitterionic form, leading to more lipophilic ion pairs. The lower R_M value of **10** could be due either to the hydrophilic character of the cinnoline N-2 atom or to the fact that it cannot form ion pairs.

At pH 1.2, whereas the carboxyl group is non-ionized, the piperazine group is ionized. Again, Eq. 11 shows a linear relationship for the compounds bearing the ionized basic group. Compounds **4**, **7**, **9** and **12** deviating from the straight line are the only non-ionized compounds in the series, and therefore the most lipophilic (plot d, Fig. 2). At this pH, **10** seems to be congeneric with the ionized subset, which should imply protonation of the cinnoline ring. However, if this were the case, the R_M value of **10** at pH 1.2 should be lower than that of **4** differing

only in the lack of the N atom in position 2. This contradictory finding might be tentatively explained by assuming the formation of an intramolecular H-bond in the protonated form of **10**:
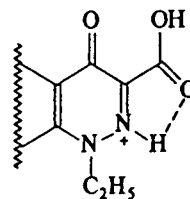
As intramolecular H-bonding is known to increase lipophilicity [9], this could to some extent counterbalance the negative contribution of the $\underset{/}{\overset{\backslash}{N^+}}=$ group.

The so far described ionization patterns also can explain the ΔR_M values between 9.0 and 1.2 in the acetone system. The quinolone derivatives with both a carboxyl and a piperazine group, i.e., **1**, **2**, **3**, **5**, **6**, **8**, **11**, **13** and **14** fitting Eqs. 8–10, have higher R_M values at pH 9.0 than at pH 1.2 (positive ΔR_M values), possibly because of the formation of ion pairs between zwitterionic forms. In contrast, **4**, **7**, **9** and **12**, bearing only the carboxyl group, are non-ionized at pH 1.2, hence their R_M values are lower at pH 9.0 than at pH 1.2 (negative ΔR_M values). The case of **10** is more complicated. This derivative, like **4**, **7**, **9** and **12**, has a negative ΔR_M value, which could be explained with the above hypothesis of an intramolecular H-bond increasing lipophilicity at pH 1.2.

However, turning back to the point at issue here, i.e., the relationship between intercepts and slopes of the TLC equations, the conclusion one can draw from the above discussion is that the definition of congenerity in chromatographic terms is still far from being clearly established. In fact, many unpredictable factors can affect chromatographic congenerity, and thereby one cannot state a priori that for a given series of structural analogues it is possible to find a linear correlation between the two parameters. This casts further doubts on the reliability of the slope of the TLC equation as a chromatographic lipophilicity parameter alternative to R_M. In any

event, the findings arising from this paper and the two earlier parts [1,2] make a contribution to a more detailed knowledge of the interrelationships between slopes and intercepts, with a view to the final assessment of the best suited alternative to the octanol–water log P values.

References

[1] G.L. Biagi, A.M. Barbaro, A. Sapone and M. Recanatini, *J. Chromatogr. A*, 662 (1994) 341.

[2] G.L. Biagi, A.M. Barbaro, A. Sapone and M. Recanatini, *J. Chromatogr. A*, 669 (1994) 246.

[3] H.J.M. Grünbauer, G.J. Bijloo and T. Bultsma, *J. Chromatogr.*, 270 (1983) 87.

[4] R.M. Smith and C.M. Burr, *J. Chromatogr.*, 475 (1989) 57.

[5] G.L. Biagi, A.M. Barbaro, M.F. Gamba and M.C. Guerra, *J. Chromatogr.*, 41 (1969) 371.

[6] G.L. Biagi, M. Recanatini, A.M. Barbaro, M.C. Guerra, A. Sapone, P.A. Borea and M.C. Pietrogrande, in H. Kalasz and L.S. Ettre (Editors), *New Approaches in Chromatography '93*, Fekete Sas Könyvkiadó, Budapest, 1993, p. 215.

[7] K.J. Bombaugh, in K. Tsuji and W. Morozowich (Editors), *GLC and HPLC Determination of Therapeutic Agents, Part I*, Marcel Dekker, New York, 1978, p. 83.

[8] L.R. Snyder and J.J. Kirkland, *Introduction to Modern Liquid Chromatography*, Wiley, New York, 1978.

[9] A. Leo, *J. Chem. Soc., Perkin Trans. 2*, (1983) 825.

Effect of the degree of substitution of (2-hydroxy)propyl-β-cyclodextrin on the enantioseparation of organic acids by capillary electrophoresis

István E. Valkó, Hugo A.H. Billiet*, Johannes Frank, Karel Ch.A.M. Luyben

Kluyver Laboratory of Biotechnology, Delft University of Technology, Julianalaan 67, NL-2628 BC Delft, Netherlands

Abstract

Optical isomers of nine organic acids were separated by high-performance capillary electrophoresis using (2-hydroxy)propyl-β-cyclodextrins, with a degree of the substitution between 3.0 and 7.3 (2-hydroxy)propyl groups/cyclodextrin molecule. The degree of substitution has a significant influence on the resolution of the enantiomers and is therefore an important tool in the optimisation of chiral separations. Accordingly, a proper description of derivatized cyclodextrins should include the degree of substitution.

1. Introduction

The separation of enantiomers by capillary electrophoresis (CE) is a quickly growing field in analytical chemistry [1–3]. Micellar electrokinetic chromatography using chiral micelles, ligand-exchange mechanism and protein- or polysaccharide-type chiral selectors were successfully used for the separation of several optical isomers. However, the type of separation mostly utilised is based on inclusion complex formation, primarily with cyclodextrins (CDs) as chiral selectors.

CDs are cyclic oligosaccharides built up from D-(+)-glucopyranose units linked by $\alpha(1,4)$ bonds. The naturally occurring α-, β- and γ-CDs consist of 6, 7 and 8 glucose units, respectively.

The glucose units form a torus with a rather hydrophobic cavity. The hydroxyl groups on the chiral carbon atoms 2 and 3 are on the wider rim of the torus. It is important to notice that these secondary hydroxyl groups cannot rotate; therefore, they provide an ideal site for chiral recognition. In contrast, the rotational primary hydroxyl groups on the narrower rim are less important for chiral recognition. Molecules can penetrate the cavity depending on their hydrophobicity, size and shape, and form an inclusion complex with the CD. Although many separation problems have been solved with the natural CDs, the application range and selectivity could be substantially enlarged by the use of synthetic derivatives. The CD derivatives often have better aqueous solubility than β-CD [4]. This can be explained by the "impure" nature of the CD derivatives. As they are mixtures of compounds with different degrees and patterns of substitu-

* Corresponding author.

tion the overall solubility can be better than that of the pure derivatives.

Heptakis(2,3,6-tri-O-methyl)-β-CD [5], heptakis(2,6-di-O-methyl)-β-CD [6], 2,6-dimethylated and 2,3,6-trimethylated α-CD [7], hydroxyethyl-β-CD, hydroxypropyl-β-CD [8] and glycosylated-α-CD [9] were successfully used for the separation of different enantiomers. In addition, the application of a series of charged CDs, e.g. mono-(6-β-aminoethylamino-6-deoxy)-β-CD [10], 6^A-methylamino- and $6^A,6^D$-dimethylamino-β-CD [11], carboxymethylated, carboxyethylated β-CD [12] and carboxylated methylethyl-β-CD [13] for the separation of optical isomers has been reported. These CDs can be used in charged form for the separation of neutral or ionic enantiomers, but after proper adjustment of the pH they can be used in the uncharged form as well [12]. Most of the derivatized CDs successfully used in CE had already been used in HPLC, GC and TLC.

Some of the derivatized CDs are commercially available or can be synthesized with different degrees of substitution (DS). DS refers to the number of hydroxyl groups per CD molecule which were substituted by other functional groups. Most of the CD derivatives are mixtures of compounds with different degrees and patterns of substitution. Therefore the DS is usually an average value, and its deviation around the average is also important for the proper characterisation of a certain CD.

(2-Hydroxy)propyl-β-cyclodextrin (HP-β-CD) is commercially available with different DS values. This CD was suitable for the resolution of the enantiomers of a series of organic acids [11]. HP-β-CD was successfully used as chiral selector in TLC [14], HPLC [15] and GC [16]. Many important aspects of the use of HP-β-CD such as the DS, the chirality of the hydroxypropyl substituent, the effect of organic modifiers etc. was addressed in chromatographic applications [14–16]. However, in CE the influence of the DS on the enantioselectivity has not been studied in detail yet. In this paper the effect of the (2-hydroxy)propylation of β-CD on the chiral separation of mandelic acid and eight of its enantiomeric analogues is reported.

2. Experimental

2.1. Chemicals

HP-β-CDs of four different DS values were purchased from Cyclolab (Budapest, Hungary). The hydroxypropyl substituents of the β-CD were racemic. β-CD was obtained from Fluka (Buchs, Switzerland). Some characteristic properties of the CDs are listed in Table 1. Mesityl oxide, DL-mandelic acid (MA), DL-3-hydroxymandelic acid (3HMA), DL-4-hydroxymandelic acid (4HMA), DL-2-phenyllactic acid (2PLA), DL-3-phenyllactic acid (3PLA), DL-2-phenylpropionic acid (2PPA), DL-α-methoxyphenylacetic acid (MPA), and DL-α-methoxy-α-trifluoromethylphenylacetic acid (MTPA) were purchased from Fluka. DL-3,4-Dihydroxymandelic acid (DMA) was from Aldrich (Steinheim, Germany). The structural formulae of the nine enantiomeric organic acids used in this study are shown in Fig. 1. Sodium hydrogenphosphate was obtained from Merck (Darmstadt, Germany). Deionised water was prepared using a Milli-Q system (Millipore, Bedford, MA, USA). All the chemicals were at least of analytical grade and were used without further purification.

2.2. Apparatus

The CE experiments were carried out on a fully automated BioFocus 3000 system (Bio-Rad, Hercules, CA, USA). An uncoated fused-silica capillary 50 cm (45.4 cm effective length) × 50 μm I.D. was used throughout the study. The capillary was filled with the run buffer. The

Table 1
Characteristic properties of β-CD and HP-β-CDs

Average degree of substitution	Average molecular mass	Solubility in water (g/100 ml)
0	1135	1.85
3.0 (± 5%)	1309	> 33
4.3 (± 5%)	1382	> 33
6.3 (± 5%)	1497	> 33 .
7.3 (± 5%)	1558	> 33

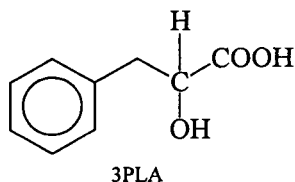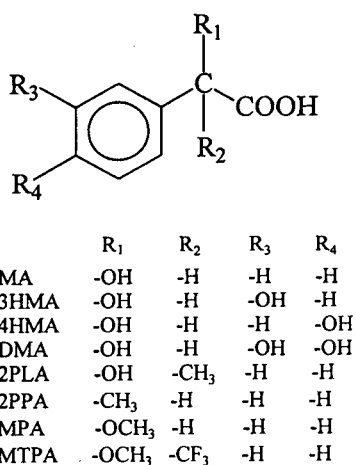|	R_1	R_2	R_3	R_4
MA	-OH	-H	-H	-H
3HMA	-OH	-H	-OH	-H
4HMA	-OH	-H	-H	-OH
DMA	-OH	-H	-OH	-OH
2PLA	-OH	-CH₃	-H	-H
2PPA	-CH₃	-H	-H	-H
MPA	-OCH₃	-H	-H	-H
MTPA	-OCH₃	-CF₃	-H	-H

Fig. 1. Structures of the enantiomeric organic acids investigated.

samples and the capillary were thermostated at 20°C. The samples were injected with 4 p.s.i.·s (1 p.s.i. = 6894.76 Pa). A constant voltage of 20 kV was applied. The analytes were detected at 206 nm.

2.3. Buffers and samples

HP-β-CD (0–80 mM) or 0–15 mM β-CD was dissolved in 50 mM phosphate buffer pH 7 or 8. These buffers were used as background electrolytes. The samples were dissolved in 5 mM phosphate buffer pH 8 in a concentration of 50 μg/ml. Mesityl oxide was used as an electroosmotic flow marker.

2.4. Calculations

The resolution (R_s) was calculated using the well known equation $R_s = 1.18(t_2 - t_1)/(w_1 + w_2)$, where t_1 and t_2 are the migration times and w_1 and w_2 are the widths of the first and the

second peak at half of the peak heights. The width of poorly resolved peaks cannot be precisely measured at the half of the peak height. In such cases the resolution was expressed as $R' = 100H'/H$, where H is the height of the first peak and H' is the depth of the valley between the first and the second peak. According to this definition $R' = 100$ means baseline resolution.

3. Results and discussion

To separate the enantiomers of organic acids with uncharged CDs like β-CD or HP-β-CDs the analytes have to be in ionic form. At a pH of 7 or higher the selected acids are predominantly in charged form. Throughout the study an uncoated capillary was used. The anions were migrating electrophoretically opposite to the detector but the intense electroosmotic flow reversed the direction of the apparent mobility. The stronger electroosmotic flow at pH 8 resulted in shorter migration times than at pH 7. Although the resolution was better at the lower pH (data not shown) the effect of the DS was studied at pH 8. With this compromise the run times could be kept reasonably low. Our intention was to show the influence of the DS on the separation of a set of compounds rather than to find the optimum conditions for the enantiomer separation.

When underivatized β-CD was dissolved in the background electrolyte no or very poor ($R' < 10$) separation was achieved for most of the enantiomeric pairs up to the maximal concentration of 15 mM. However, there are two exceptions; MTPA ($R_s = 2.31$) and 2PPA ($R_s = 1.21$). The resolution is a strong function of the chiral selector concentration. Upon increasing the CD concentration the resolution passes through a maximum [17,18]. The low aqueous solubility of the β-CD sets the limit of the chiral selector concentration so low, that often the optimum cannot be reached or even no sign of chiral recognition can be observed. One of the strategies to overcome this problem is to dissolve urea in the buffer containing β-CD, which can enhance the solubility considerably [19].

Another approach is to derivatize the β-CD so that the solubility can be increased and the enantioselectivity can be altered.

All the nine pairs of enantiomers were resolved with at least one of the HP-β-CDs. However, the resolution was in some cases remarkably different for the same components when HP-β-CD with different *average* DS was used. The resolution values of the enantiomers obtained with HP-β-CDs having different DS values are listed in Table 2.

2PLA was the worst resolved compound. Some weak enantioseparation ($R' = 13.8$) was achieved with 80 mM HP-β-CD, DS = 7.3 but no chiral separation was possible with any of the

other CDs. The resolution for 3PLA was better than for 2PLA. R' of the 3PLA enantiomers is substantially different when HP-β-CDs with different DS values are used (Fig. 2). The resolutions in the figure are expressed as R' because the R_s values for the weakly resolved peaks cannot be reliably calculated. However, the weak point of this expression is that R' stays constant after baseline separation was reached. In order to give proper information about the separation of both poorly and well resolved peaks Table 2 shows the resolution expressed as R_s but the figures indicate R' values.

Good resolution can be achieved for 2PPA with all the HP-β-CDs as shown in Fig. 3. All

Table 2
Resolution of the enantiomers of nine organic acids

DS	mM	R_s								
		MA	3HMA	4HMA	DMA	2PLA	3PLA	2PPA	MPA	MTPA
0	5	$-^a$	$-^a$	$-^a$	$-^a$	$-^a$	$-^b$	1.21	$-^a$	2.31
	10	$-^a$	$-^a$	$-^a$	$-^a$	$-^a$	$-^b$	1.03	$-^a$	2.11
	15	$-^a$	$-^a$	$-^b$	$-^a$	$-^a$	$-^b$	1.09	$-^a$	2.05
3.0	10	$-^a$	$-^a$	$-^a$	$-^a$	$-^a$	0.91	1.08	$-^a$	$-^b$
	20	$-^b$	$-^a$	$-^a$	$-^b$	$-^a$	1.02	1.35	$-^a$	0.86
	40	1.11	$-^b$	$-^a$	0.87	$-^a$	1.01	1.48	0.75	0.82
	60	1.50	1.04	$-^b$	1.28	$-^a$	0.70	1.39	1.40	0.81
	80	1.55	1.14	1.49	n.d.	$-^a$	$-^b$	1.52	1.44	$-^b$
4.3	10	$-^a$	$-^a$	$-^b$	$-^a$	$-^a$	$-^b$	0.84	$-^a$	$-^a$
	20	$-^b$	$-^b$	1.11	$-^b$	$-^a$	$-^b$	1.32	$-^b$	$-^a$
	40	1.16	0.91	1.57	$-^b$	$-^a$	$-^b$	1.56	0.96	$-^a$
	60	1.49	1.46	2.21	0.91	$-^a$	0.81	1.89	1.46	$-^a$
	80	1.89	1.30	2.63	1.97	$-^a$	0.91	2.02	2.21	$-^a$
6.3	10	$-^a$	$-^a$	$-^b$	$-^a$	$-^a$	$-^b$	1.16	$-^a$	$-^b$
	20	$-^b$	$-^a$	1.00	$-^a$	$-^a$	0.91	1.60	$-^b$	$-^b$
	40	0.94	$-^b$	1.36	$-^b$	$-^a$	0.86	1.74	0.93	$-^b$
	60	1.67	0.89	1.25	0.89	$-^a$	0.83	1.60	1.16	$-^b$
	80	2.40	1.37	1.85	1.37	$-^a$	0.89	2.05	1.72	$-^b$
7.3	10	$-^a$	$-^a$	$-^b$	$-^a$	$-^a$	$-^b$	0.81	$-^a$	$-^b$
	20	$-^b$	$-^b$	1.33	$-^b$	$-^a$	0.89	1.37	$-^b$	$-^b$
	40	1.28	1.57	2.69	1.57	$-^a$	1.04	1.70	1.98	$-^b$
	60	1.89	1.69	1.14	1.69	$-^b$	1.22	1.07	1.89	$-^b$
	80	2.34	2.57	1.27	2.58	$-^b$	1.17	0.93	2.21	$-^b$

For experimental conditions see the text. n.d. = No data.
[a] No separation.
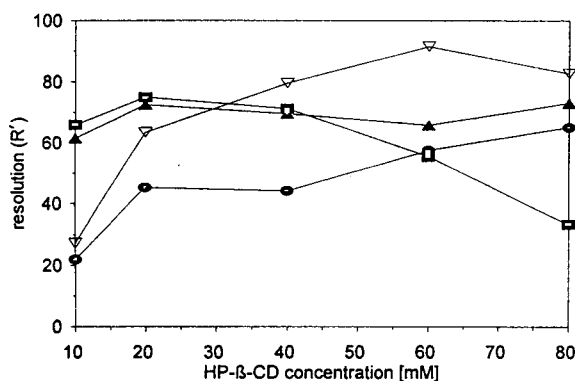[b] Poor enantioseparation, the peaks were not resolved at the half of the peak height.

Fig. 2. Resolution (R') of the 3PLA enantiomers as a function of the HP-β-CD concentration. DS values: □ = 3.0; ○ = 4.3; ▲ = 6.3; ▽ = 7.3. See the text for experimental conditions.

the four HP-β-CDs can provide baseline resolution, but resolution versus CD concentration plots are different. When HP-β-CD, DS = 7.3 is used the resolution reaches a maximum at 40 mM. With the other HP-β-CDs the maximum resolution was not achieved in the concentration range studied. The greater the affinity of the enantiomers for the chiral selector the lower is the optimum CD concentration [17]. This means that the inclusion complex of 2PPA with HP-β-CD has the highest equilibrium constant at DS = 7.3.

MTPA was the only compound that was better resolved with β-CD than with any of the HP-β-

CDs. The best resolution of MTPA with HP-β-CDs ($R' = 57.5$) was measured at DS = 3.0. At DS = 4.3 no enantioseparation was found. MTPA and 2PLA are both disubstituted on the α-carbon atom and have the worst resolution in the set of enantiomers studied. MPA differs from MTPA only at the α-carbon which is monosubstituted in MPA. This compound was well resolved with all the HP-β-CDs. The (2-hydroxy)propyl groups on the rim of the CD cavity may form a steric barrier for compounds bearing two substituents on the α-carbon. This effect can be seen in the case of MTPA, where the absolute value of the effective mobility decreases with a factor of 1.8 if 10 mM β-CD was dissolved in the phosphate buffer. This low CD concentration does not influence the electroosmotic flow considerably, so the reduced effective mobility is a consequence of the strong complexation with the β-CD. In contrast the decrease in absolute value of the effective mobility is only 1.2 if the concentration of HP-β-CD DS = 7.3 is increased from 0 to 10 mM. Fig. 4 shows the effective mobility of the MTPA and 2PLA as a function of the concentration of β-CD and HP-β-CD, DS = 7.3. The absolute value of the effective mobility is reduced significantly if β-CD is dissolved in the buffer. The decrease in the effective mobility is much less pronounced if HP-β-CD is used as a chiral selector. These findings may indicate that
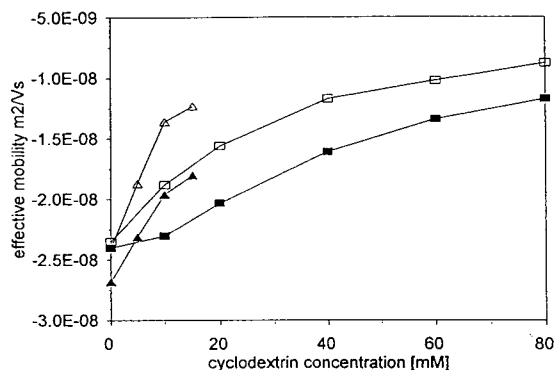

Fig. 3. Resolution (R') of the 2PPA enantiomers as a function of the HP-β-CD concentration. DS values: □ = 3.0; ○ = 4.3; ▲ = 6.3; ▽ = 7.3. See the text for experimental conditions.

Fig. 4. The effect of β-CD and HP-β-CD (DS = 7.3) concentration on the effective mobility of 2PLA and MTPA. Symbols: ■ = 2PLA + HP-β-CD (DS = 7.3); ▲ = 2PLA + β-CD; □ = MTPA + HP-β-CD (DS = 7.3); △ = MTPA + β-CD. See the text for experimental conditions.
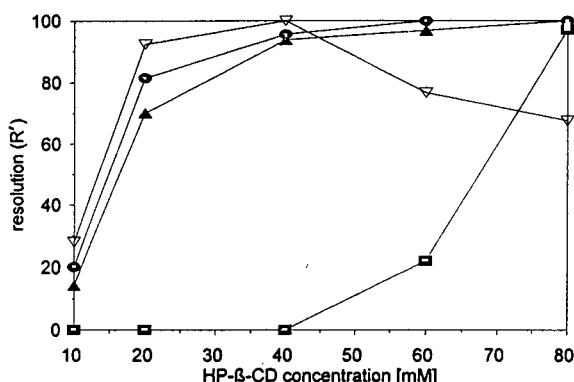
Fig. 5. Resolution (R') of the 4HMA enantiomers as a function of the HP-β-CD concentration. DS values: □ = 3.0; O = 4.3; ▲ = 6.3; ▽ = 7.3. See the text for experimental conditions.

for compounds disubstituted in the α-carbon atom, the inclusion complex formation is hindered. In addition to the less favoured formation of the complex the enantioselectivity of HP-β-CD may also be substantially different from that of β-CD.

MA and its analogues hydroxylated on the aromatic ring are well resolved with the HP-β-CDs. However, at different degrees of substitution the resolution of the same compound is sometimes very different. Fig. 5 shows how the resolution of 4HMA is effected by the concentration of different HP-β-CDs. 4HMA was the best resolved compound from the nine enantiomeric pairs investigated in this study. At 40 mM HP-β-CD, DS = 7.3 the resolution was as high as 2.69.

4. Conclusions

The enantioselectivity of derivatized CDs can be significantly influenced by changing the DS. The resolution of a certain pair of enantiomers can be very different if the DS of the chiral selector is different. In some cases the chiral

recognition can be completely lacking at a DS value but using the same type of CD at another DS the separation of the enantiomers may be possible. These effects can be successfully used for the optimization of chiral separations. On the other hand, our results emphasise that proper description of the derivatized CDs should include the information about the DS.

References

[1] J. Snopek, I. Jelínek and E. Smolková-Keulemansová, J. Chromatogr., 609 (1992) 1.
[2] R. Kuhn and S. Hoffstetter-Kuhn, Chromatographia, 34 (1992) 505.
[3] I.E. Valkó, H.A.H. Billiet, H.A.L. Corstjens and J. Frank, LC · GC Int., 6 (1993) 424.
[4] J. Szejtli, Cyclodextrin Technology, Kluwer, Dordrecht, 1988, p. 12.
[5] H. Soini, M.-L. Riekkola and M. Novotny, J. Chromatogr., 608 (1992) 265.
[6] S. Fanali, J. Chromatogr., 474 (1989) 441.
[7] M. Tanaka, M. Yoshinaga, S. Asano, Y. Yamashoji and Y. Kawaguchi, Fresenius' J. Anal. Chem., 343 (1992) 896.
[8] M. Heuermann and G. Blaschke, J. Chromatogr., 648 (1993) 267.
[9] M.J. Sepaniak, R.O. Cole and B.K. Clark, J. Liq. Chromatogr., 15 (1992) 1023.
[10] S. Terabe, Trends Anal. Chem., 8 (1989) 129.
[11] A. Nardi, A. Eliseev, P. Boček and S. Fanali, J. Chromatogr., 638 (1993) 247.
[12] T. Schmidt and H. Engelhardt, Chromatographia, 37 (1993) 474.
[13] N.W. Smith, J. Chromatogr. A, 652 (1993) 259.
[14] D.W. Armstrong, J.R. Faulkner, Jr. and S.M. Han, J. Chromatogr., 452 (1988) 323.
[15] A.M. Stalcup, S.-C. Chang, D.W. Armstrong and J. Pitha, J. Chromatogr., 513 (1990) 181.
[16] D.W. Armstrong, W. Li, C.-D. Chang and J. Pitha, Anal. Chem., 62 (1990) 914.
[17] S.A.C. Wren and R.C. Rowe, J. Chromatogr., 603 (1992) 235.
[18] S.A.C. Wren, J. Chromatogr., 636 (1993) 57.
[19] D.Y. Pharr, Z.S. Fu, T.K. Smith and W.L. Hinze, Anal. Chem., 61 (1989) 275.

Determination of inositol phosphates in fermentation broth using capillary zone electrophoresis with indirect UV detection

B.A.P. Buscher[a], H. Irth[a], E. Andersson[b], U.R. Tjaden[a,*], J. van der Greef[a]

[a]Division of Analytical Chemistry, Center for Bio-Pharmaceutical Sciences, P.O. Box 9502, 2300 RA Leiden, Netherlands
[b]Perstorp Regeno, S-284 80 Perstorp, Sweden

Abstract

The potential of capillary zone electrophoresis for the fast monitoring of a fermentation process in which inositol phosphates are enzymatically hydrolyzed has been investigated. The developed analysis consists of capillary zone electrophoresis combined with indirect UV detection, using 1-naphthol-3,6-disulfonic acid as the chromophore. The total analysis of all six inositol phosphates covering a concentration range of 0–500 μM takes only 13 min.

1. Introduction

Specific inositol phosphates, e.g. 1,4,5-inositol trisphosphate, play an important role as a second messenger in signal transduction in the body [1]. Others, such as phytic acid, are found in grains and seeds [2], whereas specific isomers of inositol trisphosphate show several interesting pharmacological properties [3]. Because of their physicochemical characteristics, fast analysis of inositol phosphates has been a problem for many years. First, inositol phosphates are, depending on the number of phosphate groups, multiply negatively charged, even at low pH values. Second, because of the absence of chromophoric or fluorophoric groups in the molecule sensitive detection is rather complicated. For the separation of the compounds ion-pair [4,5] and ion-exchange chromatography [6,7] have been applied, as well as gas chromatography after derivatization of myo-

* Corresponding author.

inositol formed after enzymatic hydrolysis [8]. However, these separation methods are rather time consuming, caused by the equilibration times in ion chromatography or by the need of laborious derivatization procedures in the case of gas chromatography. Detection methods applied include refractive index detection [9], radiometric detection [10], colorimetric detection [11], fluorometry after complexation [3] and after derivatization [12], mass spectrometry [13], postcolumn reaction detection, based on enzymatic hydrolysis of the phosphate esters and detection of the inorganic phosphate formed [14], electrochemical detection of NADH after enzymatic oxidation of inositol [15] and suppressed conductivity [16].

Since for the monitoring of the enzymatic hydrolysis of phytic acid a fast analysis of charged compounds is required, capillary zone electrophoresis (CZE) enabling indirect UV detection should be an attractive technique. Henshall et al. [17] already described this meth-

od for IP_1 (1- and 2-isomer), IP_2, IP_3 and IP_6. However, IP_4 and IP_5 were not included and for a routine analysis the method was said to be questionable because of the day-to-day variation in migration time. Capillary zone electrophoresis, which is based on the charge and size of the molecules, appeared to be appropriate for the fast separation of the multiply charged inositol phosphates. It reduces the long analysis times as obtained with chromatographic systems while the loss of material due to adsorption onto the chromatographic support material is avoided.

Indirect detection methods [18] based on either UV, fluorescence or amperometric detection offer the advantage that no derivatization of the compounds is needed. Either a chromophore [19–21], a fluorophore [22–24] or an electrochemically active substance [25] is added to the buffer thus creating a constant, large background signal. Similar mobilities of the buffer constituent and the analyte are of major importance for the resulting peak shapes. The analyte signal is derived from the signal of the buffer constituent through displacement of the electrolyte by the analyte. A severe disadvantage of indirect detection is the increased noise level by the addition of the chromophore with its detection characteristics which leads to increased detection limits.

The present paper describes the determination of myo-inositol phosphates in fermentation broth with CZE and indirect UV detection using 1-naphthol-3,6-disulfonic acid as chromophore. The only clean-up step required consisted of centrifugation of the fermentation sample, the supernatant being directly injected in the CZE system.

2. Experimental

2.1. Chemicals

1-Naphthol-3,6-disulfonic acid (NDSA) was obtained from Janssen (Beerse, Belgium). Acetic acid p.a. was purchased from Baker (Deventer, Netherlands). Both inositol monophosphate (2-IP_1), as dicyclohexylammonium

salt and hydroxypropylmethylcellulose (HPMC), with a viscosity of 4000 cP for a 2% aqueous HPMC solution, came from Sigma (St. Louis, MO, USA). Inositol bis- (1,2-IP_2), tris- (1,2,6-IP_3), tetrakis- (1,2,5,6-IP_4), pentakis- (1,2,4,5,6-IP_5) and hexakisphosphate (IP_6) were supplied as sodium salts by Perstorp Pharma (Perstorp, Sweden). For the preparation of the stock solutions of analytes and buffer solutions, deionized water was used (Milli-Q system, Millipore, Bedford, MA, USA). Calibration curves were generated by spiked fermentation buffer with different concentrations of inositol phosphates. The buffer solution was filtered through a 0.2-μm Nylon acrodisc syringe filter (Gelman Sciences, Ann Arbor, MI, USA).

2.2. Electrophoresis

The experiments were performed on a P/ACE 2200 system (Beckman, Fullerton, CA, USA), including a liquid thermostated (24°C) capillary and a UV detector. The electrophoresis medium was prepared freshly every day and consisted of 0.5 mM NDSA, 30 mM acetic acid and 0.01% HPMC to suppress the electroosmotic flow. The applied voltage was −30 kV generating a current of about 10 μA. Detection was performed at 214 nm with a data sampling rate of 5 Hz and a time constant of 0.5 s. For data collection and handling System Gold software, version 7.12 (Beckman) was used. This software did not integrate the large negative peak preceding the IP_6 peak; integration was set to start at the IP_6 peak base. Untreated fused-silica capillaries (75 μm I.D.) from SGE (Ringwood, Victoria, Australia) with a total length of 0.57 m (0.50 m to the detector) were used. New capillaries were rinsed with deionized water and electrophoresis medium, each for 2 min. Before each injection the capillary was rinsed with electrophoresis medium for 2 min. Pressurized injection during 3 s, which corresponded to 34 nl was applied.

2.3. Sample pretreatment

Samples taken from the fermentation broth containing yeast, buffer and inositol phosphates,

were centrifuged for 5 min in an Eppendorf centrifuge 5415 (Eppendorf Geraetebau, Netheler und Hinz GmbH, Hamburg, Germany) at 11 000 rpm (4000 g). The supernatant was introduced into the capillary after 1:1 dilution with fermentation buffer.

3. Results and discussion

3.1. Electrophoresis

Inositol phosphates have in general high electrophoretic mobilities due to the multiple charges of the phosphate groups. When electrophoresis takes place at pH values that are favourable regarding selectivity, the electro- osmotic flow (EOF) under these conditions (pH about 3) is rather low. At higher pH values, the EOF increases considerably, while simultaneously the selectivity between IP_4, IP_5 and IP_6 becomes unacceptably low. As a consequence, the peaks are not sufficiently separated anymore to quantitate all peaks. Because the phosphate groups are negatively charged, this implies that without electroosmotic flow the analytes migrate in the direction of the anode. Since the electrophoretic velocity is the resultant of the electrophoretic mobility and the electroosmotic mobility the net result at the applied pH is rather low electrophoretic velocities leading to unacceptably long analysis times. Therefore, it has been decided to reverse the polarity of the system (negative inlet electrode, grounded outlet electrode). In that case it is necessary to suppress the electroosmotic flow as much as possible, which is realized by modifying the electrophoresis buffer. Although the stability of dynamically coated capillary walls are not as favourable as untreated capillaries, we obtained quite acceptable systems using HPMC which is demonstrated by the validation figures.

Due to the many phosphate groups of the inositol phosphates, the pH of the electrophoresis medium is a very critical parameter in the separation of inositol phosphates: 0.2 pH units deviation already induced considerable changes in the migration time. Thirty millimolar of acetic

acid (pH 3.0) appeared to be adequate for this purpose. Migration times and relative standard deviations (R.S.D.) of all six inositol phosphates are shown in Table 1. These are mean values from 15 measurements over the whole concentration range. The R.S.D. for all the compounds is less than 2.6% allowing reliable peak identification. Because the effect of electrodispersion is more pronounced at higher concentrations, the migration times of the compounds that show fronting (IP_4, IP_5, IP_6) tend to be slightly higher at increased concentrations, whereas the migration times of the compounds that show tailing (IP_2, IP_1) are reduced at higher concentrations.

3.2. Detection

With respect to indirect detection, NDSA has been chosen as the chromophore because its electrophoretic mobility matches closely with that of the most important analyte, IP_3. The optimal matching has been obtained by adjustment of the pH of the electrophoresis buffer. As a consequence of the high optical background the noise of the baseline is considerably increased in comparison with direct UV detection. Fig. 1 presents the electropherogram of the inositol phosphates having analysis times of less than 6 min. Under these conditions the isomers are not separated. Although IP_5 and IP_6 are not baseline separated, they still can be quantified. The other inositol phosphates are completely baseline separated. From this figure it can easily be seen that IP_4, IP_5 and IP_6 have electrophoretic mobilities higher than that of the chromophore

Table 1
Migration times and relative standard deviation (R.S.D.) of the inositol phosphates

Compound	Migration time (s)	R.S.D. (%)
IP1	315.5	0.4
IP2	240.2	1.6
IP3	205.3	0.9
IP4	187.0	2.0
IP5	176.7	2.5
IP6	166.4	1.4
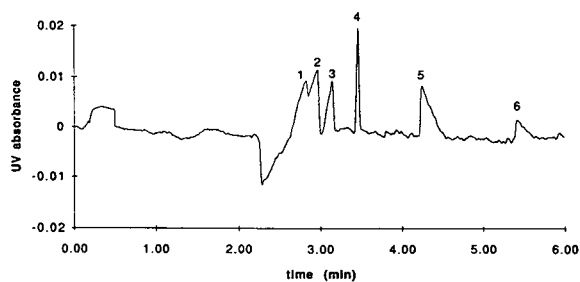
Fig. 1. Electropherogram of a standard mixture of all six inositol phosphates ($1 = 340$ μM IP$_6$, $2 = 320$ μM IP$_5$, $3 = 160$ μM IP$_4$, $4 = 170$ μM IP$_3$, $5 = 220$ μM IP$_2$, $6 = 500$ μM IP$_1$). Conditions: applied voltage: -30 kV, current: 10 μA, $\lambda = 214$ nm, fused-silica capillary: 75 μm I.D., electrophoresis buffer: 0.5 mM NDSA, 30 mM acetic acid, 0.01% HPMC.

at pH 3, which leads to fronting peak shapes. On the other hand, IP$_1$ and IP$_2$ have lower electrophoretic mobilities resulting in tailing peaks. This asymmetry of the peaks is caused by electrodispersion, deriving from local differences in conductivity and consequently differences in the local electric field strengths. This effect is more pronounced at concentrations of the analytes that are high in comparison with the chromophore [21]. IP$_3$ is the only compound with a symmetrical peak shape. By adjusting the mobility of the chromophore to that of the analyte, electrodispersion of that particular compound is suppressed and the efficiency is improved [20]. In that way the limit of determination (LOD) of the analyte can be improved. Therefore, the LOD (defined as 10 times the noise) appeared to be lowest for IP$_3$ (3.9 μM). The LODs for IP$_4$ and IP$_6$ amounted to 9.2 and 22.5 μM, respectively, applying an injection volume of 34 nl.

In a fermentation process, however, the concentrations of the main compounds of interest are in the 50–1000 μM range. For that reason the LOD of the compounds is not critical.

3.3. Quantitative aspects

Quantitative aspects have been examined by generating calibration curves for the compounds of interest. Therefore, fermentation buffer was spiked with concentrations of inositol phosphates

up to 1 mM. Calibration curves for the inositol phosphates are linear in the 0–500 μM range. For concentrations above 500 μM being the concentration of the chromophore the peak area of the inositol phosphates does not increase linearly. By increasing the chromophore concentration, higher inositol phosphate concentrations can be determined. Unfortunately, the linear dynamic range only shifts to higher concentrations but is not expanded, while the LOD is still increased. Calibration plots for the inositol phosphates were thus made from 0–500 μM. The calibration plots of IP$_1$ and IP$_6$ have the lowest correlation coefficients of 0.993 and 0.986, respectively, which is caused by the least symmetric peak shapes. The correlation coefficients for the other inositol phosphates were higher: 0.998 (IP$_2$), 0.996 (IP$_3$), 0.997 (IP$_4$) and 0.995 (IP$_5$).

The developed analysis has been validated for the most important analytes in the fermentation mixture, IP$_2$, IP$_3$, IP$_4$ and IP$_6$. The intra-day and inter-day variability, expressed as imprecision (R.S.D., %), have been examined for different concentrations of inositol phosphates (Table 2). The intra-day variability did not exceed 19.8%

Table 2
Intra-day and inter-day variability expressed as imprecision (R.S.D.) of the method

Compound	Concentration (μM)	Intra-day R.S.D. (%)	n	Inter-day R.S.D. (%), $n = 3$
IP$_2$	348	9.6	11	1.2
		14.5	8	
IP$_3$	99	4.4	20	2.4
		5.7	25	
		6.1	16	
	395	3.9	6	2.5
		8.9	8	
IP$_4$	192	13.6	20	1.4
		10.0	25	
		8.1	17	
	383	9.0	6	1.2
		12.7	8	
IP$_6$	396	19.8	20	7.8
		19.8	26	
		13.1	19	

(IP$_6$), whereas the highest inter-day variability amounted to 7.8% (IP$_6$). As can be seen from Table 2, the developed method shows a good reproducibility. Although the intra-day variability for IP$_6$ is relatively high, its value is acceptable for this application. Nevertheless, it indicates that every day a new calibration curve for the different analytes has to be constructed. The analytes for the calibration curves are dissolved in the fermentation buffer in order to simulate the real samples as much as possible thus increasing the accuracy of the analysis. Fermentation samples are diluted 1:1 with the fermentation buffer to avoid concentrations out of the linear range.

3.4. Fermentation monitoring

Fermentation monitoring, being the aim of the analysis, has been performed after a simple sample pretreatment of centrifugation which takes only 5 min. During the centrifugation the yeast is separated as a pellet from the inositol phosphates in the supernatant. Fig. 2 shows the electropherograms of the fermentation broth analyzed after 5 min (Fig. 2a), 60 min (Fig. 2b) and 22 h (Fig. 2c). From these electropherograms it is evident that the applied sample pretreatment, though in the off-line mode, is sufficient for quantification of the analytes. IP$_6$, present at a high initial concentration (Fig. 2a), has been hydrolyzed into the other inositol phosphates and free phosphate after a few hours (Fig. 2b and 2c). The potential of monitoring the fermentation process is also demonstrated in Fig. 3. The more active the yeast, the faster phytic acid is hydrolyzed. During the hydrolysis a high amount of free phosphate has been formed. Phosphate has approximately the same electrophoretic mobility as IP$_1$. For that reason IP$_1$ can not be determined in the fermentation broth. At even higher phosphate concentrations, interference with IP$_2$ also occurs. A minor drawback of the developed analysis is the off-line sample pretreatment. Instead of centrifugation which cannot easily be automated, dialysis but especially electrodialysis has to be explored as sample pretreatment. If a dialysis probe is positioned in
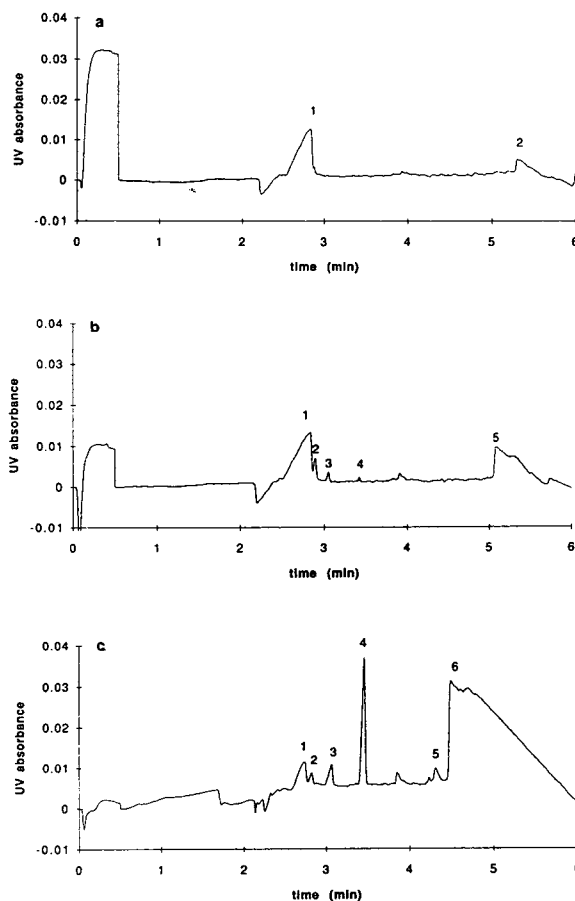
Fig. 2. Electropherograms of a sample of the fermentation broth at 5 min (a), 60 min (b) and 22 h (c). Concentrations of the inositol phosphates: (a) 1 = 480 μM IP$_6$, 2 = acetate, (b) 1 = 420 μM IP$_6$, 2 = 30 μM IP$_5$, 3 = 20 μM IP$_4$, 4 = 8 μM IP$_3$, 5 = phosphate + acetate, (c) 1 = 70 μM IP$_6$, 2 = 20 μM IP$_5$, 3 = 60 μM IP$_4$, 4 = 300 μM IP$_3$, 5 = 30 μM IP$_2$, 6 = phosphate + acetate. For conditions see Fig. 1.

the fermentation broth, a connection between the dialysis probe and a sample vial will allow the complete automation of the analytical method.

4. Conclusions

A method for monitoring the enzymatic hydrolysis of phytic acid has been developed. Fast separation and detection of all six inositol phosphates in deionized water has been achieved by using capillary zone electrophoresis with indirect
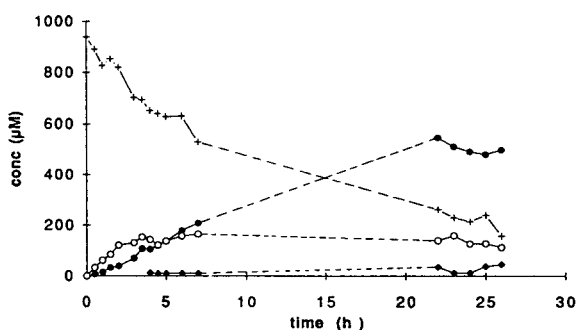
Fig. 3. Monitoring of the enzymatic hydrolysis of phytic acid. ◆ = IP$_2$, ● = IP$_3$, ○ = IP$_4$, + = IP$_6$.

UV detection. The mobility of the chromophore has to be adjusted to that of the compound to be quantified most accurately.

In the fermentation broth the high concentration of free phosphate masks IP$_1$ thus preventing it from being detected. At long reaction times the high concentration of free phosphate formed during fermentation may also interfere with the detection of IP$_2$.

References

[1] N.N. Osborne, A.B. Tobin and H. Ghazi, *Neurochem. Res.*, 13 (1988) 177.
[2] E. Graf, *J. Agric. Food Chem.*, 31 (1983) 851.
[3] H. Irth, M. Lamoree, G.J. de Jong, U.A.Th. Brinkman, R.W. Frei, R.A. Kornfeldt and L. Persson, *J. Chromatogr.*, 499 (1990) 617.
[4] J.A. Shayman and D.M. BeMent, *Biochem. Biophys. Res. Comm.*, 151 (1988) 114.
[5] A.S. Sandberg and R.J. Ahderinne, *J. Food Sci.*, 51 (1986) 547.
[6] R. Ellis and E.R. Morris, *Cereal Chem.*, 59 (1982) 232.
[7] R.E. Smith and R.A. Macquarrie, *LC-GC*, 7 (1989) 775.
[8] C.W. Ford, *J. Chromatogr.*, 333 (1985) 167.
[9] B. Tangendjaja, K.A. Buckle and M.J. Wootton, *J. Chromatogr.*, 197 (1980) 274.
[10] H. Binder, P.C. Weber and W. Siess, *Anal. Biochem.*, 148 (1985) 220.
[11] J.J.L. Cilliers and P.J. v. Niekerk, *J. Agric. Food Chem.*, 34 (1986) 680.
[12] M.E. Kargacin, G. Bassel, P.J. Ryan and T.W. Honeyman, *J. Chromatogr.*, 393 (1987) 454.
[13] W.R. Sherman, K.E. Ackerman, R.A. Berger, B.G. Gish and M. Zinbo, *Biomed. Environ. Mass Spectrom.*, 13 (1986) 333.
[14] J. Meek, *Natl. Acad. Sci.*, 83 (1986) 4162.
[15] G. Marko-Varga, E. Dominguez, B. Hahn-Hägerdal and L. Gorton, *J. Pharm. Biomed. Anal.*, 8 (1990) 817.
[16] *Dionex application note AN 65*, 1990, Dionex, Sunnyvale, CA.
[17] A. Henshall, M.P. Harrold and J.M.Y. Tso, *J. Chromatogr.*, 608 (1992) 413.
[18] E.S. Yeung and W.G. Kuhr, *Anal. Chem.*, 63 (1991) 275A.
[19] S. Hjerten, K. Elenbring, F. Kilar, J. Liao, A.J.C. Chen, C.J. Siebert and M. Zhu, *J. Chromatogr.*, 403 (1987) 47.
[20] F. Foret, S. Fanali, L. Ossicini and P. Bocek, *J. Chomatogr.*, 470 (1989) 299.
[21] G.J.M. Bruin, A.C. v. Asten, X. Xu and H. Poppe, *J. Chromatogr.*, 608 (1992) 97.
[22] W.G. Kuhr and E.S. Yeung, *Anal. Chem.*, 60 (1988) 1832.
[23] T.W. Garner and E.S. Yeung, *J. Chromatogr.*, 515 (1990) 639.
[24] M.D. Richmond and E.S. Yeung, *Anal. Biochem.*, 210 (1993) 245.
[25] T.M. Olefirowicz and A.G. Ewing, *J. Chromatogr.*, 499 (1990) 713.

Indirect UV detection as a non-selective detection method in the qualitative and quantitative analysis of heparin fragments by high-performance capillary electrophoresis

Jan B.L. Damm*, George T. Overklift

Department of Analytical Chemistry, Organon International B.V., Akzo Pharma Group, P.O. Box 20, NL-5340 BH Oss, Netherlands

Abstract

The application of capillary electrophoresis (CE) in combination with indirect UV detection for the qualitative and quantitative analysis of synthetic low-molecular-mass heparin fragments, at low pH, is described. It is demonstrated that, in contrast to direct UV detection, with indirect UV detection the signal obtained for various synthetic heparin pentasaccharides is nearly independent of their molecular structure. Moreover, the sensitivity of indirect UV detection is at least one order of magnitude higher than that of direct UV detection. CE–indirect UV detection for the qualitative and quantitative analysis of low-molecular-mass glycosaminoglycans was achieved by using 5 mM 5-sulphosalisylic acid, pH 3 or 5 mM 1,2,4-tricarboxybenzoic acid, pH 3.5 as electrophoresis buffer and chromophore. The technique is exemplified by the analysis of three pharmaceutical preparations of synthetic heparin pentasaccharides. The method employing indirect UV detection was validated with respect to repeatability, limit of detection, limit of quantitation, linearity, accuracy and ruggedness. In the indirect detection mode, the limit of detection for synthetic pentasaccharides is below 5 fmol, whereas the limit of quantitation is about 25 fmol. The method shows excellent repeatability and is linear in the femtomole–picomole range. Finally, it is demonstrated that the method is suitable for the analysis of various types of glycosaminoglycans.

1. Introduction

Recently, high-performance capillary electrophoresis (CE) was reported as a sensitive, high-resolution method for the determination of the disaccharide composition of several proteoglycans [1,2]. In extension to these studies we described the separation of complex mixtures of natural and synthetic heparin fragments by CE [3]. It was demonstrated that the resolution

obtained by CE for these mixtures was in general superior to that obtained by high-performance anion-exchange chromatography, while the amount of material needed for the analysis was about three orders of magnitude less. In the latter study the heparin fragments were detected on basis of their UV absorbance. However, the various heparin fragments may have different molar extinction coefficients, impeding a quantitative analysis by CE using UV detection. Especially in the case of synthetic pentasaccharide preparations the extinction coefficients

* Corresponding author.

of the individual sample components, viz. main product and side products, may strongly deviate.

For a reliable quantitative analysis the heparin fragments should produce an equal detection response. In principle, there are several options for non-selective detection of heparin fragments, e.g. detection after chromophoric, fluorescence or radioactive labelling, refractive index detection, or detection by mass spectrometry (MS). Furthermore, conductivity detection of uniformly charged analytes and amperometric detection may serve as (pseudo) non-selective detection modes for CE. However, in case of CE of synthetic pentasaccharides that are intended for pharmaceutical use, attachment of a chromophore or fluorescence label is not possible or suitable. CE in combination with conductivity or (indirect) amperometric detection has been reported for the quantitative analysis of carboxylic acids [4], amino acids [5] and carbohydrates [6,7]. However, at present these detectors are not yet commercially available for CE. On-column laser-based refractive index detection for CE of carbohydrates has been described by Bruno et al. [8], but also this application is not yet commercially available. Fast atom bombardment (FAB) [9,10] and electrospray ionization [11,12] MS detection and multi-channel Raman spectroscopic detection [13] are potentially powerful techniques for the on-line detection and characterization of analytes by CE, although the feasibility of these options for the analysis of glycosaminoglycans (GAGs) by CE still needs to be demonstrated. Garner and Yeung [14] reported indirect fluorescence detection as a universal detection method for CE of charged carbohydrates. Unfortunately, the high cost of laser equipment and the fact that it is not available in most commercial CE systems compromise the applicability of this method. With respect to cost and feasibility, indirect UV detection [15] seems a more straightforward approach. Indirect UV detection has already been applied successfully to the analysis by CE of inorganic [16] and organic [17] anions as well as of various monosaccharides [18]. In the latter study the monosaccharides were ionized and separated at high pH using 6 mM sorbic acid, pH 12.1 as

electrophoresis buffer and chromophore. Ionization of neutral sugars by high pH is a prerequisite as indirect UV detection is dependent on charge displacement [18]. For the analysis of synthetic heparin fragments by CE–indirect UV detection, high pH-induced ionization is not necessary since these compounds contain multiple carboxylic acid and sulphate groups. Wang and Hartwick [19] recently documented the use of binary buffers in CE–indirect UV detection, allowing for a wide range of pH of the electrophoresis buffers and mobility of the analyte ions. We have shown previously [3] that a high resolution of complex mixtures of heparin fragments can be obtained applying a single buffer system at relatively low pH and using direct UV detection. Here we report the applicability of indirect UV detection for the non-selective detection of various heparin fragments after their separation by CE at low pH using 5-sulphosalisylic acid or 1,2,4-tricarboxybenzoic acid as electrophoresis buffer and chromophore. A key question then is whether the background electrolyte that is required in the indirect detection mode does not interfere with an efficient resolution. Furthermore, it is essential that the background electrolyte has a high molar extinction coefficient at the selected detection wavelength to warrant sufficient detection sensitivity, and an effective mobility similar to that of the analyte ions in order to prevent fronting or tailing of analyte peaks. In this study the application of CE–indirect UV detection as an analytical method for the determination of the purity of GAG preparations is validated and it is demonstrated that the technique enables the qualitative and quantitative analysis of low-molecular-mass heparin fragments.

2. Experimental

2.1. Materials

Synthetic pentasaccharides were prepared at Organon (Oss, Netherlands) in cooperation with Sanofi (Toulouse, France) and the structures

were verified by ^{1}H and ^{13}C NMR spectroscopy [20–23] and FAB-MS [23]. Heparin disaccharide reference compounds were obtained from Grampian enzymes (Aberdeen, UK). Dermatan sulphate di-, tetra- and hexasaccharides were synthesized by Organon.

2.2. Capillary electrophoresis

The synthetic pentasaccharides were each dissolved in Milli-Q water (Millipore, Milford, MA, USA) to a concentration of 1 mg/ml and separated by high-performance CE essentially as described [3], except that in this study the internal diameter of the capillary was 50 μm (unless stated otherwise). Furthermore, to allow indirect UV detection, the electrophoresis buffer was changed as outlined below. The eight commercially obtained heparin disaccharides were dissolved in Milli-Q water and mixed to give a final concentration of approximately 0.1 mg/ml of each compound. On-capillary detection was performed by UV absorbance at 210 or 230 nm, using 200 mM NaH$_2$PO$_4$ (J.T. Baker, Deventer, Netherlands), adjusted to pH 2.5 or 3.0 with concentrated H$_3$PO$_4$, as CE electrophoresis buffer. The potential across the capillary was 7.5 kV (131.5 V/cm) and the thermostatted capillary was kept at 40°C. Indirect UV detection by quenching of the UV signal at 214 nm was performed by using 5 mM 5-sulphosalicylic acid (pK_a carboxylic acid group 2.27), pH 3.0 or 5 mM 1,2,4-tricarboxybenzoic acid (pK_a values 2.28, 3.58 and 4.79), pH 3.5 as electrophoresis buffer at a potential of 5 kV (87.7 V/cm) and room temperature.

2.3. Validation of CE–indirect UV detection

The application of CE in combination with indirect UV detection as an analytical method for the determination of the purity of pentasaccharide preparations was validated by use of a "golden standard" preparation of D-glucosamine-N,6-disulphate(α1-4)-L-iduronic acid-2-sulphate-(β1-4)–D-glucosamine-N,3,6-trisulphate-(α1-4)-D-glucuronic acid(β1-4)–D-glucosamine-N,3,6-trisulphate (Org 31550). The purity of this prep-

aration was determined to be at least 99.5% (mol/mol) by 360 MHz ^{13}C/^{1}H NMR spectroscopy as described [22]. The residual water content was 8.7% (w/w) ± 0.55 (standard error of the mean, S.E.M., $n = 3$) as determined by Karl Fischer titration [24] and chloride and (free) sulphate content were 0.5% (w/w) and 0% (w/w), respectively, as determined by isotachophoresis [25]. All CE validation experiments were carried out using 5 mM sulphosalicylic acid, pH 3.0 at a thermostatted temperature of 25°C, applying a potential of 5 kV across the capillary. The injection time was in each case 2 s resulting in injection of 1.8 nl of sample solution. These conditions are further referred to as standard conditions.

3. Results and discussion

All CE experiments were carried out using low pH ($\leqslant 3.5$) electrophoresis buffers to prevent dissociation of the silanol groups of the capillary inner wall, resulting in arheic or nearly-arheic separation conditions without the need for anticonvective gel filling or coating of the capillary inner wall [3,26].

Fig. 1A depicts the CE electropherogram obtained for a nearly equimolar mixture of eight heparin disaccharides (denoted 1–8, structures in Table 1) employing 200 mM NaH$_2$PO$_4$, pH 2.5 as electrophoresis buffer and using direct UV absorbance at 230 nm as detection method. Injection of ca. 5 pmol of each disaccharide yields a satisfactory signal-to-noise ratio, demonstrating the high mass sensitivity of CE. The identity of the peaks as compounds 1–8 (Table 1) was established in an earlier study [3]. Fig. 1B shows the CE pattern obtained for the same mixture applying 5 mM 1,2,4-tricarboxybenzoic acid, pH 3.5 as electrophoresis buffer and observing the quenching of the UV signal at 214 nm (further referred to as indirect UV detection). In this case only ca. 0.5 pmol of each disaccharide are injected. The disaccharides 2–4 are not completely separated under the conditions of indirect UV detection, but the three disaccharides denoted 6–8, all having two negative
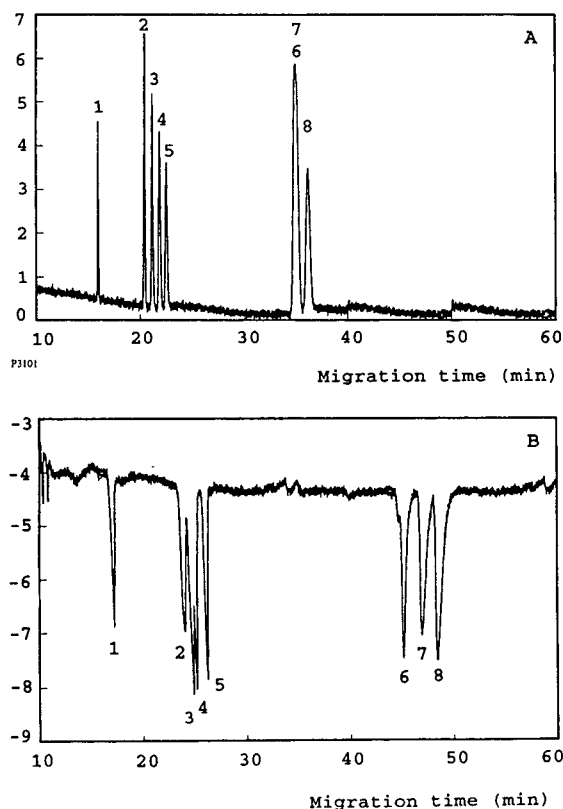
Fig. 1. CE of eight heparin disaccharides using direct (A) or indirect (B) UV detection. In case of direct UV detection the electrophoresis buffer was 200 mM Na$_2$HPO$_4$, pH 2.5 and the injection volume was 9 nl from a solution containing approximately 0.16 mg/ml of each disaccharide. The potential across the capillary was 7.5 kV (131.5 V/cm) and the thermostatted capillary was kept at 40°C. In case of indirect UV detection the electrophoresis buffer was 5 mM 1,2,4-tricarboxybenzoic acid, pH 3.5 and the injection volume was 1.8 nl from the same solution as in A, except that the concentration was approximately 0.1 mg/ml of each disaccharide. The potential across the capillary was 5 kV (87.7 V/cm) and the thermostatted capillary was kept at 25°C. The structures of disaccharides 1–8 are given in Table 1.

charges, are baseline separated which is not the case under the conditions used for direct detection. Unfortunately, the concentrations of the various disaccharides in the mixture were not exactly known, hampering a quantitative interpretation of the results.

The practical value of CE in combination with indirect UV detection for the determination of the purity of "real world" pentasaccharide prep-

arations was demonstrated by the analysis of several synthetic pentasaccharide preparations.

In Fig. 2 the CE electropherograms obtained for Org 31540, batch E using direct (A) and indirect (B) UV detection are depicted. The synthetic pentasaccharide Org 31540 (structure in Table 2) corresponds to the unique natural pentasaccharide sequence that confers the anti-coagulant activity to heparin. Prior to CE, the organic purity of Org 31540-E was established by
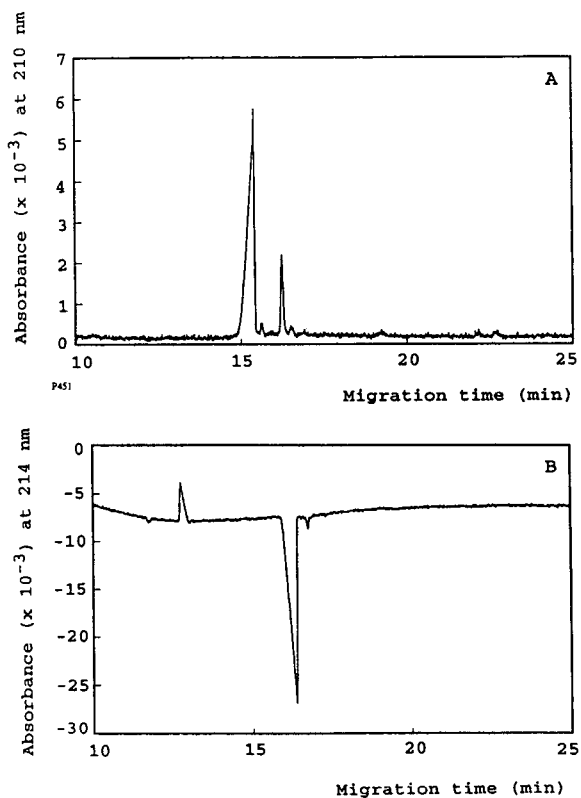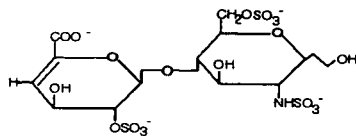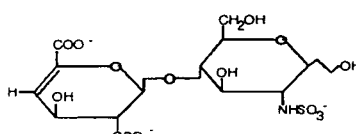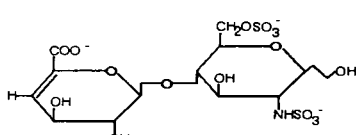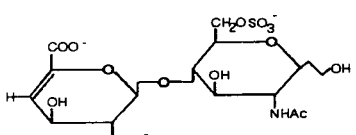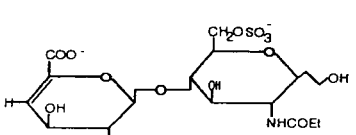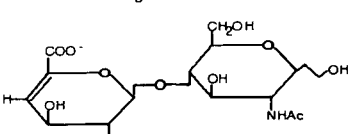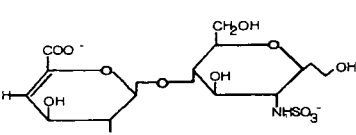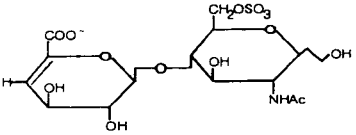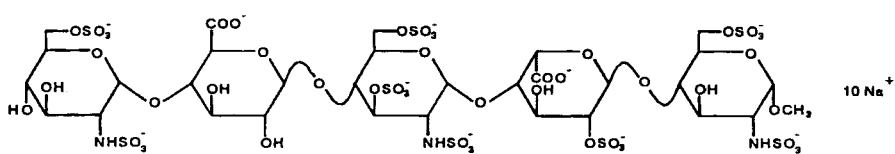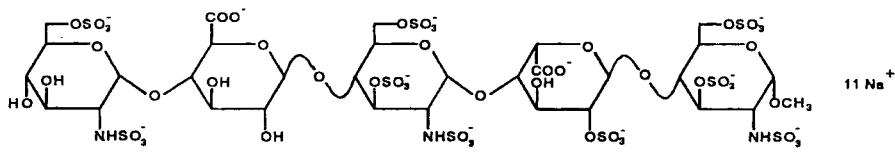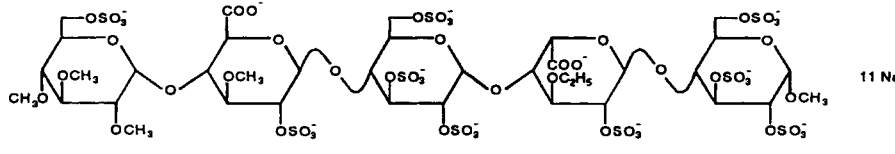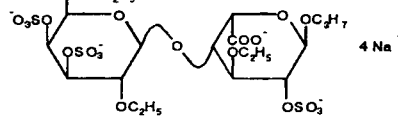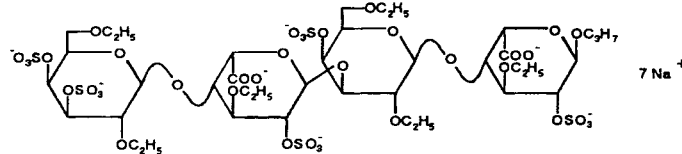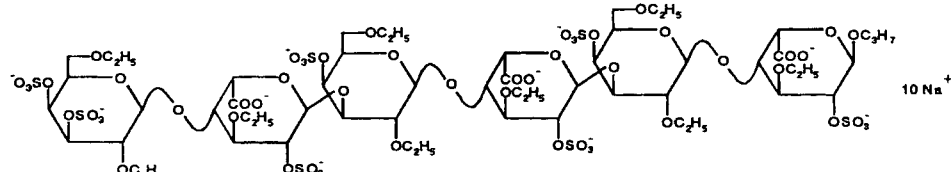

Fig. 2. Analysis of pentasaccharide preparation Org 31540-E by CE using direct (A) and indirect (B) UV detection. Direct UV detection was carried out using 200 mM Na$_2$HPO$_4$, pH 3.0 as electrophoresis buffer. The potential across the capillary (57 cm × 75 μm) was 7.5 kV (131.5 V/cm) and the thermostatted capillary was kept at 40°C. Indirect UV detection was performed applying 5 mM 5-sulphosalicylic acid, pH 3.0 as electrophoresis buffer. The potential across the capillary (57 cm × 50 μm) was 5 kV (87.7 V/cm) and the thermostatted capillary was kept at 25°C. Concentration of Org 31540 in the sample solution is 1 mg/ml, injection volume 50 nl (A) or 1.8 nl (B). The structure of Org 31540 is outlined in Table 2.

Table 1
Structures of eight heparin disaccharide reference compounds and their migration times in CE using direct or indirect UV detection

Disaccharide	Structure	Charge	Migration time (min)	
			Direct UV detection	Indirect UV detection
(1) δUA2S → GlcNS6S		4⁻	16.1	17.3
(2) δUA2S → GlcNS		3⁻	20.4	24.1
(3) δUA1 → GlcNS6S		3⁻	21.2	24.9
(4) δUA2S → GlcNAc6S		3⁻	21.8	25.2
(5) δUA2S → GlcNCOEt6S		3⁻	22.5	26.3
(6) δUA2S → GlcNAc		2⁻	34.9	45.2
(7) δUA → GlcNS		2⁻	34.9	46.9
(8) δUA → GlcNAc6S		2⁻	35.9	48.4

Electropherograms and electrophoresis conditions are reported in Fig. 1.

Table 2
Structures of Org 31540, 31550, 33232, 34275, 34276 and 34277

GAG	Structure
Org 31540	
Org 31550	
Org 33232	
Org 34277	
Org 34276	
Org 34275	

Org 33271 and Org 33263 are close derivatives of Org 33232 having twelve and eleven negative charges, respectively.

NMR spectroscopy to be 98% (mol/mol). CE in combination with direct UV detection gives rise to a major peak at 15.4 min (79% of total peak area) representing Org 31540 and three minor peaks at 15.6, 16.2 and 16.5 min stemming from contaminants. In the indirect detection mode the main peak stemming from Org 31540 migrates at 16.6 min and forms 98% of the total peak area which exactly agrees with the NMR data. The peak belonging to the main contaminant is observed at 16.9 min and accounts for 1.8% of the total peak area. This peak probably corresponds to the peak at 15.6 min in the direct detection mode. Remarkably, the contaminant that yields a major signal at 16.2 min in the direct detection mode is not observed in the

indirect detection mode, implying that it represents less than 0.5% (w/w) relative to Org 31540-E (see below). It should be noted that, apart from yielding representative peak areas enabling quantitative analysis, the sensitivity of indirect UV detection is by far superior to that of direct detection. In the latter experiment 28 pmol (50 ng) and 1 pmol (1.8 ng) of Org 31540 were injected in case of direct and indirect UV detection, respectively, yielding still a better signal-to-noise ratio for the indirect detection mode.

A second example of the practical value of CE in combination with indirect UV detection for the determination of the purity of "real world" pentasaccharide preparations is furnished by the analysis of HH2174. Sample HH2174 represents a batch of raw material of Org 31550 (structure in Table 2) that was deliberately kept from further purification. Org 31550 is a derivative of the unique natural pentasaccharide sequence responsible for the anticoagulant activity of heparin. Relative to the natural sequence, Org 31550 contains one extra 3-O-sulphate group in the first glucosamine-N,6-disulphate residue (denoted number 6 in [22]) and it was synthesized by Organon in collaboration with Sanofi via a multistep procedure. As reported earlier [3], NMR spectroscopic analysis proves that HH2174 consists for approximately 85% (mol/mol) of Org 31550. When HH2174 is subjected to CE using direct UV detection at least nine peaks are discernable in the electropherogram (Fig. 3A). From injection of pure Org 31550 it is known that the peak at 14.7 min can be attributed to Org 31550. The additional peaks, accounting for 75% of the total peak area, belong to minor contaminants. This clearly demonstrates the limitations of direct UV detection for the quantitative analysis of these type of preparations by CE. The contaminants most probably represent synthetic precursors of Org 31550 that contain strong UV absorbing groups, which is the main reason for the overestimation of the amounts present. In contrast, when HH2174 is analyzed by CE applying the indirect detection mode a pattern is obtained displaying proportionality between peak areas and the amount of the components present (Fig. 3B). The main peak at
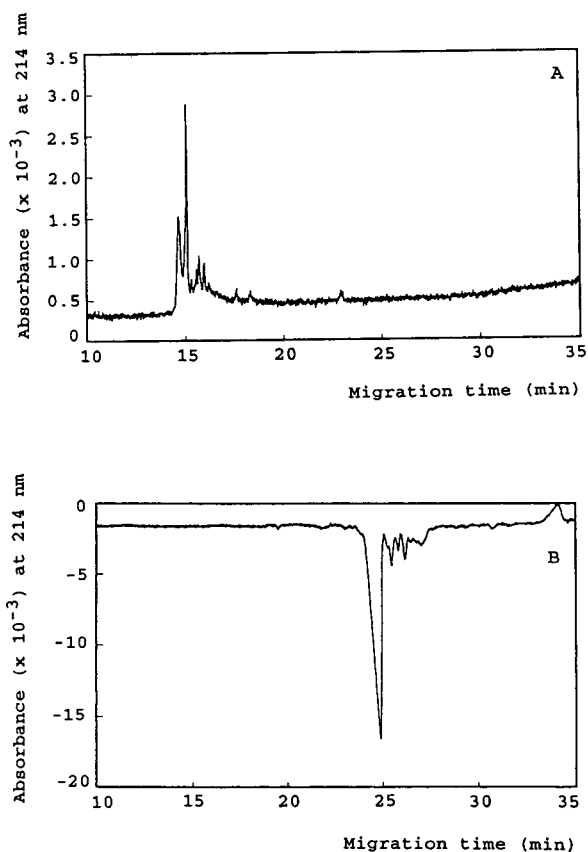

Fig. 3. Analysis of pentasaccharide preparation HH2174 by CE using direct (A) and indirect (B) UV detection. The electrophoresis conditions for direct and indirect UV detection are reported in Fig. 2, except that for indirect detection the pH of the electrophoresis buffer is 2.5. HH2174 represents a sample of Org 31550 (structure indicated in Table 2) that was deliberately kept from purification. The concentration of the pentasaccharide in the sample solution is 1 mg/ml, injection volume 50 nl (A) or 1.8 nl (B).

24.9 min corresponds with Org 31550 and constitutes 86% of the total peak area, which corresponds with the NMR data. Four minor peaks and three barely discernable peaks, all belonging to contaminants, are visible and account for 14% of the total peak area. Like in the previous example, the contaminant that gives rise to a major peak in the direct detection mode yields only a minor signal in the indirect detection mode. Note that in the latter experiment the pH of the electrophoresis buffer was 2.5 which

explains why the migration times obtained for the analytes in the indirect mode are higher than those obtained using the direct mode.

A final example of the applicability of CE–indirect UV detection for the determination of the purity of a glycosaminoglycan preparation for pharmaceutical use is presented by the analysis of Org 33263. Org 33263 is a derivative of Org 31550 in which the free hydroxyl functions have been methylated and the N-sulphate groups have been replaced by O-sulphate groups (structure of Org 31550 in Table 2). As is clear from Fig. 4 also these type of compounds are amenable to analysis by CE. Using indirect UV detection this preparation yields a major peak at 23.9 min, accounting for 95% of the total peak area which is corroborated by the NMR data.

The applicability of indirect UV absorption as a *quantitative* detection method for CE was further investigated by using known amounts of a highly purified batch of the synthetic pentasaccharide Org 31550 [> 99.5% (mol/mol) pure by NMR spectroscopy, water content 8.7% ± 0.55% (S.E.M., $n = 3$) by Karl Fischer, chloride content 0.5% (w/w) and (free) sulphate content 0% (w/w) by isotachophoresis]. This compound was used in a series of validation experiments addressing the linearity and sensitivity of indirect UV detection and the overall repeatability of the
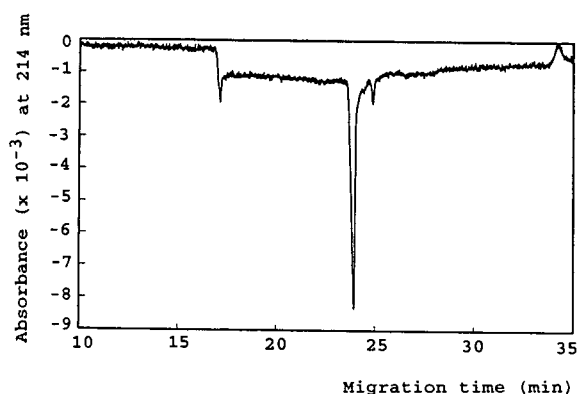

Fig. 4. Analysis of pentasaccharide preparation Org 33263 by CE–indirect UV detection. Electrophoresis conditions as in Fig. 2B, except that the pH of the electrophoresis buffer is 2.5. The concentration of Org 33263 in the sample solution is 1 mg/ml, injection volume 1.8 nl.

method. Also the influence of the presence of sodium chloride, sodium sulphate and sodium phosphate in the electrophoresis buffer on the performance of the method and the effect of the migration time and the type of analyte on the detector response were examined.

As a first step in the validation procedure, the repeatability of the method was investigated by six successive injections of 1 pmol Org 31550, employing the standard conditions as described in the Experimental section. It turns out that the method shows excellent repeatability as the average migration time of Org 31550 is 17.9 min ± 0.03 (S.E.M., $n = 6$), whereas the average integrated peak area is 17.4 ± 0.43 (S.E.M., $n = 6$) The day-to-day reproducibility of the migration time is somewhat less favourable. The average migration time found for Org 31550, analyzed on ten different days in a time interval of four weeks, keeping all analysis conditions as much as possible identical, is 17.0 ± 0.81 (S.E.M., $n = 10$), whereas the average peak area is 15.6 ± 2.44 (S.E.M., $n = 10$).

For determination of the limit of detection (LOD), limit of quantitation (LOQ) and linearity, the stock solution of Org 31550 (1 mg/ml, 546 nmol/ml) was diluted with Milli-Q water to 75, 50, 25, 2.5, 1 and 0.5% (v/v). In addition, more concentrated solutions, containing 1.25, 1.50 and 2.00 mg/ml of Org 31550, were prepared (corresponding to 125, 150 and 200% of the stock solution). From each solution 1.8 nl were injected and analyzed applying the standard conditions. The obtained peak areas (electropherograms not shown) are compiled in Table 3. Injection of 5 fmol Org 31550 (1.8 nl from the 0.5% solution) still gives a signal-to-noise ratio of 3. This means that the LOD for synthetic pentasaccharides is about 5 fmol. In Fig. 5 the peak areas vs. the injected amounts are plotted. Taking into account all data points, except that for the highest injected amount (1960 fmol), a regression line $y = 0.015x + 0.487$ and a correlation coefficient $R = 0.996$ is obtained. When all data points are taken into account, the regression line is $y = 0.018x - 0.581$ with $R = 0.981$. It should be mentioned however, that the data points found for the three lowest concentrations

Table 3
LOD, LOQ and linearity of CE–indirect UV detection

Stock solution (%)	Injected amount		Peak area	
	pg	fmol	area	area%
200	3600	1960	39.43	265
150	2700	1480	21.42	144
125	2250	1230	19.93	134
100	1800	980	14.86	100
75	1350	740	12.00	81
50	900	490	8.63	58
25	450	245	4.90	33
2.5	45	25	0.33	2.2
1.0	18	10	0.26	1.7
0.5	9	5	0.07	0.5

Four stock solutions containing 1.00 (100%), 1.25 (125%), 1.50 (150%) and 2.00 (200%) mg Org 31550 per ml Milli-Q water were prepared. The 100% solution was diluted to the concentrations indicated in the table. From each solution 1.8 nl were analyzed by CE–indirect UV detection applying the standard conditions as indicated in Fig. 2B. The injected amount of Org 31550 is given in pg and fmol. The resulting peak areas are in arbitrary units (area) and are expressed relative to the peak area obtained for injection from the 100% solution (area%).

(injected amounts 5, 10 and 25 fmol pentasaccharide) are close together and might be less reproducible. Taken together, it can be stated that the LOQ is better than 25 fmol pentasaccharide and that the method is linear at least from 25 to 1480 fmol injected pentasaccharide. Consequently, for accurate quantitative analysis, the concentration of the pentasaccharide(s) in the sample solution should be between 0.025 and
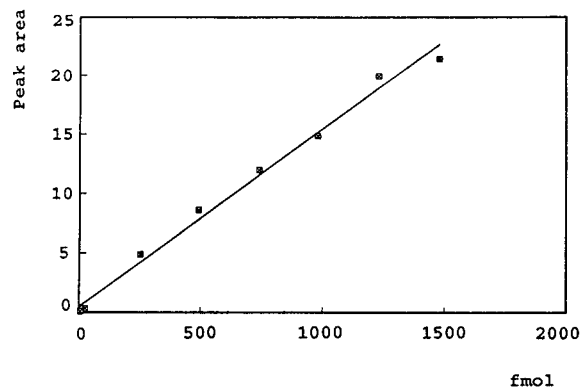

Fig. 5. Peak areas vs. injected amounts, obtained for various amounts of Org 31550 by CE–indirect UV detection. Peak areas are given in arbitrary units. Experimental details in Table 3.

1.50 mg/ml. More concentrated solutions may be diluted prior to analysis, whereas sample solutions containing less than 0.25 mg pentasaccharide per ml should be concentrated or, alternatively, the injection volume is to be increased. Furthermore, it can be deduced from the above data that for quantitative analysis of pentasaccharides in a multicomponent mixture, e.g. main component plus contaminants, the ratio between the compounds should preferably be about 1:60 (w/w) or smaller. This means that the LOQ for contaminants is about 1.7% (w/w) relative to the main component. This issue is more accurately addressed in the experiment described below.

For determination of the accuracy of the method, Org 31540 was spiked with decreasing amounts of Org 31550. Prior to CE, the purity and the residual water content of Org 31540 were established to be >98% (mol/mol) by 1H NMR spectroscopy and 19.2% (w/w) ± 0.28 (S.E.M., $n = 3$) by Karl Fischer titration, respectively. Ten mixtures of Org 31550 and Org 31540 were prepared, the total concentration of all mixtures being 1 mg pentasaccharide per ml (defined as 100%, Table 4). Analysis of a mixture containing 50% Org 31540 and 50% Org 31550 (i.e., both compounds 0.5 mg/ml) yields

Table 4
Accuracy of CE–indirect UV detection

Org 31540			Org 31550		
% Org 31540	Peak area	Area%	% Org 31550	Peak area	Area%
0	0	0	100	16.83	100
50	8.85	51.1	50	8.49	48.9
60	11.45	60.3	40	7.53	39.7
80	15.10	79.9	20	3.81	20.1
90	16.89	88.6	10	2.17	11.4
95	22.14	93.9	5	1.43	6.1
96	18.03	95.9	4	0.77	4.1
97	20.73	96.0	3	0.86	4.0
98	16.80	99.9	2	0.02	0.1
99	16.03	99.8	1	0.03	0.2
99.5	16.03	99.8	0.5	0.03	0.2
100	16.46	100	0	0	0

Ten mixtures of Org 31540 and Org 31550 having an increasing Org 31540/Org 31550 ratio were analyzed by CE–indirect UV detection applying standard conditions. In each mixture the total pentasaccharide concentration (Org 31540 + Org 31550) was 1 mg/ml (defined as 100%). Peak areas were corrected for residual water content (details in text). % Org 31540 = Percentage (w/w) of Org 31540 in the Org 31540/Org 31550 mixture; Peak area = observed peak area (in arbitrary units) in CE–indirect UV analysis; Area% = observed peak area for Org 31540 or Org 31550 in CE–indirect UV analysis of a mixture of both Org compounds. The total peak area obtained for Org 31540 + Org 31550 is taken as 100%.

two baseline-separated peaks at 15.57 and 16.09 min, followed by a minor peak at 16.47 min (Fig. 6). From injection of Org 31550 and Org 31540 separately (not shown), it is known that the signal at 15.57 min stems from Org 31550, whereas the signals at 16.09 and 16.47 min are derived from Org 31540 and an impurity in Org 31540, respectively. The peak areas found for Org 31540 (impurity not included) and Org 31550 are 8.49 and 7.83, respectively (Table 4). However, since the water contents of Org 31550 and Org 31540 are 8.7 and 19.2%, respectively, a correction factor of 1.13 for the area found for Org 31540 must be applied, determining the corrected peak area of Org 31540 as 8.85. Nine additional mixtures were made, gradually increasing the ratio Org 31540/Org 31550. In fact, in this experiment Org 31550 can be regarded as a contaminant in the Org 31540 preparation. As is clear from Fig. 6 and Table 4, the theoretical and observed ratios are in accordance with each other, indicating on the one hand that, using indirect UV detection, a nearly identical detector response is obtained for Org 31540 and Org

31550, and that on the other hand the presence of a small amount of Org 31550 (e.g., 9 pg or 4.9 fmol) can be detected in the presence of a large excess of Org 31540 (e.g., 1791 pg or 1036 fmol, Table 4). There is, however, a discrepancy between the limit of detection and the limit of quantitation of Org 31550 in the presence of excess Org 31540. Fig. 6 demonstrates that the observed signal for Org 31550 continuously decreases, relative to the signal obtained for Org 31540, as the ratio Org 31540/Org 31550 increases. Therefore, the Org 31550/Org 31540 ratio (w/w) can be assessed in a qualitative way at least up to a ratio of 0.5/99.5, i.e. the limit of detection of Org 31550 in the presence of an excess Org 31540 is about 0.5% (w/w). However, from Table 4 it will be clear that the limit of quantitation for Org 31550 in a mixture with Org 31540 is about 2% (w/w). This difference with the limit of detection is mainly due to the limited accuracy of the integration software, as it is evident from Fig. 6 that the detection signal does reflect the actual ratio. Taken together it can be concluded that CE coupled with indirect
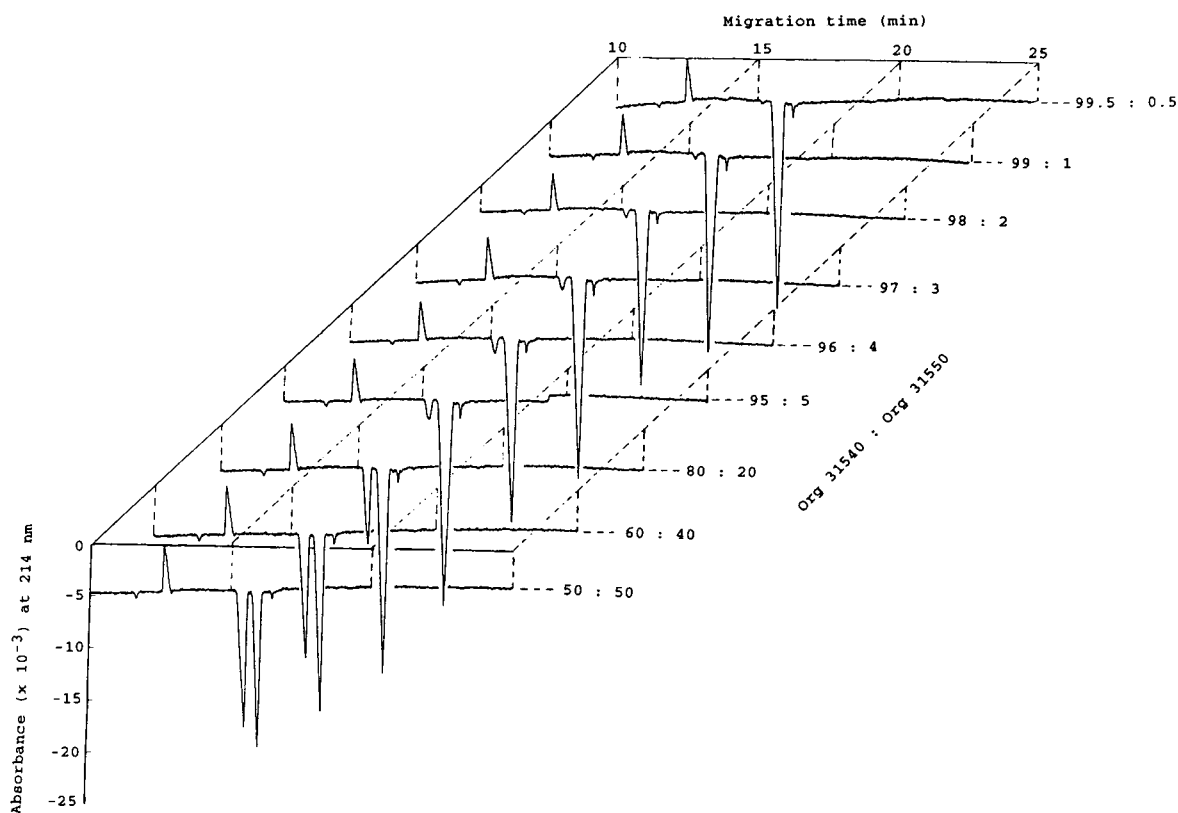
Fig. 6. CE–indirect UV detection of nine mixtures of Org 31540 and Org 31550, containing a decreasing amount of Org 31550. The electropherograms are compiled in a three-dimensional plot. The Org 31540/Org 31550 ratio (w/w) is indicated on the Z-axis. Experimental details in Table 4.

UV detection enables the non-selective detection of different types of pentasaccharides and allows the quantitative detection of small amounts ($>2\%$, w/w) of pentasaccharide contaminants.

The former experiment shows that closely related pentasaccharides yield a (nearly) identical detector response in the indirect detection mode. Moreover, determination of the purity of Org 31540-E and HH2174 (see above) demonstrates that also pentasaccharides which carry additional chromophoric substituents are registered in proportion to their relative (gravimetric) abundance. Notwithstanding these observations, it is of importance to ascertain that equal amounts of GAGs widely differing in molecular mass, charge and migration time are detected with equal sensitivity, since these parameters

could influence the detector response. The influence of the molecular mass and charge of the GAG on the detector response was investigated by CE–indirect UV analysis of equal amounts of Org 31550 and δUA2S$\rightarrow$GlcNS6S (structure in Table 1). The possible influence of the migration time is more appropriately dealt with in a separate experiment (see below). Injection of 1.8 nl from a solution containing 0.5 mg/ml Org 31550 (injected amount 0.9 ng or 0.49 pmol) and 0.5 mg/ml δUA2S$\rightarrow$GlcNS6S (injected amount 0.9 ng or 1.35 pmol) yields two peaks (Fig. 7) at 17.2 min, corresponding to Org 31550 and 20.1 min, corresponding to δUA2S$\rightarrow$GlcNS6S having nearly identical peak areas, namely 12.48 (48.2%) and 13.43 (51.8%), respectively. This convincingly demonstrates that injection of equal
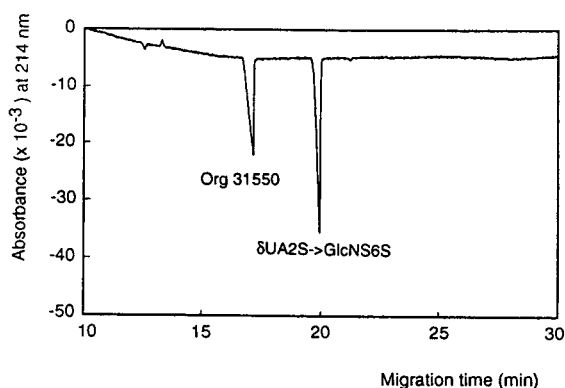
Fig. 7. CE–indirect UV detection of a mixture containing 1 mg/ml of Org 31550 and 1 mg/ml of δUA2S→GlcNS6S. The injection volume is 1.8 nl. Experimental conditions as in Fig. 2B.

Table 5
The influence of migration time on peak area

Voltage	Migration time (min)	Peak area
2.5	35.8 ± 0.10	17.8 ± 0.03
5.0	18.9 ± 0	16.1 ± 0.04
7.5	12.0 ± 0	16.7 ± 0.01
10.0	9.1 ± 0	17.6 ± 0.18
12.5	7.3 ± 0	18.2 ± 0.09

CE–indirect UV detection of Org 31550 using standard conditions, except that the voltage over the capillary was varied. In each case 1 pmol of Org 31550 was injected. Data are the mean value ± S.E.M. of two experiments.

mass amounts of different types of GAGs yield an equal detector response, enabling their quantitative analysis by CE–indirect UV detection. It is of importance to note that the detector response correlates with the gravimetric amount of the saccharide and not with the molar amount.

With respect to the ruggedness of the method two parameters were investigated, namely the possible influence of the migration time on the peak area and the influence of the presence of salts in the sample solution on the overall performance of the method.

As mentioned earlier, indirect UV detection offers a possibility to detect analytes indiscriminative of their chromophoric constituents and molecular structure. However, it cannot be excluded that the sensitivity of detection of an analyte is influenced by its migration time. This was studied by CE analysis of Org 31550 applying different voltages across the capillary. In this way the migration time of a certain analyte species can be varied, keeping the experimental conditions constant (except for the applied voltage). The migration times and peak areas obtained for Org 31550 at 2.5, 5.0, 7.5, 10.0 and 12.5 kV are compiled in Table 5. A shift in migration time from 35.8 min (2.5 kV) to 7.3 min (12.5 kV) gives rise to an increment of the peak area of Org 31550 from 17.8 to 18.2. Apparently, the migration time has little effect

on the detector response. However, when the data obtained at 2.5 kV are neglected the tendency for peak areas to increase as the migration times decrease is more pronounced (Table 5).

Since the synthetic pentasaccharide samples may contain traces of residual salts, it was relevant to test the influence of the presence of salts in the sample solution on the performance of CE–indirect UV detection. The maximal tolerated salt content of pentasaccharide preparations for pharmaceutical use is 10% (w/w). Typically, injections are made from a sample solution containing 1 mg pentasaccharide per ml, and consequently the salt concentration should be below 0.1 mg salt per ml. In Fig. 8 the electropherogram obtained for a mixture containing 1 mg Org 31550 per ml and 0.1 mg NaCl per ml is shown. Clearly, the presence of NaCl is detected by the chloride peak at 12.81 min. The minor peak, migrating at 13.35 min, belongs to sulphate ions (see below). Apparently, the NaCl used in this experiment was contaminated with Na_2SO_4. It is of note that in an earlier study applying direct UV detection [3] the presence of up to 1 M NaCl is not noticed. Similarly, the presence of 0.1 mg Na_2SO_4 or 0.1 mg NaH_2PO_4 per ml sample solution gives rise to peaks migrating at 13.72 and 33.52 min, respectively (Fig. 8). For Na_2SO_4 an additional peak at 12.48 min is noticed probably belonging to traces of NaCl that are present in the Na_2SO_4 used. These observations demonstrate that the presence of salts may compromise the interpretation of the electropherogram. Therefore it seems advisable,
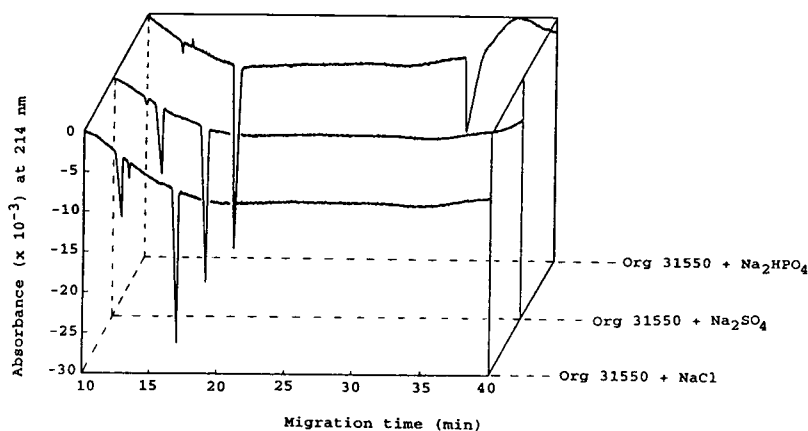
Fig. 8. Influence of the presence of NaCl, Na_2SO_4 or Na_3PO_4 in the sample solution (each at a concentration of 0.1 mg/ml) on CE–indirect UV detection of Org 31550. Experimental conditions as in Fig. 2B. The concentration of Org 31550 in the sample solution is 1 mg/ml.

especially in case of ambiguities in the interpretation of the electropherogram, to desalt the pentasaccharide sample prior to analysis by CE–indirect UV detection.

Finally, to establish the scope of the method, additional types of GAGs, comprising alkylated and O-sulphated synthetic pentasaccharides, synthetic dermatan sulphate di-, tetra- and hexasaccharides and a natural heparin disaccharide (structures indicated in Tables 1 and 2), were analyzed by CE–indirect UV detection in a single run. Fig. 9 depicts the electropherogram obtained for a mixture containing approximately 1 mg/ml of each of the mentioned GAGs, using standard conditions. The identity of the peaks was determined by injection of the pure compounds (results not shown). Evidently, all GAGs can be analyzed in a single run which demonstrates the general applicability of CE–indirect UV detection for the analysis of GAG fragments. In Table 6 the charge and migration time of the various GAG fragments are compiled. The O-sulphated, alkylated pentasaccharide Org 33271, possessing 12 negative charges migrates at 18.2 min. The N,O-sulphated pentasaccharides Org 31550 and Org 31540, having 11 and 10 negative charges, respectively, show slightly higher migration times (18.7 and 19.1 min, respectively) in line with their reduced negative charge compared to Org 33271. The relationship

between the molecular mass and charge of carbohydrate molecules and their electrophoretic mobility was recently studied in detail by Chiesa and Horváth [26] using maltooligosaccharides derivatized with 8-aminonaphthalene-1,3,6-tri-
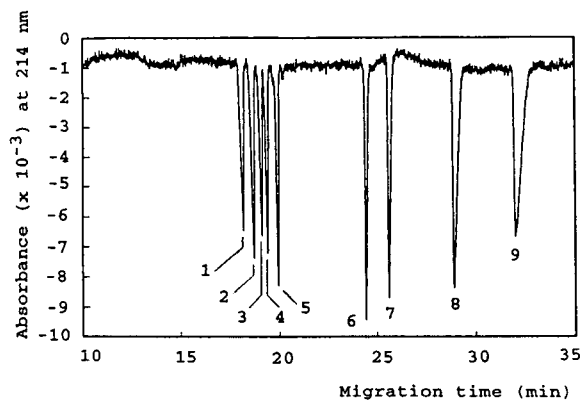

Fig. 9. CE–indirect UV detection of a mixture of various glycosaminoglycans, comprising different synthetic pentasaccharides (1 = Org 31550; 2 = Org 31540; 3 = Org 33271; 4 = Org 33263; 5 = Org 33232), synthetic dermatan sulphate hexa-, tetra- and disaccharides (6 = Org 34275; 7 = Org 34276; 8 = Org 34277, respectively) and a natural heparin disaccharide (9 = δ UA2S → GlcNAc6S). The concentration of each GAG in the mixture is approximately 1 mg/ml and the injection volume is 1.8 nl. The structures of the GAGs are compiled in Table 2. Org 33271 and Org 33263 are close derivatives of Org 33232 having twelve and eleven negative charges, respectively. Electrophoresis conditions as in Fig. 2B.

Table 6
Migration time of GAGs in CE–indirect UV detection

GAG	Type	Charge	Migration time (min)
Org 33271 (1)	Synthetic pentasaccharide	12	18.2
Org 31550 (2)	Synthetic pentasaccharide	11	18.7
Org 31540 (3)	Synthetic pentasaccharide	10	19.1
Org 33263 (4)	Synthetic pentasaccharide	11	19.4
Org 33232 (5)	Synthetic pentasaccharide	11	19.9
Org 34275 (6)	Dermatan sulphate hexasaccharide	10	24.4
Org 34276 (7)	Dermatan sulphate tetrasaccharide	7	25.6
Org 34277 (8)	Dermatan sulphate disaccharide	3	28.9
δUA2S $\rightarrow$ GlcNAc6S (9)	Heparin disaccharide	3	32.0

Experimental details in Fig 9. Org 33271, Org 33263 and Org 33232 differ from Org 31550 and Org 31540 in that they contain exclusively O-sulphated groups and methylated hydroxyl functions, whereas Org 31550 and Org 31540 possess N- and/or O-sulphated and free hydroxyl functions. The numbers in brackets refer to the peaks in Fig. 9.

sulphonic acid as model compounds. In the latter study it was shown that the electrophoretic mobility can be expressed as $\mu_{ep} = CqM_r^{-2/3}$ where μ_{ep} represents the electrophoretic mobility, C is a constant, q is the electrical charge of the analyte and M_r is the molecular mass of the analyte. Although the results presented in this study are in line with the relationship set forth by Chiesa and Horváth, for a correct interpretation of the results it should be noted that also the charge distribution of the analyte may influence the migration time [3]. The alkylated pentasaccharides Org 33263 and Org 33232, both having 11 negative charges, migrate at 19.4 and 19.9 min, respectively. The fact that the latter two compounds have higher migration times than Org 31540, in spite of containing one extra negative charge, must be ascribed to their higher molecular mass (Org 31540: 1727; Org 33263: 1917; Org 33232: 1917) and/or differences in charge distribution. Since Org 33263 and Org 33232 have an identical molecular mass and charge, the difference in migration time must be ascribed to the unequal charge distribution. The dermatan sulphate hexasaccharide, bearing ten negative charges, migrates at 24.4 min. The higher migration time of the dermatan sulphate hexasaccharide compared to the heparin pentasaccharides can be ascribed to its reduced charge and/or higher molecular mass (2108) The dermatan sulphate tetra- and disaccharides, posses-

sing 7 and 3 negative charges, respectively, migrate at 25.6 and 28.9 min, respectively. Finally, the heparin disaccharide δUA2S $\rightarrow$ GlcNAc6S, having 3 negative charges, migrates at 32.0 min.

In summary, we conclude that CE in combination with indirect UV detection enables a reliable qualitative and quantitative analysis of the purity of sub-picomole levels of low-molecular-mass heparin preparations by CE.

Acknowledgements

References

[1] S.L. Carney and D.J. Osborne, Anal. Biochem., 195 (1991) 132.
[2] A. Al-Hakim and R.J. Linhardt, Anal. Biochem., 195 (1991) 68.
[3] J.B.L. Damm, G.T. Overklift, B.W.M. Vermeulen, C.F.

Fluitsma and G.W.K. van Dedem, *J. Chromatogr.*, 608 (1992) 297.

[4] X.H. Huang, J.A. Luckey, M.J. Gordon and R.N. Zare, *Anal. Chem.*, 61 (1989) 766.

[5] T.M. Olefirowicz and A.G. Ewing, *J. Chromatogr.*, 499 (1990) 713.

[6] L.A. Colón, R. Dadoo and R.N. Zare, *Anal. Chem.*, 65 (1993) 476.

[7] T.J. O'Shea, S.M. Lunte and W.R. LaCourse, *Anal. Chem.*, 65 (1993) 948.

[8] A.E. Bruno, B. Krattiger, F. Maystre and H.M. Widmer, *Anal. Chem.*, 63 (1991) 2689.

[9] M.A. Moseley, L.J. Deterding, K.B. Tomer and J.W. Jorgenson, *Rapid Commun. Mass Spectrom.*, 3 (1989) 87.

[10] R.M. Caprioli, W.T. Moore, M. Martin, B.B. de Gue, K. Wilson and S. Moring, *J. Chromatogr.*, 480 (1989) 233.

[11] R.D. Smith, J.A. Olivares, N.T. Nguyen and H.R. Udseth, *Anal. Chem.*, 60 (1988) 436.

[12] R.W. Hallen, C.B. Shumate, W.F. Siems, T. Tsuda and H.H. Hill, Jr., *J. Chromatogr.*, 480 (1989) 233.

[13] C.Y. Chen and D. Morris, *J. Chromatogr.*, 540 (1991) 355.

[14] T.W. Garner and E.S. Yeung, *J. Chromatogr.*, 515 (1990) 639.

[15] S. Hjertén, K. Elenbring, F. Kilar, J.L. Liao, A.J.C. Chen, C.J. Siebert and M.D. Zhu, *J. Chromatogr.*, 403 (1987) 47.

[16] P. Jandik and W.R. Jones, *J. Chromatogr.*, 546 (1991) 431.

[17] F. Foret, S. Fanali, L. Ossicini and P. Boček, *J. Chromatogr.*, 470 (1989) 299.

[18] A.E. Vorndran, P.J. Oefner, H. Scherz and G.K. Bonn, *Chromatographia*, 33 (1992) 163.

[19] T. Wang and R.A. Hartwick, *J. Chromatogr.*, 589 (1992) 307.

[20] C.A.A. van Boeckel, T. Beetz, J.N. Vos, A.J.M. de Jong, S.F. van Aelst, R.H. van den Bosch, J.M.R. Mertens and F.A. van der Vlugt, *J. Carbohydr. Chem.*, 4 (1985) 293.

[21] M. Petitou, P. Duchaussoy, I. Lederman and J. Choay, *Carbohydr. Res.*, 167 (1987) 67.

[22] C.A.A. van Boeckel, T. Beetz and S.F. van Aelst, *Tetrahedron Lett.*, 29 (1988) 803.

[23] P.L. Jacobs, G.J.H. Schmeits, M.P. de Vries, A.P. Bruins and P.S.L. Janssen, presented at the *12th International Mass Spectrometry Conference, Amsterdam, 1991*.

[24] K. Fischer, *Angew. Chem.*, 48 (1935) 394.

[25] P.S.L. Janssen and J.W. van Nispen, *J. Chromatogr.*, 287 (1984) 166.

[26] C. Chiesa and Cs. Horváth, *J. Chromatogr.*, 645 (1993) 337.

Controlling electroosmotic flow in capillary zone electrophoresis

Nava Cohen, Eli Grushka*

Department of Inorganic and Analytical Chemistry, The Hebrew University, Jerusalem, Israel

Abstract

Electroosmotic flow in capillary zone electrophoresis must be controlled for precise and reproducible performance. We found that the addition of any one of several classes of compounds such as amines, amino acids or organic acids to the running buffer stabilizes electroosmotic flow. With the additives in the buffer, the precision of migration times improved to better than 1%. The reproducibilities improved to better than 5%. The system is very stable at various conditions for small molecules and for proteins at very acidic or very basic conditions.

1. Introduction

Capillary electrophoresis (CE) is an analytical separation technique capable of high resolution because of its inherent high efficiency. Unlike in chromatography, the resolution in CE should improve continuously as the migration times decrease (or as the applied voltage is increased). This potential of high efficiencies, high resolutions and short analysis times in CE have attracted the attention of researchers in various fields, and the use of CE is growing exponentially.

To be an acceptable analytical technique, the precision of migration times and peak areas need to be high. If we take chromatographic figures-of-merit as a rough guideline, then the precision of the data should be about 1% and the reproducibility less than 5% [1]. Frequently, CE done in open and untreated capillaries shows much poorer precisions and reproducibilities (viz. [2,3]). One of the reasons for the poorer precision is the difficulty of maintaining constant electroosmotic flow (EOF), which occurs when an external electric field is imposed across a capillary whose inner wall is charged [4]. In such cases, solutes migrate through the capillary as a result of electrophoresis and electroosmosis. The apparent reason for the lack in precision may be due to variations in the capillary silica surface, occurring during and between electrophoretic separations, which cause variation in the EOF.

There are many literature reports on the lack of precision in CE (e.g., [5–11]). There is also a great deal of work attempting to improve the precision of CE, mainly by manipulating EOF; for example, by the use of surface-active additives (e.g. [12–14]), of ions and zwitterions (e.g. [15]), of polymers (e.g. [16]) and of organic modifiers (e.g. [17–20]). Other attempts using pH (e.g. [18]) and chemical derivatization of the capillary wall (e.g. [21–24]) have been reported.

---

* Corresponding author.

External electric field has been used also to control EOF (e.g. [25–27]).

In spite of all the efforts mentioned above, there is still a need for a simple and a reliable way to control and maintain a constant EOF. In the present communication we report on the use of several classes of compounds which allow us to control EOF better, and thus to give stable CE systems with excellent precision in migration times without the need for capillary rinsing between injections. The rationale for the choice of the additives will be discussed.

We should stress here that the aim of the present work was to control EOF, and therefore to improve the precision of the data, and not to optimize the efficiencies of the separations. The solutes in this study were not chosen with an application in mind but rather due to convenience and availability. Thus, the results are reported mainly in terms of consistency in migration times and in efficiency and not in terms of efficiency improvement.

2. Material and methods

2.1. Apparatus

Separations were performed on a laboratory-made CE unit. A high-voltage power supply (Glassman, NJ, USA) was used to establish the electrical field across the capillary. The output voltage of the power supply was computer-controlled. Separations were done in polyimide-coated fused-silica capillaries (Polymicro Technologies, CA, USA), 50 and 100 μm I.D. and 375 μm O.D. Separation lengths of the capillaries varied from 40 to 44 cm, and the total length of the capillaries varied from 72 to 74 cm. Detection was done with a Model 200 UVIS absorbance detector (Linear Instruments, CA, USA) at 280 or 200 nm for proteins. About a 1-cm section of the capillary coating was removed by heat and it served as a UV detection window. The signals from the detector were fed to a Model 600 recorder (W + W Electronic, Switzerland) and to a Model D-2000 Hitachi integrator (Merck, Germany).

2.2. Reagents

Buffers

The running buffers were made from either NaH_2PO_4 (Baker, USA), Na_2HPO_4 (Mallinckrodt, USA), KH_2PO_4, CH_3COONa (Merck) or Tris (Serva, Germany). Final pH was adjusted with a 1 M solution of either NaOH, H_3PO_4, CH_3COOH or HCl (Frutarom, Israel). Most of the experiments were done using a 0.02 M NaH_2PO_4 buffer at pH 6.00 adjusted with 1 M NaOH.

Additives

Three classes of additives were studied. The first additive class, which were amines, included 0.01 M solutions of the following compounds: triethylamine (TEA), triethanolamine (Fluka, Switzerland), propylamine, n-pentylamine, piperidine (Sigma, MO, USA), dipropylamine, dipentylamine, tripropylamine, morpholine and histamine (Aldrich, WI, USA). The second class of additives included 0.001 M solutions of the following amino acids: alanine, arginine, asparagine, aspartic acid, cystine, glutamic acid, glycine, histidine, isoleucine, leucine, lysine, methionine, proline, serine, threonine and valine (Takara Hohsan, Japan). The aromatic amino acids (phenylalanine, tryptophan and tyrosine) were not used because of solubility and detection problems. The third class of additives, which were acids, included 0.01 M trimethylacetic acid (TMA) (Fluka) and 0.001 M imidazole-4-acetic acid (Sigma).

Solutes

Phenol (Mallinckrodt) or acetone (Frutartom) was used as a neutral marker for measuring EOF. Other solutes included the amino acid tyrosine (Sigma) and the proteins lysozyme, myoglobin and trypsinogen (Sigma). The solutes were dissolved (1 mg/ml) in the running buffer.

2.3. CE procedures

The introduction of each new additive was followed by 3 h of conditioning as described below. In addition, the capillary was conditioned

at 25 kV for 1 h at the beginning of each working day. Injection of the sample into the capillary was made by electromigration at 5 kV for a fixed period of time (1–5 s). Electrophoresis was usually run at 25 kV applied voltage. The current through the capillary did not exceed 50 μA.

2.4. Capillary treatment

Each new capillary was cleaned by flushing, sequentially, with 1 *M* KOH (Frutarom) for 15 min, then with triply distilled water for 30 min and, finally, with the running buffer containing an additive for few seconds. The capillary was conditioned for 3 h, at 25 kV, to allow equilibration of additive interactions with the capillary wall. Similar procedure was employed whenever a new additive was used. *This treatment eliminates the need for capillary washing between runs.*

3. Results and discussion

It is an experimental fact that most conventional electrophoresis buffers do not yield constant EOF. The exact causes for the variation in EOF are not known with certainty, but they are thought to be related to continuous modification of the wall surface resulting from interactions with buffer components and with solutes. Simple attempts to maintain an homogeneous surface, such as rinsing the capillary with bases, acids, triply distilled water etc. are not helpful in stabilizing EOF. Fig. 1 is a plot of migration time of the EOF marker (phenol) for sequential injections. The figure shows that the migration times decrease continuously with successive injections. This decrease was observed with every buffer studied here. The initial decrease is quite large, but is less pronounced with time; however, even after 8 working hours there is still a decrease in the migration time. The general trend is quite clear and there is very little deviation from that trend.

We control EOF, and therefore migration times, by the use of additives. Three classes of compounds, amines, amino acids and acids were investigated by us as additives. The reasons for
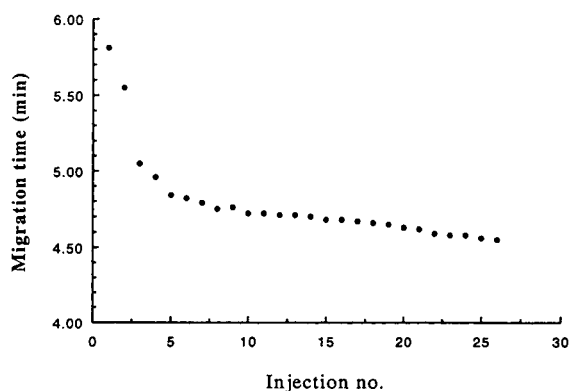
Fig. 1. Migration times of phenol as a function of injection number. No additive in buffer which was 0.02 *M* NaH$_2$PO$_4$ pH 6. Applied voltage was 25 kV.

choosing these classes of compounds are: from HPLC we know that amines interact with silanol groups, thus masking them from the solutes. Since the amines are positive at the pH used here, they should be electrostatically attracted to the capillary wall. Thus, the amines should shield the wall from impurities in the buffer that otherwise might be adsorbed onto it. The adsorption of impurities will change the nature of the double layer on the wall and therefore change EOF.

The choice of amino acids was made to negate the effects that simple amines have on the current density in the capillary. Since amino acids are zwitterions, their contribution to the conductivity of the buffer is smaller than that of amines. Yet, amino acids have an amine group which should interact with the wall surface.

Finally, since amino acids have also an acidic group, we decided to investigate the behavior of acids.

3.1. Additive type: amines

A common practice in HPLC is the addition of amines to the mobile phase to diminish, or even eliminate, the adsorption of basic solutes to the bare silica gel via silanol interactions. The accepted mechanism of the amine action is by competitive interaction with the free silanols on the silica gel. Since the capillary wall in CE also
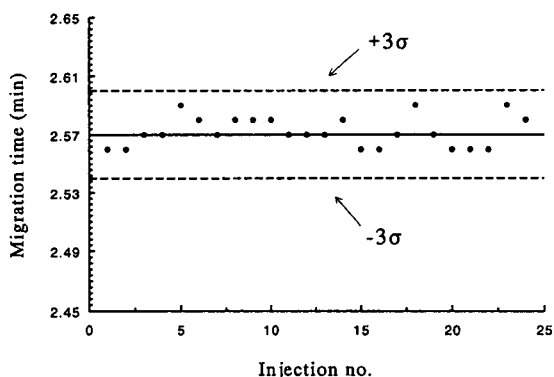
Fig. 2. Migration times of phenol as a function of injection number. 0.001 M TEA additive in buffer which was 0.02 M NaH$_2$PO$_4$ pH 6. Applied voltage was 25 kV.

possesses free silanols, which are responsible for the charge of the surface and, hence, for EOF, it was decided to add an amine to the running buffer to stabilize the wall charge. Fig. 2 shows, in a control chart fashion, the behavior of successive migration times when 0.001 M TEA was added to the buffer. Beside the fact that the migration time is shorter when TEA is present, the figure shows that t_R is constant with a coefficient of variation of about 0.4%. The solid line in Fig. 2 is the average for all the runs. The dashed lines are the $\pm 3\sigma$ lines. The variations in the migration time does not seem to have any trend, i.e. the fluctuations shown are random. The difference in t_R when TEA is present is, most likely, due to the fact that in the TEA study the capillary was not fan-cooled while the

data in Fig. 1 were obtained with temperature control.

Table 1 summarizes the results as a function of applied voltage and of TEA concentration. The data in the table show that the precision in migration time is excellent with relative standard deviations less than 1% in all cases. This precision is sufficient to recommend CE as an analytical tool for routine applications. In addition, the data in the table show that, for a given applied voltage, there is a slight increase in the migration time with an increase in TEA concentration. The increase in migration time might be explained by the increase in ionic strength of the buffer caused by the increasing amine concentration. Similar dependence of EOF on ionic strength was reported by several workers (e.g. [12,17]).

Similar results were obtained with all the amines that were examined here. Table 2 summarizes the results concerning the migration data. The presence of an amine in the buffer results in excellent precision in the migration times. The electroosmotic velocity differs from additive to additive. Table 2 shows that while there is no relationship between the migration times and the additives' pK_a values, there is a good correlation with the ratio of the dielectric constant, ε, to the viscosity, η, as anticipated from the Smoluchowski equation [4]. Undoubtedly, variation in the chemical nature of the amines influences their interaction with the capil-

Table 1
Migration times and standard deviations (in parentheses), as a function of applied voltage and concentration of TEA

Applied voltage (kV)	Migration time (min)			
	$2 \cdot 10^{-4}\,M$ TEA	$1 \cdot 10^{-3}\,M$ TEA	0.01 M TEA	0.07 M TEA
5	18.2 (0.05)	19.3 (0.05)	20.6 (0.02)	–
10	8.47 (0.02)	9.20 (0.06)	10.2 (0.03)	–
12.5	6.50 (0.01)	6.43 (0.05)	7.75 (0.03)	7.00 (0.02)
15	5.34 (0.02)	5.70 (0.04)	6.34 (0.02)	6.06 (0.01)
17.5	4.19 (0.01)	4.57 (0.04)	4.77 (0.02)	5.00 (0.01)
20	3.58 (0.02)	3.72 (0.02)	3.90 (0.01)	3.99 (0.01)
25	2.32 (0.02)	2.57 (0.01)	2.74 (0.02)	2.78 (0.02)

Migration times are averages of anywhere between 4 and 20 runs. Solute is phenol; phosphate buffer at pH 6.

Table 2
Migration times of phenol, and their standard deviations as a function of the amine used to control EOF

Amine	pK_a	ε/η	Migration time (min)	Standard deviation
Triethanolamine[a]	7.76	47.4	2.69	0.01
Propylamine	10.74	15.04	3.35	0.007
Dipropylamine	11.00	7.19	3.91	0.006
Tripropylamine	10.66		4.72	0.005
Histamine	9.83		4.74	0.008
Pentylamine	10.75	5.5	4.87	0.008
Trietylamine	10.72	7.49	5.1	0.02
Morpholine	8.3	4.41	5.32	0.01
Dipentylamine	≈11		5.69	0.016
Piperidine	11.12	4.74	6.12	0.01

Applied voltage was 25 kV; amine concentration was 0.01 M except histamine whose concentration was 0.001 M; buffer was 0.02 M NaH$_2$PO$_4$ at pH 6.0. Migration times are averages of anywhere between 4 and 20 runs. Values of dielectric constants ε, and viscosities, η, are mainly at 25°C [28].
[a] Indicates values obtained without fan-cooling of capillary.

lary wall, thus giving different EOF and migration times for each additive. In addition, some of the data were collected on various capillaries which might also cause the observed scatter in the migration data.

Day-to-day reproducibility was also examined and representative results are given in Table 3. Typical values for day-to-day reproducibilities are 5% or less as shown in the table. Similar

Table 3
Day-to-day reproducibility in migration times of phenol with TEA in buffer

Day	Migration time (min)	Standard deviation
1	5.56	0.008
2	5.89	0.006
3	6.17	0.006
4	5.80	0.02
Average	5.86	0.25[a]

Applied voltage was 25 kV; TEA concentration was 0.01 M; 0.02 M NaH$_2$PO$_4$ buffer at pH 6.0.
[a] Standard deviation of the average migration time of the daily migration time averages.

values were obtained for all amines examined irrespective of whether they are primary, secondary or tertiary amines.

3.2. Additive type: amino acids

As mentioned above, a possible disadvantage in the use of amines as buffer additives is the relatively high current which can result from their presence. Consequently, it was decided to examine amino acids which, being zwitterions, should be poorer conductors. Moreover, amino acids present an amine-type additive with additional functional groups which might influence the selectivities toward charged and uncharged solutes. Amino acids, as well as other zwitterions, were used previously in CE but mainly to eliminate surface adsorption of proteins (e.g. [15,29]). We examine here sixteen different amino acids as additives to control and stabilize EOF. Most of the common amino acids were studied with the exception of the aromatic ones (phenylalanine, tyrosine and tryptophan).

Table 4 shows typical results with four amino acid additives with different functional groups. The migration time values are the average of anywhere from 8 to 32 runs. As a further example, Fig. 3 shows the stability of the EOF, as measured by the migration times of phenol, when serine was the additive. The relative standard deviation of the data in Fig. 3 is 0.16%.

Similar results were obtained for all 16 amino acids studied irrespective of whether the additive was polar, hydrophobic, acidic or basic. Table 4 demonstrates that EOF is independent of the

Table 4
Effect of amino acids in buffer on precision of migration time

Amino acid additive	Migration time (min)	Standard deviation
Lys	4.29	0.009
Arg	4.37	0.007
Asp	4.53	0.017
Ser	4.40	0.007

Solute was phenol; applied voltage was 25 kV; buffer as in Table 3; amino acid concentration was 0.001 M.
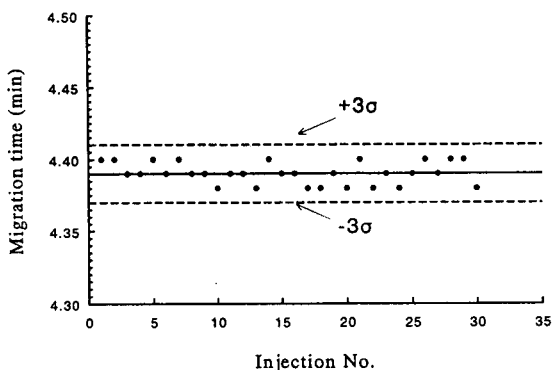
Fig. 3. Migration times of phenol as a function of injection number. 0.001 *M* Serine additive in buffer which was 0.02 *M* NaH$_2$PO$_4$ pH 6. Applied voltage was 25 kV.
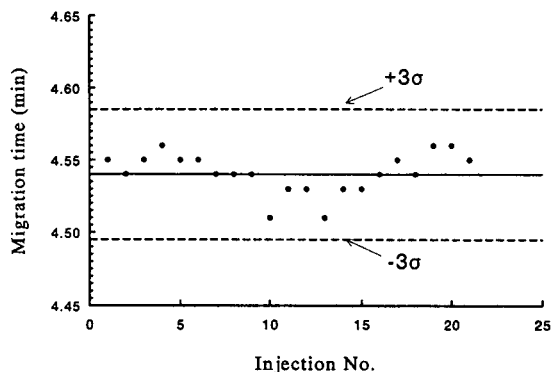

Fig. 4. Migration times of phenol as a function of injection number. 0.01 *M* TMA additive in buffer which was 0.02 *M* NaH$_2$PO$_4$ pH 6. Applied voltage was 25 kV.

nature of the amino acid additive. When tyrosine was used as a test solute, its migration times were also independent of the nature of the additive. Thus, at least for the solutes that we have examined, no selective interactions were observed with the amino acids.

Table 5 shows typical reproducibilities for some amino acid additives. The number of days over which the data were amassed is shown in the table. The results are alike those observed in chromatography. Similar results were obtained with all amino acids studied irrespective of the solutes used or the nature of amino acids.

3.3. Additive type: organic acids

Since amino acids have an acidic group as well as an amine group, organic acids were investigated as additives to control EOF. Fig. 4 shows typical results when TMA was used as an addi-

tive. Imidazole-4-acetic acid affected EOF in a similar fashion. Much to our surprise, excellent precision was also obtained with this class of additive.

3.4. Effect of buffer pH

The stabilizing effect of the amines or the acid additives occurs over a wide range of buffer pH. Fig. 5 shows the electroosmotic velocity, monitored by acetone as the solute, as a function of pH when TEA was present in the running buffer. The data were collected at pH 5 and higher, since at lower pH TEA is no longer effective as EOF stabilizer. Fig. 6 shows similar

Table 5
Effect of amino acids in buffer on the reproducibility of solute velocity

Amino acid	No. of days	Velocity (cm/min)	Standard deviation
Gly	4	9.5	0.095
Val	4	9.5	0.35
Arg	3	9.5	0.25
Cys	3	9.3	0.51

Experimental conditions as in Table 4.
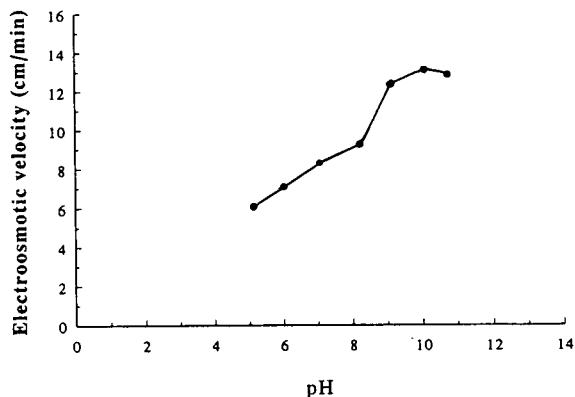
Fig. 5. Electroosmotic velocity as a function of pH. Solute was acetone. Applied voltage 25 kV; 0.02 *M* phosphate buffer, 0.01 *M* TEA in buffer.
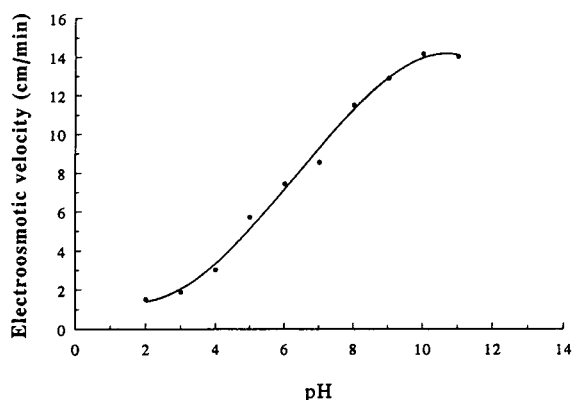
Fig. 6. Electroosmotic velocity as a function of pH. Solute was acetone. Applied voltage 25 kV; 0.02 *M* phosphate buffer, 0.01 *M* TMA in buffer.

results for TMA as additive. Acetone was chosen as solute since it is uncharged throughout the pH range studied. In both figures, the filled circles, drawn to represent the experimental points, are wider than ± 1 standard deviation of the measurements. Therefore, both types of additives can be used to stabilize EOF over a wide range of pH. To achieve the wide pH ranges shown, the phosphate buffer was prepared from either NaH_2PO_4 or Na_2HPO_4 depending on the actual pH.

Several additional observations should be made with regard to Figs. 5 and 6: (a) In the pH range studied the TMA changes from being almost completely unionized to being completely ionized (negatively charged). TMA's effectiveness in controlling EOF seems to be independent of its ionization state. TEA changes from being completely ionized (positively charged) at the low pH to being only about 50% charged. Here too, the effectiveness of TEA as EOF controller seems to be pH independent. (b) Whether the additive was an acid or a base, the electroosmotic velocity of the acetone probe was roughly the same, both in magnitude and direction, at a given pH, for both additives. The magnitude of the EOF for each additive seems to be a function of its charge, viscosity and dielectric constant. (c) The increase in EOF with an increase in pH is a well understood phenomenon (e.g. [12,23]). The sigmoid shape of the curve in Fig. 6 is typical of

acid–base titration curves. The behavior of the EOF most likely mirrors the concentration of the ionized silanol groups on the capillary surface. Thus, by measuring the EOF as a function of the pH, the titration of the capillary surface silanols can be monitored. However, and more importantly, Figs. 5 and 6 indicate that the additives used here do not control the EOF by strongly adsorbing to the capillary surface. If additive adsorption was the stabilizing mechanism, then the pH dependence of the EOF would have been much smaller [23]. It is our opinion that the additives used in this study work more like supporting electrolytes in polarography: by introducing a larger number of charge carriers a narrower wall double layer is obtained with a better defined wall ζ potential, resulting in a more stable EOF.

The discussion until now centered on small and neutral solutes. To examine the applicability of the additives to stabilize the migration times of large solutes, we used lysozyme, trypsinogen and myoglobin as test molecules. The running buffer was either Na_2HPO_4 (pH 11) or NaH_2PO_4 (pH 2). These pH values were chosen since they minimize the adsorption of the proteins to the capillary wall. Again, we found that with additives in the buffer the migration time precision improved. For example, at pH 11 the precision improved from 7% to less than 1% when using either TEA, TMA or isoleucine as the additive.

3.5. Effects of additives on peak shape

The additives discussed above affect favorably not only the migration data but also peak shape and width. For example, in the absence of additives typical relative standard deviation in plate height (*H*) measurements is between 20 and 40%. The presence of an additive improves the precision in efficiency drastically as Table 6 shows. With TEA additive the relative standard deviation is at worst about 15% and mostly less than 10%. Similar results were observed with all additives studied here.

More important is the effect of the additive on the peak shape in the case of large molecules. As

Table 6
Plate heights and standard deviations (in parentheses), as a function of applied voltage and concentration of TEA

Applied voltage (kV)	H (μm)			
	$2 \cdot 10^{-4}$ M TEA	$1 \cdot 10^{-3}$ M TEA	0.01 M TEA	0.07 M TEA
5	6.1 (0.7)	6.1 (0.7)	6.5 (0.1)	–
10	3.9 (0.1)	3.4 (0.1)	3.8 (0.3)	–
12.5	3.0 (0.2)	3.1 (0.1)	3.3 (0.1)	3.7 (0.3)
15	3.1 (0.2)	2.8 (0.2)	2.9 (0.2)	3.6 (0.4)
17.5	2.8 (0.2)	2.6 (0.1)	3.1 (0.03)	3.0 (0.01)
20	3.0 (0.3)	2.6 (0.2)	3.1 (0.2)	3.0 (0.1)
25	2.4 (0.4)	2.4 (0.4)	3.2 (0.1)	2.8 (0.3)

Other experimental conditions as in Table 1.

an example, Fig. 7 shows the peak which results from an injection of lysozyme at pH 11. Without the additive, or a pre-run wash, the resulting lysozyme peak is broad and badly tailing. The plate count was a very poor 5000. After a buffer and triply distilled water wash the peak shape improved and the plate number increased to
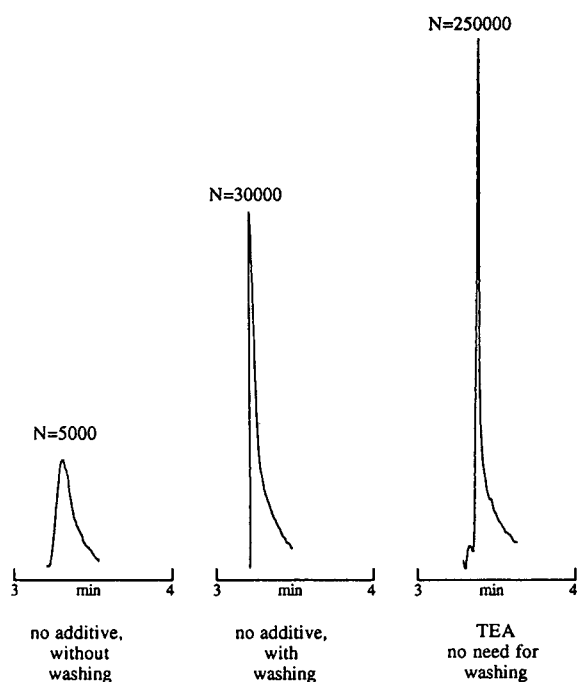
Fig. 7. The effect of adding TEA to the buffer on the efficiency and the peak shape of lysozyme. 0.02 M Na$_2$HPO$_4$ buffer pH 11, 25 kV.

30 000. With TEA in the running buffer the lysozyme peak becomes much narrower with a plate count of 250 000. All of the above values of H for lysozyme are much lower than the theoretically predicted value. The peak still tails but the overall performance is far superior with the additive in the buffer. Similar results were obtained with myoglobin and trypsinogen. Their peak shapes improved in the presence of any of the additives examined here. Note, again, that the presence of the additive eliminates the need for washing the capillary between injections.

4. Conclusions

Amines, amino acids and acids control EOF and, therefore, stabilize the migration times of solutes in CE. In the presence of these additives, the precision and reproducibility both in migration times and in plate heights improves drastically. With additives, CE can compete, as far as figures-of-merit are concerned, with more established separation techniques, such as HPLC. The additives described here work well with small as well as with large solute molecules. The results discussed above coupled with the fact that such a chemically wide range of additives work in a similar fashion indicate that their modus operandi is related probably more to the presence of charged species than to chemical interactions.

The goal of the present work was to improve

precision. While it is important to optimize CE separation, it is also vital to improve the precision of the method. Our results clearly demonstrate that the use of additives does provide the necessary precision which is essential for practical use.

Acknowledgement

References

[1] E. Grushka and I. Zamir, in P.R. Brown and R.A. Hartwick (Editors), *High Performance Liquid Chromatography*, Wiley, New York, 1989, pp. 529–561.
[2] K.A. Turner, *LC·GC*, 9 (1991) 350.
[3] A. Watzig and C. Dette, *J. Chromatogr.*, 636 (1993) 31.
[4] R.J. Hunter, *Zeta Potential in Colloid Science*, Academic Press, London, 1981.
[5] W.J. Lambert and D.L Middleton, *Anal. Chem.*, 62 (1990) 1585.
[6] J.A. Lux, H.-F. Yin and G. Schomburg, *Chromatographia*, 30 (1990) 7.
[7] T. Dülffer, R. Herb, H. Herrmann and U. Kobold, *Chromatographia*, 30 (1990) 675.
[8] S.C. Smith, J.K. Strasters and M.G. Khaledi, *J. Chromatogr.*, 559 (1991) 57.
[9] T.T. Lee and E.S. Yeung, *Anal. Chem.*, 63 (1991) 2848.
[10] Q. Wu, H.A. Claessens and C.A. Cramers, *Chromatographia*, 33 (1992) 303.
[11] M.A. Strege and A.L. Lagu, *J. Liq. Chromatogr.*, 16 (1993) 51.
[12] K.D. Altria and C.F. Simpson, *Anal. Proc.*, 25 (1988) 85.
[13] Th.P.E.M. Verheggen, A.C. Schoots and F.M. Everaerts, *J. Chromatogr.*, 503 (1990) 245.
[14] T. Kaneta, S. Tanaka and H. Yoshida, *J. Chromatogr.*, 538 (1991) 385.
[15] M.M. Bushey and J.W. Jorgenson, *J. Chromatogr.*, 480 (1989) 310.
[16] J.B. Poli and M.R. Schure, *Anal. Chem.*, 64 (1992) 896.
[17] B.V. VanOrman, G.G. Liversidge, G.L. McIntire, T.M. Olefirowicz and A.G. Ewing, *J. Microcol. Sep.*, 2 (1990) 176.
[18] A.D. Tran, S. Park, P.J. Lisi, O.T. Huynh, R.R. Ryall and P.A. Lane, *J. Chromatogr.*, 542 (1991) 459.
[19] C. Schwer and E. Kenndler, *Anal. Chem.*, 63 (1991) 1801.
[20] M. Idei, I. Mezo, Zs. Vadasz, A. Horvath, I. Teplan and Gy. Keri, *J. Liq. Chromatogr.*, 15 (1992) 3181.
[21] K.A. Cobb, V. Dolnik and M. Novotny, *Anal. Chem.*, 62 (1990) 2478.
[22] S. Hjertén and M. Kiessling-Johansson, *J. Chromatogr.*, 550 (1991) 811.
[23] J.K. Towns and F.E. Regnier, *Anal. Chem.*, 63 (1991) 1126.
[24] Z. Zhao, A. Malik and M.L. Lee, *Anal. Chem.*, 65 (1993) 2747.
[25] C.S. Lee, W.C. Blanchard and C.-T. Wu, *Anal. Chem.*, 62 (1990) 1550.
[26] M.A. Hayes and A.G. Ewing, *Anal. Chem.*, 64 (1992) 512.
[27] P. Tsai, B. Patel and C.S. Lee, *Anal. Chem.*, 65 (1993) 1439.
[28] A. Riddick and W.B. Bunger, *Organic Solvents*, Wiley-Interscience, New York, 1970.
[29] S.A. Swedberg, *J. Chromatogr.*, 503 (1990) 449.

Short Communication

Chiral resolution of 1,3-dimethyl-4-phenylpiperidine derivatives using high-performance liquid chromatography with a chiral stationary phase

Dali Yin[a], Atmaram D. Khanolkar[a], Alexandros Makriyannis[a,*], Mark Froimowitz[b]

[a]School of Pharmacy, Box U-92, University of Connecticut, 372 Fairfield Road, Storrs, CT 06268, USA
[b]McLean Hospital, Harvard Medical School, 115 Mill Street, Belmont, MA 02178, USA

Abstract

A number of racemic 1,3-dimethyl-4-phenylpiperidines which serve as intermediates in the synthesis of opioid analgesics have been resolved on two commercially available high-performance liquid chromatography columns containing cellulose-based chiral stationary phases: Chiralcel OD and Chiralcel OJ. The resolution results were complementary between the two columns. Also, the polarity of substituents appears to play an important role on the ability of the Chiralcel OD column to resolve pairs of enantiomers.

1. Introduction

4-Phenylpiperidines such as meperidine, ketobemidone and prodines are opioid analgesics [1] (Fig. 1). Various structure–activity relationship studies have shown that the prodines have different pharmacological profiles compared to
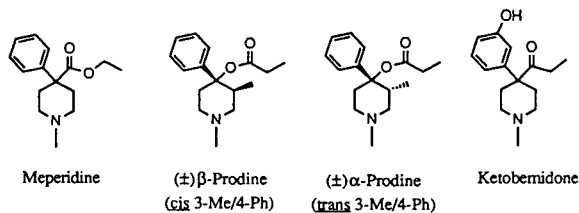
Fig. 1. 4-Phenylpiperidine opioid analgesics.

Meperidine   (±)β-Prodine   (±)α-Prodine   Ketobemidone
                    (cis 3-Me/4-Ph)   (trans 3-Me/4-Ph)

the analogues of ketobemidone and meperidine [2–4]. In order to test the predictions of a proposed model [5–7] which predicts the stereochemical requirements for opioid receptor activity, we initiated a project to study the effects of conformation on analgesic activity of these compounds. This study required the synthesis and resolution of α- and β-prodines and their analogues.

Optical resolution of prodinols, the precursor alcohols of prodines, has already been accomplished by fractional crystallization [8], but most other analogues were less amenable to this approach [9]. High-performance liquid chromatography (HPLC) with a chiral stationary phase (CSP) provides a convenient method for both analytical- and preparative-scale separation of enantiomers for all of the analogues we tested.

* Corresponding author.
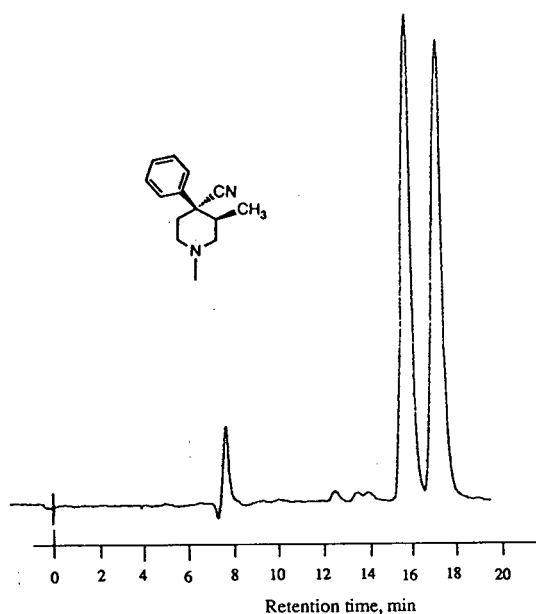
Fig. 2. Resolution of racemic β-4-cyano-1,3-dimethyl-4-phenylpiperidine on Chiralcel OD; solvent 3% isopropanol and 0.05% DEA in hexane.

However, no data concerning the resolution of the enantiomers of these compounds by HPLC on CSPs could be found in the literature.

Herein we report on the chiral resolution of α- and β-prodines, α- and β-prodinols, a ketobemidone analogue as well as precursors of two ketobemidone analogues by HPLC on two cellulose-based CSP columns viz. Chiralcel OD and Chiralcel OJ.
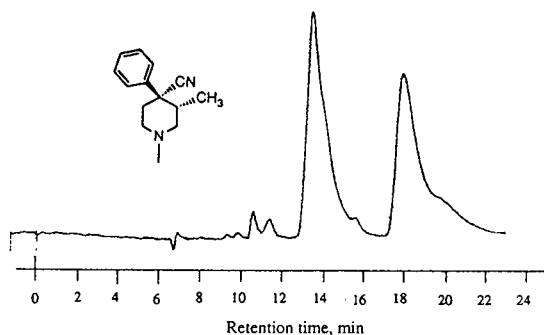
Fig. 3. Resolution of racemic α-4-cyano-1,3-dimethyl-4-phenylpiperidine on Chiralcel OD; solvent 10% isopropanol and 0.1% DEA in hexane.
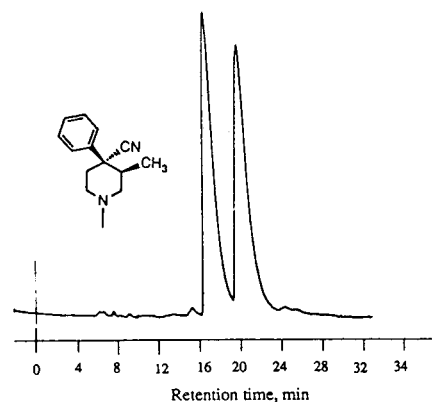
Fig. 4. Resolution of racemic β-4-cyano-1,3-dimethyl-4-phenylpiperidine on Chiralcel OJ; solvent 10% isopropanol and 0.1% DEA in hexane.

2. Experimental

2.1. Chromatography

Chromatography was performed using a Waters Model 590 pump, an U6K injector, a Model 450 variable-wavelength UV detector detecting at 254 nm and a Fisher Recordall recorder. Chiralcel OD and Chiralcel OJ (both 25 × 0.46 cm, 0.5-μm particles, from Daicel) were used. The flow-rate was 0.5 ml/min.
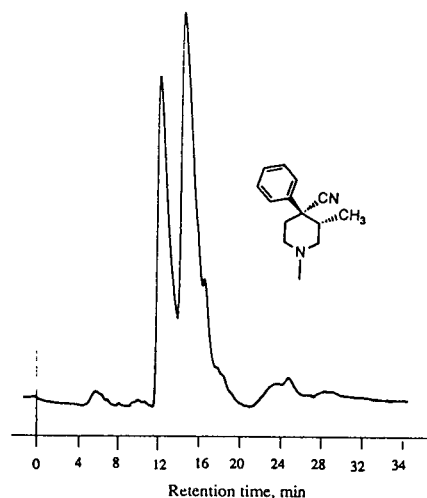
Fig. 5. Resolution of racemic α-4-cyano-1,3-dimethyl-4-phenylpiperidine on Chiralcel OJ; solvent 10% isopropanol and 0.1% DEA in hexane.
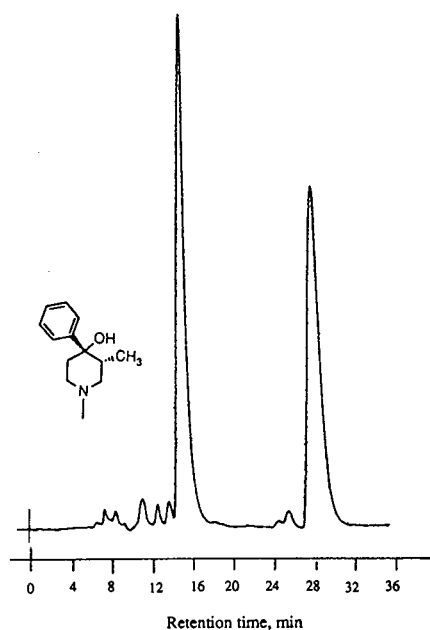
Fig. 6. Separation of enantiomers of α-prodinol on Chiralcel OD; solvent 10% isopropanol and 0.1% DEA in hexane.

2.2. Reagents and materials

The compounds used in this study were synthesized in our laboratory following literature procedures. The racemic diastereomers were first separated and purified by column chromatography before injecting into the chiral HPLC columns. The solvents used were HPLC grade. Diethylamine (DEA) used as a modifier was of analytical-reagent grade.

3. Results and discussion

Chiralcel OD and Chiralcel OJ are derivatized cellulose stationary phases. Although the mechanism of chiral recognition by this kind of CSP is not quite clear, there are numerous examples demonstrating the wide range of solutes which have been resolved [10,11]. Since we were interested in direct resolution of our analogues as free bases without derivatization, we chose Chiralcel

Table 1
Resolution of 1,3-dimethyl-4-phenylpiperidine derivatives
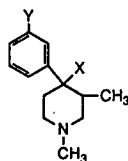
Compound			Chiralcel OD				Chiralcel OJ			
X	Y	3-Me/4-Ph	k_1'	k_2'	α	Solvent	k_1'	k_2'	α	Solvent
OH	H	(±) α	1.70	5.89	3.45	A	1.38	1.50	1.09	A
		(±) β	1.17	4.35	3.70	A	–	–	–	
CN	H	(±) α	1.00	1.95	1.95	A	0.87	1.25	1.42	B
		(±) β	0.97	1.12	1.15	A	1.56	2.02	1.32	B
OCOEt	H	(±) α	1.04	1.14	1.09	C	1.38		1.00	A
		(±) β	0.62	0.74	1.19	C	1.31	2.00	1.53	A
COEt	H	(±) α	0.88	0.98	1.12	A	0.56	0.68	1.22	A

Solvents: A = 5% isopropanol and 0.1% DEA in hexane; B = 10% isopropanol and 0.1% DEA in hexane; C = 3% isopropanol and 0.05% DEA in hexane.

OD and Chiralcel OJ [12,13], which are thought to be the best and the most practical among this type of CSPs.

The retention time could be adjusted by modifying the percentage of isopropanol in the mobile phase. Also a small amount of DEA was used as a modifier to decrease peak broadening and tailing. We found that increasing the proportion of DEA in the mobile phase did not influence the retention time dramatically, but more than 0.5% DEA caused disturbance of the baseline.

The resolution data for prodines and their analogues on Chiralcel OD and Chiralcel OJ columns are summarized in Table 1. From these data it is clear that the resolution abilities of the two columns are quite different. The best resolution on Chiralcel OD column was obtained when X = OH (for both β and α isomers); α = 3.70 for the β and α = 3.45 for the α diastereomer. However, the α diastereomer showed very poor resolution on Chiralcel OJ column. When X = CN, both β and α isomers had good resolutions on either columns. The best separation on Chiralcel OJ was obtained for β-prodine which showed much less satisfactory resolution on Chiralcel OD. For all the compounds that were tested, the (+)-enantiomer had a shorter retention time than the (−)-enantiomer. Overall, better resolutions were obtained on Chiralcel OD compared to Chiralcel OJ. It appears that for the Chiralcel OD column polarity is a key factor in the chiral recognition; the more polar the substituents, the better the resolution.

The resolution results of compounds described above indicated that the two columns, Chiralcel OD and Chiralcel OJ, perform in a complementary fashion. As a result, we were able to resolve all of the racemic diastereomers synthesized in our laboratory. Some of these compounds were also resolved on a preparative scale using a semipreparative Chiralcel OD column.

Acknowledgements

References

[1] A.E. Jacobson, E.L. May and L.J. Sargent, in A. Burger (Editor), Medicinal Chemistry, Part II, Wiley-Interscience, New York, 3rd ed., 1970, pp. 1327–1350.

[2] D.M. Zimmerman, R. Nickander, J.S. Horng and D.T. Wong, Nature (London), 275 (1978) 332.

[3] T. Oh-ishi and E.L. May, J. Med. Chem., 16 (1973) 1376.

[4] A.H. Beckett and A.F. Casy, in G.P. Ellis and G.B. West (Editors), Progress in Medicinal Chemistry, Vol. 2, Butterworth, London, 1962, p. 43.

[5] H. Tecle and G. Hite, in Problems of Drug Dependence 1976, National Academy of Sciences; Washington, DC, 1976, pp. 464–470.

[6] D.S. Fries and P.S. Portoghese, J. Med. Chem., 19 (1976) 1155.

[7] M. Froimowitz, P. Salva, G.J. Hite, G. Gianutsos, P. Suzdak and R. Heyman, J. Comp. Chem., 5 (1984) 291.

[8] D.L. Larson and P.S. Portoghese, J. Med. Chem., 16 (1973) 195.

[9] M. Froimowitz, A.D. Khanolkar, D. Yin, A.I. Brooks, G.W. Pasternak and A. Makriyannis, J. Med. Chem., submitted.

[10] H.Y. Aboul-enein and M.R. Islam, J. Liq. Chromatogr., 13 (1990) 485.

[11] Y. Okamoto, R. Aburatani and K. Hatada, J. Chromatogr., 389 (1987) 95.

[12] Y. Okamoto and M. Kawashima, Chem. Lett., (1986) 1237.

[13] T. Ohkubo, T. Uno and K. Sugawara, Chromatographia, 33 (1992) 287.

Short Communication

Gel permeation chromatographic properties of poly(vinyl alcohol) gel particles prepared by freezing and thawing

Ryoichi Murakami*, Hiroshi Hachisako, Kimiho Yamada, Yoshiaki Motozato

Department of Applied Chemistry, Kumamoto Institute of Technology, Kumamoto 860, Japan

Abstract

The gel permeation chromatographic properties of poly(vinyl alcohol) gel particles prepared by a freezing-and-thawing procedure were investigated. From the calibration graph established with poly(ethylene glycol) and poly(ethylene oxide) samples, it was found that the value of the excluded molecular mass increased from 2500 (original) to 6000 (fifteen repeated cycles of freezing and thawing). In addition, the treated gels showed a favourable pressure-resisting property.

1. Introduction

We have been investigating the preparation of macroporous gel particles of poly(vinyl alcohol) [1]. These particles are obtained by the saponification of particles of poly(vinyl acetate) formed in the polymerization of vinyl acetate in a suspension process. The poly(vinyl alcohol) gel particles have been used as a column packing for aqueous separations. However, the gels have a disadvantage with regard to pressure-resistant properties because of their poor mechanical strength. We considered that a poly(vinyl alcohol) gel might have a potential high enough to realize excellent mechanical stability, because a poly(vinyl alcohol) aqueous solution more than 5 wt.-% was found to become strong hydrogel following a freezing-and-thawing procedure [2–4].

We report here that the freezing-and-thawing procedure is suitable for improving the performance of poly(vinyl alcohol) gel particles for use as a column packing for gel permeation chromatography in aqueous media.

2. Experimental

Vinyl acetate was freed from inhibitor by washing with a 5% aqueous solution of sodium hydrogensulfite and distilled water. Suspension polymerization of vinyl acetate was conducted in the presence of benzoyl peroxide as an initiator in a 300-ml round-bottomed flask equipped with an agitator and a reflux condenser. After the reaction product had been processed, the dry gel particles of poly(vinyl acetate) [degree of polymerization (DP) = 1000] was classified with a testing sieve. The classifier settings were chosen to give a particle size distribution with particle diameters in the range 200–250 μm. The sapon-

* Corresponding author.

ification from poly(vinyl acetate) to poly(vinyl alcohol) was carried out at 30°C for 1 month by immersing the gel particles in a solution containing sodium hydroxide and methanol in an aqueous saturated sodium sulfate solution [5]. The completion of saponification was confirmed by IR measurement. The gel particles of poly-(vinyl alcohol) obtained above have enough mechanical stability in water below 70°C without treatment for cross-linking. Observations by optical microscopy suggested that the diameter of a dry particle increased by a factor of ≤1.38 on swelling with water.

The gel particles of poly(vinyl alcohol) swollen in water were subjected to repeated freezing and thawing. The temperature range was between −30 and 20°C. This was realized simply by placing the swollen gel particles in and removing them from a freezer at 3-h intervals; in this way the temperature was lowered from 20 to −30°C in 1 h, kept at that temperature for 3 h, then raised from −30 to 20°C and kept at 20°C for 3 h. The slurry of the gel particles was packed into a 150 × 4 mm I.D. stainless-steel column at a pressure of about 5 MPa.

High-performance gel permeation chromatographic (HP-GPC) separations were performed with a Shimadzu LC6-AD instrument employing distilled water as eluent. Solutions (40 μl) of individual solutes were injected with an off-column syringe–septum arrangement. Detection of solutes was performed with a Shimadzu Model RID-6A Refracto Monitor (cell volume = 10 μl, aqueous reference). The samples of poly-(ethylene oxide) (PEO) were narrow-distribution standards supplied by Showa Science (Tokyo Japan). The samples of poly(ethylene glycol) (PEG) are designated with a number indicating the molecular mass provided by the suppliers (Kanto Chemicals, Tokyo, Japan). The calibration graph was established at a flow rate of 0.4 ml/min with a PEG concentration of 2.0% (w/v) and a PEO concentration of 1.0% (w/v).

X-ray experiments were carried out using a Rigaku wide-angle X-ray diffractometer with nickel-filtered copper Kα_1 radiation. Its power setting was at 35 kV and 20 mA.
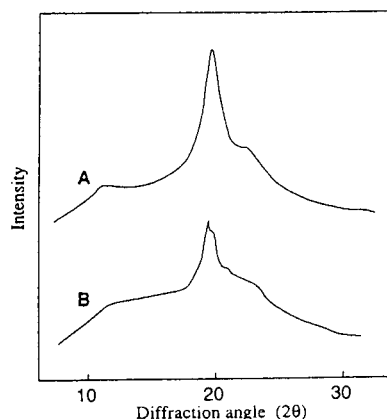
Fig. 1. X-ray diffraction patterns of poly(vinyl alcohol) gel particles. A, Original; B, after fifteen repeated cycles of freezing and thawing.

3. Results and discussion

Fig. 1 shows plots of X-ray diffraction intensity versus 2θ for particles subjected to the freezing-and-thawing treatment. The original sample shows clear (101) reflections in the angle regions 2θ = 19.40–19.60°. The main peak position in the X-ray pattern of the gel particles freezing and thawing on treatment by does not change. However, the intensity and sharpness of the profiles decrease compared with the original sample. In contrast, the halo portions in the angle range 2θ = 10–15° increase. This may be due to an increase in disordered domains.

The calibration graphs established with PEG and PEO samples are shown in Fig. 2. The value of the excluded molecular mass (M_{lim}) increased from 2500 (original) to 6000 with increasing number of repeated cycles of freezing and thawing (N). Above ten repeated cycles this value becomes independent of N. This result suggests that the fine structure of the gel particles prepared by the freezing-and-thawing procedure changes to a structure having larger pores because of the higher excluded molecular mass of the treated particles. In general, the cross-linking point in the network structure of gels is the crysalline relations which consist of aggregates of extended molecular chains associated by
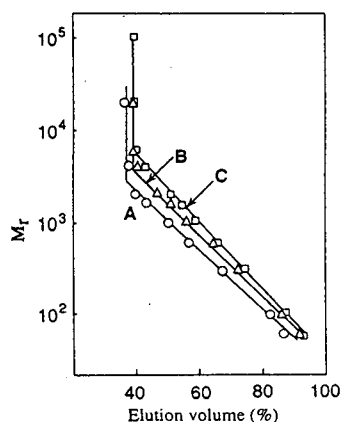
Fig. 2. Molecular mass calibration graphs for GPC column containing poly(vinyl alcohol) gel particles. A, Original; B, after five repeated cycles of freezing and thawing; C, after fifteen repeated cycles of freezing and thawing.
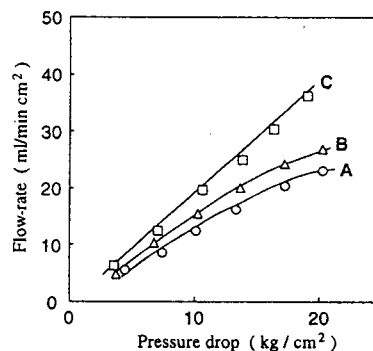

Fig. 3. Relationship between the flow-rate and pressure drop for poly(vinyl alcohol) gel particles. A, Original; B, after five repeated cycles of freezing and thawing; C, after fifteen repeated cycles of freezing and thawing.

many hydrogen bonds [6]. Considering the results of X-ray scattering, in this case the development of a network structure having larger pores is not caused by an increase of crystalline regions, but probably by water interacting with amorphous chains between the cross-linking points.

HP-GPC is desirable in aqueous systems. In this case, the pressure resistence is an important property. Fig. 3 shows the relationship between the flow-rate and the pressure drop, compared with the behaviour observed for untreated poly(vinyl alcohol) gels. The straight line in Fig. 3 indicates that the gel particles prepared by the freezing-and-thawing procedure form rigid and stable packing materials for high-speed chromatography. When the gel particles are repeatedly treated by freezing and thawing, the hydrogen bonds between chain molecules and water become stronger. This results in an increase in the rigidity of the particles. From the above results it is clear that the freezing-and-thawing treatment is useful for improving the performance of poly(vinyl alcohol) particles as packing materials.

References

[1] C. Hirayama and Y. Motozato, Nippon Kagaku Kaishi, (1972) 1087.
[2] M. Nanbu, Kobunshi Kako, 32 (1983) 523.
[3] M. Watase and K. Nishinari, J. Polym. Sci., Polym. Phys. Ed., 23 (1985) 1803.
[4] M. Watase and K. Nishinari, Makromol. Chem., 189 (1988) 871.
[5] R. Murakami and Y. Motozato, Kobunshi Ronbunshu, 47 (1990) 1005.
[6] M. Nagura, T. Hamano and H. Ishikawa, Polymer, 30 (1989) 762.

Short Communication

Preparative separation of ganglioside GM₃ by high-performance liquid chromatography

R.F. Menzeleev[a],* Yu.M. Krasnopolsky[a], E.N. Zvonkova[b], V.I. Shvets[b]

[a]Biolek Company, Pomerki 70, Kharkov, 310070, Ukraine
[b]Department of Biotechnology, M.V. Lomonosov Institute of Fine Chemical Technology, Moscow, Russian Federation

(First received January 7th, 1993; revised manuscript received March 15th, 1994)

Abstract

A preparative high-performance liquid chromatographic method for the purification of ganglioside GM₃ is described. The method utilizes a Zorbax-NH₂ column and methanol–2-propanol–acetonitrile–phosphate buffer as the eluent. The elution profile was monitored by flow-through detection of UV absorbance at 215 nm. The purification of ganglioside GM₃ was performed in a total elution time of less than 15 min.

1. Introduction

Gangliosides are normal membrane components, located almost exclusively at the outer leaflet of plasma membranes [1]. Dramatic changes in ganglioside composition and metabolism during ontogenesis, differentiation and oncogenic transformation suggest a specific role of gangliosides in the regulation of cell growth and cellular interaction [2]. The observation of effects on growth factor-stimulated receptor phosphorylation was the first evidence of the participation of gangliosides in the molecular mechanism associating cell growth control [3,4]. Confirmation and extension of these results are important. Usually 1– 20 mg of GM₃ of purity not less than 99% are sufficient for experiments with cell cultures. The aim of this work was to develop a convenient and inexpensive HPLC

procedure appropriate for the preparative isolation of GM₃ from a mixture containing other gangliosides and non-ganglioside impurities. This paper describes a procedure for the preparative HPLC of gangliosides GM₃-NeuGc and GM₃-NeuAc with on-line UV detection.

2. Experimental

HPLC-grade acetonitrile (LiChrosolv) was purchased from Merck (Darmstadt, Germany). Water was purified with a Milli-Q system (Millipore). All other solvents were redistilled before use. Commercial chemicals were of analytical-reagent grade or the highest grade available.

Precoated high-performance thin-layer chromatographic (HPTLC) plates with Kieselgel 60 were obtained from Merck and DEAE Sephadex A-25 from Pharmacia (Uppsala, Sweden).

Ganglioside GM₃ and N-acetylneuraminic acid from Sigma (St. Louis, MO, USA) and GM₃-

---

* Corresponding author. E-mail: (Internet) root @ ramil. kharkov.ua.

NeuGc from equine erythrocytes, prepared according to Miyazaki et al. [5], were used as standards.

The procedure for extraction and phase separation was similar to a previously described method [6] for the isolation of total gangliosides from male Wistar rat (3–6 months old) liver (160 g) and equine erthrocytes (5 1). Monosialogangliosides from the upper methanol–water phase were prepared by DEAE-Sephadex A-25 (acetate form) column chromatography (7 × 3 cm I.D. column) with 0.03 M ammonium acetate in methanol as eluent, as described [1]. The desalting of gangliosides was carry out on LiChroprep RP-18 column (4 × 3 cm I.D.) similarly to a described method [7]. The methanol solutions were evaporated and lipids were dissolved in water and lyophilized. The yield of monosialogangliosides was 23 mg from rat liver and 420 mg from equine erythrocytes.

HPLC was performed on a Gilson apparatus, equipped with a Rheodyne Model 7125 sample injector.

2.1. Preparative HPLC separation of ganglioside GM_3

Ganglioside GM_3-NeuGc was dissolved in 2-propanol–water (1:2, v/v) to give a 10 mg/ml concentration and 0.1–2.0 ml of this solution was introduced into the sample injector. Ganglioside was then purified on a Zorbax-NH_2 (8 μm) column (250 × 21.4 mm I.D.) (DuPont) with methanol–2-propanol–acetonitrile–30 mM sodium phosphate buffer (pH 5.6) (168:84:24:35, v/v) as eluent at a flow-rate of 20 ml/min and UV detection at 215 nm.

Monosialogangliosides from equine erythrocytes were separated under the same conditions as standard GM_3-NeuGc.

Methanol–2-propanol–acetonitrile–30 mM sodium phosphate buffer (168:96:23:20, v/v) was used for the separation of GM_3-NeuAc from the monosialoganglioside fraction of the rat liver by injection of up to 1 ml (10 mg/ml) of sample solution.

2.2. Analytical HPLC

A 1 mg/ml solution of ganglioside GM_3 in water was introduced into the injector and then separated on a Diasorb-130-NH_2 (6 μm) column (150 × 4 mm, I.D.) with a Diasorb-130-NH_2 (6 μm) guard column (50 × 4 mm I.D.) (BioChimMak, Russian Federation) with methanol–2-propanol–acetonitrile–30 mM sodium phosphate buffer (pH 5.6) (168:96:23:20, v/v) as eluent at a flow-rate of 1.5 ml/min and UV detection at 215 nm.

2.3. Analytical methods

Chloroform–methanol–0.2% $CaCl_2$ (60:35:8, v/v) was used as the mobile phase for HPTLC. Spots were revealed with orcinol–iron(II) chloride (Sigma) and resorcinol–HCl spray reagents [8], ninhydrin and a solution of sulphuric acid in ethanol.

Sialic acid was measured quantitatively with resorcinol–HCl reagent [9]. Pure N-acetylneuraminic acid was used as the standard.

3. Results and discussion

Several methods for the separation of gangliosides by preparative HPLC have been developed [10–13]. 2-Propanol–hexane–water and chloroform–methanol water are used as eluents with HPTLC control of the collected fractions. Unfortunately, on-line monitoring of the separation by short-wavelength UV detection cannot be used in these procedures, because gradient elution and highly absorbing eluents were used. The aim of this study was to establish appropriate conditions for the rapid preparative HPLC separation of ganglioside GM_3 with UV flow-through detection.

Gazzotti et al. [14] presented an HPLC method with an aminopropyl-modified silica gel stationary phase and UV detection at 215 nm. However, the eluent used (acetonitrile–phosphate buffer) is not suitable for preparative purposes because of the low solubility of the

gangliosides. Replacement of acetonitrile by methanol, in which gangliosides show better solubility, resulted in a significant decrease in the capacity factor (k'). That is why we introduced a component with a smaller elution strength than

methanol–2-propanol. The proportions of the components in the eluent were optimized to achieve the maximum and rapid yield of ganglioside with 99% purity. An example of the purification of 1, 10 and 20 mg of ganglioside GM_3-NeuGc is shown in Fig. 1. The recovery of ganglioside after HPLC purification and desalting was more then 96% by measurement of the sialic acid content.

Fig. 2 illustrates the preparative separation of the equine erythrocyte monosialoganglioside fraction. A 4.5-mg amount of mixture was separated within 14 min using 250 ml of eluent. The 3.1-mg yield of pure GM_3-NeuGc was homogeneous according to analytical HPLC under the same conditions (Fig. 4) and HPTLC (Fig. 5).

The optimum capacity factor for the preparative isolation of ganglioside GM_3-NeuAc from rat liver was obtained with a small change in the eluent composition. Fig. 3 illustrates the preparative separation of GM_3-NeuAc from a mixture containing non-ganglioside impurities. The collected substance was homogeneous according to analytical HPLC and HPTLC (Figs. 4 and 5).

Both gangliosides obtained by the developed preparative HPLC method did not contain im-
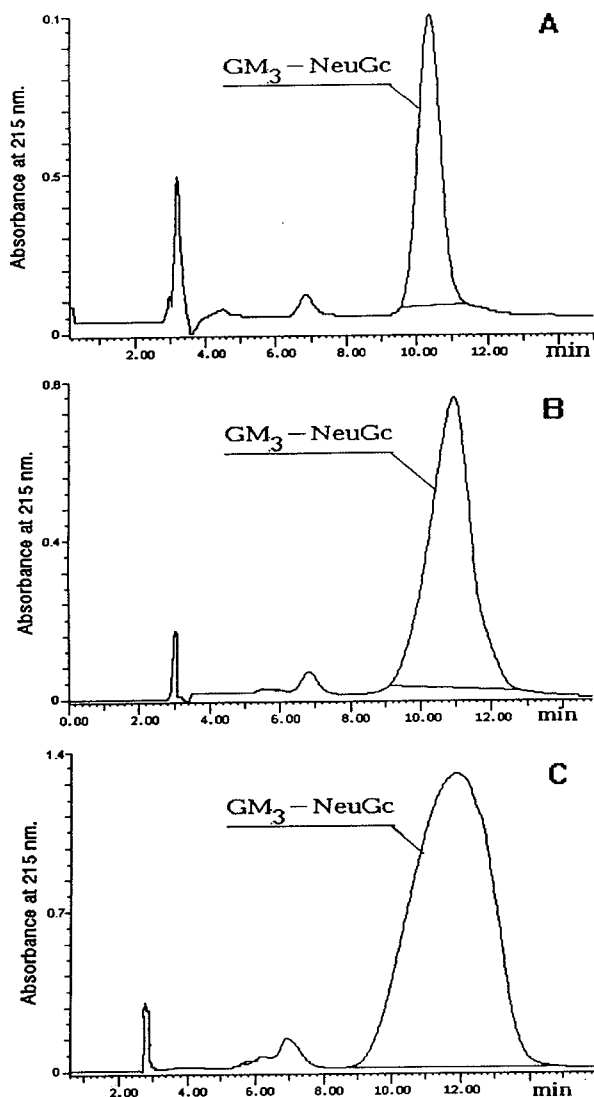
Fig. 1. Application of the preparative HPLC method to the purification of ganglioside GM_3-NeuGc. Amount: (A) 1; (B) 10; (C) 20 mg. The substance was dissolved in 2-propanol–water (1:2, v/v) to give a 10 mg/ml concentration and 0.1, 1.0 and 2.0 ml of sample solution were injected.
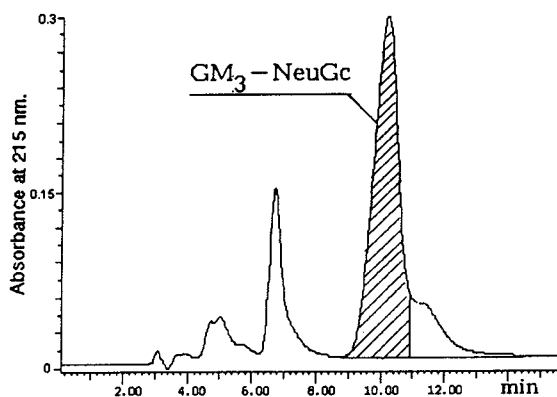
Fig. 2. Application of the preparative HPLC method to the isolation of the ganglioside GM_3-NeuGc from 4.5 mg of monosialoganglioside fraction of equine erythrocytes. The substance was dissolved in 2-propanol–water (1:2, v/v) to give a 10 mg/ml concentration and 0.45 ml of sample solution was injected.
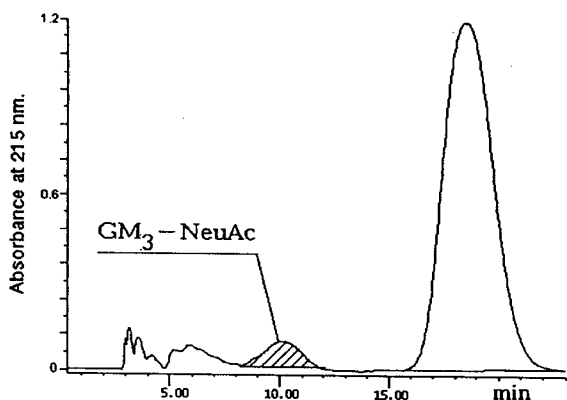
Fig. 3. Application of the preparative HPLC method to the isolation of the ganglioside GM$_3$-NeuAc from 3 mg of monosialoganglioside fraction of rat liver. The substance was dissolved in 2-propanol–water (1:2, v/v) to give a 10 mg/ml concentration and 0.3 ml of sample solution was injected.
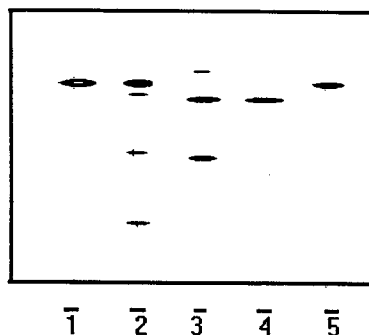

Fig. 5. HPTLC of gangliosides 1 = Standard of GM$_3$-NeuAc; 2 = monosialogangliosides from rat liver; 3 = monosialogangliosides from equine erythrocytes; 4 = GM$_3$-NeuGc purified by HPLC; 5 = GM$_3$-NeuAc purified by HPLC. Spots were revealed using both resorcinol–HCl spray reagent and a solution of sulphuric acid in ethanol.

purities detectable with ninhydrin and sulphuric acid reagents.

In conclusion, we have demonstrated the application of an aminopropyl-modified silica gel column for the preparative separation of ganglioside GM$_3$ from equine erythrocytes and rat liver with methanol–2-propanol–acetonitrile–30 mM sodium phosphate buffer as eluent and UV detection. The same combination of stationary phase and eluent can be used for the analytical HPLC of ganglioside GM$_3$.

References

[1] W. Ledeen and R.K. Yu, in N. Marks and R. Rodnight (Editors), Research Methods in Neurochemistry, Vol. 4, Plenum Press, New York, 1978, p. 371.
[2] S.-I. Hakomori, Annu. Rev. Biochem., 50 (1981) 733.
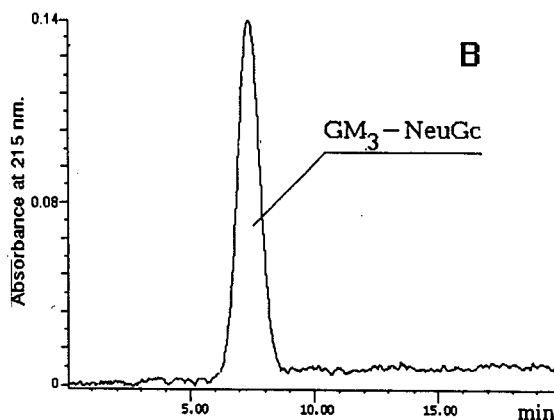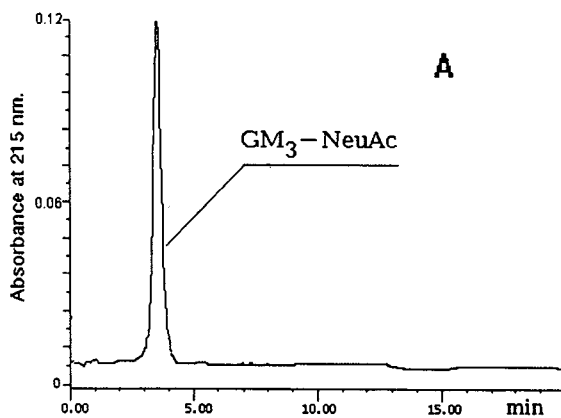
Fig. 4. Application of the analytical HPLC method to verification of ganglioside GM$_3$ purity after preparative separation. (A) GM$_3$-NeuAc; (B) GM$_3$-NeuGc, The substance was dissolved in water to give a 1.0 mg/ml concentration; 20 and 30 μl of sample solution were injected.

[3] E.G. Bremer, J. Schlessinger and S.-I. Hakomori, *J. Biol. Chem.*, 261 (1986) 2434.

[4] W. Song, M.F. Vacca, R. Welti and D.A. Rintoul, *J. Biol. Chem.*, 266 (1991) 10174.

[5] K. Miyazaki, N. Okamura and Y. Kishimoto, *Biochem. J.*, 235 (1986) 755.

[6] I.A. Mesin, G.K. Menzeleeva, R.F. Menzeleev, A.N. Pinchuk, Yu. M. Krasnopolsky and V.I. Shvetz, *Biol. Membr.*, 6 (1992) 395.

[7] H. Kubo and M. Hoshi, *J. Lipid Res.*, 26 (1985) 638.

[8] L. Svennerholm, *Biochim. Biophys. Acta*, 24 (1957) 604.

[9] L.D. Bergelson, E.V. Dyatlovitskaya, Jul.G. Molotkovsky, S.G. Batrakov, L.I. Barsukov and N.V. Prokazova, *Preparative Biochemistry of Lipids*, Nauka, Moscow, 1981, p. 23.

[10] J. Bushler, U. Galili and B.A. Macher, *Anal. Biochem.*, 164 (1987) 521.

[11] R. Kannagi, E. Nodelman, S.B. Levery and S. Hakomori, *J. Biol. Chem.*, 257 (1982) 14865.

[12] S.K. Kundu and D. Dunn Scott, *J. Chromatogr.*, 19 (1982) 232.

[13] J. Gottfries, P. Davidsson, J.E. Mansson and L. Svennerholm, *J. Chromatogr.*, 490 (1989) 263.

[14] G. Gazzotti, S. Sonnio and R. Ghidoni, *J. Chromatogr.*, 348 (1985) 371.

Analytical Applications of Circular Dichroism

Edited by **N. Purdie** and **H.G. Brittain**

Techniques and Instrumentation in Analytical Chemistry Volume 14

Circular dichroism is a special technique which provides unique information on dissymmetric molecules. Such compounds are becoming increasingly important in a wide variety of fields, such as natural products chemistry, pharmaceutics, molecular biology, etc. The content of this book has been selected in order to feature the unique aspects of circular dichroism, and how these strengths can be of assistance to workers in the field.

Substantial discussions have been provided regarding the particular phenomena associated with dissymmetric compounds which give rise to the circular dichroism effect. Reviews are also given of the type of instrumentation available for the measurement of these effects. A number of chapters cover the wide range of applications illustrating the power of the method.

Owing to its broad appeal, the book will be of interest to workers in all areas of chemistry and pharmaceutical science.

Contents:

© 1994 360 pages Hardbound
Price: Dfl. 355.00 (US $ 202.75)
ISBN 0-444-89508-6

ORDER INFORMATION
For USA and Canada
ELSEVIER SCIENCE INC.
P.O. Box 945
Madison Square Station
New York, NY 10160-0757
Fax: (212) 633 3880
In all other countries
ELSEVIER SCIENCE B.V.
P.O. Box 330
1000 AH Amsterdam
The Netherlands
Fax: (+31-20) 5862 845
US$ prices are valid only for the USA & Canada and are subject to exchange rate fluctuations; in all other countries the Dutch guilder price (Dfl.) is definitive. Customers in the European Community should add the appropriate VAT rate applicable in their country to the price(s). Books are sent postfree if prepaid.

ELSEVIER
SCIENCE B.V.

PUBLICATION SCHEDULE FOR THE 1994 SUBSCRIPTION

Journal of Chromatography A and *Journal of Chromatography B: Biomedical Applications*

MONTH	1993	J–J	J	A	S	O	
Journal of Chromatography A	652–657	Vols. 658–672	673/1 673/2 674/1 + 2 675/1 + 2 676/1	676/2 677/1 677/2 678/1	678/2 679/1 679/2 680/1	680/2	The publication schedule for further issues will be published later.
Bibliography Section		Vol. 681			682/1		
Journal of Chromatography B: Biomedical Applications		Vols. 652–656	657/1 657/2	658/1 658/2	659	660/1 660/2	

INFORMATION FOR AUTHORS

(Detailed *Instructions to Authors* were published in *J. Chromatogr. A*, Vol. 657, pp. 463–469. A free reprint can be obtained by application to the publisher, Elsevier Science B.V., P.O. Box 330, 1000 AH Amsterdam, Netherlands.)

Types of Contributions. The following types of papers are published: Regular research papers (full-length papers), Review articles, Short Communications and Discussions. Short Communications are usually descriptions of short investigations, or they can report minor technical improvements of previously published procedures; they reflect the same quality of research as full-length papers, but should preferably not exceed five printed pages. Discussions (one or two pages) should explain, amplify, correct or otherwise comment substantively upon an article recently published in the journal. For Review articles, see inside front cover under Submission of Papers.

Submission. Every paper must be accompanied by a letter from the senior author, stating that he/she is submitting the paper for publication in the *Journal of Chromatography A* or *B.*

Manuscripts. Manuscripts should be typed in **double spacing** on consecutively numbered pages of uniform size. The manuscript should be preceded by a sheet of manuscript paper carrying the title of the paper and the name and full postal address of the person to whom the proofs are to be sent. As a rule, papers should be divided into sections, headed by a caption (*e.g.*, Abstract, Introduction, Experimental, Results, Discussion, etc.). All illustrations, photographs, tables, etc., should be on separate sheets.

Abstract. All articles should have an abstract of 50–100 words which clearly and briefly indicates what is new, different and significant. No references should be given.

Introduction. Every paper must have a concise introduction mentioning what has been done before on the topic described, and stating clearly what is new in the paper now submitted.

> **Experimental conditions** should preferably be given on a *separate* sheet, headed "Conditions". These conditions will, if appropriate, be printed in a block, directly following the heading "Experimental".

Illustrations. The figures should be submitted in a form suitable for reproduction, drawn in Indian ink on drawing or tracing paper. Each illustration should have a caption, all the *captions* being typed (with double spacing) together on a *separate sheet*. If structures are given in the text, the original drawings should be provided. Coloured illustrations are reproduced at the author's expense, the cost being determined by the number of pages and by the number of colours needed. The written permission of the author and publisher must be obtained for the use of any figure already published. Its source must be indicated in the legend.

References. References should be numbered in the order in which they are cited in the text, and listed in numerical sequence on a separate sheet at the end of the article. Please check a recent issue for the layout of the reference list. Abbreviations for the titles of journals should follow the system used by *Chemical Abstracts.* Articles not yet published should be given as "in press" (journal should be specified), "submitted for publication" (journal should be specified), "in preparation" or "personal communication".

> Vols. 1–651 of the *Journal of Chromatography; Journal of Chromatography, Biomedical Applications* and *Journal of Chromatography, Symposium Volumes* should be cited as *J. Chromatogr.* From Vol. 652 on, *Journal of Chromatography A* (incl. Symposium Volumes) should be cited as *J. Chromatogr. A* and *Journal of Chromatography B: Biomedical Applications* as *J. Chromatogr. B.*

Dispatch. Before sending the manuscript to the Editor please check that the envelope contains four copies of the paper complete with references, captions and figures. One of the sets of figures must be the originals suitable for direct reproduction. Please also ensure that permission to publish has been obtained from your institute.

Proofs. One set of proofs will be sent to the author to be carefully checked for printer's errors. Corrections must be restricted to instances in which the proof is at variance with the manuscript.

Reprints. Fifty reprints will be supplied free of charge. Additional reprints can be ordered by the authors. An order form containing price quotations will be sent to the authors together with the proofs of their article.

Advertisements. The Editors of the journal accept no responsibility for the contents of the advertisements. Advertisement rates are available on request. Advertising orders and enquiries can be sent to the Advertising Manager, Elsevier Science B.V., Advertising Department, P.O. Box 211, 1000 AE Amsterdam, Netherlands; courier shipments to: Van de Sande Bakhuyzenstraat 4, 1061 AG Amsterdam, Netherlands; Tel. (+31-20) 515 3220/515 3222, Telefax (+31-20) 6833 041, Telex 16479 els vi nl. *UK*: T.G. Scott & Son Ltd., Tim Blake, Portland House, 21 Narborough Road, Cosby, Leics. LE9 5TA, UK; Tel. (+44-533) 753 333, Telefax (+44-533) 750 522. *USA and Canada*: Weston Media Associates, Daniel S. Lipner, P.O. Box 1110, Greens Farms, CT 06436-1110, USA; Tel. (+1-203) 261 2500, Telefax (+1-203) 261 0101.

Trace Element Analysis in Biological Specimens

Edited by **R.F.M. Herber** and **M. Stoeppler**

Techniques and Instrumentation in Analytical Chemistry Volume 15

The major theme of this book is analytical approaches to trace metal and speciation analysis in biological specimens. The emphasis is on the reliable determination of a number of toxicologically and environmentally important metals. It is essentially a handbook based on the practical experience of each individual author. The scope ranges from sampling and sample preparation to the application of various modern and well-documented methods, including quality assessment and control and statistical treatment of data. Practical advice on avoiding sample contamination is included.

In the first part, the reader is offered an introduction into the basic principles and methods. Quality control and all approaches to achieve reliable data are treated as well.

The chapters of the second part provide detailed information on the analysis of thirteen trace metals in the most important biological specimens.

The book will serve as a valuable aid for practical analysis in biomedical laboratories and for researchers involved with trace metal and species analysis in clinical, biochemical and environmental research.

Contents:
Part 1. Basic Principles and Methods. 1. Sampling and sample storage (A. Aitio, J. Järvisalo, M. Stoeppler). 2. Sample treatment of human biological materials (B. Sansoni, V.K. Panday). 3. Graphite furnace AAS (W. Slavin). 4. Atomic absorption spectrometry. Flame AAS (W. Slavin). 5. Atomic emission spectrometry (P. Schramel). 6. Voltammetry (J. Wang). 7. Neutron activation analysis (J. Versieck). 8. Isotope dilution mass spectrometry (IDMS) (P. de Bièvre). 9. The chemical speciation of trace elements in biomedical specimens: Analytical techniques (P.H.E. Gardiner, H.T. Delves). 10. Interlaboratory and intralaboratory surveys. Reference methods and reference materials (R.A. Braithwaite). 11. Reference materials for trace element analysis (R.M. Parr, M. Stoeppler).

12. Statistics and data evaluation (R.F.M. Herber, H.J.A. Sallé).
Part 2. Elements. 13. Aluminium (J. Savory, R.L. Bertholf, S. Brown, M.R. Wills). 14. Arsenic (M. Stoeppler, M. Vahter). 15. Cadmium (R.F.M. Herber). 16. Chromium (R. Cornelis). 17. Copper (H.T. Delves, M. Stoeppler). 18. Lead (U. Ewers, M. Turfeld, E. Jermann). 19. Manganese (D.J. Halls). 20. Mercury (A. Schütz, G. Skarping, S. Skerfving). 21. Nickel (D. Templeton). 22. Selenium (Y. Thomassen, S.A. Lewis, C. Veillon). 23. Thallium (M. Sager). 24. Vanadium (K.-H. Schaller). 25. Zinc (G.S. Fell, T.D.B. Lyon). Subject index.

© 1994 590 pages Hardbound
Price: Dfl. 475.00 (US$ 271.50)
ISBN 0-444-89867-0

ORDER INFORMATION
ELSEVIER SCIENCE B.V.
P.O. Box 330
1000 AH Amsterdam
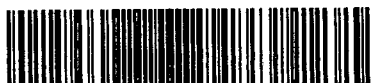The Netherlands
Fax: (+31-20) 5862 845
For USA and Canada
P.O. Box 945
Madison Square Station
New York, NY 10159-0945
Fax: (212) 633 3680
US$ prices are valid only for the USA & Canada and are subject to exchange rate fluctuations; in all other countries the Dutch guilder price (Dfl.) is definitive. Customers in the European Union should add the appropriate VAT rate applicable in their country to the price(s). Books are sent postfree if prepaid.

ELSEVIER SCIENCE